
**Extraction of Dietary Bioactive Components from Sea Buckthorn Leaves and
Whole Berries using Organic Solvent and Supercritical CO₂, and Its
Application in the Synthesis of Silver Nanoparticles**

A thesis submitted for the award of the Degree

of

DOCTOR OF PHILOSOPHY

By

Abebe Moges Tadesse

(Roll No 166107031)



Department of Chemical Engineering

Indian Institute of Technology Guwahati

Guwahati-781 039, India

March 2023









Department of Chemical Engineering
Indian Institute of Technology Guwahati, Assam, India

STATEMENT

I hereby that the matter embodied in this thesis is the result of investigations carried out by me in the Department of Chemical Engineering, Indian Institute of Technology Guwahati, Assam, India under the supervision of Professor Vaibhav V. Goud.

In keeping with the general practice of reporting scientific observations, due acknowledgment has been made wherever the work described is based on the finding of other observations.

Abebe Moges

Department of Chemical Engineering
Indian Institute of Technology Guwahati

March 2023







Department of Chemical Engineering

Indian Institute of Technology Guwahati, Assam, India

CERTIFICATE

It is certified that the work contained in this thesis entitled “**Extraction of Dietary Bioactive Compounds from Sea Buckthorn using Organic Solvent and Supercritical CO₂, and Its Application for the Synthesis of Silver Nanoparticles**” by Mr. Abebe Moges (Roll No. 166107031) for the award of Ph.D. degree, is a record of original research carried out by him at the Department of Chemical Engineering, Indian Institute of Technology Guwahati, under my guidance and supervision. The work embodied in this thesis has not been submitted to any other University or Institute for the award of any other degree or diploma.

Vaibhav V. Goud

Professor

Department of Chemical Engineering

Indian Institute of Technology Guwahati





ACKNOWLEDGMENTS

It is my great pleasure to sincerely thank the people who have supported me throughout my doctoral studies.

First and foremost, I would like to acknowledge and give my warmest thanks to my supervisor **Prof. Vaibhav V. Goud** who provides inspiration and valuable guidance through all the stages of the course. I owe him a debt of gratitude for his constant and intelligent remarks, recommendations, and encouragement.

A debt of gratitude is also owed to my doctoral committee members **Prof. Chandan Das** and **Prof Pallab Gosh**, Department of Chemical Engineering, and **Dr. Siddhartha Singha**, School of Agro and Rural Technology. Their keen interest to provide their strategic insight, comments, and constructive suggestion during the research progress kept the research work in the right direction.

I am grateful to the Analytical Laboratory of the Department of Chemical Engineering and Central Instrument Facility, IIT Guwahati, for providing me with the necessary support during sample analysis.

I am extremely thankful and pay my gratitude to all Faculty and Staff members of the Department of Chemical Engineering and School of Energy Science and Engineering, IIT Guwahati.

I am very grateful to the Ethiopian Ministry of Science and Higher Education for providing me with full sponsorship throughout my Ph.D. study at IIT Guwahati. My appreciation also extends to my home University, Haramaya University for facilitating the opportunity to pursue my study.

I am always indebted to my lab mates and colleagues **Mr. Sukumar Purohit, Mr. Chitta Ranjan Barik Miss. Sutapa Das, Miss. Debni Debi, Mr. Atanu Kumar, Dr. Dipshika Kalita, Miss**

Kakali Borah, and **Saptarshi Gupta** for their help and support in all possible ways throughout my Ph.D. study.

Last, but not least, my wholehearted gratitude goes to my family, my mam, brothers, and sisters.

And beyond all, I thank those invisible hands of the **Almighty God**, who always strengthen me throughout my work.

Sincerely,

Abebe Moges



TABLE OF CONTENTS

CONTENTS	Pages
TABLE OF CONTENTS	I
LIST OF FIGURES	XI
LIST OF TABLES	XVI
LIST OF ABBREVIATIONS	XIX
ABSTRACT	XXII
CHAPTER 1	1
INTRODUCTION AND REVIEW OF LITERATURE	1
1.1 Sea buckthorn	1
1.2 Sea buckthorn distribution	2
1.3 Sea buckthorn varieties in India	2
1.4 The biological aspect of Indian sea buckthorn species	3
1.5 Chemical composition and nutritional value	3
1.6 Sea buckthorn oil	4
1.7 Pharmaceutical properties of sea buckthorn	8
1.8 Sea buckthorn products and their biological properties	9
1.9 Extraction of bioactive compounds	10

1.9.1	Conventional Soxhlet extraction	11
1.9.2	Successive extraction	12
1.9.3	Supercritical carbon dioxide extraction	14
1.10	Antioxidant and antibacterial properties of sea buckthorn extract	15
1.11	Biosynthesis of silver nanoparticles from sea buckthorn extract	17
1.12	Antibacterial properties of Ag NPs	21
2.13	Motivation of the research	21
2.14	Knowledge gap	22
CHAPTER 2		26
MATERIALS AND METHODS		26
2.1	Collection of Sea buckthorn berries and leaves	26
2.2	Chemicals and reagents	26
2.3	Bacterial culture	27
2.4	Physicochemical characterization	27
2.4.1	Proximate analysis	27
2.4.2	Ultimate analysis	28
2.4.3	Elemental composition	28
2.4.4	Total soluble sugar	28
2.4.5	Reducing sugar	29
2.4.6	Non-reducing sugar	29
2.4.7	Total protein content	29

2.4.8	Vitamin C analysis	30
2.4.9	Total tannin content	31
2.5	Extraction experiments	31
2.5.1	Successive Soxhlet extraction	31
2.5.2	Supercritical CO ₂ extraction	32
2.5.2.1	SC-CO ₂ extraction of polyphenols from sea buckthorn leaves	32
2.5.2.2	SC-CO ₂ extraction of oil from sea buckthorn berries	33
2.5.3	Supercritical CO ₂ extraction procedures	34
2.5.4	Experimental design for polyphenol extraction	35
2.5.5	Experimental design for oil extraction from sea buckthorn berries	35
2.5.6	ANOVA and model fitting	36
2.5.7	Soxhlet extraction	36
2.6	Characterization of extracts	37
2.6.1	Phytochemical screening	37
2.6.2	Fourier transform infrared spectroscopy analysis	37
2.6.3	Total phenolic content (TPC)	37
2.6.4	Total flavonoid content (TFC)	38
2.6.5	Identification of phenolic and flavonoid compounds by HPLC	39
2.6.6	Limit of detection (LOD) and limit of quantification (LOQ)	39
2.6.7	In-vitro antioxidant activity	39
2.6.7.1	DPPH assay	40
2.6.7.2	ABTS assay	40
2.6.7.3	Global antioxidant score (GAS)	40

2.6.8	Antibacterial activity	41
2.6.8.1	Minimum inhibitory concentration (MIC)	41
2.6.8.2	Zone of inhibition (ZOI)	42
2.7	Characterization of oil	42
2.7.1	β -carotene analysis	42
2.7.2	Total tocopherol analysis	43
2.7.3	Fatty acid methyl esters analysis	43
2.7.4	Physico-chemical characterization of oil	44
2.7.4.1	Refractive index (AOCS Cc 7-25)	44
2.7.4.2	Specific gravity (AOCS Cc 10a-25)	44
2.7.4.3	Saponification value (AOCS Cd 3-35)	45
2.7.4.4	Unsaponifiable matter (AOCS Ca 6a-40)	45
2.7.4.5	Peroxide value (AOCS Cd 8-53)	46
2.7.4.6	Acid value (AOCS Cd 3d-63)	47
2.7.4.7	Iodine value (AOCS Cd 1-25)	47
2.7.5	Thermogravimetric analysis	48
2.7.6	Rheological measurements	49
2.8	Synthesis of silver nanoparticles	50
2.8.1	Preparation of plant extract	50
2.8.2	Synthesis Ag NPs	50
2.8.3	Preliminary study	50
2.8.4	Parameters optimization	51
2.8.5	Ag NPs yield at optimum condition	51

2.9	Characterization of synthesized silver nanoparticles	52
2.9.1	UV–Visible spectrophotometer	52
2.9.2	X-Ray Diffraction analysis	52
2.9.3	Dynamic and light scattering	53
2.9.4	Field Emission Transmission Electron Microscope	53
2.9.5	Field Emission Scanning Electron Microscope	53
2.9.6	FTIR spectrometer	53
2.10	Statistical analysis	54
CHAPTER 3		55
DIETARY AND BIOACTIVE PROPERTIES OF THE BERRIES AND THE LEAVES OF <i>HIPPOPHAE SALICIFOLIA D. DON</i>		55
3.1	Background	55
3.2	Overview	56
3.4	Results and Discussion	57
3.4.1	Proximate and CHNS analysis	57
3.4.2	Elemental analysis	58
3.4.3	Quantitative phytochemical analysis	60
3.4.4	Successive extraction	62
3.4.5	Qualitative phytochemical screening	63
3.4.6	FTIR Analysis	64
3.4.7	Total phenolic and flavonoid contents	66
3.4.8	HPLC analysis	69

3.4.9 In vitro antioxidant activity	74
3.4.10 Antibacterial activity	77
3.5 Summary	81
CHAPTER 4	83
OPTIMIZATION OF POLYPHENOL EXTRACTION FROM <i>HIPPOPHAE SALICIFOLIA</i> LEAF USING SUPERCRITICAL CO₂ BY RESPONSE SURFACE METHODOLOGY	83
4.1 Background	83
4.2 Overview	83
4.3 Results and Discussion	85
4.3.1 Preliminary studies	85
4.3.1.1 Comparison between leaves from the male and female plant	85
4.3.1.2 Effect of leaf powder-to-entrainer ratio	86
4.3.1.3 Effect of extraction time	86
4.3.2 Fitting the Models and analysis of ANOVA	86
4.3.3 Influence of extraction variables on the yield of extraction, TPC, and IC50	89
4.3.4 Effect of pressure and temperature	90
4.3.5 Effect of pressure and CO ₂ flow rate	93
4.3.6 Effect of pressure and amount of co-solvent	94
4.3.7 Effect of temperature and CO ₂ flow rate	94
4.3.8 Effect of temperature and co-solvent	95
4.3.9 Effect of CO ₂ flow rate and co-solvent	97

4.3.10	Process optimization for higher extraction yield, TPC, and lower IC50	98
4.3.11	Validation of SC-CO ₂ extraction parameters	98
4.3.12	Characterization of extract obtained at optimum SC-CO ₂ extraction conditions	98
4.3.13	Antibacterial activity of extract obtained at optimum conditions	103
4.3.14	Comparison between SC-CO ₂ extracts of FL, ML, and the mixture of leaves.	105
4.3.4	Summary	105
CHAPTER 5		107
OPTIMIZATION AND CHARACTERIZATION OF SUPERCRITICAL CO₂ EXTRACTED OIL FROM <i>HIPPOPHAE SALICIFOLIA</i> BERRIES		107
5.1	Background	107
5.2	Overview	107
5.3	Results and Discussion	109
5.3.1	Models fitting and analysis of ANOVA	109
5.3.2	Effect of extraction variables on the oil yield	110
5.3.3	Effect of extraction variables on the β -carotene content in the oil	114
5.3.4	Effect of extraction variables on the total tocopherol content	116
5.3.5	Optimization of process parameters	116
5.3.6	Conventional organic solvent extraction	117
5.3.7	Fatty acids composition	119
5.3.8	Physicochemical characteristics of oil	121
5.3.9	Total phenolic and flavonoid content	123
5.3.10	Antioxidant activity	124

5.3.11	Antibacterial activity	125
5.3.12	Thermal stability	126
5.3.13	Rheological measurement	129
5.4	Summary	131
CHAPTER 6		133
OPTIMIZATION, CHARACTERIZATION, AND EVALUATION OF ANTIOXIDANT AND ANTIBACTERIAL ACTIVITIES OF SILVER NANOPARTICLES SYNTHESIZED FROM <i>HIPPOPHAE SALICIFOLIA</i>		133
6.1	Background	133
6.2	Overview	134
6.3.	Results and discussion	135
6.3.1.	Optimization study	135
6.3.1.1	Effect of extract concentration	135
6.3.1.2	Effect of AgNO ₃ concentration	137
6.3.1.3	Effect of pH	139
6.3.1.4	Effect of temperature	140
6.3.1.5	Effect of time	141
6.3.2	Ag NPs yield at optimum condition	142
6.3.3	Characterization of Ag NPs	143
6.3.3.1	Particle size analysis	143
6.3.3.2	Crystallinity Analysis	144
6.3.3.3	Shape and size analysis	145

6.3.3.4 Morphological analysis	148
6.3.4 FTIR analysis	148
6.3.5 Total phenolic and flavonoid content	150
6.3.6 Antioxidant activity	152
6.3.7 Antibacterial activity	153
6.3.7.1 Minimum inhibitory concentration (MIC)	153
6.3.7.2 Zone of Inhibition (ZoI)	153
6.4 Summary	156
CHAPTER 7	158
OVERALL SUMMARY AND CONCLUSIONS	158
7.1 Overall summary	158
7.2 Conclusions	159
RESEARCH CONTRIBUTIONS AND FUTURE WORK RECOMMENDATIONS	158
CHAPTER 8	162
RESEARCH CONTRIBUTIONS AND FUTURE WORK RECOMMENDATIONS	162
8.1 Research contribution	162
8.2 Future work recommendations	162
References	164
APPENDIX	I



LIST OF FIGURES

Fig. No.	Figure titles	Page No
Fig. 1.1	Structure of some biologically active phytochemicals	5
Fig. 3.1	Graphical Abstract	56
Fig. 3.2	FTIR spectral transmission band for (a) powdered berries (b) mixture of powdered leaves, (c) berries extracts, and (d) leaves extracts, HX-hexane, CL-chloroform, EA-ethyl acetate, AC-acetone, MT-methanol, AQ-aqueous	65
Fig. 3.3	HPLC chromatograms for identification of phenolic acids. (a) HPLC profile of standards: gallic acid (GA), caffeic acid (CA), p-coumaric acid (P-CA), and ferulic acid (FA). (b) Identification of phenolic acids in berries extracts: ethyl acetate (BEA), acetone (BAC), methanol (BMT), and aqueous (BAQ) extracts at 310 nm. (c) Identification of phenolic acids in leaves extracts: ethyl acetate (LEA), acetone (LAC), methanol (LMT), and aqueous (LAQ) extracts at 310 nm	72
Fig. 3.4	HPLC chromatograms of flavonoid compounds. (a) HPLC profile of standards rutin (RT), myricetin (MRC), quercetin (QRC), and kaempferol (KMP) at 368 nm. (b) Identification of flavonoids in berries extracts: ethyl acetate (BEA), acetone (BAC), methanol (BMT), and aqueous (BAQ) extracts; (c) Identification of phenolic acids in leaves	73

	extracts: ethyl acetate (LEA), acetone (LAC), methanol (LMT), and aqueous (LAQ) extracts	
Fig.3.5	The antioxidant activity of extracts of (a) berries extract, (b) leaves extracts in DPPH and ABTS assays, (c) global antioxidant score for berries extracts, and (d) global antioxidant score for leaves extracts. AA- Ascorbic acid HX- hexane. CL- Chloroform, EA- Ethyl acetate, AC- acetone, MT- Methanol, and AQ- aqueous	77
Fig. 4.1	Graphical Abstract	84
Fig. 4.2	Plots of model predicted values versus actual experimental values for (a) yield of extraction, (b) TPC, and (c) IC ₅₀ of SC-CO ₂ extracts	92
Fig. 4.3	Influence of extraction variables on extraction yield (a-f), total phenolic content (g-l)	96
Fig. 4.4.	Influence of extraction variables on IC ₅₀ (a-d)	97
Fig. 4.5.	HPLC chromatograms for identification of phenolic acids. (a) HPLC profile of standards: gallic acid (GA), caffeic acid (CA), p-coumaric acid (P-CA), and ferulic acid (FA). (b) Identification of phenolic acids in extracts at 310 nm: FL(Sox) and ML(Sox) – extracts from female and male leaf obtained by Soxhlet extraction, respectively. FL(1:1)-female leaf, ML(1:1)-male leaf, MIX(1:1)- mixture of FL and ML extracts obtained from SC-CO ₂ extraction at optimum condition	101
Fig. 4.6.	HPLC chromatograms of flavonoid compounds. (a) HPLC profile of standards rutin (RT), myricetin (MRC), quercetin (QRC), and	102

	kaempferol (KMP) at 368 nm. (b) Identification of flavonoids in extracts: FL(Sox) and ML(Sox) – extracts from female and male leaves obtained by Soxhlet extraction, respectively. FL(1:1)-female leaf, ML(1:1)-male leaf, MIX(1:1)- mixture of FL and ML extracts obtained from SC-CO ₂ extraction at optimum condition	
Fig. 5.1	Graphical Abstract	108
Fig. 5.2	Plots of actual experimental values versus model predicted values for (a) Oil yield, (b) β -carotene, and (c) Total tocopherol content	113
Fig. 5.3	Effect of pressure, temperature, and CO ₂ flow rate time on oil yield (a–c), on β -carotene (d–f), and Total tocopherol content of the oil (g–i)	115
Fig. 5.4	HPLC chromatograms of (a) standards, (b) SC-CO ₂ extracted oil, and (c) Soxhlet extracted oil. 1- α -tocopherol, 2 - γ -tocopherol, and 3 - δ -tocopherol	118
Fig. 5.5	Gas chromatograms of (a) SC-CO ₂ extracted oil and (b) Soxhlet extracted oil FAMES	121
Fig. 5.6	(a) TGA, (b) DTG, and (c) Arrhenius plots for SC-CO ₂ and Soxhlet extracted oils	127
Fig. 5.7	(a) Flow behavior, (b) Effect of the shear rate on the viscosity, (c) Effect of the temperature on the viscosity of SC-CO ₂ and Soxhlet extracted oils	131
Fig. 6.1	Graphical Abstract	134
Fig. 6.2	Schematic diagram	135

-
- Fig. 6.3 UV-vis spectrum of Ag nanoparticle: (a - d) Effect of extract concentration on (a) LM-Ag NPs, (b) LA-Ag NPs, (c) BM-Ag NPs, (d) BA-Ag NPs. (f - h) Effect of AgNO₃ concentration on (e) LM-Ag NPs, (f) LA-Ag NPs, (g) BM-Ag NPs, (h) BA-Ag NPs. LM-Ag NPs - nanoparticles from leaves-methanol extract, LA-Ag NPs - nanoparticles from leaves-aqueous extract, BM-Ag NPs - nanoparticles from berries-methanol extract, BA-Ag NPs - nanoparticles from berries-aqueous extract 136
- Fig. 6.4 Effect of PH on UV-vis spectrum of Ag nanoparticle: (a - d) Effect of PH on (a) LM-Ag NPs, (b) LA-Ag NPs, (c) BM-Ag NPs, (d) BA-Ag NPs. (e - h) Effect of temperature and time on (e) LM-Ag NPs, (f) LA-Ag NPs, (g) BM-Ag NPs, (h) BA-Ag NPs. LM-Ag NPs - nanoparticles from leaves-methanol extract, LA-Ag NPs - nanoparticles from leaves-aqueous extract, BM-Ag NPs - nanoparticles from berries-methanol extract, BA-Ag NPs - nanoparticles from berries-aqueous extract 138
- Fig. 6.5 XRD pattern of LM-Ag NPs (nanoparticles synthesized from leaves-methanol extract), LA-Ag NPs (nanoparticles synthesized from leaves-aqueous extract), BM-Ag NPs (nanoparticles synthesized from berries-methanol extract), and BA-Ag NPs (nanoparticles synthesized from berries-aqueous extract) 144

Fig. 6.6	FETEM analysis: Histograms - a, e, i, and m; SEM images - b, f, j, and n; Selected area electron diffraction (SAED) pattern - c, g, k, and o; Elemental (EDX) analysis - d, h, l, and p. LM-Ag NPs - nanoparticles synthesized from leaves-methanol extract, LA-Ag NPs – nanoparticles synthesized from leaves-aqueous extract, BM-Ag NPs - nanoparticles synthesized from berries-methanol extract, BA-Ag NPs - nanoparticles synthesized from berries-aqueous extract	146
Fig. 6.7	SEM images of synthesized Ag nanoparticles. a - nanoparticles synthesized from leaves-methanol extract, b – nanoparticles synthesized from leaves-aqueous extract, c - nanoparticles synthesized from berries-methanol extract, d - nanoparticles synthesized from berries-aqueous extract	147
Fig. 6.8	FTIR spectra of (a) LME (leaves-methanol extract), LM-Ag NPs (nanoparticles synthesized from leaves-methanol extract), LMS (supernatant from LM-Ag NPs suspension), (b) LAE (leaves-aqueous extract), LA-Ag NPs (nanoparticles synthesized from leaves-aqueous extract), LAS (supernatant from LA-Ag NPs suspension), (c) BME (berries-methanol extract), BM-Ag NPs (nanoparticles synthesized from berries-methanol extract), BMS (supernatant from BM-Ag NPs suspension), (d) BAE (berries-aqueous extract), BA-Ag NPs (nanoparticles synthesized from berries-aqueous extract), BAS (supernatant from BA-Ag suspension)	149





LIST OF TABLES

Table No.	Table Titles	Page No.
Table 1.1	Concentrations of different bioactive compounds in sea buckthorn	7
Table 1.2	Summary of previously published reports on total phenolic content, antioxidant and antibacterial properties of sea buckthorn extracts	13
Table 1.3	Review of literature review on SC CO ₂ extraction from sea buckthorn berries and leaves	16
Table 1.4	A literature review on Ag NP synthesis from various plants	19
Table 1.5	Review of literature on the optimization of silver nanoparticle synthesis	20
Table 3.1	Composition of sea buckthorn berries and leaves	58
Table 3.2	Elemental composition of sea buckthorn berries and leaves	59
Table 3.3	Nutritional composition of sea buckthorn berries and leaves	61
Table 3.4	Yield (%) of successive extraction from sea buckthorn berries and the leaves	63
Table 3.5	Phytochemical screening results of sea buckthorn berries and leaves extracts	64
Table 3.6	The yield of extraction, total phenolic content (TPC), and total flavonoid content (TFC) of extracts	67
Table 3.7	HPLC analysis of phenolic and flavonoid compounds in sea buckthorn berries and leaves extract	71

Table 3.8	The percentage scavenged at 50 µg/mL extract concentration in DPPH and ABTS assay	76
Table 3.9	Minimum inhibitory concentration (µg/mL) study of sea buckthorn berries and leaves extracts	78
Table 3.10	Zone of Inhibition (mm) of sea buckthorn berries and leaves extracts	80
Table 4.1	Yield, TPC, TFC, and IC50 of extracts obtained from Soxhlet and SC-CO ₂ extraction	85
Table 4.2	Extraction process variables and their levels for central composite design	87
Table 4.3	Central Composite Design and actual data of performed experiments	88
Table 4.4	ANOVA for extraction yield, total phenolic content, and IC50 obtained from central composite design	90
Table 4.5	Regression coefficients, Standard Deviation (Std. dev.), and Coefficient of the variation (CV%) for extraction yield, TPC, and IC50.	91
Table 4.6	Extraction yield, TPC, TFC, IC50, and HPLC analysis of extracts	99
Table 4.7	Retention time, regression equation, LOD, and LOQ of analyzed compounds	100
Table 4.8	Antibacterial analysis of extracts obtained at optimized conditions	104
Table 5.1	Extraction process variables and their levels	109

Table 5.2	Central Composite Design for supercritical CO ₂ extraction and the corresponding responses	111
Table 5.3	ANOVA for yield, β -carotenoid, and total tocopherol extraction efficiency for the results obtained from CCD	112
Table 5.4	The oil yield, β -carotene, and tocopherol content of sea buckthorn oils	117
Table 5.5	Fatty acid composition of SC-CO ₂ and Soxhlet extracted oils	120
Table 5.6	Physico-chemical characteristics of sea buckthorn oils	123
Table 5.7	Zone of Inhibition (mm) of SC-CO ₂ and Soxhlet extracted oils	126
Table 5.8	TGA characteristic properties for active pyrolysis stages of SC-CO ₂ and conventional Soxhlet extracted oils	128
Table 6.1	Optimum conditions for the synthesis of Ag NPs	142
Table 6.2	Size of NPs using DLS, XRD, and FETEM analysis	143
Table 6.3	TPC, TFC, and antioxidant activities of extracts and Ag NPs obtained at optimized conditions	151
Table 6.4	Minimum inhibitory concentration ($\mu\text{g/mL}$) of extracts and Ag NPs synthesized at optimal conditions	154
Table 6.5	Zone of Inhibition (mm) of extracts and Ag NPs synthesized at optimal condition	155



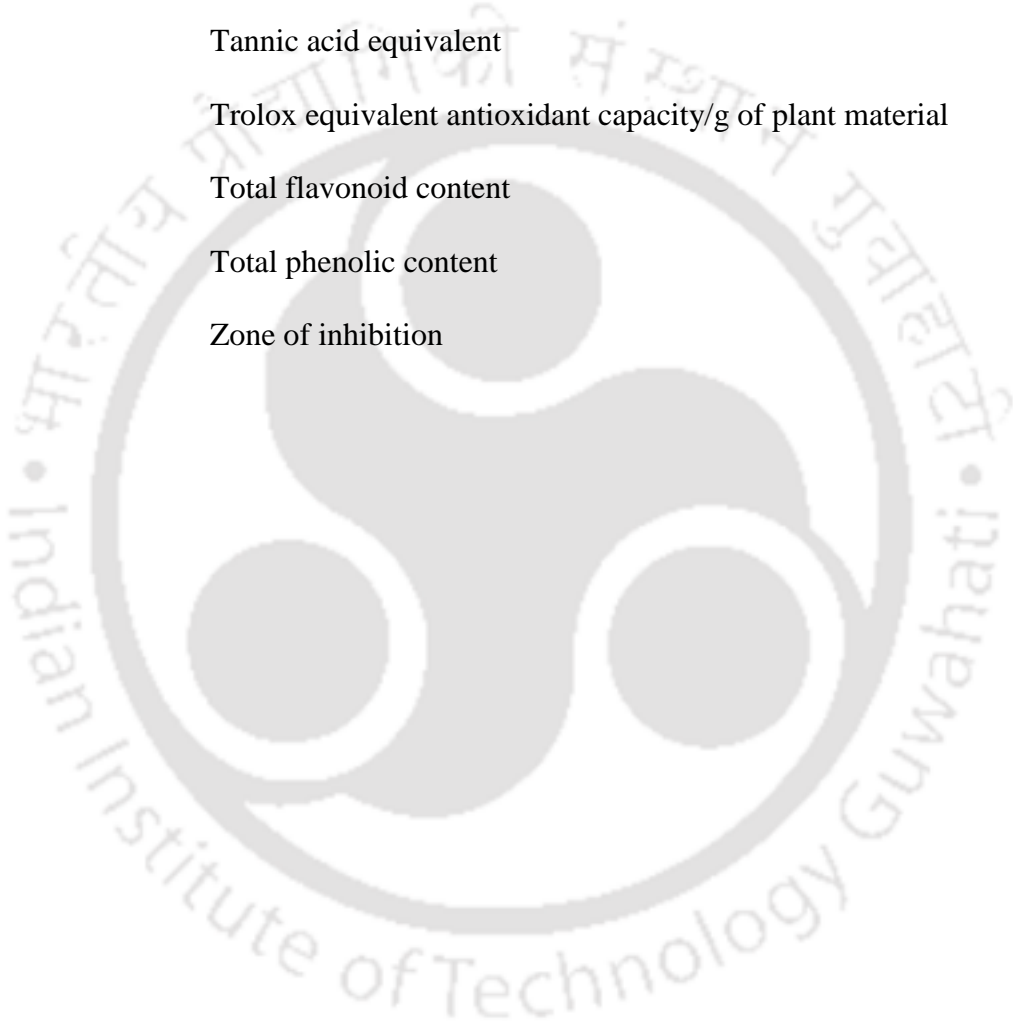


LIST OF ABBREVIATIONS

AA	Ascorbic acid
AAE	Ascorbic acid equivalent
ABTS	2,2'-azino-bis (3-ethylbenzothiazoline-6-sulfonic acid) diammonium salt
AC	Acetone
Ag NPs	Silver nanoparticles
AOA	Antioxidant activity
BA-Ag NPs	Nanoparticles synthesized from berries-aqueous extract
BAE	Berries-aqueous extract
BASE	Bovine serum albumin equivalent
BM-Ag NPs	Nanoparticles synthesized from berries-methanol extract
BME	Berries-methanol extract
BS	<i>Bacillus subtilis</i>
CCD	Central composite design
CE	Catechin equivalent
CL	Chloroform
DMSO	Dimethyl sulfoxide
DPPH	1,1-Diphenyl-2-picrylhydrazyl
DW	Dry weight
EA	<i>Enterobacter aerogenes</i>
EA	Ethyl acetate

<i>EC</i>	<i>Escherichia coli</i>
EC50	Extract concentration required to scavenge 50% of radicals in vitro
FL	Leaves from female plant
FW	Fresh weight
GAE	Gallic acid equivalent
GAS	Global antioxidant score
GE	Glucose equivalent
HX	Hexane
<i>KP</i>	<i>Klebsiella pneumonia</i>
LA-Ag NPs	Nanoparticles synthesized from leaves-aqueous extract
LAE	Leaves-aqueous extract
LM-Ag NPs	Nanoparticles synthesized from leaves-methanol extract
LME	Leaves-methanol extract
MIC	Minimum inhibitory concentration
MIX	50-50% mixture of FL and ML
ML	Leaves from male plant
<i>ML</i>	<i>Micrococcus luteus</i>
MT	Methanol
<i>PA</i>	<i>Pseudomonas aeruginosa</i>
QE	Quercetin equivalent
RE	Rutin equivalent
RSM	Response surface methodology
<i>SA</i>	<i>Staphylococcus aureus</i>

SBT	Sea buckthorn
SBTB	Sea buckthorn berry
SBTL	Sea buckthorn leaves
SC-CO ₂	Supercritical carbon dioxide
<i>SE</i>	<i>Staphylococcus epidermis</i>
TAE	Tannic acid equivalent
TEAC	Trolox equivalent antioxidant capacity/g of plant material
TFC	Total flavonoid content
TPC	Total phenolic content
ZoI	Zone of inhibition







ABSTRACT

Sea buckthorn berries and leaves have received a lot of attention in the field of nutraceuticals, cosmeceuticals products, and natural food preservatives due to their high content of minerals, sugars, vitamins, and bioactive compounds such as phenolics, flavonoids, tocopherols, carotenoids, phytosterols, unsaturated lipids, and volatile compounds. This served as the impetus for research into dietary, antioxidant, and antibacterial characteristics of sea buckthorn (*Hippophae salicifolia*) leaves and whole berries, as well as the application of bioactive substances in the synthesis of silver nanoparticles.

The first section investigates the dietary and bioactive properties of the berries and the mixture of leaves (from male and female plants) of *Hippophae salicifolia*. The berries and leaves of *Hippophae salicifolia* have nutritional and bioactive characteristics, with the leaves being more nutritious and physiologically active than the berries. Vitamin C was the most abundant phytonutrient in the berries (256.1 ± 1.3 mg/100g), whereas the leaves had the highest total soluble sugar concentration (138.64 ± 3.3 mg GE/g). Further, the berries and mixture of leaves were successively extracted using n-hexane, chloroform, ethyl acetate, acetone, methanol, and distilled water, which were then investigated for their polyphenolic content, and antioxidant and antibacterial properties. Total phenolic content (TPC) was highest in the leaves-methanol extract (157.97 ± 2.09 mg GAE/g) and berries-aqueous extract (48.45 ± 1.94 mg GAE/g). In contrast, total flavonoid was predominant in the leaves- acetone extract (75.64 ± 3.21 mg QE/g) and berries-methanol extract (28.93 ± 2.08 mg QE/g). The primary polyphenols validated by HPLC analysis were gallic acid, caffeic acid, and rutin, with a higher amount in the leaves. Gallic acid in the leaves extract was approximately 4 to 23-fold higher than the whole berries extracts. Berries-aqueous and

leaves-methanol extracts showed excellent global antioxidant scores. Methanol extracts observed the best antibacterial activity against eight different strains.

Further, the thesis presents the extraction of polyphenolic compounds from *Hippophae salicifolia* leaves using supercritical carbon dioxide (SC-CO₂). The process of SC-CO₂ extraction was optimized using central composite design (CCD) followed by response surface methodology (RSM) to achieve maximum yield of extraction, TPC and antioxidant activity. Central composite design as a tool of response surface methodology was used to examine the effect of pressure, temperature, amount of co-solvent, and CO₂ flow rate on the extraction yield, TPC, and antioxidant activity. Under optimized condition (25.13 MPa pressure, 47.53°C temperature, 14.47 g/min CO₂ flow rate, and 2.43% amount of cosolvent), the experimental data (yield of extraction: 4.38%, TPC: 84.31 mg GAE/g, and IC₅₀: 41.94 µg/mL) showed good agreement with the predicted values (yield of extraction: 4.53%, TPC: 83.37 mg GAE/g, and IC₅₀: 40.2 µg/mL). Using HPLC, nine polyphenolic compounds (gallic acid, caffeic acid, ferulic acid, vanillic acid, p-coumaric acid, quercetin, myricetin, kaempferol, and rutin) were examined in the SC-CO₂ extract. SC-CO₂ extraction was more selective for the extraction of ferulic acid, myricetin, and quercetin. SC-CO₂ extracts demonstrated notable antibacterial activity when tested against eight different strains in the antibacterial activity assays. The study results revealed SC-CO₂ extracts of *Hippophae salicifolia* as a potential candidate for functional foods and ingredients, food supplements, and food preservatives.

In the thesis, the process variables (pressure, temperature, and CO₂ flow rate) for SC-CO₂ extraction of oil from *Hippophae salicifolia* berries are also optimized with the objective to achieve maximum oil yield, β-carotene and total tocopherol. The results revealed that CO₂ flow rate had a maximum effect on oil yield, while pressure showed a significant influence on β-carotene and total

tocopherol contents of oil. 2nd order polynomial model sufficiently represented the relationship between the process variables and responses. The optimum extraction conditions for oil yield of $12.82 \pm 1.4\%$, β -carotene content of 126.67 ± 2.9 mg/100, and total tocopherol content of 679.42 ± 1.3 mg/100 g was 27.02 MPa pressure, 48.46 °C temperature, 16.45 g/min CO₂ flow rate. The berry oil extracted using conventional solvent extraction and SC-CO₂ contained 92.72 and 91.42% UFA, with omega-seven fatty acids (palmitoleic acid) content of 42.98 and 41.14%, respectively. The physicochemical properties of both the oils were within the edible range. The oil extracted by SC-CO₂ had a higher TPC and antioxidant activity than conventional solvent-extracted oil. The oil extracted using both methods showed significant antibacterial activity against eight pathogenic bacterial strains. The thermogravimetric profile of SC-CO₂ extracted oil exhibited lower thermal stability up to 185 °C. The mechanical stress resistance of SC-CO₂ extracted oil was higher than that of conventional solvent-extracted oil.

The thesis also incorporates the applications of *Hippophae salicifolia* leaves and berries extracts for the synthesis of silver nanoparticles (Ag NPs). Ag NPs synthesized using methanol and aqueous extracts of *Hippophae salicifolia* leaves and berries were characterized and analyzed for their antioxidant and antibacterial activity. The parameters such as extract concentration, AgNO₃ concentration, pH, temperature, and time were optimized to achieve a higher Ag NPs yield. The pH was the most critical parameter in regulating the size and NPs yield. Ag NPs were successfully synthesized at optimum conditions and characterized by DLS, FTIR, UV-Vis spectrophotometry, XRD, EDX, FESEM, and FETEM. The FTIR analysis revealed that compounds such as phenolics, proteins, benzenes, and sulforaphane are responsible for converting Ag⁺ to Ag⁰ and acting as stabilizing agents. TEM analysis showed that sea buckthorn leaves and berries extract mediated Ag NPs were monodispersed and spherical with an average particle size of 7.87 ± 2.9 nm

(nanoparticles synthesized from leaves-aqueous extract) to 13.86 ± 5 nm (nanoparticles synthesized from berries-aqueous extract). Ag NPs synthesized using aqueous extracts were smaller than those synthesized using methanol. Whereas Ag NPs produced from methanolic extract of leaves exhibited the highest antioxidant of 1.29 ± 0.3 $\mu\text{g/mL}$ and antibacterial activity of 1.9 $\mu\text{g/mL}$. Overall, the findings indicate that Ag NPs synthesized from sea buckthorn leaves and berries extract have significant antioxidant and antibacterial potential for controlling and preventing bacterial infections.

Key words

Hippophae salicifolia, Sea buckthorn, Successive extraction, Supercritical CO₂ extraction, Polyphenol, Oil characteristics, Optimization, Thermal property, Rheological property, Silver nanoparticles, Antioxidant activity, Antibacterial activity.



The logo of the Indian Institute of Technology Guwahati is a circular emblem. It features a central stylized figure with three rounded protrusions, resembling a traditional Indian motif. The figure is surrounded by a circular border containing text in both Assamese and English. The Assamese text at the top reads 'সম্বলীয প্ৰৌদ্যোগিকী সংস্থান গুৱাহাটী' and the English text at the bottom reads 'Indian Institute of Technology Guwahati'.

INTRODUCTION AND REVIEW OF LITERATURE



INTRODUCTION AND REVIEW OF LITERATURE

In this chapter, a summary of the dietary properties, phenolic and flavonoid contents, and antioxidant and antibacterial properties of sea buckthorn berries and leaves are presented. It also includes a comprehensive assessment of published literature on various extraction processes and extraction yield of different sea buckthorn species. The impact of extraction factors on polyphenols and extraction of oil using supercritical CO₂ has been elaborated. This chapter also includes the literature review on the application of extracts of sea buckthorn berries and leaves as a reducing agent for the synthesis of silver nanoparticles. The knowledge gaps in the investigation are thoroughly discussed. Finally, the aims and specific objectives of this research work are presented.

1.1 Sea buckthorn

Sea buckthorn (*Hippophae*) is a nutritious and medicinal plant belonging to the Elaeagnaceae family with extensive applications in the fields of food, medicine, and cosmeceuticals. The plant has a wide range of nutritive and health-promoting properties in its seeds, pulp, leaves, stems, and roots. It is a dioecious hardy, thorny willow-like shrub with separate male and female plants, usually 2 to 4 m in height, growing at an altitude of 2,500 - 4,300 m in temperatures ranging from - 40 °C to + 40 °C (Ding et al., 2015; Negi et al., 2005). Sea buckthorn is a wild fruit-bearing plant that starts bearing fruit three years after plantation and remains productive for about 25 to 30 years. The color and the shape of ripe berries range typically from yellow to orange in color and globose to oval in form. The weight of berries is often in the range of 4 - 60 g per 100 pieces and usually tastes sour, depending on the cultivar and maturity (Ciesarová et al., 2020). The average production

of sea buckthorn is 15 tons of fruit per hectare per year. The leaves are narrow and lanceolate with a silver-gray color on the upper side. The plant has an extensive root system with nitrogen-fixing actinomycetes and can hold the soil on fragile slopes (Li and Schroeder, 1996). *Hippophae* is classified into three species based on morphological variations: *H. rhamnoides* L., *H. salicifolia* D. Don, and *H. tibetana* Schlecht. *Hippophae rhamnoides* is further divided into nine subspecies: *carpatica*, *caucasica*, *gyantsensis*, *mongolica*, *sinensis*, *turkestanica*, *yunnanensis*, *rhamnoides*, and *fluviatilis*. *Hippophae rhamnoides* is the most widespread species, followed by *Hippophae salicifolia* and *Hippophae tibetana* (Li and Schroeder, 1996).

1.2 Sea buckthorn distribution

Sea buckthorn is cultivated in different countries like India, China, Asia, Europe, etc. The global distribution of sea buckthorn, including wild and cultivated, is estimated to cover 3 million hectares. China, Russia, Mongolia, Canada, and Northern Europe cover approximately 90% of the world's sea buckthorn (Singh et al., 2019). Sea buckthorn covers around 1.2 million hectares of land in China, the world's most significant producer, followed by Mongolia, the second-leading producer with 20,000 ha (Wild collection). In India, the total area under sea buckthorn is 13,000 ha, leading to an annual yield of 600 tons of berries (Husain et al., 2018).

1.3 Sea buckthorn varieties in India

India produces three species of sea buckthorn: *H. rhamnoides*, *H. salicifolia*, and *H. tibetana*. The primary site for natural sea buckthorn resources is located in northern India near Karakoram (Ladakh) and the westernmost Himalayan mountain. Sea buckthorn has been distributed in the Himalayan regions of Ladakh (9,267 ha), Himachal Pradesh (1,000 ha), Uttaranchal (2,000 ha),

and Sikkim (800 ha) (Stobdan and Phunchok, 2021). *H. rhamnoides* are widely distributed in the country, followed by *H. salicifolia* while species *H. salicifolia* is the most abundant species in the Sikkim (Stobdan et al., 2011a, 2011b).

1.4 The biological aspect of Indian sea buckthorn species

The phytonutrient composition and the biological activities of sea buckthorn berries and leaves vary from species to species. Among the three species of Indian sea buckthorn, *H. salicifolia* berries are considered to be the best in terms of high-quality fruit, high yield, less thorn, and high lipophobic constituents such as vitamin C, total phenolic, and flavonols (Ahmed and Gupta, 2009; Lu, 1992; Ranjith et al., 2006). On the other hand, the berries of *H. rhamnoides* and *H. tibetana* have a higher amount of lipophilic carotenoids and tocopherols content (Ranjith et al., 2006). Regarding the leaves, it is reported that the aqueous extract of *H. salicifolia* leaves has a higher level of total phenolic content with more potent protective and adaptogenic activity compared to *H. rhamnoides* (Rathor et al., 2015).

1.5 Chemical composition and nutritional value

Sea buckthorn berries and leaves have acquired significant attention due to their high contents of minerals, sugars, vitamins, and bioactive compounds such as phenolics, flavonoids, tocopherols, carotenoids, phytosterols, unsaturated lipids, and volatile (Upadhyay et al., 2010). Sea buckthorn berries and leaves also contain macro and micronutrient elements, including K, Na, Mg, Mn, Al, As, Ca, Cd, Cr, Cu, Fe, Ni, Pb, and Zn (Beveridge et al., 1999). However, sea buckthorn leaves are non-edible but contain more nutrients and biologically active hydrophilic polyphenolic compounds with better antioxidant, antibacterial, antitumoral, and anti-inflammatory properties

than berries (Criste et al., 2020). Phenolics are compounds consisting of one (monophenol) or more (polyphenol) aromatic rings with one or more hydroxyl substituents. According to their structure, they are subgrouped into simple phenols, hydroxybenzoic acids, hydroxycinnamic acids, stilbenes, flavonoids, lignans, and tannins. Polyphenolic flavonoids, with diphenyl propane ($C_6C_3C_6$) skeleton, consist of two aromatic rings (A ring and B ring) interconnected through a heterocyclic pyran ring (C ring). Based on the hydroxylation, absence, or presence of a double bond of the pyran ring and the number of hydroxyls in the A and B ring, flavonoids are classified into flavonols, flavanones, flavones flavanols, anthocyanidins, and isoflavonoids (Lin et al., 2016; Kumar & Pandey, 2013). The structure of some phenolic compounds is shown in **Fig. 1.1**. The biologically active polyphenolic compounds in sea buckthorn leaves and berries include catechin, epicatechin, gallic acid, p-coumaric acid, caffeic acid, ferulic acid, rutin, quercitrin, isoquercitrin, narcissoside, isorhamnetin, kaempferol, and protocatechuic acid (Bittová et al., 2014; Dong et al., 2017). The berries of sea buckthorn, on the other hand, are among the most nutritious and vitamin-rich fruits in the plant kingdom, containing more oil and essential fatty acids and vitamins (carotenoids and tocopherols) than leaves. The unique trait of sea buckthorn fruit is its high Vitamin C content, approximately 5 to 100-fold higher than other fruits or vegetables (Bal et al., 2011). Chinese subspecies *Sinensis* (600-2500 mg/100 g) was reported to contain the highest vitamin C, followed by Indian sea buckthorn (*Hippophae rhamnoides*) (168.3-509 mg/100 g) and European Subspecies *H. rhamnoides* (28-310 mg/100 g) (Bal et al., 2011).

1.6 Sea buckthorn oil

The oil, which makes up 20-24% of the berry, is the other most valuable component of sea buckthorn fruit. Sea buckthorn oil is an excellent source of carotenoids, tocopherols, sterols, and

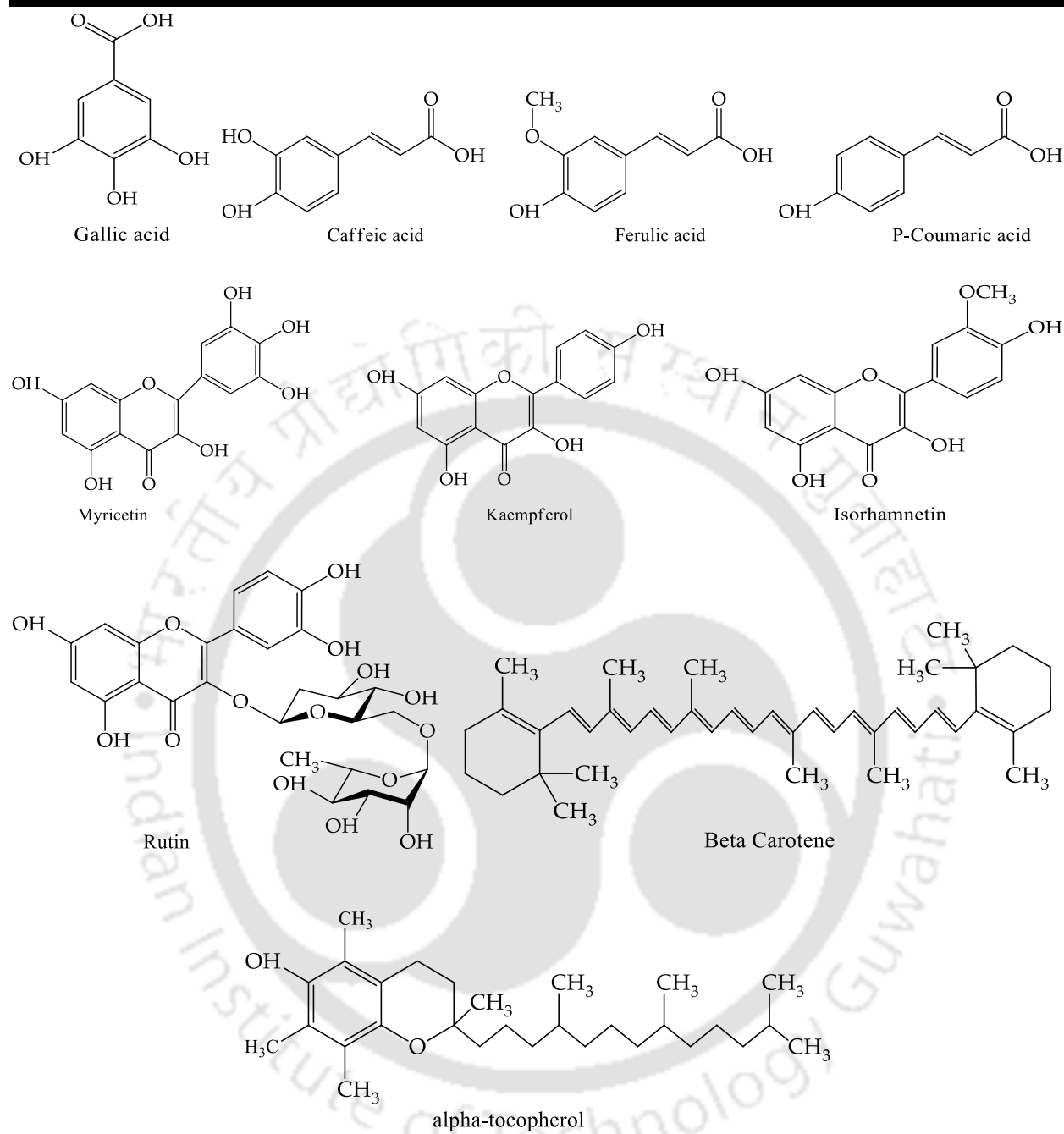


Fig. 1.1: Structure of some biologically active phytochemicals

saturated and unsaturated fatty acids (Kagliwal et al., 2012; Kaminskas et al., 2006; Yang and Kallio, 2002), and other natural antioxidant substances (Anbarasu et al., 2015). Carotenoids are the common form of tetraterpenoids that mainly exist in the soft parts, giving the sea buckthorn

berries beautiful intensive golden color. If the oil is applied directly to the skin, it provides a fresh and healthy appearance. The major carotenoids in sea buckthorn oil are zeaxanthin, β -carotene, β -cryptoxanthin, lutein, lycopene, and γ -carotene, of which 15-55% of the total carotenoid comprised of β -carotene followed by lycopene and zeaxanthin (Andersson et al., 2009; Bal et al., 2011; Yang and Kallio, 2002). Carotenoids and tocopherols are fat-soluble antioxidants that contribute to the stability of berries, protecting cell membranes from oxidation by quenching singlet oxygen and lipid peroxy radicals. The oil of sea buckthorn is rich in tocopherols. Tocopherols are critical bioactive compounds in sea buckthorn berries, defining the quality of berries and berries oil (**Fig. 1.1**). The four forms, α -, δ -, γ , and β -are recognized by the position of the methyl group on the aromatic ring. The sea buckthorn fruits contain 101.4-128.3 mg /100 g of oil tocopherol. α -tocopherol is the predominant tocopherol found in the oil, constituting 76-89% of the total tocopherols (Zadernowski et al., 2003).

Sea buckthorn oil is also a valuable source of fatty acids, especially unsaturated fatty acids. The whole fruit oil contains 11 distinguished fatty acids, which constitute 31% to 33% of the oil, and 75% of these are unsaturated fatty acids that enhance the nutritional and medicinal value of the oil (Kagliwal et al., 2012). The main fatty acids in the oil include myristic acid (0.81%), Pentadecanoic acid (0.22%), palmitoleic acid (38.07%), palmitic acid (23.87%), oleic acid (33.18%), 5,8,11,14-Eicosatetraenoic acid (0.13%), 11-Eicosenoic acid (0.2%), Eicosanoic acid (0.41), and omega-7 fatty acid (palmitoleic acid) (38.07%), which provides sea buckthorn fruit oil a remarkable quality (Kagliwal et al., 2012). The physicochemical and phytonutrient characteristics of the leaves and berries depend on various factors such as cultivar, geographic location, harvesting time, processing technologies, storage conditions, and analysis method. The chemical compositions of sea buckthorn berries and leaves are listed in **Table 1.1**.

Table 1.1: Concentrations of different bioactive compounds in sea buckthorn

Chemical compounds	Berries	Leaves	Reference
Vitamin C	310 - 2500 mg/100 g berries	370 mg/100 g berries	(Bal et al., 2011; Krejcarová et al., 2015)
Vitamin E	6.98 - 29.91 mg/g FW	71.54–153.99 mg/g FW	(Sytařová et al., 2020)
Tocopherols:			
α-tocopherol	74.0 mg/100 g oil	66 - 83 mg/100 g dry leaf	(Burčová et al., 2017; Kanayama et al., 2013;
δ-tocopherol	36.3 mg/100 g oil	ND	Zadernowski et al., 2003)
γ-tocopherol	Trace	ND	
Carotenoids:			
β-carotene	11.8 mg /100 g dry berries	0.7 - 0.9 mg /100 g dry leaf	(Andersson et al., 2009; Raluca Maria Pop et al., 2014)
Zeaxanthin	6.52 mg /100 g dry berries	0.5 – 0.6 mg /100 g dry leaf	
lycopene	6.52 mg /100 g dry berries	-	
Total phenolic content	38.7 mg GAE/g DW 3.57 - 4.44 mg/g DW 1.88 - 3.72 mg GAE/g FW	134.96 mg GAE/g DW 56.28 mg GAE/g DW 0.70 - 3.62 mg GAE/g FW	(Asofiei et al., 2016; Guo et al., 2017; Sytařová et al., 2020; Upadhyay et al., 2010; Zadernowski et al., 2005)
Total flavonoid content	51.5 mg CE/g DW 0.55 - 4.11 mg R E/g FW	20.76 (mg RE/g DW 14.40–49.44 mg RE/g FW	(Guo et al., 2017; Sytařová et al., 2020; Upadhyay et al., 2010)
Total Soluble sugar (mg GE/g)	130 mg/g	272.9	(Hussain et al., 2014; Kashif and Ullah, 2013)
Reducing sugar (mg GE/g)	9.7-59.1 mg/g	173.7	(Kashif and Ullah, 2013; Tang and Tigerstedt, 2001)
Total protein (mg BSAE/g)	3.99 - 45.35 mg%	150-200	(Oprica et al., 2007), (Stobdan, et al., 2011)
Total tannin (mg TAE/g)	1.99 - 5.74 mg/g	80 mg/g	(Krejcarová et al., 2015; Kuhkheil et al., 2017)
Ash	1.76-2.83%	1.98-5.09%	(Bal et al., 2011; Ion et al., 2019; Jaroszewska et al., 2017; Tiller et al., 2020)

FW - fresh weight, DW - dry weight, GAE - gallic acid equivalent, CE - catechin equivalent, RE - rutin equivalent, BSAE - bovine serum albumin equivalent, TAE - tannic acid equivalent.

1.7 Pharmaceutical properties of sea buckthorn

The effects of sea buckthorn on cardiovascular diseases are known in Tibetan traditional medicine as early as the eighth century. The versatile properties of sea buckthorn are used in daily life for a variety of purposes, including food, animal fodder (young shoots and leaves), and traditional medicine to cure many ailments and sicknesses, including gastrointestinal diseases, hepatitis, skin disorders, asthma, and as a way of preventing rheumatism in all-around Asia, Russia, and Europe (Olas, 2016). The medicinal uses and research on modern medicinal uses of sea buckthorn have been initiated and well documented in Asia, Europe, and Russia. Currently, hundreds of distinguished sea buckthorn-based formulations are reported in various pharmacopeias. In India, in the Ladakh region where 70% of the site is found, sea buckthorn is used for the treatment of throat infection, indigestion, gynecological problem, gastritis, ulcer, acidity, bronchitis, diarrhea, blood disorder, hypertension, fever, tumor, cough, gallstone, cold, food poisoning, etc (Stobdan and Phunchok, 2021).

Recent scientific studies revealed that the pharmaceutical properties of sea buckthorn berries and leaves ascribed to have phenolic and flavonoid compounds, carotenoids, tocopherols, and essential fatty acids, which inhibit lipoxigenase, chelate metals, and scavenge free radicals (Michel et al., 2012; Olas et al., 2018). In addition to antioxidant activities, the bioactive compounds in sea buckthorn berries and leaves can also contribute to antimicrobial properties. Extracts from the leaves and the berries were reported to have wide-range activities, including anti-inflammatory (Padwad et al., 2006), cytotoxic (Yang & Kallio, 2002), antiviral (Ursache et al., 2017), antiulcer (Xing et al., 2002), anti-atherogenic (Basu et al., 2007), cardioprotective and anticancer (Olas, 2016; Olas et al., 2018). Vitamins and essential polyunsaturated fatty acids of sea buckthorn oils are known to have several physiological functioning in human systems and antioxidant,

antibacterial antiatherogenic, and cardioprotective activities (Burčová et al., 2017; Hussain et al., 2013; Lushchak and Semchuk, 2012). Sea buckthorn oil is also used in the treatment of many diseases including removal of toxins from the body (Zielińska and Nowak, 2017), preventing oxidative stress (Zeb and Ullah, 2015), UV-induced ROS generation (Geçotek et al., 2018), and membrane destabilization and chronic inflammation (Dubey et al., 2017), reducing gastric ulcers (Jianfeng Xing, 2012), infections, allergies, and eliminates inflammation (Zielińska and Nowak, 2017), and enhance wound healing activity (Upadhyay et al., 2009). Apart from vitamins and fatty acids, sea buckthorn oils also contain phenolic and flavonoid compounds (Rop et al., 2014), organic acids (Zakynthinos et al., 2016), and other different microelements (Bekker and Glushenkova, 2001). As a result, they are critical in the pharmaceutical, cosmetic, and therapeutic industries.

1.8 Sea buckthorn products and their biological properties

Sea buckthorn berries are too delicate, highly perishable, and commonly used fresh by local people. They are frequently used in many products around the world in fresh, preserved, and dried forms and need to be processed immediately or require cold-chain facilities for preservation. Sea buckthorn products can be classified into dietary supplements, food, and beverage, cosmetics, pharmaceuticals, etc. Nowadays, sea buckthorn berries are being domesticated by various manufacturers. Plenty of different nutritional and pharmaceutical market products such as oil, digestive support herbal candy, oil capsules, and immune-enhancing ingredients are available (Patel et al., 2012). They are widely used in oils, juice, and teas for various health issues. They are also used in food product development as an ingredient in food product formulation to impart the food's desirable aroma, taste, consistency, and antioxidant activity. Additionally, the use of sea

buckthorn in feed products is also accustomed to derives into a higher quality final product (e.g. meat quality, egg quality) (Vilas-Franquesa et al., 2020). In India, Defence Food Research Laboratory produces various sea buckthorn-based products like bakery products, jelly, health drinks, wine, food colorants, and yogurt. There are also different animal feeds from sea buckthorn byproducts.

Sea buckthorn leaves are hardly used in food production because they have not been used significantly as food and food supplements in specific areas of the world (i.e. Europe). However, attempts are made to introduce the scope and procedure of Novel Food Regulation in European Union to use sea buckthorn leaves as food, food supplement, or spice (Kauppinen, 2017). The leaves are made into sea buckthorn tea (Vilas-Franquesa et al., 2020) or aqueous extracts because of their potent antioxidant, antibacterial, and cytoprotective effects (Upadhyay et al., 2010). Indian Defence Institute of High Altitude Research industrialized several antioxidant-rich products from berries and leaves of sea buckthorn to combat high altitude-related oxidative damage.

1.9 Extraction of bioactive compounds

The initial stage of utilizing sea buckthorn as a functional food and pharmaceutical ingredient frequently involves extracting, separating, and isolating bioactive components from plant tissue. Some parts of the sea buckthorn fruit, like the seed oil, are characterized by high medicinal value and are not directly edible. Likewise, sea buckthorn leaves are known for their nutritional and pharmacological importance but are not recognized as edible food. The utilization of either edible or non-edible parts of the plant requires the development of an efficient, effective, and selective method for the extraction and isolation of natural bioactive compounds. The extraction yield and constituents of the extract are dependent on different factors such as extraction methods,

procedures, temperature and time, and the type of solvent. The method of extraction may vary depending on the biomolecules of interest. The most prevalent methods for extraction of oils and aromatic compounds from sea buckthorn berries include solvent extraction, mechanical cold pressing, and hydrodistillation techniques (water distillation, steam distillation, and water and steam distillation). While, maceration, hot continuous (Soxhlet), aqueous-alcoholic, microwave-assisted, and ultrasound extractions are all common methods for extracting polyphenolic components from sea buckthorn leaves. The most extensively used extraction method is standard Soxhlet extraction with an organic solvent.

1.9.1 Conventional Soxhlet extraction

Soxhlet extraction is one of the most widely used extraction methods which is still used extensively. It has been for extracting valuable bioactive compounds from various natural sources. Soxhlet extraction assembly can be considered as a batch system when solvent acts stepwise, however, assembly bears continuous character when the solvent is recirculated through the sample. The selection of the solvent is crucial for solvent extraction and it should be based on solubility, selectivity, and cost. Solvents with different polarities are used in the assembly. The extraction begins with the low polar solvent and completes with the high polar solvent. The most commonly used solvents are n-hexane, chloroform, ethyl acetate, acetone, ethanol, methanol, ethanol, and water. The former two solvents are targeted for oil and fat-soluble compounds like those used in the case of sea buckthorn berries. The other moderately polar and strongly polar solvents are used to extract phenolic and flavonoid compounds from the leaves.

Ahmad and Ali, (2013) have reported that acetone extract of *Hippophae rhamnoides* L. leaves offered the highest extraction yield with higher antimicrobial activity than aqueous, methanolic,

and ethanolic extracts. Upadhyay et al., (2010) indicated that aqueous and ethanolic extract of *Hippophae rhamnoides* L. leaves exhibited potent antioxidant activity when analyzed by DPPH, ABTS, and FRAP assay. In another study, the total phenolic content and antioxidant capacity of *Hippophae rhamnoides* L. leaves extracts (water, methanol, acidic 50% methanol, 70% acetone, acidic 50% methanol, and 70% acetone) were compared, and in general, the 70% acetone and acidic 50% methanol extract was found to contain significantly higher total phenolic content than other organic solvents. A positive correlation exists between phenolic concentration and antioxidant activity (Korekar et al., 2011). The total phenolic content of extracts of *Hippophae rhamnoides* L. leaves obtained by microwave (MAE) and conventional (CSE) extraction in ethanol:water solvent showed no significant difference, whereas MAE extracts exhibited higher antioxidant activity than CSE (Galan et al., 2017). The total phenolic and flavonoid content and the antioxidant and antibacterial activity of sea buckthorn berries and leaves extracts are highlighted in **Table 1.2**.

1.9.2 Successive extraction

Successive extraction is a typical extraction approach that involves a succession of extractions with increasing solvents polarity from nonpolar (hexane) to polar (water) to ensure that all phytochemicals with a wide polarity range are exhaustively extracted. The successive exhaustive extraction technique effectively extracts all of the polar and nonpolar metabolites with antibacterial and antioxidant effects (Ngouana et al., 2021). The successive extraction method ensures the extraction of primary metabolites (chlorophyll pigments, carotenoids) as well as secondary metabolites (phenols, flavonoids, and alkaloids). Michel et al., (2012) fractionated ethanol extracts of sea buckthorn leaves by liquid-liquid extraction into hexane fraction (HF), ethyl acetate fraction

Table 1.2: Summary of previously published reports on total phenolic content, antioxidant and antibacterial properties of sea buckthorn extracts

Type of extract	Variety	Origin	TPC (mg/g)	TFC (mg/g)	AOA (DPPH assay)	MIC ($\mu\text{g/mL}$)	References
Whole berry extract							
Methanol	<i>H. rhamnoides</i>	Iran	20.78-34.6 ¹	0.98-2.8 ¹	-	-	Kuhkheil et al., (2017)
Ethanol	<i>H. rhamnoides</i>	India	4.9 ¹	-	8.33 (TEAC) ¹	-	Sharma et al., (2008)
80% Methanol	<i>H. rhamnoides</i>	Byelorussia	8.82-14.42 ¹	-	-	-	Zadernowski et al., (2005)
Ethanol:water:acetic acid (70:30:1(v/v/v))	<i>H. rhamnoides</i>	Finland	0.77 -0.86 ²	-	-	-	Tian et al., (2017)
Leaves extract							
Methanol	<i>H. salicifolia</i>	India	98.7 ³	-	-	250	(Saikia and Handique, 2013)
Acetone	<i>H. salicifolia</i>	India	64.6 ³	-	-	250	
chloroform	<i>H. salicifolia</i>	India	42.4 ³	-	-	250	
Petroleum ether	<i>H. salicifolia</i>	India	25.9 ³	-	-	ND	
Ethanol	<i>H. rhamnoides</i>	-	9.7 ^{1,a}	3.12-21 ^{1,b}	37.16(TEAC) ^{1,a}	-	Sharma et al., (2008) ^a , Tsering Stobdan, et al. (2011) ^b
Aqueous extract	<i>H. rhamnoides</i>	India	40.49 ¹	14.90 ¹	109.03(TEAC) ¹	-	Upadhyay et al., (2010)
Hydroalcoholic extract	<i>H. rhamnoides</i>	India	56.28 ¹	20.76 ¹	143.21(TEAC) ¹	-	Upadhyay et al., (2010)
Ethanol:water:acetic acid(70:30:1(v/v/v))	<i>H. rhamnoides</i>	Finland	60.47-78.56 ²	-	-	-	Tian et al., (2017)
Water	<i>H. rhamnoides</i>	Baekjangaeng Co.	70.68 ³	-	-	-	(Kim et al., 2017)
LCE			245.65 ¹	-	-	-	(Kumar et al., 2013)
HF			197.33 ¹				
HAF			319.33 ¹				
WF			206 ¹				

AOA – Antioxidant activity, TPC- total phenolic content, TFC- total flavonoid content, TEAC - trolox equivalent antioxidant capacity/g of plant material, superscripts 1,2, and 3 refer to results per g of dry weight, fresh weight, and extract, respectively; Leaves crude extract (LCE): an extract obtained by maceration using 70% ethanol, LCE was successively extracted with water, hexane, and ethyl acetate. Phenolic rich fraction (PRF) is ethyl acetate fraction, MIC $\mu\text{g/MI}$ for *B. subtilis*.

(EAF), and water fraction (WF). The major phenolic and tannin compounds contained in the crude ethanol extract are established in WF, which has higher antimicrobial and antioxidant activity than EAF.

1.9.3 Supercritical carbon dioxide extraction

Supercritical carbon dioxide (SC-CO₂) is a non-toxic, abundantly accessible, eco-friendly alternative approach that allows quicker extraction at a reduced temperature and provides solvent-free extract. SC-CO₂ is a good solvent for the extraction of heat-sensitive compounds due to its low critical temperature (31 °C) and pressure (73.82 bar). Pressure and temperature are the essential parameters to tune the solvating properties of SC-CO₂ by altering its density and diffusivity. SC-CO₂ extraction's efficiency depends on the solubility of the target compound, plant material, moisture content, particle size, cosolvents, and working conditions. Optimization of pressure, temperature, and CO₂ flow rate is crucial for SC-CO₂ extraction of oil. The optimization of SC-CO₂ extraction to maximize the tocopherol, β-carotene, and antioxidant activity of the *Hippophae rhamnoides* berry oil has been reported in the range of 27.6-34.5 MPa, 34-44 °C, 17 L/hr (CO₂ flow rate), and 80-82 min (Kagliwal et al., 2012; Xu et al., 2008). Pure CO₂, on the other hand, is non-polar and is ineffective in extracting polar polyphenolic and large molecular mass compounds. Therefore, the cosolvent is used as a modifier and/or entrainer to possibly augment the solvating power of SC-CO₂ for the extraction of polar molecules (Herrero et al., 2006). Since ethanol is generally regarded as safe, it is often chosen as a cosolvent for SC-CO₂ extraction of polyphenols from vegetable matrices. SC-CO₂ extract of sea buckthorn leaves is reported to exhibit adjuvant activity by effectively enhancing antibody and cell-mediated immunity in response to inactivated rabies antigen (Jayashankar et al., 2017, 2016). Several reports

are available on SC-CO₂ extraction of isorhamnetin (Jayashankar et al., 2014), oleoresin, fat-soluble vitamins, carotenoids (Sajfrtova and Sovova, 2012), and flavonoids (Ghatnur et al., 2012) from the leaves of *H. rhamnoides*. Sajfrtova and Sovova (2012) studied the SC-CO₂ extraction of oleoresin, fat-soluble vitamins, and carotenoids from sea buckthorn leaves (*H. rhamnoides* L.) in the range of 40-60 °C temperature, 20-28 MPa pressure, and 0-6.9% w/w co-solvent. Previous reports on SC-CO₂ extraction of the berries and leaves of sea buckthorn are presented in **Table 1.3**.

1.10 Antioxidant and antibacterial properties of sea buckthorn extract

An oxidation-reduction reaction is one of the metabolic biochemical reactions which contributes to several functions in cellular respiration that provides cellular energy. Oxygen is attributed to the formation of numerous chemical compounds known as reactive oxygen species that causes oxidative stress and may destroy or kill body cells. Antioxidants defend cells from damage triggered by oxidative stress. Antioxidants are bioactive substances that inhibit free radical-induced tissue damage by averting the formation of radicals, scavenging them, or by endorsing their disintegration. The functioning modes of antioxidants are related to scavenging free radicals, chelating transition-metal involved in free radical production, and inhibiting the enzymes participating in free radical generation (Halliwell et al., 2000). Extracts obtained by conventional Soxhlet and SC-CO₂ extraction from the leaves and berries of sea buckthorn have been investigated for their antioxidant and antimicrobial properties.

The antioxidant property of extracts is mainly due to phenolic and flavonoid compounds, carotenoids, and tocopherols (Kagliwal et al., 2012; Korekar et al., 2011; Xu et al., 2008). The antioxidant potency and microbial inhibitory characteristics of phenols are related to the site(s)

Table 1.3: Review of literature review on SC CO₂ extraction from sea buckthorn berries and leaves

Plant material	Range of parameters	Optimum condition	Response	% yield (recovery)	Reference
<i>H. rhamnoides</i> berries	Particle size (340 µm), Sample = 25g CO ₂ flow rate 10 g/min, T = 35-55 °C P =15-35 MPa, t = 30-90 min	T = 44 °C P =34.5 MPa t = 80min	Tocopherol Carotene EC50 (DPPH assay)	85.15% 71.73% 29.02mg/ml	(Kagliwal et al., 2012)
<i>H. rhamnoides</i> berries	Sample = 300 g, T = 40-60°C, P = 20-40 MPa, t = 30-90 min, CO ₂ = 10-20 L/hr	T= 34.5 °C P = 27.6 Mpa t = 82 minutes CO ₂ = 17 L/hr	Oil yield Vitamin E Carotenoid	620 mg/kg (96.5%) 288.7 mg/kg (125.6%) 620 mg/kg dry berry (98.7%)	(Xu et al., 2008)
<i>H. rhamnoides</i> berries	Sample~0.650 kg, T=34.51 °C, P=27.6 MPa, t= 82.0 min CO ₂ =22.93 kg/h		Oil Carotenoids	121.10 g /kg dried berries 4517.54 mg/kg dried berries.	(Mihalcea et al., 2017)
<i>H. rhamnoides</i> seed	Particle size of 225µm, Sample =25 g CO ₂ flow rate 10g/min, T = 35-55 °C P =15-35MPa, t = 30-90 min	T = 35 °C P =30.5 MPa t= 90 min	Tocopherol Carotene EC50	77.2% 75.5% 49.9 mg/ml	(Kagliwal et al., 2011)
<i>H. rhamnoides</i> seed	Sample = 7g, T = 40-80 °C, P = 15–60 MPa, Time = 9 h	T = 40 °C, P = 15 MPa	Oil yield β-sitosterol	99.3–109.3 mg/g 0.31 mg/g (0.5%)	(Sajfrtová et al., 2010)
<i>H. rhamnoides</i> seed	Sample 25 g, Sample size-225 µm, CO ₂ =10 g/min, T=60 and 90 min, 2-propanol 30%, T=35 °C, P = 10 and 40 MPa	T= 35 °C P= 40 MPa T=60 min	Tocopherol Carotene EC50	77.2% 75.5% 49.9 mg/mL	(Kagliwal et al., 2011)
<i>H. rhamnoides</i> pomace	T= 40 °C, 60 °C & 80 °C P= 30 MPa , 38 MPa & 46MPa	T= 60 °C P = 46 MPa	Carotene Tocopherol	180 mg/kg 450 mg/kg	(Cossuta et al., 2007)
<i>H. rhamnoides</i> leaves	Sample= 10 g, P= 20-28 MPa T= 40-60 °C, Ethanol concentration in CO ₂ = 0-6.9 % w/w, CO ₂ = 0.5 g/min	P= 28 MPa T= 60 °C Ethanol in CO ₂ =6.9%	Yield	91.1 mg/g leaves ⁻¹	(Sajfrtova and Sovova, 2012)

T – temperature, P – pressure, t – time, EC50 - the extract concentration required to scavenge 50% of radicals in vitro, DPPH - 1,1-

Diphenyl-2-picrylhydrazyl radical assay.

and the number of conjugated hydroxyl groups. Toxicity to microorganisms increases with hydroxylation, with highly oxidized phenols inhibiting more. Phenolic compounds are thought to be toxic to microorganisms because of the inhibition of enzymes by oxidized compounds, probably due to the reaction between sulfhydryl groups or through more nonspecific interactions and the proteins (Cowan, 1999; Rice-Evans et al., 1996). Extracts from the berries and leaves of sea buckthorn are reported to act against the growth of human and food pathogen bacterial strains *Listeria monocytogenes*, *Staphylococcus aureus*, *Bacillus cereus*, *Escherichia coli*, *Salmonella enterica* sv. Typhimurium, *Pseudomonas aeruginosa*, *Enterobacter aerogenes*, and *Klebsiella pneumonia* (Saikia and Handique, 2013; Tian et al., 2018). Many plant resources have also been employed to create diverse metal nanoparticles because plant metabolites have reducing potential.

1.11 Biosynthesis of silver nanoparticles from sea buckthorn extract

Nanotechnology is an important area of modern research dealing with particle structure design, synthesis, and manipulation. It has a wide range of applications in cosmetics, health care, environmental health, food and feed, mechanics, biomedical sciences, optics, chemical industries, space industries, energy science, optoelectronics, catalysis, and drug-gene delivery, etc. Nanoparticles are made of several noble metals like Au, Fe, Ag, Pd, Zn, etc., in the order of 100 nm or less. Among numerous metallic nanoparticles, silver nanoparticles have received considerable attention for their effective antiviral, antioxidant, and antimicrobial activity (Banerjee and Narendhirakannan, 2011; Haider and Kang, 2014; Singh et al., 2018).

Although NPs can be synthesized through a range of conventional procedures such as chemical reduction, ion sputtering, sol-gel, etc, green routes like plants and microorganisms are

environmentally affable and cost-effective. Plant extract-mediated Ag NPs synthesis is a safe, cheap, and eco-friendly method and is free of hazardous material (Padalia et al., 2015). Normally, a plant extract-mediated bioreduction involves mixing the plant extract with an aqueous solution of the appropriate metal salt (Ahmed et al., 2016b).

Table 1.4 shows a literature review on Ag NP synthesis from various plant extracts. Various researchers reported that phytochemicals such as phenols, flavonoids, proteins, carbohydrates, glycosides, tocopherols, and lipids are actively involved in the Ag NP synthesis process as a bio-reducing agent. Biomolecules are also acting as bio-capping and efficiently stabilize the Ag NPs (Riaz et al., 2021; Sharma and Deswal, 2018; Sivakumar et al., 2012). Sea Buckthorn is a rich source of bioactive compounds such as; vitamins, phenols, lipids, tocopherols, carotenoids, phytosterols, omega-3 fatty acids, and other volatile compounds (Pop et al., 2013; Stobdan et al., 2010; Vuorinen et al., 2015). Due to their redox properties, these bioactive compounds can neutralize free radicals and avert oxidative stress-induced cardiovascular and other degenerative diseases like cancer (Singh et al., 2018).

The optimization, characterization, antioxidant and antibacterial activities of the bioinspired syntheses of silver, gold, and palladium nanoparticles using *Hippophae rhamnoides* have been reported (Ahmad et al., 2013; Nasrollahzadeh et al., 2014; Sharma and Deswal, 2018; Siakavella et al., 2020). A detailed review of literature on the optimization of silver nanoparticle synthesis is presented in **Table 1.5**.

Table 1.4: A literature review on Ag NP synthesis from various plants

Plant extracts	Parameters	Biomolecules involved	NP	Size	Shape	Reference
<i>H. rhamnoides</i> berries	0.3 mM HAuCl ₄ .3H ₂ O + 3 mL Aq extract	flavonoids	Au	55± 4.5 nm	Anisotropic/nano triangles	(Sharma and Deswal, 2018)
<i>H. rhamnoides</i> leaves	0.3 mM HAuCl ₄ .3H ₂ O + 0.3 mL Aq extract	polyphenolics	Au	27±3.2 nm	monodispersed spherical	(Sharma and Deswal, 2018)
<i>H. rhamnoides</i> leaves	50 mL 0.003 M PdCl ₂ + 10 mL extract	flavonoid	Pd	5 ± 2.5 nm	spherical morphology	(Nasrollahzadeh et al., 2014)
<i>Lantana camara</i> fruit	90 mL (1 mM) AgNO ₃ + 10 mL extract	flavonoids, carbohydrates glycosides	Ag	12.55 to 12.99 nm	spherical	(Sivakumar et al., 2012)
<i>Chaenomeles sinensis</i> fruit	1 mM HAuCl ₄ .3H ₂ O + extract (70 %) for 10 s at room temp. 1 mM AgNO ₃ + extract (70 %) for 65 min at 80 °C	flavonoids triterpene acids	Au Ag	Au 20–40nm Ag 5–20nm	Au - spherical icosahedral Ag - spherical	(Oh et al., 2018)
<i>Boerhaavia diffusa</i> extract	0.1 M AgNO ₃ (50 mL) + extract (5 mg/mL) at 100 °C	Phenols	Ag	25 nm	spherical	(Kumar et al., 2014)
<i>Azadirachta indica</i> leaf extract	1 mM - 5 mM AgNO ₃ (10 mL) + 1 - 5 mL extract	flavonoids terpenoids	Ag	34 nm	spherical	(Ahmed et al., 2016b)
Olive leaf extract	1 mM AgNO ₃ (10 mL) + 0.2 - 9 mL extract	hydroxyl carboxylate	Ag	20–25 nm	spherical	(Khalil et al., 2014)
Magnolia leaves	1 mM AgNO ₃ (190 mL) + 10 mL extract	-	Ag	15 to 50 nm	spherical	(Song and Kim, 2009)

Table 1.5: Review of literature on the optimization of silver nanoparticle synthesis

Extracts	Parameters	Experimental design	Responses	Optimized condition	Size	Reference
<i>H. rhamnoides</i> leaves	AgNO ₃ conc. = 0.25, 0.5, 0.75, 1 and 2 mM T = 25, 35, 45, 55, 65, 75 and 85°C pH = 4, 5, 6, 7 and 8 t = 10, 20, 30, 40, 50, 60, and 70 min Extract to AgNO ₃ ratio = 0.5:99.5, 1:99, 2.5:97.5, 5:95 and 10:90	One factor-at-a time	Yield	AgNO ₃ concentration = 1mM T = 75°C pH = 7 incubation time = 1 h extract to AgNO ₃ ratio = 5:95	Highest intensity of UV spectroscopy peak	(Ahmad et al., 2013)
<i>Eucalyptus oleosa</i> leaves	Extract conc. = 1, 3, 5 (%w/w) AgNO ₃ conc. = 1, 5, 10 (mmol/L) Time = 8, 16, 24 h T = 25, 50, 100 °C Response = Size of silver particles	Taguchi Method	Size	1% 10mmol 24hr 100°C	21 nm	(Pourmortazavi et al., 2015)
<i>Aegle marmelos</i> leaves	pH = 5,6,7,8.5 Media = water, Acacia, Reetha, Shikakai T= 10 °C 25 °C 40 °C 55 °C Light = dark. white, blue, red Proportion=AgNO ₃ (HAuCl ₄)/LE 1/0.3, 1/1.5, 1/0.5, 1/1.0	Taguchi Method	Size	Ag NP pH = 7 Media = Acacia T= 55 °C Light = white Proportion= 1/0.3	13 nm spherical	(Rao and Paria, 2015)

1.12 Antibacterial properties of Ag NPs

Silver has the most effective antibacterial activity and is least toxic to animal cells compared to other metals with antimicrobial properties (Ahmed et al., 2016a). Several studies have proved the potent antibacterial action of Ag NPs against various human pathogenic bacteria such as *Bacillus subtilis*, *Staphylococcus aureus*, *Escherichia coli*, and *Pseudomonas aeruginosa* (Abalkhil et al., 2017). Silver-containing materials are used in medicine to reduce infections in burn treatment (Parikh et al., 2005) and arthroplasty (Alt et al., 2004), bacteria colonization on prostheses (Alt et al., 2004), urinary catheters (Rupp et al., 2004), vascular grafts, dental materials (Ohashi et al., 2004), human skin-irritation (Lee and Jeong, 2005), Human immunodeficiency virus (HIV) (Elechiguerra et al., 2005), and SARS-Covid-19 (Jeremiah et al., 2020). The interaction of Ag ions to scavenging oxygen-based free radicals to inhibit bacterial growth is mainly due to the specific surface area of Ag NPs and other physicochemical characteristics such as shape, composition, charge, and solubility (Galocchio et al., 2015; Gurunathan et al., 2009). Sea buckthorn berries and leaf extract-mediated nanoparticles have potent antioxidant and antibacterial properties (Sharma and Deswal, 2018; Siakavella et al., 2020).

2.13 Motivation of the research

Nowadays, the nutritional composition of fruits and vegetables has taken a great deal of interest since the information from numerous clinical trials and epidemiological studies point to the tendency to reduce human disease if diets rich in fruits and vegetables are consumed. The health benefits of phytonutrients in fruits and vegetables to avert the risk of disease are more likely allied to their free radical scavenging and antioxidative properties which provide protection to DNA, RNA, proteins, and lipids from oxidative stress. Sea buckthorn is amongst those plants reported as

a natural source of antioxidants and compounds with antiplatelet activity to prevent and/or cure disorders associated with oxidative stress and changes in platelet activation. As a result, this research is especially motivated to evaluate and characterize sea buckthorn and sea buckthorn components for a variety of therapeutic and dietary goals.

2.14 Knowledge gap

India holds four biodiversity hotspots, of which the Himalayas and Indo-Burma regions are found in the Northeast part of India. The Himalayan region, which includes Northeast India, Bhutan, and the central and eastern parts of Nepal, is home to over 10,000 species of flora, many of which have not been thoroughly investigated yet (Samant et al., 1998). The nutritional and pro-health properties of Indian *H. rhamnoides* L. seeds, pulp, leaves, stems, and roots are extensively documented. Research on *H. salicifolia* species from Northeast India is scarce despite the nutritional and physiological benefits. In addition, despite their nutritional and health benefits, sea buckthorn leaves end up as agricultural waste after harvesting berries. Moreover, the pomace and seeds are also thrown away or utilized as calf feed after the juice extraction. Sea buckthorn is a dioecious species; both its male and female plants coexist in close proximity in the wild. Local people and the scientific community also do not differentiate between these male and female leaves very often. For most of the published research, the gender of the leaves is also not correctly mentioned. There is no evidence of any coactivity of the mixture of male and female sea buckthorn leaves. Characterization of the leaf mixture could aid in utilizing sea buckthorn leaves without prior gender identification, allowing for more efficient use of natural resources. Phytonutrients derived from the leaves mixture could potentially have synergetic effects.

Chapter 1

The amount of phytonutrients in plant extract varies greatly depending on many factors, including the extraction method and type of solvent used for extraction. Bioactive compounds in sea buckthorn berries and leaves are in a wide range of polarities. Identification and evaluation of all extractable biomolecules require exhaustive extraction from non-polar to polar compounds. Based on polarity and solubility differences, few attempts have been undertaken to extract phytochemicals from *H. salicifolia* leaves and berries. Similarly, very few reports in the literature have investigated the composition and bioactivities of phytochemicals from *H. salicifolia* in Northeast India.

Extracting bioactive compounds from sea buckthorn leaves and berries for food and pharmaceutical systems requires an efficient, selective, and environmentally friendly approach. Organic solvents have several disadvantages, including high temperatures that cause thermal destruction of bioactive chemicals, hydrolysis, and the presence of harmful solvent residues in the final product. To overcome these challenges, emerging methods, particularly SC-CO₂ extraction, have been used to extract bioactive compounds from plant resources. SC-CO₂ extraction is a safe, inert, non-toxic, and eco-friendly alternative approach that allows quicker extraction at a reduced temperature and provides a solvent-free product. Nevertheless, pure CO₂ is non-polar and not useful to extract polar and high molecular mass compounds. Employing cosolvent as a modifier and/or entrainer makes the extraction possible by augmenting the fluid density and diffusivity towards polar compounds embedded in the cell wall (Khaw et al., 2017). Ethanol is the most preferred modifier in SC-CO₂ extraction to recover phenolics, flavonoids, tannins, oleoresins, gingerols-rich oleoresin, and triterpenic acids. However, limited information is available on extracting bioactive compounds from *H. salicifolia* leaves using SC-CO₂. Therefore, polyphenol

extraction from *H. salicifolia* leaves using SC-CO₂ needs to be optimized to achieve the highest extraction yield with maximum TPC and the best antioxidant activity.

Supercritical CO₂ is also a viable solvent for extracting oil containing labile unsaturated fatty acids. The most beneficial component of sea buckthorn berries is the oil, which contains more unsaturated fatty acids. It is an excellent source of biologically active phytochemicals such as carotenoids, tocopherols, sterols, saturated, unsaturated fatty acids, and other natural antioxidant substances. Therefore, optimization of the process parameters for extracting *H. salicifolia* berries oil using SC-CO₂ is required to maximize the oil yield, β -carotene, and total tocopherol content. So far, in the literature, there is no report on the optimization and characterization of SC-CO₂ extraction of oil from a less explored variety of *H. salicifolia* berries grown in Northeast India. The active ingredients such as terpenoids, phenols, alkaloids, flavonoids, quinines, or tannins contained in plants have antibacterial and antioxidant abilities and reduce metal salts and stabilize nanoparticles.

Due to this reducing ability of plant metabolites, many plant materials have been used to synthesize various metallic nanoparticles. Plant extract-mediated Ag NPs synthesis is a cheap and eco-friendly technique. Phytochemicals such as phenols, flavonoids, proteins, carbohydrates, glycosides, tocopherols, and lipids are actively implicated as bio-reducing agents and bio-caps to keep Ag NPs stable. Although several earlier authors have addressed the matter of synthesis of gold and silver nanoparticles using plant extracts, studies on the synthesis of silver nanoparticles using successive extracts (methanol and water) of berries and leaves of *Hippophae Salicifolia* are limited. Many studies in the literature have reported using a known volume of crude extract: without quantifying the dry mass composition of the aliquot for the synthesis of nanoparticles. However, by removing the solvent from crude extract, the concentration of plant extract used in

the synthesis of nanoparticles may be controlled. In addition, the antioxidant and antibacterial activities of *Hippophae Salicifolia* extract-mediated silver nanoparticles have not yet been investigated. The shape and size of particles that are known to affect the activities of silver nanoparticles significantly have not been discussed. Based on the state-of-the-art and research gaps discussed above, it is therefore proposed to conduct a detailed and systematic study on the extraction of dietary bioactive components of *Hippophae Salicifolia* berries and leaves using organic solvent and supercritical CO₂, and its application in the synthesis of silver nanoparticles with the following specific objectives:

Objectives of the thesis

- Characterization of the dietary and bioactive properties of berries and leaves of *Hippophae salicifolia*.
- Optimization of supercritical carbon dioxide extraction of polyphenols from *Hippophae salicifolia* leaves and analysis of the extracts.
- Process optimization and characterization of oil extracted from *Hippophae salicifolia* berries using supercritical carbon dioxide.
- Optimization and characterization of *Hippophae salicifolia* berries and leaves extract-mediated silver nanoparticles synthesis and evaluate their antioxidant and antibacterial properties.



MATERIALS AND METHODS







MATERIALS AND METHODS

2.1 Collection of Sea buckthorn berries and leaves

The berries and leaves of sea buckthorn, *Hippophae salicifolia* D. Don variety, were collected from Arunachal Pradesh, Northeast India (Sikkim), during its fruiting season when both plant types can easily be distinguished morphologically. The leaves of male and female plants of sea buckthorn were collected separately. All samples were dried in the shade, milled, and stored in a plastic bag. For physicochemical characterization and subsequent successive extraction studies, an equal mass of powdered leaves from the male and female plants (50%-50% DW) was mixed.

2.2 Chemicals and reagents

HPLC grade methanol, ethanol, acetonitrile, other solvents (hexane, chloroform, ethyl acetate, acetone), and analytical grade chemicals such as glacial acetic acid, phosphoric acid, gallic acid, caffeic acid, ferulic acid, vanillic acid, and p-coumaric acid, quercetin, myricetin, kaempferol, rutin, β -carotene, and α -, δ -, and γ -tocopherols were all of purchased from Merck India Pvt. Ltd. and Himedia. Folin-Ciocalteu reagent was procured from Merck India Pvt. Ltd. DPPH (2, 2-diphenyl-1-picryl- hydrazyl) and ABTS [2, 2'-azino-bis (3-ethylbenzothiazoline-6-sulphonic acid)] were purchased from Sigma Aldrich. Resazurin and bacteriological grade media were bought from Himedia. Carbon dioxide (98% pure) was procured from Assam Air Products, India.

2.3 Bacterial culture

Bacterial cultures of *Staphylococcus aureus* (MTCC 9886), *Micrococcus luteus* (MTCC 2848), *Bacillus subtilis* (MTCC 1133), *Staphylococcus epidermidis* (MTCC 9040), *Enterobacter aerogenes* (MTCC 8558), *Klebsiella pneumonia* (MTCC 4030), *Pseudomonas aeruginosa* (MTCC 8727), and *Escherichia coli* (MTCC 1687) were purchased from Institute of Microbial Technology (Chandigarh, India).

2.4 Physicochemical characterization

2.4.1 Proximate analysis

The moisture and total ash content were estimated according to A.O.A.C method (2012). The powdered sample was dried at 105 ± 1 °C in a pre-weighed crucible and frequently weighed until the weight is constant. The difference between the initial and the final weights gives the moisture content. Total ash was estimated by igniting the sample at 550 °C for 6 h in a muffle furnace. The obtained ash was used to quantify acid-insoluble and water-soluble ash using the methods reported by Bhargava et al., (2013). For acid-insoluble ash determination, 12.5 mL HCl (70 g/L) was added to a test tube that contain 100 mg ash. The tube was immersed in a boiling water bath for 5 min. the solution was then filtered with ashless filter paper and washed out with hot water. The insoluble residual material in the filter paper was dried in a crucible and ignited in a furnace. The ash in a crucible refers to the acid-insoluble ash. Likewise, water-soluble ash was analyzed using 12.5 mL of distilled water instead of HCl.

Volatile matter and fixed carbon content were quantified by the method outlined by Piltz and Law (2007). A dry sample (1 g) was combusted at 900 °C for 7 min in a crucible that is tightly covered with a lid. After combusting, the crucible was cooled and re-weighed. The difference between

Chapter 2

weights gives the amount of volatile matter. The fixed carbon content was computed from the combustible residue.

2.4.2 Ultimate analysis

The carbon (C), hydrogen (H), nitrogen (N), sulfur (S), and oxygen (O) analyses were carried out using CHNSO analyzer (Make: Eurovector, Model: EA3000). A dried sample (1 mg) was used for C, H, N, and S percentage composition analysis. The percentage of O was calculated by difference.

2.4.3 Elemental composition

The finely powdered dry sample was mounted on a carbon tape and analyzed at different magnifications to determine the compositional elements using Field Emission Scanning Electron Microscope (FESEM) (Make: Zeiss, Model: Sigma 300).

2.4.4 Total soluble sugar

The total soluble sugar content of the samples was evaluated using the method described by Sadasivam & Manickam, (2008). A sample of 10 mg sample was hydrolyzed with 5mL HCl (2.5 N) at 100 °C for 3 h. After cooling, it was neutralized by Na₂CO₃ powder until the effervescence ceased. The volume of the solution was adjusted to 50 mL and centrifuged at 10,000 rpm. A chilled supernatant of 1 mL and 4 mL of ice-cold Anthrone reagent were mixed and heated in a water bath at 100 °C for 8 min. The mixture was rapidly cooled using running water and the absorbance was measured at 630 nm. Different glucose concentrations (1-5 µg/mL) were used to establish a calibration curve ($R^2 > 0.99$), and the total soluble sugar and reducing sugar contents were

extrapolated from the curve. The total soluble sugar and reducing sugar were expressed in mg glucose equivalent (mg GE) per gram (g) of the dry sample.

2.4.5 Reducing sugar

The amount of reduced sugar was quantified using the procedure described by Sadasivam and Manickam, (2008). A powdered sample of 100 mg was dispersed in 2.5 mL of 80% methanol. Reducing sugar was extracted twice by heating the mixture in a water bath at 65 °C for 10 min. After cooling the mixture, it was centrifuged at 10,000 rpm for 10 min, and the liquor (supernatant) was collected. Then, the solvent was removed from the supernatant and dried in an oven. The dried matter obtained from the supernatant refers to the reducing sugar. The reducing sugar was re-dissolved in distilled water. The reducing sugar solution (0.2 mL) and alkaline copper tartrate (1mL) were mixed in a test tube. The mixture was heated in boiling water for 10 min. After cooling the mixture with running tap water, 1 mL arsenomolybdate reagent was added to the solution. The volume was adjusted to 10 mL and incubated for 10 min before measuring the absorbance at 620 nm.

2.4.6 Non-reducing sugar

The concentration of non-reducing sugar in the berries and the leaves of sea buckthorn was determined by taking the difference between total sugar and reducing sugar.

2.4.7 Total protein content

Total crude protein was determined by Lowry's method (Lowry et al.,1951). A powdered sample of 300 mg was defatted by maceration for 24 h using n-hexane. The protein was extracted from

Chapter 2

the dry defatted samples with 5 mL extraction buffer (a mixture of 1M TrisHCl (5 mL), glycerol (1 mL), ethanol (1 mL), and 43 mL distilled water) at 6.8 PH and 4 °C for 14 h. A volume of 0.2 mL extracted protein was mixed with a 2mL alkaline copper sulfate reagent. After 10 min, 1 N Folin-Ciocalteu reagent (0.2 mL) was added to the mixture, and it was incubated in the dark for another 30 min at room temperature. The absorbance of the solution was measured at 660 nm using a UV-vis spectrophotometer. Various concentrations (10-50 µg/mL) of bovine serum albumin solution were used to plot the calibration curve, and protein content was extrapolated from the curve. Total protein content was expressed in mg bovine serum albumin equivalent (BSAE) per gram (g) of dry sample.

2.4.8 Vitamin C analysis

Vitamin C was quantified according to the protocol elaborated by Arimboor et al., (2006) using HPLC (Shimadzu Corporation, Kyoto, Japan) equipped with a C-18 column and PDA detector set at 246 nm. Vitamin C was extracted by homogenizing a 0.5 g sample in 0.01 M meta-phosphoric acid (10 mL) and centrifuging at 10,000 rpm for 10 min (repeated six times). The supernatant was filtered through a 45 µm filter (Axiva) and subjected to HPLC analysis. The mobile phase was 3.7 mmol/L phosphate buffer (PH 4) with a 1 mL/min flow rate. A 20 µL was the injection volume. Various ascorbic acid concentrations (1-10 µg/mL) were used to establish a calibration curve ($R^2 > 0.99$), and quantification was done by comparing the retention times of the peaks of the sample with known standards.

2.4.9 Total tannin content

The total tannin content in the samples was determined by the method elaborated by Polshettiwar et al., (2007). Tannin was extracted from a 500 mg sample using 50% methanol. The mixture was kept in the water bath at 95 °C for 10 min, followed by cooling and centrifugation. The supernatant was collected and its volume was adjusted to 10 mL. After diluting the tannin extract (100 µL) with distilled water (900 µL), it was mixed with 5 mL saturated sodium carbonate solution and kept at room temperature for 10 min. Finally, it was vigorously mixed with 0.5 mL, 1N Folin-Ciocalteu reagent and incubated in the dark for 30 min before measuring the absorbance at 700 nm. Various concentrations of tannic acid solutions (40-200 µg/mL) were used to establish a calibration curve. Tannin was quantified in mg tannic acid equivalent (mg TAE) per gram (g) of dry sample.

2.5 Extraction experiments

2.5.1 Successive Soxhlet extraction

The powdered samples (berries and the mixture of leaves) were successively extracted using *n*-hexane, chloroform, ethyl acetate, acetone, methanol, and water, respectively, for 6 to 24 h until the solvent in the siphon tube is clear. At first, oil and nonpolar compounds were extracted by *n*-hexane. After the extraction is completed, the raffinate was dried in an oven and extracted again using chloroform. Likewise, subsequent extraction of the raffinate was carried out using ethyl acetate, acetone, methanol, and water. The solvent was removed from each extract using a vacuum rotary evaporator. The extraction yield from each solvent was calculated using equation (2.1). Extracts were collected in separate amber glass vials and stored in a fridge (4 °C).

$$\text{Yield} = \frac{\text{Weight of extract}}{\text{Weight of sample}} \times 100\% \quad (2.1)$$

2.5.2 Supercritical CO₂ extraction

The leaves and berries of sea buckthorn were also extracted using supercritical CO₂ (SC-CO₂). The leaves and berries of sea buckthorn powder were sieved to find a powder of average particle size ranging from 60 to 40 µm mesh size and the moisture content of the samples was determined before extraction. Sample preparation and extraction methods for SC-CO₂ extraction of the leaves and berries powder were different. For the leaves, ethanol was used as a cosolvent (modifier) as well as an entrainer to support the extraction of polar compounds. In this context, cosolvent (modifier) is defined as a solvent mixed with SC-CO₂, while an entrainer is a solvent used to soak the sample. On the other hand, SC-CO₂ extraction of oil from the berries powder was performed by using only CO₂.

2.5.2.1 SC-CO₂ extraction of polyphenols from sea buckthorn leaves

In the preliminary studies, conventional Soxhlet extraction of the leaf from the female (FL) and male (ML) plants of *H. salicifolia* was performed separately using ethanol. The extracts obtained from each leaf sample were compared in terms of yield of extraction, TPC, and antioxidant activity (IC₅₀). Based on these criteria, the extract from the female plant (FL) was found to be better than the male. Results are discussed in the result and discussion section (Section 4.3.1). In the next step, SC-CO₂ extraction of FL leaves was carried out at the minimal extraction variables employed in the optimization study (18 MPa, 40°C, 10 g/min CO₂ flow rate, and 1% cosolvent). The extraction time was 1 h. It has been noticed that SC-CO₂ extract resulted in a much lower yield of extraction, TPC, and antioxidant activity than Soxhlet extract. Thus, an attempt has been made to improve the

yield of extraction, TPC, and antioxidant activity of SC-CO₂ extract by using ethanol as an entrainer by increasing the extraction time.

Effect of entrainer: Before starting the optimization study, a single parameter optimization process was followed to decide the optimum FL powder-to-entrainer ratios (w/v). The effect of entrainment (ethanol) on SC-CO₂ extraction was performed at minimum limits of extraction variables used in the optimization study. The leaves sample for SC-CO₂ extraction was prepared by soaking 50 g (DW) of powdered leaves overnight in entrainer (ethanol) at powder-to-entrainer ratios of 1:0.5, 1:1, and 1:1.5 (w/v) at room temperature (25 ± 1 °C). The yield of extraction, the TPC, and the antioxidant activity of extracts were studied and the powder-to-entrainer ratio of FL(1:1) resulted in a higher yield of extraction with higher TPC, and lower IC₅₀ value. Therefore, FL(1:1) was selected for the optimization study. Results are discussed in the result and discussion section (Section 4.3.1).

Effect of time: After deciding the appropriate powder-to-entrainer ratios (FL(1:1)), the effect of extraction time on the yield of extraction, TPC, and antioxidant activity was also studied at 1 h, 2 h, and 3 h. The extract obtained from 2 h extraction time was found to offer a higher yield of extraction with maximum TPC and minimum IC₅₀. Therefore, the time of extraction chosen for the optimization study was 2 h.

2.5.2.2 SC-CO₂ extraction of oil from sea buckthorn berries

Powdered sea buckthorn berries (20 g) were uniformly mixed with spherical glass beads (2 mm diameters) with a 1:4 (w/w) ratio. Glass beads were used to increase the space occupied by the

sample inside the extraction vessel, to enhance the diffusion surface area of SC-CO₂ into the sample matrix, and to minimize the caking possibility.

2.5.3 Supercritical CO₂ extraction procedures

The SC-CO₂ extraction of samples was carried out using a supercritical fluid extractor, SFE 500 Systems (Waters, USA) equipped with a 500 mL extraction vessel and separator. An electric heating coil was used to heat the extractor vessels and the temperature was regulated by using thermostats. Extraction pressure, temperature, and CO₂ flow rate were monitored by program logic control. The sample was packed in a double-layered pocket-size muslin cloth and loaded into the high-pressure extraction vessel. The vessel was tightly closed with a screw equipped with a pressure gauge. Before the start of the extraction, the CO₂ pump, ABPR, and the heat exchanger were all kept in switched-on mode. The shut-off valve of the CO₂ cylinder was open and liquid CO₂ was allowed to flow through the chiller to the CO₂ pump and reached the heat exchanger before the extraction vessel. In the case of polyphenols extraction from the leaves, cosolvent and CO₂ were mixed before reaching the heat exchanger. The heat exchanger and the extraction vessel were kept at desired temperature and pressure that keeps the solvent in a supercritical state. The solvent carrying the extract flows through the automated back pressure regulator (that maintains the solvent in the supercritical state) and while exiting, the system pressure is reduced to atmospheric conditions, causing the solvent to lose its solvating power. The extract was continuously precipitated into the separator (cyclone) held at 30 °C during the entire extraction time (2 h). Later, the extract was collected in the amber-colored vials, weighed to obtain the yield of extraction, and stored in a freezer (-20 °C) until the subsequent analysis.

2.5.4 Experimental design for polyphenol extraction

The combined effect of independent variables on the yield of extraction, TPC, and IC50 was judged by RSM. Four highly responsible variables: X_1 , pressure (MPa); X_2 , temperature ($^{\circ}\text{C}$); X_3 , CO_2 flow rate (g/min); and X_4 , amount of cosolvent (%) were chosen to study their effect. The range of independent variables used in the study was: temperature (X_1), 40-60 $^{\circ}\text{C}$, pressure (X_2), 180-320 MPa, CO_2 flow rate (X_3), 10-20 g/min, and amount of cosolvent (X_4), 1-3%. The lower and upper limits of variables were decided based on published literature (Ghatnur et al., 2012; Maran et al., 2015; Rodrigues et al., 2018; Sajfrtova and Sovova, 2012). Design expert was used for devising the full factorial CCD experimental design and also for analysis and processing of the data.

2.5.5 Experimental design for oil extraction from sea buckthorn berries

Optimization of process variables for SC- CO_2 extraction of sea buckthorn berry oil was performed using Central Composite Design (CCD). Optimization of extraction variables: X_1 - pressure; X_2 - temperature; and X_3 - CO_2 flow rate was carried out to maximize oil yield, β -carotene, and total tocopherol content. The lower and upper permissible limits of each independent variable, X_1 , 150-330 MPa; X_2 , 40-60 $^{\circ}\text{C}$; and X_3 , 10-20 g/min, were established based on published literature (Kagliwal et al., 2012; Xu et al., 2008). A 2^3 full factorial design CCD of three independent variables coded at five levels (-1.682, -1, 0, +1, +1.682) which gave 20 ($2^n + 2n + 6$) experiments: 8-factorial points, 6-axial points, and 6-center points ('n' is the number of independent variables) were used for the optimization study.

2.5.6 ANOVA and model fitting

The extraction behavior was studied based on the experimental runs. The regression coefficient was determined using the design expert software 11.0 trial version to predict each response as a function of independent variables. The independent variables were mathematically related to dependent variables using the following 2nd-order polynomial equation (Eq 2.2):

$$Y = \beta_0 + \sum_{i=1}^4 \beta_i X_i + \sum_{i=1}^4 \beta_{ii} X_{ii}^2 + \sum_{i,j=1}^4 \beta_{ij} X_i X_j \quad (2.2)$$

Where: Y stands for response variables (for polyphenol extraction from the leaves: yield of extraction (%), TPC (mg GAE/g), or IC50 ($\mu\text{g/mL}$); for oil extraction from the berries: (oil yield (%), β -carotene (mg/100 g oil), and tocopherol (mg/100 g oil)); β_i , β_{ii} , and β_{ij} are linear, quadratic, and interaction coefficients, respectively; and X_i and X_j are independent extraction variables. ANOVA was applied to estimate the effect of model coefficients and their interaction on responses in the response surface multiple regression analysis. The best fit and goodness of the model were estimated by a regression coefficient R^2 . The response surface and contour plots were obtained from the fitted quadratic equation generated from regression analysis by varying two of the independent variables at a time while keeping the other(s) at the central point (0).

2.5.7 Soxhlet extraction

Dried powdered sea buckthorn leaves and berries were extracted for 2 h by Soxhlet apparatus using ethanol (at 78 °C) and *n*-hexane (at 69 °C), respectively. After removing the solvent, extracts were kept in a desiccator for 24 h and stored in the refrigerator until analysis. Conventional Soxhlet extracts were used as a control (100%) for SC-CO₂ extraction studies.

2.6 Characterization of extracts

2.6.1 Phytochemical screening

Phytochemical screening was carried out according to the method described by Khandelwal, (2008). The presence of carbohydrates (Benedict's and Barfoed's test), glycosides (Keller-Killiani and Foam test), proteins (Biuret and Precipitation test), amino acids (Ninhydrin test), alkaloids (Dragendorff's and Mayet's test), tannins and phenols (5% FeCl₃ and dilute potassium permanganate solution), and flavonoids (Sulphuric acid and NaOH test) was qualitatively determined in the sea buckthorn berries and leaves extracts.

2.6.2 Fourier transform infrared spectroscopy analysis

The functional groups inherently present in the whole berry and mixtures of leaves and extractives were determined by comparing the vibrational frequencies with respect to percentage transmittance and wave number obtained using Fourier transform infrared red (FTIR) spectrometer "IR Affinity1" (Shimadzu Corporation, Japan). A dry sample and potassium bromide (KBr) at the weight ratio of 1:100 were crushed in a mortar and pestle and compressed into a thin pellet before analyzing using FTIR. Infrared spectra were recorded within the wavenumbers between 4000-400 cm⁻¹, at a resolution of 4 cm⁻¹ and 30 scans per spectrum. Variations in the frequency and baseline corrections were employed with Shimadzu IR solution 1.5 software provided with the spectroscopy.

2.6.3 Total phenolic content (TPC)

Estimation of TPC present in the berries and leaves extracts was carried out by using a method outlined by Sen et al., (2013). Briefly, 0.5 mL extract and 2.5 mL Folin-Ciocalteu reagent (10%)

were thoroughly mixed. Then, 2 mL Na₂CO₃ (2% (w/v)) was poured into the mixture and vortexed. After 20 min of incubation in dark, absorbance was measured against blank at 765 nm. The calibration curve ($R^2 > 0.99$) was plotted using 10-100 µg/mL gallic acid solution. TPC was expressed in mg gallic acid equivalent (mg GAE) per g of extract. The TPC per gram of dry berries and leaves (mg GAE/g DW) of each extract was calculated by multiplying the yield of extraction by TPC per gram of extract using equation (2.3).

$$TPC \text{ (mg GAE/ g DW sample)} = \text{Yield of extraction} \times TPC \text{ (mg GAE/ g extract)} \quad (2.3)$$

Further, for successive Soxhlet extraction studies, the grand total TPC obtained from the entire extraction process was obtained by adding the TPC per gram of dry sample in each extract.

2.6.4 Total flavonoid content (TFC)

TPC in each extract was analyzed according to the protocol reported by Sen et al., (2013). About 0.5 mL sample, 100 µL potassium acetate (1 M), and 100 µL aluminum nitrate (10%) were added into a tube containing 4.3 mL ethanol and vigorously shaken. After 40 min incubation, absorbance was measured at 415 nm. Various concentrations of quercetin solution (10-100 µg/mL) were used to establish a calibration curve. TFC was expressed in mg quercetin equivalent (mg QE) per g of the extract. The TFC per gram of dry berries and leaves (mg QE/g DW), was calculated using equation (2.4).

$$TFC \text{ (mg QE/ g DW sample)} = \text{Yield of extraction} \times TFC \text{ (mg QE/ g extract)} \quad (2.4)$$

For successive Soxhlet extraction studies, the grand total TFC was computed by adding the TFC per gram of dry sample in each extract.

2.6.5 Identification of phenolic and flavonoid compounds by HPLC

Quantification of phenolic (gallic acid, caffeic acid, ferulic acid, vanillic acid, and p-coumaric acid) and flavonoid (quercetin, myricetin, kaempferol, and rutin) compounds in the extracts was carried out using HPLC (Shimadzu Corporation, Kyoto, Japan) equipped with a UV-Vis detector and C18 (250 x 4.6 ID) column. The detection wavelengths were 280 nm for gallic acid, 270 nm for vanillic acid, 296 nm for caffeic acid and ferulic acid, and 310 nm for p-coumaric acid. Quercetin, myricetin, kaempferol, and rutin were detected at 368 nm. The mobile phases for phenolic compound analysis were milli-Q water (63%) and acetonitrile (37%), each with 1% phosphoric acid (flow rate 1 mL/min), while for flavonoids it was a mixture of methanol (40%): acetonitrile (15%): milli-Q water (45%) with 1% glacial acetic acid (flow rate 0.5 mL/min). Extracts were dissolved in HPLC-grade methanol and filtered through a 0.45 µm filter (Axiva). The injection volume was 20 µL. The standard compounds were prepared in the quantification range of 1-100 µg/mL and calibration curves ($R^2 \geq 0.99$) were established.

2.6.6 Limit of detection (LOD) and limit of quantification (LOQ)

LOD (lowest concentration in a sample that can be detected) and LOQ (lowest concentration of analyte that can be determined) were calculated using the formula $LOD = 3.3 \times SD/S$ and $LOQ = 10 \times SD/S$, where SD = standard deviation of response and S = slope of the calibration curve (Alquadeib, 2019).

2.6.7 In-vitro antioxidant activity

The antioxidant potential of the leaves and berries extracts was carried out using DPPH and ABTS analysis. The antioxidant activity of extracts was calculated from the percentage scavenged

Chapter 2

according to equation (2.5). The percentage scavenged was used to calculate the IC₅₀ value of each extract. IC₅₀ is the extract concentration required to scavenge 50% of radicals in vitro. The experimental procedures of DPPH and ABTS assays are briefly described below.

$$\text{Percentage scavenged} = \frac{A_{\text{control}} - A_{\text{sample}}}{A_{\text{control}}} \times 100\% \quad (2.5)$$

Where, A_{control} = Absorbance of control, A_{sample} = Absorbance of sample

2.6.7.1 DPPH assay

The DPPH assay was implemented using the method described by Sen et al., (2013). The DPPH reagent (1 mL, 0.1 mM) was added to a 3 mL extract solution and vigorously vortexed. After incubated at room temperature in dark for 30 min, absorbance was measured at 517 nm. Solvent (3 mL) without extract was used as a control.

2.6.7.2 ABTS assay

The ABTS antioxidant assay was carried out following the protocol reported by Re et al., (1999). ABTS free radical was prepared by mixing 7 mM ABTS solution and 2.45 mM potassium persulfate solutions with a 1:1 ratio followed by 12-16 h of incubation in dark. Before the use, the ABTS free radical solution was diluted with purified water (50-52 mL) until the absorbance at 734 nm was about 0.7 ± 0.05. The ABTS solution was added to a 0.5 mL extract solution. The solution was thoroughly shaken and incubated in a dark for 20 min. Finally, the absorbance was measured at 734 nm. The IC₅₀ values from DPPH and ABTS assays were compared with pure ascorbic acid.

2.6.7.3 Global antioxidant score (GAS)

T-score was used to calculate the GAS value. T-score is calculated by using Equation (2.6):

$$T - \text{score} = (X - \text{min}) / (\text{max} - \text{min}) \quad (2.6)$$

Where, max and min represent the maximum and minimum values of variable X among the investigated extract, respectively (Leeuw et al., 2014). The variables assigned were TPC, TFC, and the percentage scavenged at 50 µg/mL extract concentration in DPPH, and ABTS assay. The percentage scavenged was calculated using equation 2.5.

2.6.8 Antibacterial activity

2.6.8.1 Minimum inhibitory concentration (MIC)

MIC of leaves and berries extracts was estimated through the procedure outlined by Sarker et al., (2007) with slight modifications. The broth used for microbial growth and inoculation was: nutrient broth (for *Bacillus subtilis*, *Micrococcus luteus*, *Staphylococcus epidermis*, *Enterobacteraerogenes*, and *Pseudomonas aeruginosa*); luria broth (for *Escherichia coli* and *Klebsiella pneumonia*); and tripton soy broth (for *Staphylococcus aureus*). An inoculum of 10 µL was subcultured in 5 mL broth and incubated at 30 or 37 °C until the optical density of the culture was 0.50 at 600 nm. The 100 µL culture was serially diluted 10⁵ times in 900 µL broth and the number of colony-forming units per mL (CFU/mL) was quantified. Stoke solutions were prepared by dissolving extracts in dimethyl sulfoxide (DMSO). Subsequently, the extracts were appropriately diluted with doubled autoclaved distilled water to attain the final concentration of 1000 µg/mL in 10% DMSO. The sample was sterilized with a 0.22 µm sterilizing Millipore express filter and serially diluted until the concentrations of extracts were between 1000 µg/mL and 0.98 µg/mL. A 96 well plate was prepared under aseptic conditions. A volume of 30 µL broth, 50 µL sample and 10 µL (about 5 x 10⁶ CFU/mL) of each bacterium were pipetted into the wells. The plate was kept in an incubator at 30 or 37 °C (at the respective bacterium growth temperature) for 12-14 h and 10 µL of 1 mg/mL resazurin indicator solution was added to the wells. The final

Chapter 2

concentration of bacterium in the well was about 5×10^5 CFU/mL. The MIC of each extract was determined with a color change from blue to pink.

2.6.8.2 Zone of inhibition (ZoI)

Agar diffusion assay was applied to quantify the zone of inhibition (ZoI) of extracts using the method outlined by Bauer et al., (1966). A 100 μ L culture of the bacterium was swabbed on the solidified agar surface on a plate. After the culture is being absorbed, three holes (0.5 mm in diameter) were pierced into the surface of the agar. Sterilized solutions of three different extracts each 50 μ L of 1 mg/mL was drained into the holes. The plates were kept in a laminar flow hood until the sample was well diffused into the solidified agar. The plates were incubated with appropriate bacterium growth temperature, and the ZoI was measured after 12 to 14 h of incubation.

2.7 Characterization of oil

2.7.1 β -carotene analysis

Sea buckthorn berry oils extracted using SC-CO₂ (obtained at the optimal extraction condition) and Soxhlet were characterized. The β -carotene content of oils was quantified by the method outlined by Gao et al., (2000). An aliquot of oil sample (100 mg/mL) and 0.5 mL of 5% NaCl were vigorously mixed, and the mixture was centrifuged at 3,000 rpm for 10 min. The supernatant (25 μ L) was suitably diluted in hexane (975 μ L) and the absorbance of the solution was measured at 460 nm using a UV-Visible spectrophotometer (Make: Shimadzu, Singapore; Model: UV-2600). An authentic standard of β -carotene (2-10 μ g/mL) was used to establish a calibration curve ($R^2 \geq 0.99$).

2.7.2 Total tocopherol analysis

Total tocopherol (the sum of three tocopherols; α , γ , and δ -tocopherol) analysis was conducted by using HPLC (Shimadzu Corporation, Kyoto, Japan) coupled with PDA detector and Shim-pack Solar C18 column (5 μ m, 250 \times 4.6 mm ID, 15L03232) (Kagliwal et al., 2011). HPLC grade methanol running at 0.5 mL/min at ambient temperature (25 ± 2 °C) was used as a mobile phase. Tocopherols were detected at 292 nm by injecting 20 μ L of oil sample using a system autosampler. The α , γ , and δ -tocopherol standard compounds run at various concentrations ranging from 10-100 μ g/mL were used to establish a calibration curve ($R^2 \geq 0.99$) for each tocopherol. Oil solutions (1 mg/mL) were prepared in ethanol, followed by a filter with a 0.45 μ m filter (Axiva). The retention time of α , γ , and δ -tocopherols was compared with individual standard compounds. The analysis of each tocopherol was carried out using a linear equation of the standard calibration curves. The total tocopherol was obtained by adding α , γ , and δ -tocopherols.

2.7.3 Fatty acid methyl esters analysis

The fatty acid methyl esters (FAME) composition of oils was analyzed by GC-FID. FAME of each oil was prepared by the method outlined by Morrison and Smith, (1964). An aliquot of oil (10 mg in 1 mL BF3) was sonicated in a screw-capped tube for 15 min using an ultrasonic bath, followed by incubation in an ultra-sonic bath at 100 °C for 30 min. Then milliQ water and HPLC grade hexane, each 2 mL, was vigorously mixed with the oil solution and centrifuged at 3000 rpm for 10 min. The supernatant was carefully pipetted out and poured into the appendroff tube, dried in a vacuum drier, and then analyzed for its FAME composition using GC. The FAME solution was prepared in 1 mL HPLC grade hexane, followed by filtering through a 0.2 μ m filter. FAME

composition was analyzed using Gas chromatography (PerkinElmer Clarus 590) coupled with an FID detector and BPX-70 capillary column. The oven temperature was preset to rise from 100 °C to 240 °C at 3 °C/min, with an initial and final hold of 10 min and 20 min, respectively. Helium was used as a carrier gas at a flow rate of 2 mL/min. The temperature of the injector and the detector was held at 250 °C. FAME composition was quantified by comparing the retention time between sea buckthorn oil samples and the standard (Supelco 37 component FAME mix).

2.7.4 Physico-chemical characterization of oil

2.7.4.1 Refractive index (AOCS Cc 7-25)

The refractive index of the oil sample was measured at 25 °C using a refractometer (Advanced research instrument company, New Delhi). Two or three drops of oil sample were placed on the prism and the prism was closed and allowed to stand for 2 min. The lens and lighting were adjusted to obtain the distinct reading, and the value was recorded from the display.

2.7.4.2 Specific gravity (AOCS Cc 10a-25)

The specific gravity of the oil sample was measured by using a pycnometer. The pycnometer was filled with the oil sample and immersed in a water bath at 25 °C for 30 min. Any oil that has come out of the capillary opening was carefully wiped off. The bottle was taken out of the bath and cleaned thoroughly. The weight was measured after removing the cap of the side arm and the specific gravity of oil was measured as follows.

$$\text{Specific gravity at } 25^{\circ}\text{C} = \frac{(A - B)}{(C - B)} \quad (2.7)$$

Where; A = weight in gm of specific gravity bottle with oil; B = weight in gm of specific gravity bottle; C = weight in gm of specific gravity bottle with water.

2.7.4.3 Saponification value (AOCS Cd 3-35)

About 500 mg of oil was dissolved in 15 mL potassium hydroxide solution in ethanol and refluxed for 1 h until the saponification was complete, as indicated by the appearance of a clear solution. After being cooled, the excess potassium hydroxide in the solution was titrated against 0.5 N hydrochloric acid, using a few droplets of phenolphthalein indicator. Blank was run with a similar procedure. The saponification value in mg KOH/g of the oil was calculated using the following equation.

$$\text{Saponifiable matter} = \frac{56.1 \times (B - S) \times N}{W} \quad (2.8)$$

Where; B - Volume of standard hydrochloric acid required for the blank; S - Volume of standard hydrochloric acid required for the sample; N - Normality of the standard hydrochloric acid; and W - Weight in gm of the oil/fat taken for the test.

2.7.4.4 Unsaponifiable matter (AOCS Ca 6a-40)

About 500 mg oil was dissolved in 50 mL potassium hydroxide solution in ethanol and refluxed until the saponification is complete. The saponified mixture was transferred to a separating funnel, into which 50 mL of petroleum ether was added, shaken vigorously, and allow the layers to separate. The lower layer was extracted again using petroleum ether. The petroleum extract was washed with a hydro-alcoholic solution and distilled water, respectively, and was transferred into a pre-weighed Erlenmeyer flask. The Erlenmeyer flask was kept in a water bath to evaporate the petroleum ether. After the removal of petroleum ether, 2-3 mL acetone was added. To remove the

Chapter 2

last traces of ether, it was dried at 100°C for 30 minutes till constant weight is obtained and the residue was dissolved in 50 mL of hot ethanol which has been neutralized to a phenolphthalein end point. Finally, it was titrated with 0.02 N NaOH. The unsaponifiable matter was calculated using the following equation.

$$\text{Unsaponifiable matter} = \frac{(A - B) \times 100\%}{W} \quad (2.9)$$

Where; A - Weight in g of the residue; B - Weight in g of the free fatty acids in the extract; W - Weight in g of the sample.

2.7.4.5 Peroxide value (AOCS Cd 8-53)

About 100 mg of oil was dissolved in 15 mL of glacial acetic acid:chloroform mixture (3:2) in a stoppered conical flask. A 0.2 mL of saturated potassium iodide solution was added and the solution was kept for 1min in dark with occasional shaking. Then about 30 mL of water was added and it was titrated against 0.1 N sodium thiosulphate solution with vigorous shaking until the yellow color disappeared. Titration was again continued until the blue color disappeared after adding 0.5 mL starch solution. Blank determination was carried out using the same procedure and the peroxide value in mg eq/kg oil was calculated using the following equation (Eq 2.10).

$$\text{Peroxide value} = \frac{(S - B) \times N \times 1000}{W} \quad (2.10)$$

Where; S - volume of sodium thiosulphate used to titrate the oil sample; B - volume of sodium thiosulphate used to titrate the blank; N - Normality of sodium thiosulphate solution.

2.7.4.6 *Acid value (AOCS Cd 3d-63)*

Approximately 100 mg of oil was dissolved in 25 mL ethanol. About 2-3 droplets of phenolphthalein indicator solution were added and the mixture was heated in a water bath at 70 °C for 15 min. The solution was titrated against standard 0.1 N KOH solution in ethanol shaking vigorously during the titration until the color of the solution turned pink. The acid value in mg KOH/g of oil was calculated using equation (2.11).

$$\text{Acid value} = \frac{56.1 \times V \times N}{W} \quad (2.11)$$

Where; V - Volume in ml of potassium hydroxide used; N - Normality of the potassium hydroxide solution; and W - Weight in g of the oil.

2.7.4.7 *Iodine value (AOCS Cd 1-25)*

About 600 mg of oil was vigorously mixed with 25 mL carbon tetrachloride. Wij's solution (25 mL) was added and the solution was swirled until the proper mixing. After keeping the solution in dark at room temperature for 30 min, 15 mL of potassium iodide solution was added, followed by 100 mL distilled water. The solution was titrated against 0.1 N sodium thiosulphate solution, using starch as an indicator until the formed blue color disappears after thorough shaking. The blank was carried out simultaneously. The iodine value of the oil sample was calculated using the following equation (Eq 2.12):

$$\text{Iodine value} = \frac{12.69 (B-S) \times N}{W} \quad (2.12)$$

Where, B, S, N, and W are the volume of standard sodium thiosulphate solution required for the blank, volume of standard sodium thiosulphate solution required for the sample, normality of the standard sodium thiosulphate solution, weight in g of the sample, respectively.

2.7.5 Thermogravimetric analysis

The thermal stability and thermal degradation properties of sea buckthorn berries oil were determined using a thermogravimetric analyzer (Model No.: TG 209 F1 Libra; Make: M/s Netzsch Germany) under a nitrogen atmosphere. Approximately 20 mg of oil sample was weighed in an alumina crucible and heated from 30 to 800 °C at a constant heating rate of 10 °C/min. An inert nitrogen gas (99.9% purity) was used as purge gas at a flow rate of 40 mL/min during the analysis. Further, TGA data were used to find out the activation energy of the sample with the help of Coats-Redfern method. Considering the Arrhenius temperature dependency for a constant heating rate, the Coats-Redfern model for non-isothermal decomposition rate for first-order reaction can be expressed as follow (Eq 2.13).

$$d\alpha/dT = (A/\beta)e^{(-E_a/RT)}(1-\alpha)^n \quad (2.13)$$

where α , T, β , A, E_a , R, and n refer to the degree of decomposition, temperature (K), heating rate (°C/min), frequency factor (1/min), activation energy (J/mol), universal gas constant (8.314 J/mol K), and order of reaction, respectively. The value of α at the appropriate temperature was calculated from TG data using (Eq 2.14):

$$\alpha = (\omega_0 - \omega_T)/(\omega_0 - \omega_f) \quad (2.14)$$

where ω_0 , ω_T , and ω_f are the initial weight, the weight at temperature T, and the final weight, respectively. Assuming first-order reaction ($n = 1$), Eq (2.13) can be solved as:

$$\ln \left[-\ln(1-\alpha)/T^2 \right] = \ln \left[AR/\beta E_a(1-2RT/E_a) \right] - E_a/RT \quad (2.15)$$

The activation energy was obtained from a plot $[\ln(-\ln(1-\alpha)/T^2)]$ against $1/T$ (Eq 2.15), resulting in a straight line of slope $-E_a/R$.

2.7.6 Rheological measurements

Rheological measurements of SC-CO₂ and Soxhlet extracted oils were carried out using an MCR 301 interfacial rheometer (Model No.: Physica MCR 301, Make: Anton Paar, Austria). The flow curves of the samples were studied by plotting shear stress versus shear rate data (shear rate range from 1 s⁻¹ to 1000 s⁻¹ at 25 °C) and were fitted to Bingham plastic model (Eq. 2.16) by using linear regression.

$$\tau = \tau_{oB} + \eta_B \gamma \quad (2.16)$$

where τ , τ_{oB} , η_B , and γ represent shear stress (mPa), Bingham yield stress (mPa), Bingham plastic viscosity (mPa.s), and shear rate (sec⁻¹). Further, the dependence of the viscosity of the oils on shear stress and temperature was investigated. The temperature sweep test was carried out from 5 to 100 °C at a shear rate of 10 s⁻¹. The viscosity versus temperature data was tailored to the Arrhenius equation (Eq. 2.17) and the activation energy of the samples was obtained from the slope of $(\ln \eta)$ versus $1/T$ plot.

$$\eta = A \times e^{(-E_a/RT)} \quad (2.17)$$

where η - viscosity (Pa.s), A - Arrhenius constant (min⁻¹), E_a - flow activation energy (kJ/mol), T - temperature (K), and R - universal gas constant (8.314 J/ mol/K).

2.8 Synthesis of silver nanoparticles

2.8.1 Preparation of plant extract

The leaves (FL) and berries of *Hippophae salicifolia* were successively and exhaustively extracted with methanol and water using the Soxhlet apparatus. After extraction, the solvent was evaporated using a vacuum rotary evaporator and dry extracts were collected in brown vials. Methanol and aqueous extracts of each sample were used to synthesize silver nanoparticles (Ag NPs).

2.8.2 Synthesis Ag NPs

Briefly, a beaker containing a 9.5 mL aqueous solution of AgNO_3 was placed on a heating mantle with a magnetic stirrer (set at 500 rpm). The beaker was covered with aluminum foil as a barrier to light. A volume of 0.5 mL plant extract solution dissolved in Dimethyl sulfoxide (DMSO) was slowly poured into the beaker. The pH of the mixture was adjusted to the required level using 0.1 N NaOH and then, allowed to react. The reduction of Ag^+ to Ag^0 was recognized by the color change of the solution from greenish-yellow to brown. The formation of Ag NPs was further confirmed by UV-Visible spectroscopy.

2.8.3 Preliminary study

Based on the preliminary findings and published literature, the lower and upper bounds of variables were determined as follows. The main purpose of the preliminary study was to determine the minimum concentration of plant extract required for the synthesis of Ag NPs at 0.5 mM AgNO_3 concentration, 7 PH, 30 °C, and 1 h. From the preliminary experiment, it was noticed that 0.5 mg/mL of leaves extract and 1 mg/mL of berries extract were sufficient for the formation Ag NPs. Therefore, the following variables were used in the optimization study: extract concentration (0.5-

2 mg/mL for leaves, 1-4 mg/mL for berries), AgNO₃ concentration (0.5-2 mM), PH (7-11), temperature (30 °C-40 °C), and time (1-100 h).

2.8.4 Parameters optimization

A single parameter optimization technique was followed to optimize the biosynthesis of Ag NPs. The concentration levels for the leaves and the berries extract were 0.5, 1, 1.5, and 2 mg/mL, and 1, 2, 3, and 4 mg/mL, respectively. Initially, the concentration of plant extracts varied in the given range, while other parameters are kept constant (0.5 mM AgNO₃ concentration, 7 pH, 30 °C, 1 h). The variables that give the highest yield of Ag NPs could be easily identified by the height of surface plasmon resonance (SPR) band intensity (Bar et al., 2009). After deciding on the appropriate plant extract concentration, the effect of AgNO₃ concentration (0.5, 1, 1.5, and 2 mM) on the formation of NPs was also studied keeping other variables constant. Similarly, the pH (7, 8, 9, 10, and 11) of the suspensions was optimized at optimal concentrations of the plant extract and AgNO₃ solution. Finally, temperature (30 °C, 40 °C, 50 °C, and 60 °C) and time (0.08-100 h) were optimized simultaneously. The time required for the complete transformation of Ag⁺ to Ag⁰ at a particular temperature was determined from the plot of maximum SPR peak versus reaction time.

2.8.5 Ag NPs yield at optimum condition

Ag NPs were successfully produced at the optimum conditions. Ag NPs suspension was centrifuged for 30 minutes at 10,000 rpm. The settling Ag NPs were collected and re-suspended in distilled water. The solution was then transferred to pre-weighed appendroff tubes and centrifuged again at 3,000 rpm until the supernatant was clear. The supernatant was gently pipetted

out, and the Ag NPs-containing tubes were vacuum-dried. The dried Ag NPs containing appendroff tubes were re-weighed and the mass of Ag NPs was estimated by the difference.

Equation (2.18) was used to compute the yield of Ag NPs at optimum conditions:

$$\text{Yield} = \frac{\text{Weight of silver nanoparticle}}{\text{Weight of silver ion in the solution}} \times 100\% \quad (2.18)$$

Weight of silver nanoparticles - the weight of collected Ag NPs using a centrifuge, and weight of silver ion in the solution - the amount of silver ion employed at optimum condition.

2.9 Characterization of synthesized silver nanoparticles

2.9.1 UV-Visible spectrophotometer

The suspension was scanned using a UV-vis spectrophotometer (Make: Shimadzu, Singapore; Model: UV-2600,) in the range from 300 nm to 800 nm to confirm the formation of Ag NPs.

2.9.2 X-Ray Diffraction analysis

The crystallinity of silver nanoparticles was examined by Powder X-Ray Diffraction System (XRD), (Make: Rigaku Technologies, JAPAN, Model: Smartlab). Ag NPs were dissolved in sterilized double distilled water and a small amount of suspension was sprayed on a glass slide to make a thin film. The thin film was dried in an oven and was scanned with X-ray (45 kV, 200 mA) at the measurement conditions of 8 deg/min and 1 nm incident slit in the range 2θ angle of 20-90 °C. The crystalline size of silver nanoparticles was calculated from the width of XRD peaks using the Debye-Scherrer equation shown in equation (2.19).

$$D = \frac{K\lambda}{\beta \cos\theta} \quad (2.19)$$

Where, D - thickness of the nanocrystal, K - constant (0.94), λ - wavelength of X-rays (1.5406×10^{-10}), β - width at half maxima of reflection at Bragg's angle 2θ , and θ - Bragg angle.

2.9.3 Dynamic and light scattering

Dynamic and light scattering (DLS) (Make: M/s Beckman Coulter, Switzerland; Model: Delsa Nano C) was used to determine the size of Ag NPs in the suspension.

2.9.4 Field Emission Transmission Electron Microscope

Field Emission Transmission Electron Microscope (FETEM) with Element EDS Detector, (Make: JEOL, Model: 2100F (HR)) was applied to characterize the shape, size, SAED pattern, and the composition of synthesized Ag NPs. The Ag NPs film for FETEM analysis was prepared by dissolving Ag NPs a small amount of suspension was sprayed on carbon-coated copper grids.

2.9.5 Field Emission Scanning Electron Microscope

Field Emission Scanning Electron Microscope (FESEM), (Make: Zeiss, Model: Sigma 300) was used to study the morphology of Ag NPs. Dried Ag NPs were mounted on the carbon tape and FESEM analysis was performed.

2.9.6 FTIR spectrometer

FTIR spectrometer (Shimadzu Corporation, Japan) analysis of extracts, dried supernatant, and synthesized silver nanoparticles was performed to identify functional groups present in the extract and to determine the functional group absorbed or involved in the reaction. Infrared spectra were recorded within wavenumbers between $4000-400 \text{ cm}^{-1}$, at a resolution of 4 cm^{-1} .

2.10 Statistical analysis

For the optimization study, Design Expert 7.0.0 (Stat-Ease, Minneapolis, USA) software was used. Experiments were performed in duplicate of two individual experiments. All the data were reported as mean \pm standard deviation. ANOVA using MATLAB 2019a software was considered to check the significance level.







**DIETARY AND BIOACTIVE
PROPERTIES OF THE BERRIES AND
LEAVES OF *HIPPOPHAE SALICIFOLIA***

D. DON

Published in

Journal of Food Science and Biotechnology. 30 (10), 2021, 1555–1569.





DIETARY AND BIOACTIVE PROPERTIES OF THE BERRIES AND THE LEAVES OF *HIPPOPHAE SALICIFOLIA* D. DON**3.1 Background**

Sea buckthorn is a dioecious hardy shrub in *Hippophae* genus. It is an economically important nutritional and medicinal plant cultivated in countries like India, China, Asia, Europe, North America at 2,500-4,300 m altitude (Negi et al., 2005). *H. salicifolia*, *H. rhamnoides*, and *H. tibetana* are species of *Hippophae* genus, disseminated in the highlands of the Indian sub-continent (Singh et al., 2019). The berries and the leaves of sea buckthorn contain plenty of minerals, sugars, vitamins, phenolics, flavonoids, tocopherols, carotenoids, phytosterols, unsaturated lipids, and volatile compounds. Therefore, this study focused on investigating the phytochemical and nutritional composition of the 50-50% mixture of dry leaves and the whole berries of *Hippophae salicifolia* from Northeast India. The leaves of sea buckthorn of both types are reported to be a good source of bioactive compounds with slight differences in total phenolic and flavonoid contents, and antioxidant and antibacterial activity. The physicochemical analyses of mixed leaves and berries (CHNS, ash, protein, vitamin C, sugar, tannin, FTIR) were performed. Some important polyphenol compounds were extracted following successive solvent extraction and further identified by HPLC analysis. Additionally, the antioxidant potential, global antioxidant score, and antibacterial activities of different extracts were evaluated. The nutritional and polyphenolic content and the antioxidant activity of extracts were compared with the previously reported data of the berries and either of individual plant leaves.

3.2 Overview

The physicochemical, polyphenols, antioxidant, and antibacterial properties of berries and the mixture of male and female leaves of *Hippophae salicifolia* were investigated. The mineral, vitamin C, sugar, total protein, and total tannin contents of the berries and the leaves were evaluated. Further, the extracts of berries and mixture of leaves samples obtained by successive solvent extraction were investigated for their polyphenols, antioxidant and antibacterial properties. The work flow of this chapter is shown in **Fig 3.1**. Total phenolic content was highest in leaves-methanol extract (157.97 ± 2.09 mg GAE/g) followed by berries-aqueous extract (48.45 ± 1.94 mg GAE/g), while total flavonoid was predominant in leaves-acetone extract (75.64 ± 3.21 mg QE/g) and berries-methanol extract (28.93 ± 2.08 mg QE/g). Gallic acid, caffeic acid, and rutin were the major polyphenols confirmed by HPLC analysis. Berries-aqueous and leaves-methanol extracts showed excellent global antioxidant scores. Best antibacterial activity was observed by methanol extracts against eight different strains. Overall, the leaves and berries of *Hippophae salicifolia* collected from Northeast India exhibited good antioxidant and antibacterial activity and can be utilized by the food and pharmaceutical sectors.

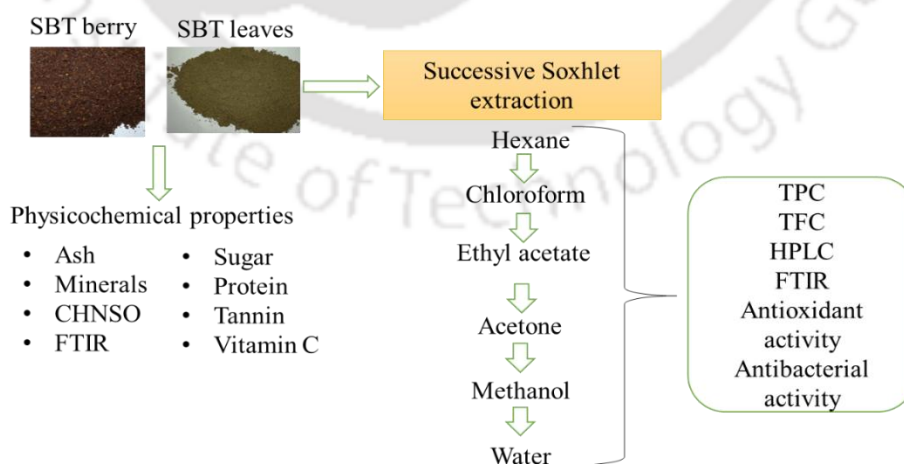


Fig. 3.1: Graphical Abstract

3.4 Results and Discussion

In this section, the physicochemical properties of the whole berries and the 50-50% mixture of leaves of the male and female *H. Salicifolia* were investigated. The berries and the leaves of *H. Salicifolia* were successively extracted using hexane, chloroform, ethyl acetate, acetone, methanol, and water; and the yield of extraction, polyphenolic content, and the antioxidant and antibacterial activities of extracts were evaluated.

3.4.1 Proximate and CHNS analysis

The proximate and CHNS analysis of the whole berries and mixture of sea buckthorn leaves are presented in **Table 3.1**. Results of the study revealed slightly higher ash content in sea buckthorn leaves ($3.85 \pm 0.06\%$) than in berries ($3.23 \pm 0.01\%$). The ash content of the sample used in the present study closely matches the value reported by Attrey et al., (2012) for Indian *H. rhamnoides*. Leaves of Indian *H. Salicifolia* showed a significant difference in their ash content when compared with Poland *H. rhamnoides* variety (4.79-5.09%). Ash content in the berries was observed to be higher than the Romanian (2.83%) (Ion et al., 2019) and Indian (1.76%) (Bal et al., 2011) varieties of *H. rhamnoides*. In both samples (berries and leaves mixture), the portion of acid-insoluble ash was higher than water-soluble ash. Ash content of berries and leaves sample is under acceptable limits which suggests less physiological (plant tissue) and non-physiological (sand or soil) contamination.

The berries used in the present work exhibited 1.7-fold higher fixed carbon content than the leaves, while leaves had higher volatile matter. The volatile matters are mainly alcohols and esters of short-chain, branched, or n-fatty acids that affect the aroma and sensory characteristics of fruit and vegetables.

Table 3.1: Composition of sea buckthorn berries and leaves

Compositions (W %)	Berries	Leaves
Moisture content	7.54 ± 0.01	12.5 ± 0.01
Ash content	3.23 ± 0.01	3.85 ± 0.06
Acid-insoluble ash	1.97 ± 0.4	2.23 ± 1.3
Water-soluble ash	0.98 ± 0.7	1.34 ± 1.4
Volatile matter	69.25 ± 1.1	71.66 ± 2.7
Fixed carbon	19.98 ± 1.0	11.99 ± 2.6
CHNS analysis		
Carbon	45.93 ± 0.35	47.10 ± 0.33
Hydrogen	5.88 ± 0.2	6.73 ± 0.12
Nitrogen	1.93 ± 0.11	3.75 ± 0.14
Sulphur	0.05 ± 0.02	0.08 ± 0.01
Oxygen	42.71 ± 0.25	37.94 ± 0.14

All values are presented in mean ± SD, n = 3, W% - weight percentage.

3.4.2 Elemental analysis

Elemental analysis of sea buckthorn berries and leaves by EDX analyzer showed 15 microelements that are necessary for human nutrition (**Table 3.2**). Potassium was the predominant element in both samples, while sodium and calcium were the second most abundant element in the berries and leaves, respectively. Other microelements such as calcium, silicon, magnesium, and

phosphorus content of the leaves were substantially higher than in berries. The composition of minerals like Potassium, Sodium, Magnesium, and some other elements of the berries were as stated for Chinese, Indian, and Romanian *H. rhamnoides* L. (Bal et al., 2011; Ion et al., 2019). However, compared to the reported literature, elements such as phosphorus, magnesium, calcium, zinc, iron, and silver showed significant variation. This variation could be attributed to the genetic difference and water holding capacity of the soil. Despite the well-documented sea buckthorn leaves and berries, no data is available in the literature on the mineral composition of sea buckthorn leaves.

Table 3.2: Elemental composition of sea buckthorn berries and leaves

Element (W %)	Berries	Leaves
Potassium	46.92 ± 3.1	29.99 ± 3.1
Calcium	5.72 ± 1.46	26.31 ± 3.4
Silicon	3.49 ± 1.4	6.68 ± 0.3
Sodium	10.30 ± 2.2	4.42 ± 1.6
Magnesium	2.56 ± 0.23	6.78 ± 1.1
Phosphorus	1.74 ± 1.6	6.12 ± 0.67
Iron	ND	5.09 ± 1.59
Phosphorus	1.63 ± 0.1	1.73 ± 0.02
Zinc	ND	1.1 ± 0.01
Aluminium	6.76 ± 1.7	4.92 ± 0.44
Chromium	3.60 ± 1.1	1.0 ± 1.34
Manganese	3.05 ± 1.5	0.35 ± 0.01
Lead	2.45 ± 0.01	4.03 ± 0.7
Selenium	3.49 ± 0.7	1.1 ± 0.7
Copper	2.34 ± 0.5	0.35 ± 0.01
Nickel	0.95 ± 0.9	ND
Arsenic	1.55 ± 1.4	ND

All values are presented in mean ± SD, n = 3, ND-not detected, W% - weight percentage.

3.4.3 Quantitative phytochemical analysis

The results of soluble and reducing sugar, protein, tannin, and vitamin C contents of sea buckthorn berries and leaves are presented in **Table 3.3**. Several authors have reported the sugar, protein, tannin, and vitamin C content in European and Chinese sea buckthorn (*Hippophae rhamnoides* L. species). *Despite numerous benefits to nutritional values and biological activities*, information on sugar content, protein, and tannin content in Indian *H. salicifolia* berries and leaves is rather limited. The total soluble sugar of leaves and berries was found to be 138.64 ± 3.3 and 120 ± 1.4 mg GE/g, respectively. The non-reducing sugar content was 30.51 ± 0.7 and 41.14 ± 2.3 mg GE/g for berries and leaves, respectively. Interestingly, the sugar content was found higher in leaves than in berries. A similar trend was also reported by Akšić et al., (2019) in different varieties of Blueberry and Strawberry, where the sugar content in leaves was higher than in fruits. They described that the ratio of sugar between fruits and leaves of a plant is dependent on the translocation of sugars from leaves to fruits which is strongly controlled by ecological factors such as light, CO₂ concentration, temperature, etc. Another study also suggests that higher sugar content in plant tissue leads to higher production of secondary plant metabolites, specifically, phenolic and flavonoid (Ibrahim et al., 2011). The present study also reveals that there is a higher concentration of TPC and TFC in sea buckthorn leaves than in the berries. The results of the present study could be supported by the above discussed two possible reasons. The results obtained in the present study are in the range of the total soluble sugar content (130 mg/g) of Chinese (Hussain et al., 2014) and reducing sugar content (9.7 - 59.1 mg/g) of Finnish (Tang and Tigerstedt, 2001) in the berries of *H. rhamnoides*.

The content of protein is a good indicator of food value and the potential of dietary supplementation of sea buckthorn berries and leaves. The protein content of sea buckthorn leaves

Chapter 3

(102.86 ± 1.1 mg BSAE/g) was found to be higher than the berries (41.87 ± 1.6 mg BSAE/g). These values are similar to that reported in the berries of Romanian *H. rhamnoides* L. (3.99 - 45.35 mg/g) by Oprica et al., (2007). Similarly, the protein content of leaves in the present study is in accord with Kashif and Ullah, (2013) and Stobdan et al., (2011).

Table 3.3: Nutritional composition of sea buckthorn berries and leaves

	Berries		Leaves	
	Present study	Literatures	Present study	Literatures
Total Soluble sugar (mg GE/g)	120 ± 1.4	130 mg/g ^a	138.64 ± 3.3	272.9 ^b
Reducing sugar (mg GE/g)	89.5 ± 1.2	9.7-59.1 mg/g ^c	97.5 ± 1.4	173.7 ^b
Non-reducing sugar (mg GE/g)	30.51 ± 0.7	-	41.14 ± 2.3	-
Total protein (mg BSAE/g)	41.87 ± 1.6	3.99 - 45.35 mg% ^d	102.86 ± 1.1	150-200 ^e
Vitamin C (mg AAE/100g)	256.10 ± 1.3	147 - 896 ^f	106.47 ± 3.6	370 ^g
Total tannin (mg TAE/g)	42 ± 0.65	1.99 - 5.74 mg/g ^f	80.1 ± 2.63	80 mg/g ^g

The results are presented in mean ± SD, n = 3; GE-glucose equivalent, BSAE-bovine serum albumin equivalent, TAE-tannic acid equivalent, and AAE-ascorbic acid equivalent. a-(Hussain et al., 2014), b-(Kashif and Ullah, 2013), c-(Tang and Tigerstedt, 2001), d-(Oprica et al., 2007), e-(Stobdan, et al., 2011), f-(Kuhkheil et al., 2017), g-(Krejcarová et al., 2015).

Vitamin C is the main component of sea buckthorn with a 5 to 100-fold higher concentration than any other fruits or vegetables (Bal et al., 2011). Vitamin C content in the berries closely matched with the reported values for Canada ‘Terhi’ and ‘Tytti’ cultivars (200 - 300 mg/100 g) (Karhu, 2003), European (28 - 310 mg/100 g) (Yao et al., 1992), and Indian *rhamnoides* (168.3 - 509 mg/100 g) (Arimboor et al., 2006), but lower than Chinese *Sinensis* (200 - 2500 mg/100 g) (Bal et al., 2011). For leaves, Krejcarová et al., (2015) reported that the vitamin C content of Czech *H. rhamnoides* levels up to 370 mg/100 g which is higher than the present work. This variation in

Vitamin C is mainly due to genotype, cultivar, ripening stage, and time of harvest. Ascorbic acid is an essential vitamin for the human body for its nourishment, oxidation scavenger, antibacterial, and other potent physiological actions.

Tannin-rich foods are considered to be of low nutritional value due to the adverse effect of tannins on protein digestibility. However, recent studies indicated that tannins are the leading contributors to antioxidant (Šne, et al., 2013) and antimicrobial (Ncube et al., 2017) potency and provide positive health benefits. The total tannin content in the leaves was in agreement with the report of 80 mg/g by Krejcarová et al., (2015) and the range between 59 and 350 mg/g by Stobdan et al., (2011) for Indian *H. rhamnoides*. However, it was 11-fold higher than the values reported by Kuhkheil et al., (2017) for Iranian *H. rhamnoides* which range from 1.99 to 5.74 mg/g. The difference in tannin between the *Hippophaë* genus is mainly attributed to the difference in species, extraction method, type of solvent, etc (Heinäaho et al., 2006; Stobdan et al., 2011b).

3.4.4 Successive extraction

The successive Soxhlet extraction of sea buckthorn berries and leaves resulted in a total yield of 66.37% and 39.19%, respectively (**Table 3.4**). In both cases, methanol offered the highest yield because it dissolves a wide range of polar and non-polar compounds. On the other hand, acetone extract from berries and chloroform extract from leaves resulted in the lowest yield. The fat content in berries ($14.54 \pm 0.47\%$) was found 3-fold higher than in leaves ($3.93 \pm 0.13\%$). These values are consistent with the result reported by Biel and Jaroszevska, (2017) with *H. rhamnoides* variety from Poland and *sinensis* species from China (Yang and Kallio, 2001).

Table 3.4: Yield (%) of successive extraction from sea buckthorn berries and the leaves

Extract	Berries extracts	Leaves extracts
HX	14.54±0.47	3.93±0.13
CL	2.41±0.02	1.60±0.13
EA	17.62±0.29	1.78±0.32
AC	1.46±0.3	2.60±0.28
MT	22.14±1.4	14.84±0.84
AQ	8.20±0.89	14.41±1.1
Total yield	66.37	39.19

All values are presented in mean, n = 2; HX-hexane, CL-chloroform, EA-ethyl acetate, AC-acetone, MT-methanol, and AQ- aqueous.

3.4.5 Qualitative phytochemical screening

The phytochemical screening results of sea buckthorn berries and leaves extracts are presented in **Table 3.5**. Carbohydrate, glycoside, protein, and amino acid were more noticeable in polar and moderately polar solvents. The alkaloid test was more appreciable in hexane and declined as the extraction progressed from non-polar to polar solvents and was not noticed in the aqueous extract of the berries and aqueous and methanol extracts of the leaves. It is confirmed from the qualitative analysis that all extracts contained tannin, phenolic, and flavonoid compounds. These compounds were more noticeable in acetone, methanol, and aqueous extracts followed by ethyl acetate, chloroform, and hexane extracts. A similar finding was reported by Ahmad and Ali, (2013) in that many phytochemicals were presented in methanol extracts. Qualitative phytochemical screening of leaves extracts was better than berries extracts.

Table 3.5: Phytochemical screening results of sea buckthorn berries and leaves extracts

Phytochemicals	Berries extracts						Leaves extracts					
	HX	CL	EA	AC	MT	AQ	HX	CL	EA	AC	MT	AQ
Carbohydrates	ND	ND	+	++	++	+++	ND	ND	+	+	+++	+++
Glycosides	ND	ND	++	+++	++	+	+	+	+	+	+++	+++
Proteins	ND	ND	ND	+	+	++	ND	ND	+	+	+++	++
Amino acids	ND	ND	ND	ND	+++	+	ND	ND	ND	+	++	+
Alkaloids	+++	++	++	+	+	ND	++	+	++	+	ND	ND
Tannins	+	+	+++	+++	+++	+++	+	+	++	+++	+++	+++
Phenols	++	++	++	++	+++	+++	++	++	++	+++	+++	+++
Flavonoids	+	++	++	++	++	+++	++	++	++	+++	+++	+++

HX-hexane, CL-chloroform, EA-ethyl acetate, AC-acetone, MT-methanol, and AQ-aqueous, + small quantity, ++ average quantity, +++ large quantity, ND = not detected.

3.4.6 FTIR Analysis

FTIR transmission plots of berries powder, leaf powder, and respective successive extractives are presented in **Fig. 3.2**. The characteristic absorption bands of the berries and leaves (**Fig. 3.2. (a)** and **(b)**) at 3296 cm^{-1} correspond to the O-H stretching and H-bond that confirmed the presence of phenols and alcohols. The presence of aromatic rings of polyphenols and flavonoids in the berries, leaves, and successive extracts was confirmed with the peaks at 3436 cm^{-1} (OH), $1734 - 1743\text{ cm}^{-1}$ (O=C), and in the $3650 - 3584\text{ cm}^{-1}$ region which belongs to O-H stretching vibrational bands. The peaks at 2922 and 2853 cm^{-1} for berries and leaves samples attributed to CH_2 antisymmetric and symmetric stretching of an aliphatic chain of lipids, respectively. The sharp signal of these peaks for the berries is evidence of higher fat content. Moreover, these peaks reappeared in hexane and chloroform extracts of both berries and leaves (**Fig. 3.2 (c)** and **(d)**). The spectra of extracts

imparted the identical pattern of absorption bands with a minor difference revealing the presence of various functional groups including alkanes (2853), alkenes (2800 - 3000), aromatic rings (1365), and carbonyl (1734 - 1743) groups. This is the first report on *H. Salicifolia* to the best of our knowledge. Similar results of FTIR analysis have been reported for various cultivars of Romanian *H. rhamnoides* ssp. *carpatica* (Pop et al., 2014).

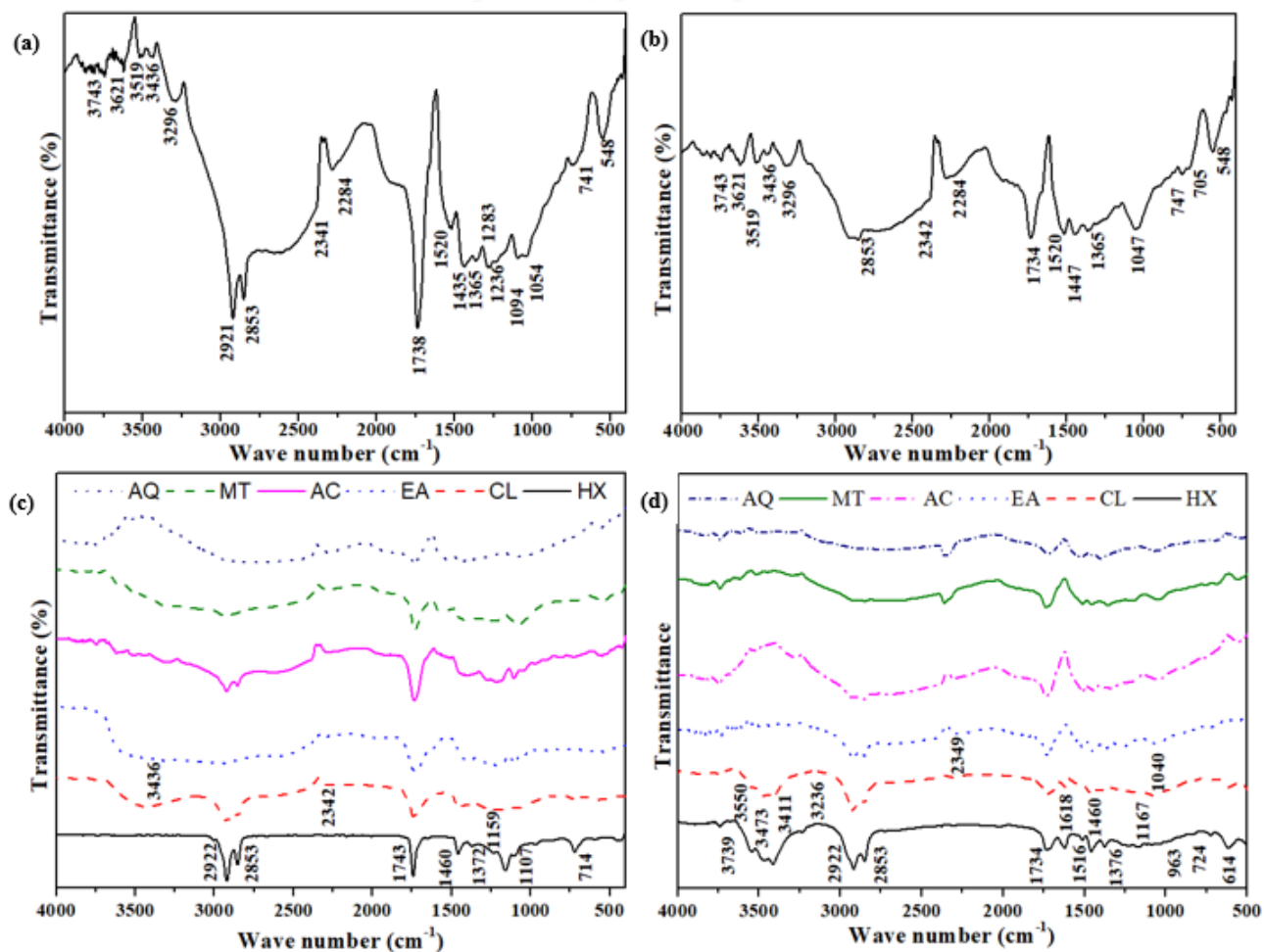


Fig. 3.2: FTIR spectral transmission band for (a) powdered berries (b) mixture of powdered leaves, (c) berries extracts, and (d) leaves extracts, HX-hexane, CL-chloroform, EA-ethyl acetate, AC-acetone, MT-methanol, AQ-aqueous

3.4.7 Total phenolic and flavonoid contents

The total phenolic (TPC) and flavonoid (TFC) contents of all the successive extracts are presented in **Table 3.6**. The TPC of berry extracts ranged from 11.99 ± 0.82 to 48.45 ± 1.94 mg GAE/g of extract. The aqueous extract had the highest concentration of TPC, followed by methanol, and the lowest in ethyl acetate extract. But in the case of the leaves, methanol extract (157.97 ± 0.86 mg GAE/g of extract) was found to contain the highest TPC followed by aqueous extract (144.63 ± 0.47 mg GAE/g) and the least TPC in chloroform extract (15.18 ± 0.53 mg GAE/g). TFC of methanolic extract of berries was highest (28.93 ± 2.08 mg QE/g), followed by aqueous (24.81 ± 0.64 mg QE/g), and lowest in the ethyl acetate extract (9.73 ± 1.61 mg QE/g). On the other hand, TFC of leaves extracts ranged from 16.1 ± 2.08 to 75.64 ± 3.21 mg QE/g of extract, being highest in acetone extract followed by methanol extract.

Computation of TPC/TFC per gram of sample (dry weight) in each extract was important to compare the amount of polyphenols extracted by a given solvent. The successive solvent extract gives the advantage to understand the TPC/TFC distribution cumulatively in each sample (berries or leaves). For instance; the concentration of TPC per gram of methanolic extracts of berries was lower (39.24 ± 1.3 mg GAE/g) than the concentration in aqueous extract (48.45 ± 1.94 mg GAE/g), but because of the higher extract yield, the TPC dry weight value of methanolic extract (8.68 mg GAE/g DW) was more than the aqueous extract (3.97 mg GAE/g DW). The TFC yield in acetone and methanol extracts of the leaves also showed an identical phenomenon with the TFC yield in methanol (10.58 mg QE/g DW) being higher than in acetone (2 mg QE/g DW) extract. The grand total TPC achieved from the entire successive extraction of berries and leaves was 19.12 mg GAE/g of berries (DW) and 49.75 mg GAE/g of leaves (DW). Similarly, the TFC was found to be 13.58 mg QE/g of berries (DW), and 23.24 mg QE/g of leaves (DW), respectively. Overall, the

Table 3.6: The yield of extraction, total phenolic content (TPC), and total flavonoid content (TFC) of extracts

Berries extracts	Yield (%)	TPC (mg GAE/g of extract)	TPC* (mg GAE/g of DW)	TFC (mg QE/g of extract)	TFC* (mg QE/g of DW)
HX	14.54 ± 0.47	24.99 ± 2.12	3.63	19.5 ± 0.63	2.83
CL	2.41 ± 0.02	19.49 ± 0.24	0.47	15.52 ± 0.48	0.37
EA	17.62 ± 0.29	11.99 ± 0.82	2.11	9.73 ± 1.61	1.71
AC	1.46 ± 0.3	17.7 ± 0.53	0.26	15.75 ± 1.77	0.23
MT	22.14 ± 1.4	39.24 ± 1.3	8.68	28.93 ± 2.08	6.41
AQ	8.2 ± 0.89	48.45 ± 1.94	3.97	24.81 ± 0.64	2.03
Grand total			19.12		13.58
Leaves extracts					
HX	3.93 ± 0.13	19.66 ± 0.12	0.77	16.1 ± 2.08	0.63
CL	1.6 ± 0.13	15.18 ± 0.53	0.24	18.74 ± 0.48	0.3
EA	1.78 ± 0.32	51.66 ± 1.06	0.92	42.69 ± 1.12	0.76
AC	2.6 ± 0.28	136.3 ± 0.94	3.54	75.64 ± 3.21	2
MT	14.84 ± 0.84	157.97 ± 0.86	23.44	71.32 ± 2.89	10.58
AQ	14.41 ± 1.1	144.63 ± 0.47	20.84	62.23 ± 1.61	8.97
Grand total			49.75		23.24

The results are presented in mean ± SD, n = 3; Total phenolic content (TPC), Total flavonoid content (TFC), Gallic acid equivalent (GAE), Quercetin equivalent (QE), * TPC/TFC per gram of dry powdered sample (DW) obtained by multiplying yield of extraction by TPC/ TFC, Grand total (TPC obtained from the entire extraction process were obtained by adding the TPC per gram of dry berries and leaves in each extract), HX-hexane, CL-chloroform, EA-ethyl acetate, AC-acetone, MT-methanol, AQ-aqueous.

extracts from leaves had higher TPC and TFC than berries. The results of TPC per g of extract of berries extracts were comparable with Romanian *H. rhamnoides* extract (10.12 to 18.66 mg GAE/g) (Criste et al., 2020). A noteworthy result is that the grand total TPC (19.12 mg GAE/g DW) was higher than the methanol extract (8.68 mg GAE/g DW) as shown in **Table 3.6**, and comparable with previously reported TPC values ranging from 20.78 to 34.60 mg GAE/g DW (crude methanolic extract) and 20.78 to 34.60 mg GAE/g DW (crude ethanol extract) for Iranian and Turkian *H. rhamnoides*, respectively (Kuhkheil et al., 2017; Ercisli et al., 2007). Likewise, TFC values for berries (13.58 mg QE/g DW) in this study were approximately similar to those reported in other varieties of sea buckthorn (5.63 - 14.37 mg rutin equivalent/g (DW) (Pop, et al., 2013) for Romanian and 3.54 - 8.54 mg/g for European *H. rhamnoides* variety. On the other hand, TFC per gram of extract of berries was found to be higher than that obtained by Criste et al., (2020) for Romanian *H. rhamnoides* cultivars (6.57 - 9.01 mg QE/g of extract). Regarding leaves extract, Saikia and Handique, (2013) reported that the crude methanolic extract of Indian *H. salicifolia* (from Sikkim-Himalayas region) had the highest concentration of TPC (98.7 mg GAE/g of extracts), followed by acetone, chloroform, and petroleum ether extracts. These values were lower than the TPC per gram of acetone, methanol, and aqueous extracts obtained from the current successive extraction. Criste et al., (2020) worked with four Romanian varieties of sea buckthorn leaves and observed TPC ranging from 41.6 - 48.12 mg GAE/g, emphasizing that the leaves had significantly higher TPC than berries ($p < 0.05$). According to Kumar et al., (2011), TPC in ethanol extracts of leaves of Indian *rhamnoides* ranges from 43.77 to 77.85 mg GAE/g DW, which is in agreement with the grand TPC (48.75 mg GAE/g DW) of the present study. In comparison, Upadhyay et al., (2010) analyzed aqueous and hydroalcoholic extracts of *H. rhamnoides* from North-West Himalayas and reported the TPC of 40.49 and 56.28 mg GAE/g DW, respectively.

The TFC of acetone, methanol, and aqueous extracts of *H. salicifolia* leaves was approximately 2-fold higher than the Romanian *H. rhamnoides* which contains 31.53 - 36.58 mg QE/g of extract. The grand total TFC (23.24 mg QE/g DW) of *H. Salicifolia* agreed with the previous report by Upadhyay et al., (2010). A large variation of TPC and TFC designates the composition of sea buckthorn is dependent on many parameters such as extraction method, time and temperature, type of solvent, harvest time, subspecies and cultivars, genotype, and geographic factors. Phenolic and flavonoid compounds are the most important bioactive compound which plays an important role as antioxidant and antibacterial agent, with significant nutritional and health-promoting abilities (Pop et al., 2014). Hence, it could be concluded that acetone, methanol, and aqueous extracts of the berries and the leaves of *H. salicifolia* could be potent sources of phenolic compounds. In general, successive extracts (ethyl acetate, acetone, methanol, and aqueous extracts) of whole berries and the mixture of leaves in the present study showed a higher concentration of TPC and TFC than the previous studies on either male or female leaves individually (Gupta and Kaul, 2017; Singh et al., 2014; Šne et al., 2013).

3.4.8 HPLC analysis

The identification and quantification of different phenolic and flavonoid compounds present in sea buckthorn leaf and berry extracts are presented in **Table 3.7**. While the HPLC chromatograms of the standards and extracts of berries and leaves are given in **Fig. 3.3 (a-c)** and **Fig. 3.4 (a-c)**, respectively. In this study, different polyphenols identified in berries and leaves were gallic acid, caffeic acid, ferulic acid, p-coumaric acid, myricetin, quercetin, kaempferol, and rutin. These compounds were identified mostly in methanolic, acetone, aqueous, and ethyl acetate extracts and were found below the detection limit in hexane and chloroform extracts.

The concentration of polyphenolic compounds found in leaves extracts was higher than in berries extracts. Gallic acid was the most abundant analyte in the leaves (50.93 ± 0.33 to 144.09 ± 0.64 mg/g) and berries (6.25 ± 0.16 to 30.18 ± 0.78 mg/g) extracts. It was the only compound detected in the highest concentration in the aqueous extract of berries compared to other phenolic compounds. The gallic acid content of Indian *H. salicifolia* leaves in the current study was in agreement with the ethyl acetate fraction of *H. rhamnoides* (Kumar et al., 2013). However, it was found to be less than Indian (West Himalaya) *H. rhamnoides* leaf extracts (314.09 mg/g). The content of caffeic acid in berries extracts was considerably lower ranged from (0.88 ± 0.02 mg/g (ethyl acetate)) to 1.18 ± 0.01 mg/g (methanol)), while it was the second major phenolic compound in leaves ranging from 9.73 ± 0.01 mg/g (ethyl acetate) to 64.47 ± 0.56 mg/g (methanol). The p-coumaric acid content of the leaves in the present study was comparatively higher than reported (0.032 mg/g of extract) by Criste et al., (2020).

Rutin was a predominant dietary flavonoid found in both berries and leaves extract. The rutin content in berries ranged from 0.45 mg/g (acetone) to 1.48 ± 0.02 mg/g (methanol) and in leaves, 3.04 ± 0.01 mg/g (ethyl acetate) to 9.5 ± 1.4 mg/g (aqueous) which was higher than other flavonoid aglycones (myricetin, quercetin, and kaempferol). The rutin content in berries and leaves extracts was in the range of previously reported values in other varieties of *rhamnoides* from different countries (Cho et al., 2017; Dong et al., 2017; Fatima et al., 2015; Kumar et al., 2013; Sharma et al., 2008). Besides, Criste et al., (2020) reported that the leaves and berries of four different Romanian *H. rhamnoides* cultivars as a rich source of phenolic compounds, particularly quercetin and hydrocinnamic acid derivatives. Quercetin was found to be in the range of 0.01 mg/g (aqueous) to 0.15 ± 0.001 mg/g (ethyl acetate) in berries and 0.04 mg/g (aqueous) to 2.62 ± 0.01 mg/g (ethyl acetate) in leaves extracts. But, kaempferol was detected in acetone, ethyl acetate, and aqueous

Table 3.7: HPLC analysis of phenolic and flavonoid compounds in sea buckthorn berries and leaves extract

Berries Extract	Phenolic Compounds(mg/g)					Flavonoid compounds(mg/g)					References
	Gallic acid	Caffeic acid	Ferulic acid	P-coumaric acid	Total	Myricetin	Quercetin	Rutin	Kaempferol	Total	
EA	11.16±0.22	0.88±0.02	1.17±0.32	0.86±0.23	14.07	0.01±0.003	0.15±0.001	0.56	0.02±0.01	0.74	Present study
AC	6.25±0.16	0.97±0.28	1.05±0.04	0.73±0.01	9	0.03	0.12±0.01	0.45	0.02±0.01	0.62	Present study
MT	14.21±0.97	1.18±0.01	1.1±0.02	0.72±0.01	17.21	0.08±0.01	0.12±0.01	1.48±0.02	ND	1.68	Present study
AQ	30.18±0.78	ND	ND	ND	30.18	0.02±0.003	0.01	1.04±0.03	0.02	1.04	Present study
Previous Study											
50%ethanol	0.065-0.194	ND	ND	0.032		ND	0.11-0.122	ND	0.013-0.019		(Criste et al., 2020)
Ethanol ^{DW}	NA	NA	NA	NA		0.0173	ND	0.136	0.0037		(Sharma et al., 2008)
Acidified water ^{FW}	0.002-0.008	0.009-0.03	0.003-1.3	0.07-0.13		0.036-0.17	0.07-0.18	ND	0.03-0.07		(Fatima et al., 2015)
Leaves Extract											
EA	50.93±0.33	9.73±0.01	2.38±0.32	1.25±0.00	64.29	ND	2.62±0.01	3.04±0.01	0.52	6.18	Present study
AC	134.27±0.04	24.48±0.07	1.16±0.7	1.1±0.01	161.01	ND	0.62±0.28	ND	0.21±0.01	0.83	Present study
MT	144.09±0.64	64.47±0.56	9.1±0.00	0.73±0.00	218.39	ND	0.94±0.12	ND	0.09±0.01	1.03	Present study
AQ	135.73±1.57	61.66±0.13	ND	ND	197.39	ND	0.04	9.5±1.4	0.06	9.6	Present study
Previous Study											
50%ethanol	0.047-0.09	0.024	0.014-0.04	0.032		0.194-0.34	15.2-73.3	0.058-0.26	0.015-0.03		(Criste et al., 2020)
Ethanol ^{DW}	NA	NA	NA	NA		0.1368	NA	0.3188	0.0458		(Sharma et al., 2008)
LCE ^{EW}	314.08	NA	NA	NA		0.19	0.26	0.41	0.2		(Kumar et al., 2013)
PRF	191.89	NA	NA	NA		1.93	2.912	0.52	2.85		(Kumar et al., 2013)
Acidified water ^{FW}	0.495-0.18	0.24-0.53	0.15-0.5	0.11-0.48		ND	0.44-1.1	0.24-1.35	0.51-1.48		(Fatima et al., 2015)
80%MeOH ^{DW}	29.94 - 37.25	NA	NA	NA		NA	0.2 - 0.54	NA	1.2 - 1.4		(Cho et al., 2017)
70%ethanol ^{DW}	NA	NA	NA	NA		ND	0.07-0.47	2.82-7.31	0.008-0.029		(Dong et al., 2017)
60% MeOH ^{DW}	0.689	0.018	0.044	0.001		NA	NA	NA	NA		(Arimboor, et al., 2008)

The results are presented in mean ± SD, n = 3; ND-not detected, NA-data not available, HX-hexane, CL-chloroform, EA-ethyl acetate, AC-acetone, MT-methanol, AQ-aqueous, Leaves crude extract (LCE): an extract obtained by maceration using 70% ethanol, LCE was successively extracted with water, hexane, and ethyl acetate. Phenolic rich fraction (PRF) is ethyl acetate fraction., * extracted by methanol + butylated hydroxyanisole (2 g/L) + 10% acetic acid. ^{FW} - results are given per gram of fresh weight, ^{DW} - results are given per gram of dry plant material, ^{EW} - results are given per gram of extract.

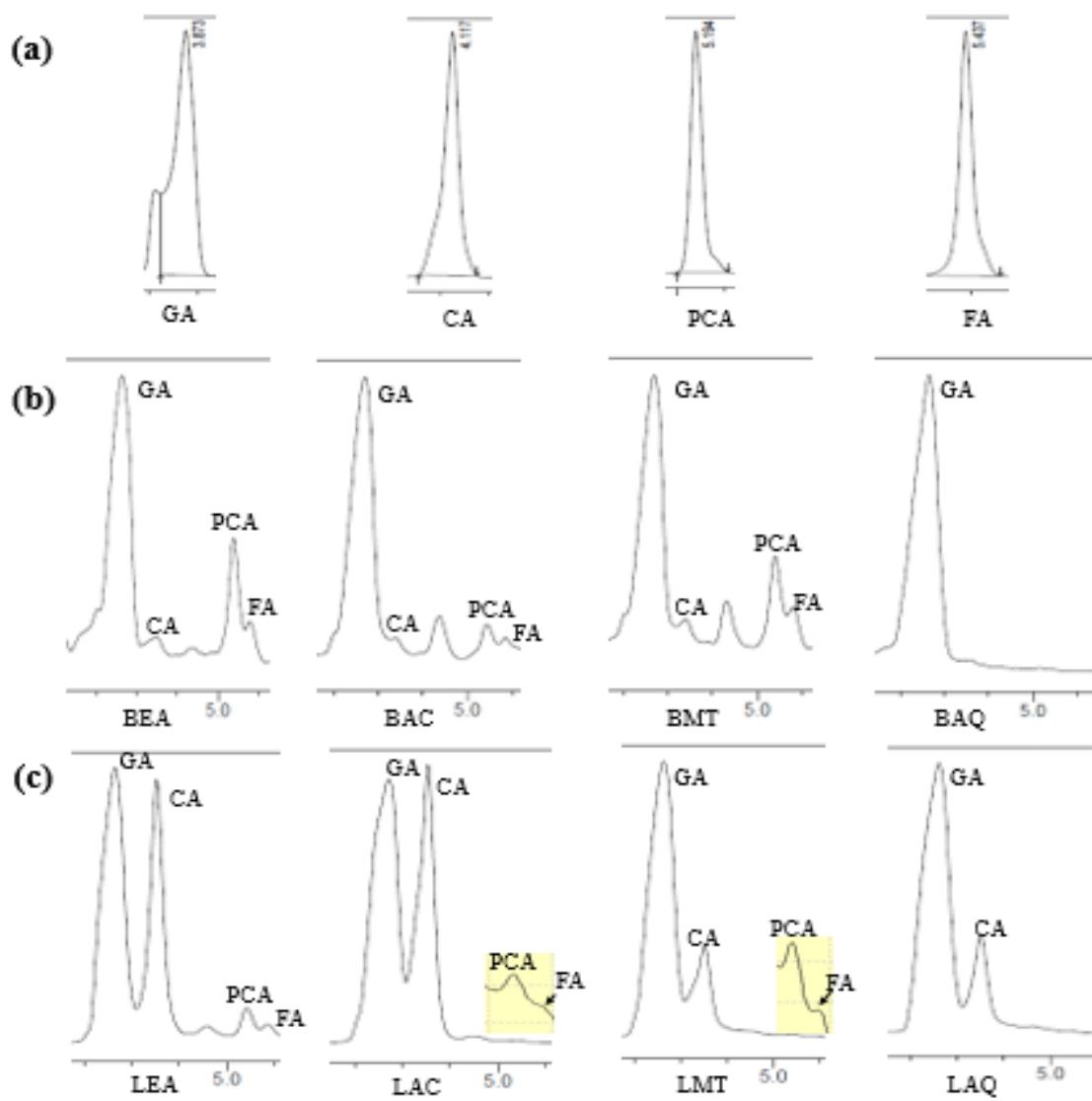


Fig. 3.3: HPLC chromatograms for identification of phenolic acids. (a) HPLC profile of standards: gallic acid (GA), caffeic acid (CA), p-coumaric acid (PCA), and ferulic acid (FA). (b) Identification of phenolic acids in berries extracts: ethyl acetate (BEA), acetone (BAC), methanol (BMT), and aqueous (BAQ) extracts at 310 nm. (c) Identification of phenolic acids in leaves extracts: ethyl acetate (LEA), acetone (LAC), methanol (LMT), and aqueous (LAQ) extracts at 310 nm

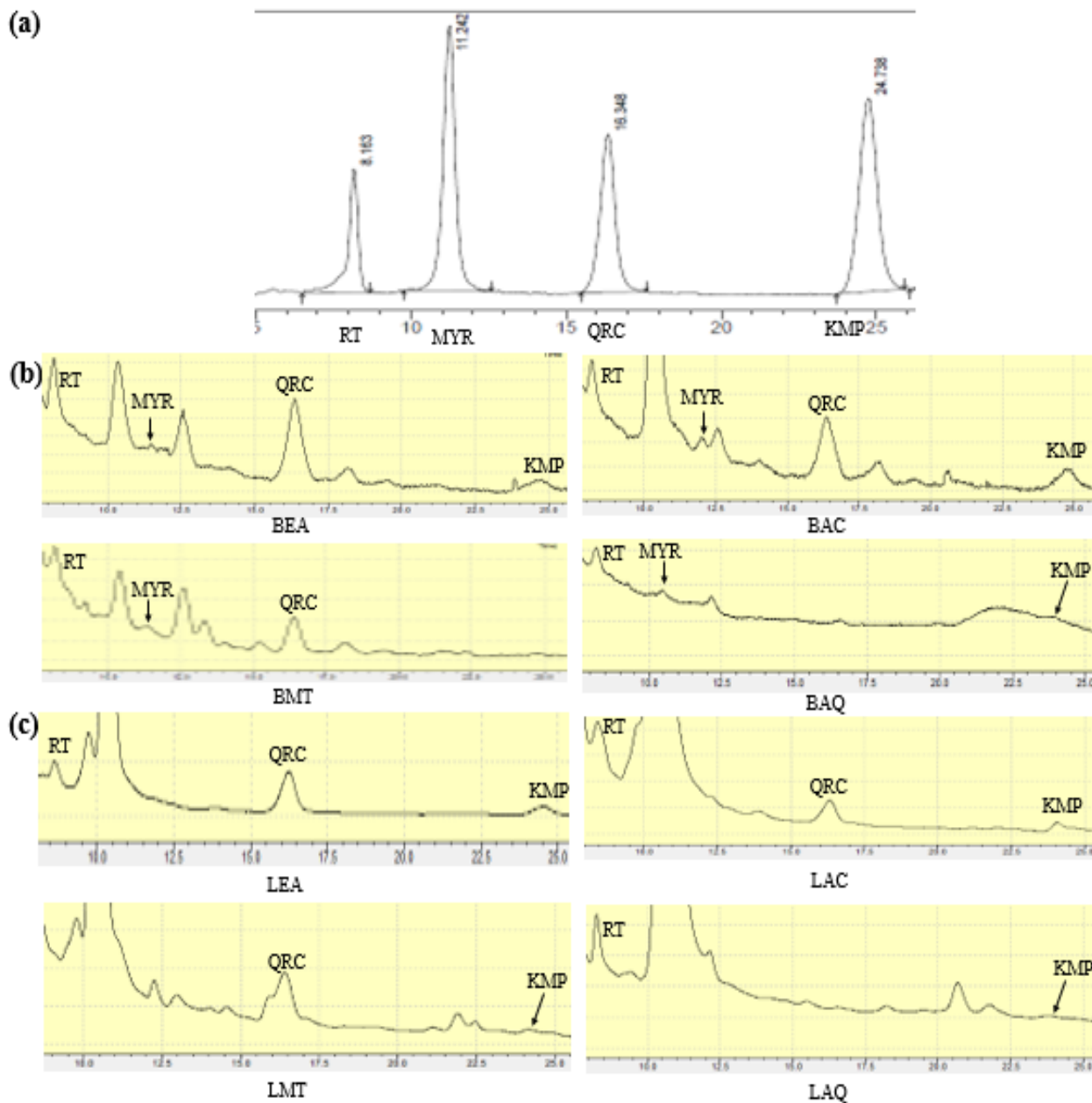


Fig. 3.4: HPLC chromatograms of flavonoid compounds. (a) HPLC profile of standards rutin (RT), myricetin (MRC), quercetin (QRC), and kaempferol (KMP) at 368 nm. (b) Identification of flavonoids in berries extracts: ethyl acetate (BEA), acetone (BAC), methanol (BMT), and aqueous (BAQ) extracts; (c) Identification of phenolic acids in leaves extracts: ethyl acetate (LEA), acetone (LAC), methanol (LMT), and aqueous (LAQ) extracts

extract of berries. The values of quercetin and kaempferol contents of berries and leaves extracts were similar to those reported for Romanian, Korean, Chinese, and Indian *H. rhamnoides* (Cho et al., 2017; Dong et al., 2017; Fatima et al., 2015; Kumar et al., 2013; Sharma et al., 2008). Another flavonoid compound, myricetin was found only in berries ranging from 0.01 ± 0.003 to 0.08 ± 0.01 mg/g. Studies by Fatima et al., (2015) and Sharma et al., (2008) on sea buckthorn berries from Canada and India reported the myricetin content from 0.036 to 0.17 mg/g FW, and 0.0173 mg/g DW, respectively. Kumar et al., (2013) demonstrated that sea buckthorn leaves extracts were rich in quercetin-3-glucoside, quercetin-3-galactoside, quercetin, rutin, and kaempferol, which matched closely with sea buckthorn *H. salicifolia* variety in the current study.

3.4.9 In vitro antioxidant activity

The antioxidant potency of sea buckthorn berries and the mixture of leaves extracts were evaluated by comparing the 50% inhibition concentration (IC₅₀) of the extracts with ascorbic acid (AA) in DPPH and ABTS assays (**Fig. 3.5 (a) and (b)**). All the extracts revealed significant antioxidant activity.

Among all the extracts, berries-hexane extracts, leaves-hexane, and -chloroform extracts had shown the lowest antioxidant activity. This is because of the presence of lower scavenging molecules compared to extracts obtained from polar and moderately polar solvents. The acetone, methanol, and aqueous extracts showed greater antioxidant activity for both assays. For berries, aqueous extract had highest antioxidant capacity with IC₅₀ of 16.6 ± 0.48 µg/mL, followed by 22.35 ± 1.1 µg/mL (methanol) and 33.72 ± 2.3 µg/mL (acetone) in DPPH assay. The highest antioxidant activity of aqueous extracts of berries could mainly be due to their highest content of TPC and gallic acid.

Chapter 3

A similar trend of antioxidant activity for successive solvent extracts of sea buckthorn leaves (hexane (87 mg TE/g) and ethyl acetate (161 mg TE/g) and water (275 mg TE/g)) was also observed by Michel et al., (2012). Among the leaves extracts, acetone ($2.42 \pm 0.1 \mu\text{g/mL}$), methanol ($2.65.78 \pm 0.2 \mu\text{g/mL}$), and aqueous ($3.68 \mu\text{g/mL}$) extracts depicted the highest scavenging activity in DPPH assay. Moreover, acetone ($9.48 \pm 0.13 \mu\text{g/mL}$) and methanol ($8.78 \pm 0.11 \mu\text{g/mL}$) extracts of leaves has shown exceptionally stronger antioxidant capacity than pure ascorbic acid ($10.35 \pm 0.1 \mu\text{g/mL}$) in ABTS assay. The activity of aqueous extract ($10.48 \pm 0.23 \mu\text{g/mL}$) of leaves was also found to be almost equivalent to ascorbic acid. The in vitro antioxidant activity of the mixture of leaves in the current study was found to be better than the reported values for individual male and female leaves of sea buckthorn (Gupta and Kaul, 2017; Singh et al., 2014; Šne et al., 2013)

The results obtained in the current work suggest that the antioxidant capacity of extracts is more likely due to concentrations of phenolic and flavonoid contents of the extracts. A similar trend was described in other studies published earlier which also found a strong correlation between phenolic contents of extracts and antioxidant capacity evaluated by different assays (Guo et al., 2017; Sen et al., 2013). The antioxidant potency of phenolic and flavonoid compounds is mainly influenced by the extra OH group (Rice-Evans et al., 1996), thus the presence of more OH groups on the aromatic ring of polyphenol favors the IC₅₀ results of DPPH and ABTS assays of acetone, methanol, and water extracts in the current study.

In most cases, leaves extracts had shown better antioxidant capacity than the berries extracts and these results are analogous to the previous reports by (Criste et al., 2020). Sharma et al., (2008) estimated the Trolox equivalent antioxidant capacity (TEAC) of ethanol extract of berries and leaves of Indian *H. rhamnoides* L. using DPPH and ABTS assay and observed it to vary in the

range of 8.33 and 31.37 mg/g and 37.16 and 39.55 mg/g, respectively. As discussed above, it is very difficult to identify the best antioxidant extract based on the TPC, TFC, or antioxidant activity. Thus, the global antioxidant score (GAS) was calculated and the results are presented in **Fig. 3.5 (c) and (d)**. The results of GAS were derived by integrating the raw data of TPC, TFC (**Table 3.6**), and the percentage scavenged at 50 µg/mL extract concentration in DPPH, and ABTS assay (**Table 3.8**). The GAS results were presented on a scale of 0 to 4 from worst to best antioxidant-containing extract.

Table 3.8: The percentage scavenged at 50 µg/mL extract concentration in DPPH and ABTS assay

	Berries extracts		Leaves extracts	
	DPPH	ABTS	DPPH	ABTS
HX	26.42±0.16	9.63±0.97	32±0.49	17.63±1.6
CL	13.69±2.6	11.68±1.2	25.13±1.3	11.53±1.7
EA	18.48±1.7	13.2±0.3	87.38±1.2	60.78±0.36
AC	67.42±1.1	17.41±1.6	99±1.5	98±0.13
MT	88.37±1.5	36.61±0.96	99.99±2.1	99.4±0.11
AQ	82.78±1.2	56.79±0.53	98.26±1.8	97.2±0.23

The results are presented in mean ± SD, n = 3; HX-hexane, CL-chloroform, EA-ethyl acetate, AC-acetone, MT methanol, and AQ-aqueous.

From GAS calculation, it was observed that aqueous extracts of berries had a maximum overall GAS value of 3.71, followed by methanol and acetone extracts. Whereas, among leaves extract, methanol extract exhibited a maximum GAS score of 3.93. These GAS values give a clear idea of understanding the best overall antioxidant extract and this mathematical calculation is now a day popular in many food and beverage industries (Purohit et al., 2021). For instance, in the case of berries extract, the TFC value of the berries-methanol extract was higher than its aqueous counterpart, whereas in the DPPH assay the results were in reverse order. GAS analysis computed

the overall antioxidant parameters (as explained above) and presented an overall best extract (aqueous in this case, despite TFC of methanol being higher).

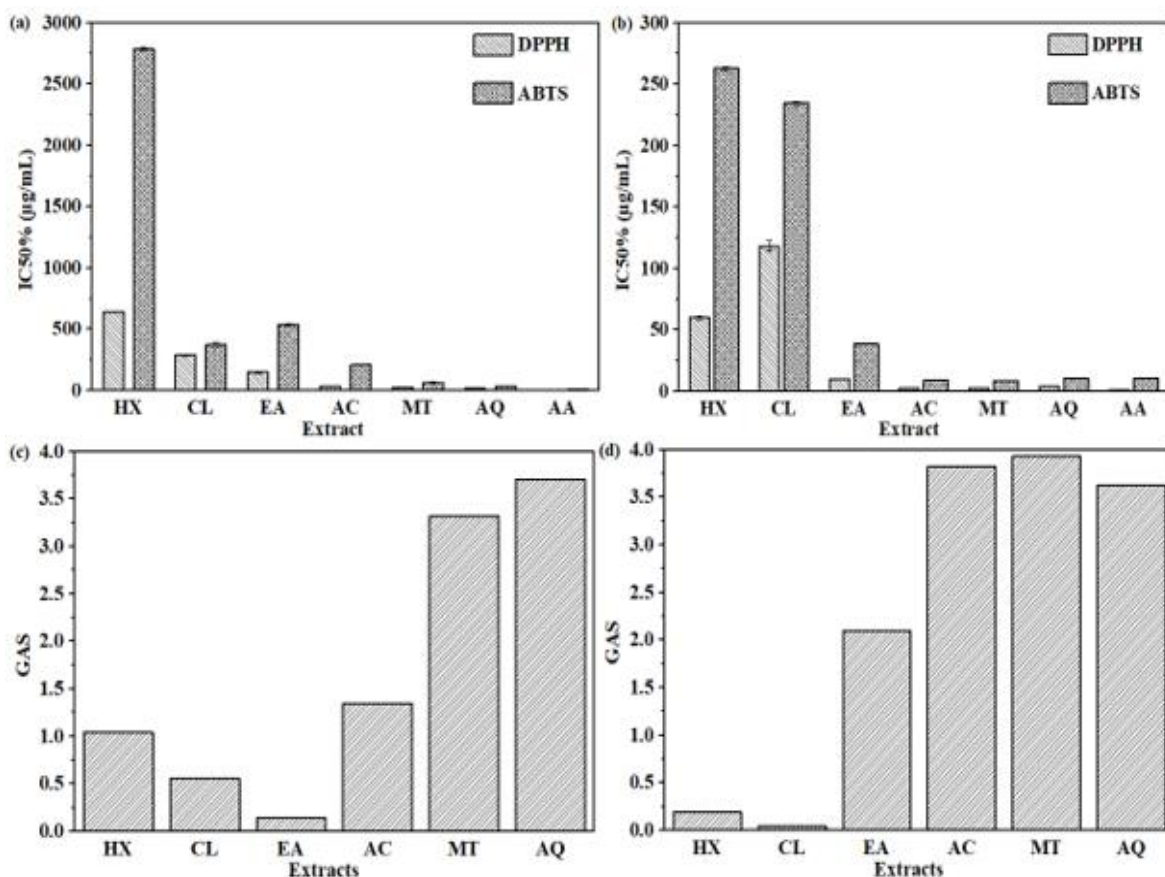


Fig.3.5: The antioxidant activity of extracts of (a) berries extract, (b) leaves extracts in DPPH and ABTS assays, (c) global antioxidant score for berries extracts, and (d) global antioxidant score for leaves extracts. AA- Ascorbic acid HX- hexane. CL- Chloroform, EA- Ethyl acetate, AC- acetone, MT- Methanol, and AQ- aqueous

3.4.10 Antibacterial activity

Sea buckthorn leaves and berries extracts were subjected to minimum inhibitory concentration (MIC) and zone of inhibition (ZoI) study to examine the antibacterial activity and the results obtained are presented in **Table 3.9** and **Table 3.10**, respectively. The bacterial strains used in this

study are reported to be foodborne pathogens that cause serious food poisoning or infections in humans (Jeong et al., 2010; Purohit, et al., 2021).

Table 3.9: Minimum inhibitory concentration ($\mu\text{g/mL}$) study of sea buckthorn berries and leaves extracts

Berries extracts	Gram-positive bacteria				Gram-negative bacteria			
	<i>S. aureus</i>	<i>B. subtilis</i>	<i>S. epidermidis</i>	<i>M. luteus</i>	<i>E. coli</i>	<i>K. pneumonia</i>	<i>E. aerogenes</i>	<i>P. aeruginosa</i>
HX	ND	ND	ND	ND	ND	ND	ND	ND
CL	ND	ND	ND	ND	ND	ND	ND	ND
EA	500	1000	1000	500	1000	1000	1000	500
AC	125	125	125	125	125	125	125	125
MT	125	125	125	125	125	125	125	125
AQ	500	250	500	250	250	250	250	250
Leaves extracts								
HX	500	500	1000	1000	1000	1000	1000	1000
CL	1000	1000	1000	1000	1000	1000	1000	1000
EA	62.5	125	125	62.5	250	125	125	125
AC	62.5	62.5	125	62.5	62.5	125	125	62.5
MT	31.3	31.3	62.5	62.5	62.5	125	62.5	125
AQ	125	125	250	125	125	500	125	250

ND-MIC not found, HX-hexane, CL-chloroform, EA-ethyl acetate, AC-acetone, MT-methanol, AQ-aqueous.

Chapter 3

All extracts (except hexane and chloroform extracts of berries) showed a noticeable antibacterial property. Acetone and methanol extracts of the berries showed strong antibacterial potency against all bacterial strains at 125 µg/mL MIC, followed by aqueous, and ethyl acetate extract. Despite higher TPC and antioxidant capacity, the aqueous extracts of whole berries (250 - 500 µg/mL) and leaves (125 - 500 µg/mL) exhibited lower antibacterial activity than methanol and acetone extracts. A similar trend was observed by Babaeekhou and Ghane, (2020) during their study on successive extraction of *Z. Officinale* rhizome with n-hexane, ethyl acetate, methanol, and distilled water. Criste et al., (2020), found the MIC of 12.5 - 25 g/mL with berries extracts and 6.2 - 25 g/mL with leaves extracts against *S. aureus*.

The methanol extracts of leaves exhibited maximum antibacterial activity with the lowest MIC of 31.3 µg/mL for *S. aureus* and *B. subtilis*. Similarly, acetone and ethyl acetate extracts showed MIC of 62.5 µg/mL for *S. aureus*, *M. luteus*, *E. coli*, *P. aeruginosa*, and *S. aureus*, *M. luteus*, respectively. The MIC of ethyl acetate, acetone, and methanol extracts of leaves in the current was lower than the crude (methanol, acetone, chloroform, and petroleum ether) leaf extracts of Indian *H. salicifolia* D. Don reported by Saikia and Handique, (2013) in the range from 250 to 500 µg/mL against *Staphylococcus aureus*, *Bacillus subtilis*, *Escherichia coli*, *Enterobacter aerogenes*, *Klebsiella pneumonia*, and *Pseudomonas aeruginosa*.

The ZoI analysis gave a clear idea about the antibacterial nature of various extracts from the leaves and berries of sea buckthorn. All the berries extracts (except hexane and chloroform) showed the highest ZoI against *B. Subtilis* strain (aqueous extract = 11.5 ± 2.1 mm) followed by *S. Epidermidis* and *M. luteus*. On the contrary, leaves extracts of sea buckthorn were effective for all four strains of gram-positive bacteria. Similarly, the leaves extracts (except chloroform extract) showed remarkable inhibition for gram-negative bacteria. Most of the leaves extracts were effective against

Table 3.10: Zone of Inhibition (mm) of sea buckthorn berries and leaves extracts

	Gram-positive bacteria				Gram-negative bacteria			
	<i>S. aureus</i>	<i>B. subtilis</i>	<i>S. epidermidis</i>	<i>M. luteus</i>	<i>E. coli</i>	<i>K. pneumonia</i>	<i>E. aerogenes</i>	<i>P. aeruginosa</i>
Berries								
extracts								
HX	ND	ND	ND	ND	ND	ND	ND	ND
CL	ND	ND	ND	ND	ND	ND	ND	ND
EA	ND	2.5±0.7	ND	ND	ND	ND	2±0.7	ND
AC	ND	6.5±0.7	5.5±2.1	6	ND	ND	5.5±2.1	2±0.8
MT	2±1.4	8±1.4	5	5±1.4	ND	6.5±0.7	5	ND
AQ	0.5	11.5±2.1	4.5±0.7	3	ND	ND	ND	ND
Leaves								
extracts								
HX	2.5±0.7	6±1.4	8.5±0.7	3	ND	ND	2.5±0.1	4.5±0.7
CL	2±0.7	4±1.4	3	3±0.7	ND	ND	ND	ND
EA	6.5±0.7	15.5±0.7	15	7.5±2.1	10.5±0.7	10.5±0.7	9	6±1.4
AC	8±1.4	18±1.4	16±1.4	10	12	12.5±0.7	13.5±1.4	12.5±1.4
MT	13±2.8	19	17.5±0.7	9.5±0.7	14	15.5±2.1	17.5±0.7	13.5
AQ	7.5±0.7	5	9.5±0.7	5	9	6±0.8	12.5±0.7	10

The results are presented in mean ± SD, n = 3; ND, no zone of inhibition, HX-hexane, CL-chloroform, EA-ethyl acetate, AC-acetone, MT methanol, and AQ-aqueous.

Chapter 3

the tough *E. coli* (methanol extract = 14 mm) which makes the sea buckthorn leaves extract a tough antibacterial agent. Minimum to zero inhibition by berries extracts could be because of the poor penetration capacity of these extracts into the hard peptidoglycan layer of the gram-negative bacteria. The antibacterial activity of leaves extracts against *S. aureus* and *E. coli* was in the range of those obtained by Kumar et al., (2013). Upadhyay et al., (2010) compared the antibacterial properties of sea buckthorn leaf extracts and found that hydroalcoholic extract (19 mm) has better activity than aqueous extract (14 mm) with higher ZoI (19 mm) for *B. cereus*.

The difference in antibacterial activity of extracts is attributed to the content of bioactive compounds such as vitamins, tannins, and polyphenol compounds, especially quercetin derivatives, gallic acid, caffeic acid, and ferulic acid. It was also noticed that the antibacterial effect of phenolic compounds was more prominent than flavonoids (El-chaghaby et al., 2014). The inhibitory characteristics of phenols are related to the site(s) and the number of conjugated hydroxyl groups in such a way that more hydroxylation results in more toxicity to microorganisms (Cowan, 1999). Successive solvent extracts of berries and leaves of *H. salicifolia* were more effective against Gram-positive bacteria than Gram-negative. This renders Gram-negative bacteria providing hydrophilic molecules deposited in the outer membrane that objects to the leakage of hydrophobic materials into the cytoplasm.

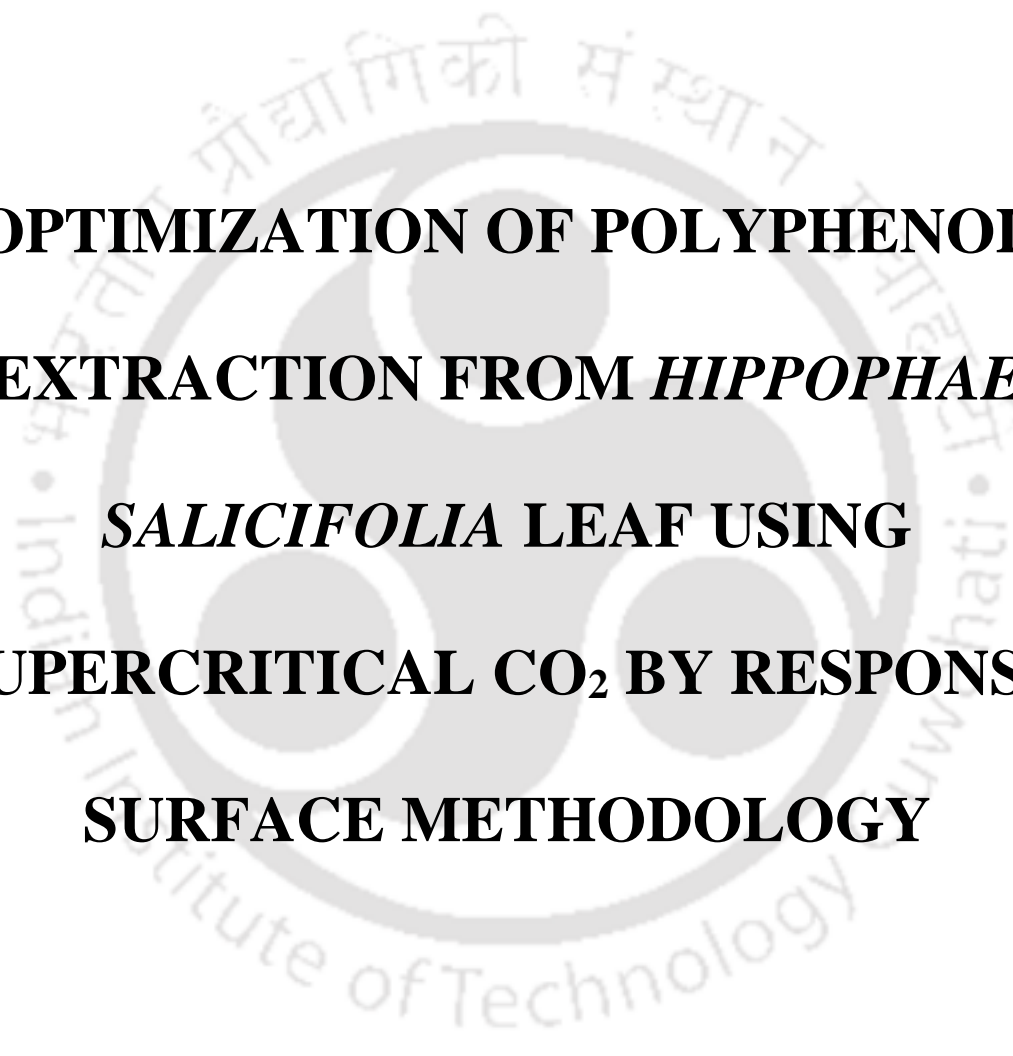
3.5 Summary

The berries and the leaves of *H. salicifolia* grown in North-East India showed significant dietary and bioactive properties. The conclusions are summarized as follows:

- The leaves are found to be more nutritious and biologically active than the berries. Vitamin C was found to be the predominant phytonutrient found in the berries, while the total soluble sugar content of the leaves was the highest. Potassium was the predominant element found in the berries and

leaves. Sodium and calcium were the second most abundant element in the berries and leaves, respectively.

- Extracts of berries and the mixture of leaves samples obtained by successive solvent extraction were investigated for their polyphenols, antioxidant and antibacterial properties. Total phenolic content was highest in leaves-methanol extract (157.97 ± 0.86 mg GAE/g) followed by berries-aqueous extract (48.45 ± 1.94 mg GAE/g), while total flavonoid was predominant in leaves-acetone extract (75.64 ± 3.21 mg QE/g) and berries-methanol extract (28.93 ± 2.08 mg QE/g).
- The methanol extract of the leaves had approximately ≥ 4 to 23-fold higher levels of gallic acid at 144.09 ± 0.64 mg/g than extracts from the whole berry.
- The acetone and methanol extracts of the leaves, with IC₅₀ of 9.48 ± 0.13 and 8.78 ± 0.11 $\mu\text{g/mL}$, respectively, exhibited a better antioxidant efficacy than pure ascorbic acid (10.3 ± 0.1 $\mu\text{g/mL}$) in ABTS assay.
- Best antibacterial activity was observed by methanol extracts against eight different strains, with higher activities for leaves extract than the berries. The methanol extract of the leaves had the least MIC (31.3 $\mu\text{g/mL}$) for *S. aureus*, *B. subtilis*, *M. luteus*, *E. coli*, and *E. aerogenes* and the highest ZoI (19 mm) against *B. subtilis*.
- Overall, the present research demonstrates the importance of *H. salicifolia* berries and leaves as an option to be utilized as bioactive ingredients, dietary supplements, food preservatives, and pharmaceuticals.



**OPTIMIZATION OF POLYPHENOL
EXTRACTION FROM *HIPPOPHAE
SALICIFOLIA* LEAF USING
SUPERCRITICAL CO₂ BY RESPONSE
SURFACE METHODOLOGY**

Published in

Journal of 3 Biotech. 12 (11):292, 2022.



OPTIMIZATION OF POLYPHENOL EXTRACTION FROM *HIPPOPHAE SALICIFOLIA* LEAF USING SUPERCRITICAL CO₂ BY RESPONSE SURFACE METHODOLOGY**4.1 Background**

Phenolic and flavonoid compounds are described to be the major contributor to the biological activity of sea buckthorn leaf. The most widely practiced extraction methods for polyphenolic compounds involve organic solvents at high temperatures that led bioactive compounds to thermal degradation, hydrolysis, and detrimental solvent residues in the final product. Supercritical carbon dioxide (SC-CO₂) extraction is a safe, inert, non-toxic, and eco-friendly alternative approach that allows quicker extraction at a reduced temperature and provides a solvent-free product. Nevertheless, pure CO₂ is inherently non-polar and not useful to extract high molecular mass polar compounds. The use of cosolvent as a modifier and/or entrainer makes the extraction of polar compounds possible by augmenting the fluid density and diffusivity towards polar compounds embedded in the cell wall. Hence, this chapter is aimed to optimize polyphenols extraction from *Hippophae salicifolia* leaves using SC-CO₂ for the highest yield of extraction with maximum TPC and best IC₅₀ and to understand the effect of extraction parameters.

4.2 Overview

In this study, an eco-friendly SC-CO₂ extraction of phenolic compounds from *Hippophae salicifolia* leaves was investigated. The process of SC-CO₂ extraction was optimized using a central composite design followed by a response surface methodology to achieve maximum yield of extraction, TPC, and

antioxidant activity. The central composite design (CCD) was used to establish an experimental design for RSM. The effect of the pressure, temperature, carbon dioxide flow rate, and co-solvent amount was scrutinized using analysis of variance (ANOVA). Under optimized condition (25.13 MPa, 47.53°C, 14.47 g/min, and 2.43%), the experimental data (yield of extraction: 4.38%, TPC: 84.31 mg GAE/g, and IC₅₀: 41.94 µg/mL) showed good agreement with the predicted values (yield of extraction: 4.53%, TPC: 83.37 mg GAE/g, and IC₅₀: 40.2 µg/mL). Nine polyphenolic compounds: gallic acid, caffeic acid, ferulic acid, vanillic acid, p-coumaric acid, quercetin, myricetin, kaempferol, and rutin were analyzed using HPLC. SC-CO₂ extraction was more selective for ferulic acid, myricetin, and quercetin extraction. The study results revealed that SC-CO₂ extract had significant antibacterial activity against eight bacterial strains. The result of the research indicates the status of utilizing SC-CO₂ extract of *Hippophae salicifolia* leaf as functional foods and ingredients, food supplements, and food preservatives.

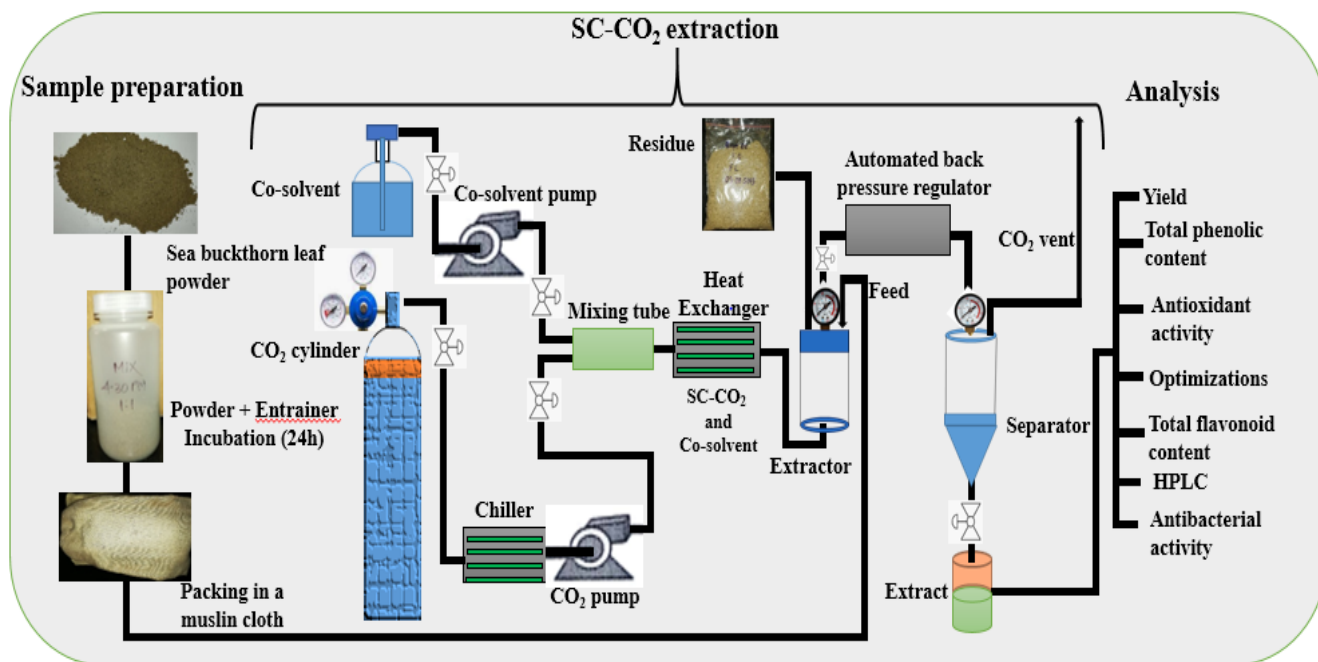


Fig. 4.1: Graphical Abstract

4.3 Results and Discussion

4.3.1 Preliminary studies

4.3.1.1 Comparison between leaves from the male and female plant

Conventional Soxhlet extraction of FL and ML of *H. salicifolia* was performed under reflux conditions using ethanol. To select the best sample for the SC-CO₂ extraction study, a comparison between the yield of extraction, TPC, and IC₅₀ of Soxhlet extracts from female (FL) and male leaf (ML) of sea buckthorn plant was conducted. FL extract had a higher extraction yield and higher TPC, TFC, and antioxidant activity than ML extract (**Table 4.1**). Thus, FL was chosen for the optimization study due to the higher yield of extraction, TPC, and antioxidant activity.

Table 4.1. Yield, TPC, TFC, and IC₅₀ of extracts obtained from Soxhlet and SC-CO₂ extraction

Sample	Yield (%)	TPC (mg GAE/g)	TFC (mg QE/g)	IC ₅₀ (µg/mL)
FL (Sox)	8.97	221.28±3.84	120.29±2.68	4.78±0.05
ML(Sox)	8.27	158.69±6.11	73.2±0.67	6.62±0.28
FL(1:0) _{1h}	1.46	43.04±2.34	69.63±2.09	127.94±0.37
FL(1:0.5) _{1h}	1.53	53.36±4.35	80.81±2.69	106.11±0.75
FL(1:1) _{1h}	1.96	56.31±1.47	87.9±2.11	96.94±1.76
FL(1:1.5) _{1h}	2.07	57.93±3.7	89.96±3.87	95.48±1.25
FL(1:1) _{2h}	3.16	65.19±2.1	82.62±3.01	83.97±1.34
FL(1:1) _{3h}	3.82	59.97±1.04	79.16±3.63	82.58±1.63

Results are given as mean ± SD, n = 3, FL(Sox) and ML(Sox) – extracts from female and male leaves obtained by Soxhlet extraction, respectively. FL (1:0), FL (1:0.5), FL (1:1), FL (1:1.5) extracts obtained from SC-CO₂ extraction with leaf-to-entrainer ratio of 1:0, 1:0.5, 1:1, and 1:1.5, respectively. The subscripts, 1 h, 2 h, and 3 h refers to extraction time.

4.3.1.2 Effect of leaf powder-to-entrainer ratio

SC-CO₂ extraction of FL leaves was carried out at the minimal extraction variables utilized in the optimization study (18 MPa, 40°C, 10 g/min CO₂ flow rate, and 1% co-solvent). Ethanol was used as a co-solvent and entrainer. The solubility of the solute, TPC, and antioxidant activity of the extracts as a function of powder-to-entrainer ratios of 1:0.5, 1:1, and 1:1.5 (w/v) were studied. As the leaf-to-entrainer ratio varied from (1:0) to (1:1), the extraction yield, the TPC, and the antioxidant activity of extracts were progressively increased, as shown in **Table 4.1**. FL(1:1.5) extract resulted in the highest extraction yield, while the TPC, TFC, and antioxidant activity were lower than the FL(1:1) extract. The powder-to-entrainer ratio (FL(1:1)), which gives a higher yield of extraction with higher TPC, TFC, and lower IC₅₀ value was selected for the optimization study.

4.3.1.3 Effect of extraction time

Following the determination of the best powder-to-entrainer ratios, the influence of extraction time on extraction yield, TPC, TFC, and IC₅₀ was also examined at 1 h, 2 h, and 3 h (**Table 4.1**). When extraction time varied from 1 h to 3 h, the extraction yield increased from 1.16% to 3.82%, while TPC, TFC, and antioxidant activity of the extract decreased as extraction time is extended from 2 h to 3 h. In other words, a 2 h extraction period was found to provide an extract with a higher TPC and a lower IC₅₀. Hence, a 2 h extraction time was chosen for the optimization study.

4.3.2 Fitting the Models and analysis of ANOVA

A CCD technique was used for the optimization of extraction yield, TPC, and IC₅₀. A CCD of four independent variables coded at five levels (-2, -1, 0, +1, -2) was applied and gives 30 ($2^n + 2n + 6$) experiments (**Table 4.2**). Evaluation of yield of extraction, TPC, and IC₅₀ of all experimental runs was performed (**Table 4.3**), and the results were analyzed by multiple regression analysis. Sources of

Chapter 4

variances were used to determine optimum extraction conditions (**Table 4.4** and **Table 4.5**). The objective of this study was to achieve the extraction condition that provides the highest yield of extraction with the highest TPC and lowest IC50. The quadratic model equations fitted to the experimental data to predict the yield of extraction, TPC, and IC50 are given in equations (4.1-4.3):

$$\begin{aligned} \text{Yield (\%)} = & -16.6 + 0.27X_1 + 0.37X_2 + 0.57X_3 + 3.47X_4 + 0.003X_1X_2 + 0.0006X_1X_3 - 0.04X_1X_4 \\ & - 0.002X_2X_3 - 0.0002X_2X_4 - 0.03X_3X_4 - 0.01X_1^2 - 0.004X_2^2 \\ & - 0.02X_3^2 - 0.35X_4^2 \end{aligned} \quad (4.1)$$

$$\begin{aligned} \text{TPC (mg GAE / g)} = & -177.8 + 4.04X_1 + 5.94X_2 + 6.05X_3 + 22.94X_4 - 0.04X_1X_2 - 0.03X_1X_3 \\ & - 0.02X_1X_4 + 0.03X_2X_3 + 0.16X_2X_4 - 0.47X_3X_4 - 0.03X_1^2 - 0.06X_2^2 \\ & - 0.19X_3^2 - 5.26X_4^2 \end{aligned} \quad (4.2)$$

$$\begin{aligned} \text{IC50 (\mu g / mL)} = & +590.15 - 8.06X_1 - 13.75X_2 - 8.74X_3 - 68.39X_4 + 0.12X_1X_2 + 0.003X_1X_3 \\ & - 0.49X_1X_4 - 0.02X_2X_3 + 0.2X_2X_4 + 0.32X_3X_4 + 0.07X_1^2 + 0.12X_2^2 \\ & + 0.3X_3^2 + 14.81X_4^2 \end{aligned} \quad (4.3)$$

Table 4.2. Extraction process variables and their levels for central composite design

Independent variables	Symbol	Unit	Variable levels				
			$-\alpha$	-1	0	+1	$+\alpha$
Pressure	X_1	MPa	11	18	25	32	39
Temperature	X_2	° C	30	40	50	60	70
CO ₂ flow rate	X_3	g/min	5	10	15	20	25
Amount of cosolvent	X_4	%	0	1	2	3	4

The results of second-order response surface models were thoroughly analyzed with ANOVA to ensure the model fit and estimate individual model coefficients test for lack-of-fit (**Table 4.4**). The greater F values of the models for the yield of extraction, TPC, and IC50 (453.55, 1887.07, and 3958.52,

Table 4.3. Central Composite Design and actual data of performed experiments

Std	X ₁ : Pressure(MPa)	X ₂ : Temperature(°C)	X ₃ : CO ₂ flow rate (g/min)	X ₄ : Amount of cosolvent (%)	Yield (wt.%)	TPC (mg GAE/g)	IC50 (µg/mL)
1	18 (-1)	40 (-1)	10 (-1)	1 (-1)	2.21	62.51±0.5	78.45±4.8
2	32 (+1)	40 (-1)	10 (-1)	1 (-1)	2.28	73.26±1.1	75.74±1.7
3	18 (-1)	60 (+1)	10 (-1)	1 (-1)	2.21	51.41±0.9	84.11±0.1
4	32 (+1)	60 (+1)	10 (-1)	1 (-1)	3.11	51.81±2.6	114.5±3.1
5	18 (-1)	40 (-1)	20 (+1)	1 (-1)	2.33	67.12±4.8	78.49±1.4
6	32 (+1)	40 (-1)	20 (+1)	1 (-1)	2.34	73.53±1.9	75.43±6.8
7	18 (-1)	60 (+1)	20 (+1)	1 (-1)	1.92	62.41±3.4	79.94±5.6
8	32 (+1)	60 (+1)	20 (+1)	1 (-1)	2.97	57.54±4.3	111.45±4.2
9	18 (-1)	40 (-1)	10 (-1)	3 (+1)	4.16	69.07±6.5	64.77±1.5
10	32 (+1)	40 (-1)	10 (-1)	3 (+1)	2.86	79.18±5.7	48.45±9.3
11	18 (-1)	60 (+1)	10 (-1)	3 (+1)	4.07	64.33±2.7	78.54±0.2
12	32 (+1)	60 (+1)	10 (-1)	3 (+1)	3.77	64.28±2	95.11±5.1
13	18 (-1)	40 (-1)	20 (+1)	3 (+1)	3.54	64.35±6.4	71.43±1.3
14	32 (+1)	40 (-1)	20 (+1)	3 (+1)	2.35	70.15±4.9	54.69±1.9
15	18 (-1)	60 (+1)	20 (+1)	3 (+1)	3.14	65.93±5.6	80.42±2.1
16	32 (+1)	60 (+1)	20 (+1)	3 (+1)	2.95	60.57±0.9	98.59±1.3
17	11 (-α)	50 (0)	15 (0)	2 (0)	3.12	74.55±2.5	48.82±1.5
18	39 (+α)	50 (0)	15 (0)	2 (0)	2.91	80.34±2.9	63.17±0.8
19	25 (0)	30 (-α)	15 (0)	2 (0)	2.51	68.01±5.3	65.43±3.2
20	25 (0)	70 (+α)	15 (0)	2 (0)	3.07	47.58±8.1	114.14±1.4
21	25 (0)	50 (0)	5 (-α)	2 (0)	3.25	63.13±6.2	71.41±0.9
22	25 (0)	50 (0)	25 (+α)	2 (0)	2.51	64.83±3.6	73.89±4.3
23	25 (0)	50 (0)	15 (0)	0 (-α)	2.15	57.09±6.3	115.17±0.3
24	25 (0)	50 (0)	15 (0)	4 (+α)	4.03	66.41±2.1	88.25±0.0
25	25 (0)	50 (0)	15 (0)	2 (0)	4.35	82.32±2.1	43.13±0.6
26	25 (0)	50 (0)	15 (0)	2 (0)	4.38	82.47±3.2	43.01±0.1
27	25 (0)	50 (0)	15 (0)	2 (0)	4.53	82.11±2.1	43.67±1.4
28	25 (0)	50 (0)	15 (0)	2 (0)	4.47	82.53±4.7	42.84±0.07
29	25 (0)	50 (0)	15 (0)	2 (0)	4.49	82.76±1.2	42.52±3.1
30	25 (0)	50 (0)	15 (0)	2 (0)	4.41	83.06±3.8	42.11±1.3

Results are given as mean ± SD, n = 3, GAE-gallic acid equivalent.

Chapter 4

respectively) with very fewer p -values (<0.0001) indicate that the three models are extremely important to represent the relationship between the independent variables and responses. All the linear terms (X_1 , X_2 , X_3 , and X_4); all the quadratic terms (X_1^2 , X_2^2 , X_3^2 , X_4^2); and the majority of the cross-terms (X_1X_2 , X_1X_4 , X_2X_3 , X_3X_4) are significantly important parameters with lower P -values. On the other hand, the interaction between X_1X_3 , X_2X_4 on the yield of extraction, X_1X_4 on TPC, and X_1X_3 on IC50 are not significant. The lack of fit for each response was insignificant, with F -value and P -value of 0.5324 and 0.8147 (for extraction yield); 1.04 and 0.5145 (for TPC); and 0.9759 and 0.547 (for IC50), indicating that the developed model was suitable for the experimental data and showed good correlations between the reproducible results.

Regression coefficients, Standard Deviation (Std. dev.), and Coefficient of the variation (CV %) for responses obtained from CCD are shown in **Table 4.5**. The model's accuracy was judged by the regression coefficient (R^2) and the suitability of the model was confirmed by its value. The values of R^2 implied that 99.76%, 99.94%, and 99.97% of the model behavior could be interpreted for the extraction yield, TPC, and IC50, respectively. The predicted R^2 agreed with the adjusted R^2 , which signifies the noticeable statistical correlation between each response's actual and predicted values. The plot of model-predicted values against experimental data of the yield of extraction, TPC, and IC50 envisioned the fitting qualities of the developed model equations, as shown in **Fig. 4.2 (a-c)**.

4.3.3 Influence of extraction variables on the yield of extraction, TPC, and IC50

To estimate the best extraction condition for the maximum yield of extraction, TPC, and minimum IC50, the effects of the linear, cross, and square extraction variables on the extraction process were studied with the help of three-dimensional response surface plots. The plots were established by varying two

process variables at a time while keeping the others at their central point (0) using design expert software as shown in **Fig. 4.3 (a-l)** and **Fig 4.4 (a-d)**.

Table 4.4. ANOVA for extraction yield, total phenolic content, and IC50 obtained from central composite design

Sources of variance	Yield		Total Phenolic Content		IC50	
	<i>F</i> -value	<i>p</i> -value	<i>F</i> -value	<i>p</i> -value	<i>F</i> -value	<i>p</i> -value
Model	453.55	< 0.0001	1887.07	< 0.0001	3958.52	< 0.0001
X ₁ -Pressure	23.59	0.0002	439.79	< 0.0001	1110.02	< 0.0001
X ₂ -Temperature	127.9	< 0.0001	5392.32	< 0.0001	12700.9	< 0.0001
X ₃ -CO ₂ flow rate	267.12	< 0.0001	30.46	< 0.0001	36.7	< 0.0001
X ₄ -Cosolvent	1585.13	< 0.0001	1178.19	< 0.0001	3794.59	< 0.0001
X ₁ X ₂	282.37	< 0.0001	1006.6	< 0.0001	4082.95	< 0.0001
X ₁ X ₃	1.81	0.1983	201.78	< 0.0001	0.846	0.3722
X ₁ X ₄	473.23	< 0.0001	2.62	0.1265	659.6	< 0.0001
X ₂ X ₃	28.52	< 0.0001	301.09	< 0.0001	46.71	< 0.0001
X ₂ X ₄	0.017	0.8981	357.89	< 0.0001	219.77	< 0.0001
X ₃ X ₄	130.41	< 0.0001	766.12	< 0.0001	147.52	< 0.0001
X ₁ ²	1102.94	< 0.0001	430.73	< 0.0001	1114.27	< 0.0001
X ₂ ²	1468.97	< 0.0001	9365.24	< 0.0001	13654.22	< 0.0001
X ₃ ²	1316.28	< 0.0001	5306.57	< 0.0001	5553.69	< 0.0001
X ₄ ²	992.57	< 0.0001	6637.92	< 0.0001	21406.42	< 0.0001
Lack of Fit	0.5324	0.8147	1.04	0.5145	0.9759	0.547

4.3.4 Effect of pressure and temperature

The effect of extraction variables on the yield of extraction, TPC, and IC50 is presented in **Fig. 4.3 (a-f)**, **Fig. 4.3 (g-l)**, and **Fig. 4.4 (a-d)**, respectively. The regression analysis of the source of variances of the yield of extraction, TPC, and IC50 of leaves extract data revealed that the extraction yield was

Chapter 4

significantly ($p < 0.05$) affected by pressure, temperature, and the interaction between pressure and temperature. Increasing pressure at lower temperatures reduces SC-CO₂ diffusivity, initiates solid matrix compaction, lowers the void fraction, minimizes solvent interaction with matrix pores, and hence hinders solute dissolution and solubility. Because of this reason, at a lower temperature (40 °C) the increase in pressure from 25 to 32 MPa resulted in a gradual reduction in extraction yield (**Fig. 4.3 (a)**). At higher temperatures (60 °C), however, the opposite phenomenon was observed, since the increase in pressure at elevated temperatures upsurges the density of the solvent and the solvating power. The extraction yield improved with an increase in temperature up to 55 °C at higher pressure (32 MPa), while the extraction yield was best around 50 °C at lower pressure (18 MPa). At 25 MPa and 50 °C, the maximum extraction yield achieved was 4.35%. Gadkari et al., (2013) observed similar behavior while studying SC-CO₂ extraction from fresh frozen tea leaves.

Table 4.5. Regression coefficients, Standard Deviation (Std. dev.), and Coefficient of the variation (CV%) for extraction yield, TPC, and IC50

	Yield	TPC	IC50
Std. Dev.	0.0576	0.3384	0.53
Mean	3.21	68.49	72.92
CV%	1.79	0.4942	0.7268
R^2	0.9976	0.9994	0.9997
Adjusted R^2	0.9954	0.9989	0.9995
Predicted R^2	0.9914	0.9975	0.9988
Adeq Precision	61.08	146.92	193.6

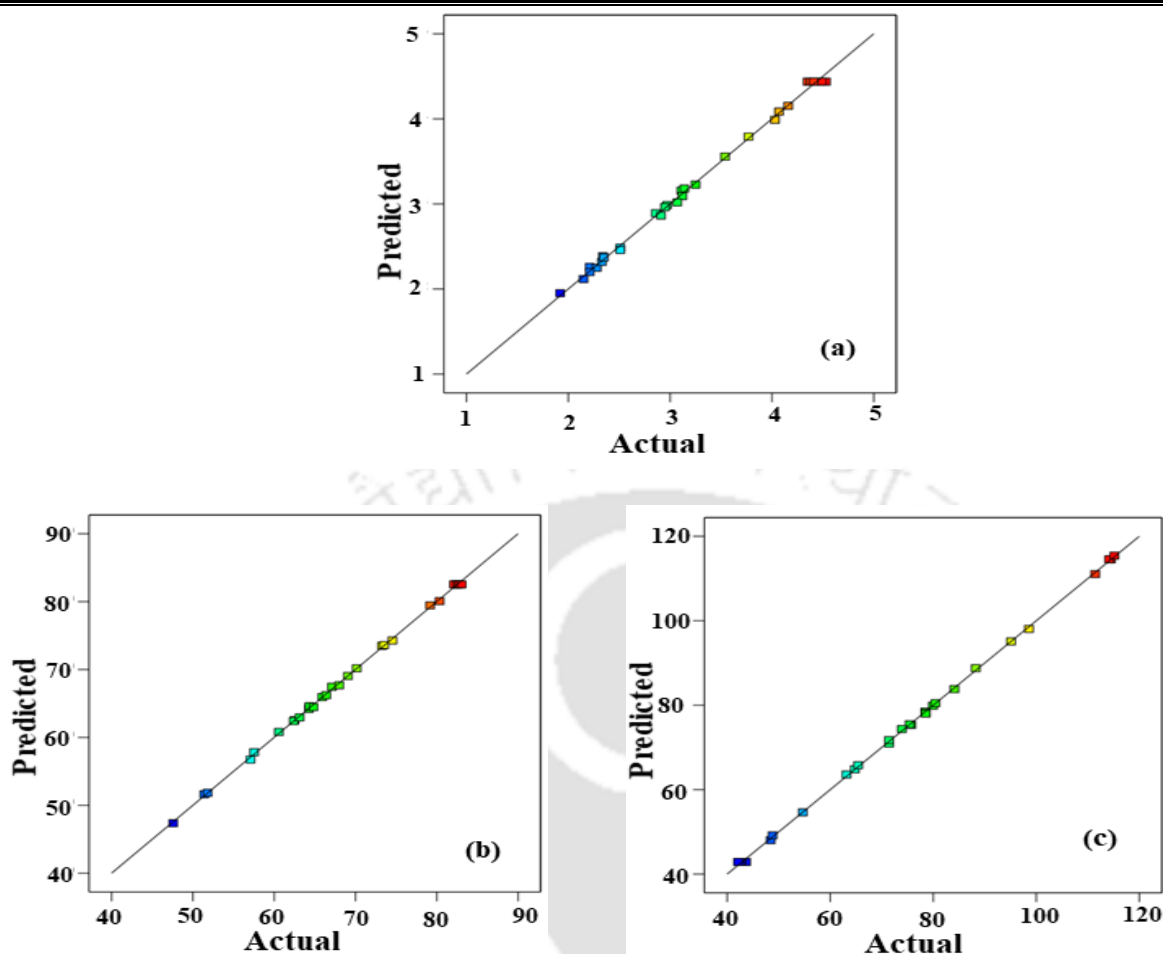


Fig. 4.2: Plots of model predicted values versus actual experimental values for (a) yield of extraction, (b) TPC, and (c) IC₅₀ of SC-CO₂ extracts

The effect of pressure and temperature on the TPC of extracts is related to alterations in the selectivity of SC-CO₂ to solutes, which depends on amendments in the polarity and density of SC-CO₂. TPC was highest at higher pressures and lower temperatures and its value decreased with temperature (**Fig. 4.3 (g)**). In the temperature range from 40-50 °C, the increase in pressure resulted in a slight increase in TPC, and beyond 50 °C, TPC decreased with increased pressure. Even though an increase in temperature favors the extraction of phenolic compounds from plant tissues, the TPC of extracts was limited because of the thermal degradation that occurs above 50 °C. Zulkafli et al., (2014) have reported that the phenolic compound extraction was reduced by increasing the temperature at reduced pressure and vice versa.

Chapter 4

The concentration of phenolic compounds contained in the extracts is usually ascribed to the antioxidant activity. Thus, at the greater pressure and lower temperature, where TPC was lowest, the IC₅₀ value reached its maximum, as shown in **Fig. 4.4 (a-d)**. At lower pressure, the IC₅₀ value decreased when the temperature increased from 45 °C to 60 °C. A similar phenomenon was reported on the antioxidant activity of SC-CO₂ rosemary extract by Genena et al., (2008).

The interaction of pressure and CO₂ flow rate significantly impacted TPC but not extraction yield. The best yield of extraction was achieved at around 25 MPa and 14.5 g/min CO₂ flow rate. The RSM plateau of pressure versus CO₂ flow rate indicated that an increase in the pressure at a lower CO₂ flow rate (10 g/min) improved TPC extraction (**Fig. 4.3 (h)**). As reported by Roberto et al., (2010), the increase in pressure at a constant temperature increases the CO₂ density, resulting in increased solvation power and hence solubility of polyphenolic compounds. Whereas variation in the pressure at a higher CO₂ flow rate (20 g/min) did not affect the TPC.

4.3.5 Effect of pressure and CO₂ flow rate

The interaction of pressure and CO₂ flow rate significantly impacted TPC but not the extraction yield. The best yield was achieved at around 25 MPa and 14.5 g/min CO₂ flow rate. The RSM plateau of pressure versus CO₂ flow rate indicated that an increase in the pressure at a lower CO₂ flow rate (10 g/min) improved TPC extraction (Fig. 2 (h)). As reported by Roberto et al., (2010), the increase in pressure at constant temperature increases the CO₂ density, resulting in increased solvation power and hence solubility of polyphenolic compounds. Whereas variation in the pressure at a higher CO₂ flow rate (20 g/min) did not affect the TPC.

4.3.6 Effect of pressure and amount of cosolvent

The interaction between pressure and amount of cosolvent significantly ($P < 0.05$) affected the yield of extraction and IC₅₀. The increase in co-solvent concentration resulted in a greater extraction yield across all pressure ranges, as presented in **Fig. 4.3 (c)**. Co-solvent had a maximum effect on the yield of extraction (4.5%) towards the maximum percentage (3%) and minimum pressure (18-20 MPa). The extent of yield increment as a function of the percentage of the co-solvent was faster at a lower pressure. This means employing co-solvent at lower pressure improves extraction efficiency, while an increase in pressure decreases the diffusivity of co-solvent into the matrix and deteriorates the extraction efficiency. This could be considered an economic benefit of using co-solvent in the SC-CO₂ extraction. On the other hand, the interaction between pressure and co-solvent amount did not significantly affect TPC. TPC was at its peak at approximately 2.4% co-solvent, as presented in **Fig. 4.3 (i)**.

The cosolvent was found to be the most important factor in extracting biologically active phenolic compounds from sea buckthorn leaves. The addition of co-solvent influences the extraction by distorting the matrix-analyte diffusion process and increasing the analyte's solubility and desorption. However, the incorporation of surplus co-solvent might alter the state of SC-CO₂ and lead to a decrease in extraction selectivity and efficiency. That might be the reason for a slight decrease in TPC after 2.4% co-solvent. Co-solvent flow rate showed the most substantial affirmative effect on the radical scavenging activity. These results granted the findings of Floch et al., (1998) and Sajfrtova and Sovova, (2012) on the SC-CO₂ extraction yield of a polar component from leaves of Olive and sea buckthorn, respectively.

4.3.7 Effect of temperature and CO₂ flow rate

The effect of the CO₂ flow rate on the extraction yield is depicted in **Fig. 4.3 (d)**. As the CO₂ flow rate increased up to 16 g/min, the extraction yield increased. This could be attributed to the enhancement of mass transfer of the system by SC-CO₂. However, a further increase in CO₂ flow rate moderated the yield

Chapter 4

of extraction. This could be due to a reduction in the required contact time between CO₂ and the plant matrix for the equilibrium separation process. Yet, at higher temperatures, the extraction yield decreased due to the reduced density of SC-CO₂.

The effect of temperature and the CO₂ flow rate was one of the most critical factors for the extraction of phenolic compounds. TPC was at its highest around 47°C, with a CO₂ flow rate of 14 g/min, as presented in **Fig. 4.3 (j)**. An identical effect of temperature on the extraction of bioactive compounds from *Camellia sinensis* L. leaves was reported by Maran et al., (2015). A rise in temperature results in the upsurge of solute vapor pressure which eventually increases the solubility of phenolic compounds with the increase in vapor pressure. Though the solvating power of SC-CO₂ decreased with density, an increase in temperature improved the extraction rate, perhaps due to the dominance effect of vapor pressure over density.

4.3.8 Effect of temperature and co-solvent

The yield of extraction was highest at around 47°C and 2.4% co-solvent (**Fig. 4.3 (k-l)**). An increase in the co-solvent up to around 2.4% augmented the TPC of extracts in all ranges of extraction temperatures. Though the increase in co-solvent intensifies the extraction yield, TPC was not eternally in an affirmative proportion to the yield. As ethanol is polar, it is expected that the solubility of polyphenols increases with the increase in the density of the binary mixture.

The increases in the density of the binary mixture enhance co-solvent-solute interactions, assists matrix swelling, improve the osmotic diffusion process, and the solubilization of polar compounds (Veggi et al., 2014). Hence, extraction with better TPC and antioxidant activity could be achieved when cosolvent is employed. Our findings on the effect of co-solvent are in favor of reports of various researchers on the

extraction of bioactive compounds (Maran et al., 2015; Rodrigues et al., 2018; Solana et al., 2014; Song et al., 2019; Valadez-Carmona et al., 2018; Zulkafli et al., 2014).

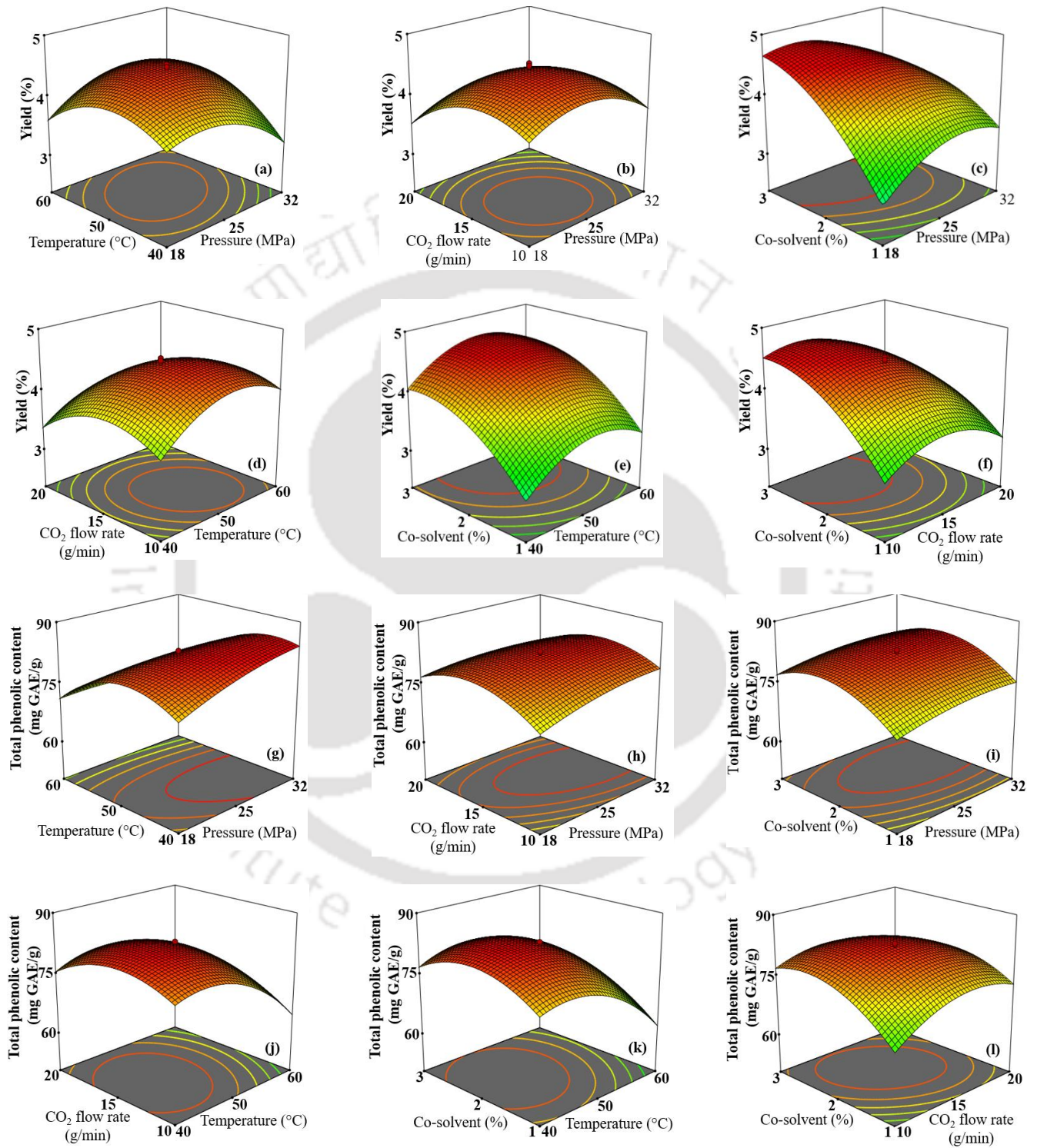


Fig. 4.3. Influence of extraction variables on extraction yield (a-f), total phenolic content (g-l)

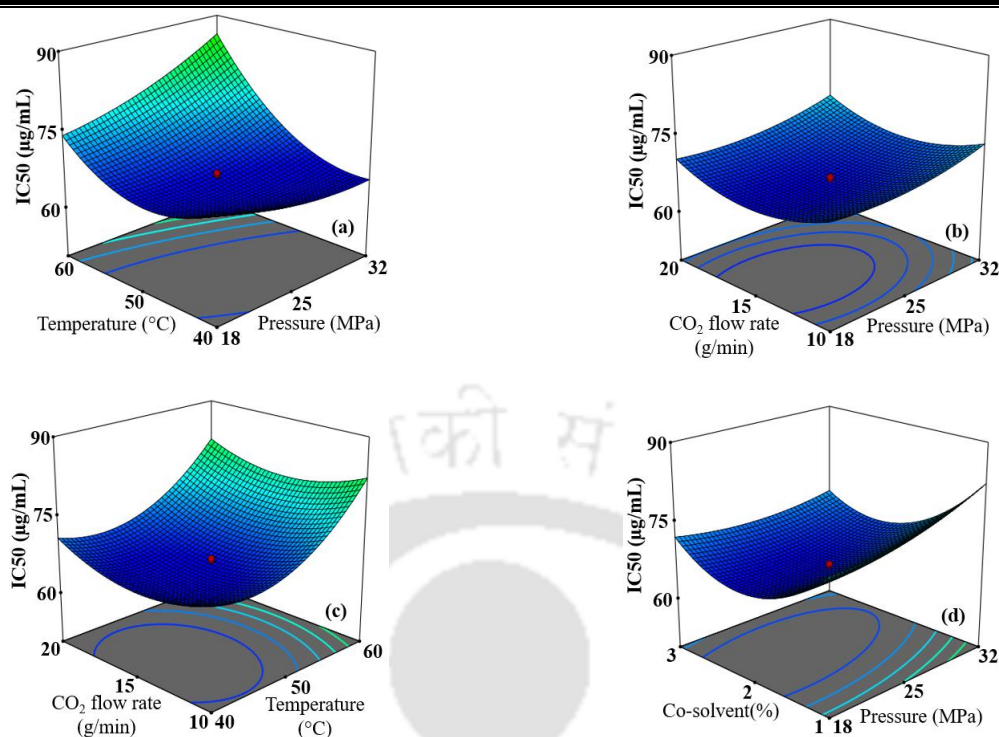


Fig. 4.4. Influence of extraction variables on IC50 (a-d)

4.3.9 Effect of CO₂ flow rate and cosolvent

Fig. 4.3 (f) shows that a higher yield of extraction was viewed when the amount of cosolvent reached its highest level at the lower ranges of CO₂ flow rate. This is because, at a lower CO₂ flow rate, the lipid can efficiently be removed from the sample matrix and the inner matrix containing desired polyphenolic compounds can be extracted with co-solvent. **Fig. 4.3 (l)** shows that a continuous rise in the co-solvent percentage increased the extraction yield but not the content of polyphenolic compounds. Ariff et al., (2018) have reported the effect of CO₂ flow rate, and co-solvent flow rate in the range from 15 to 35 g/min and 5 to 30%, respectively, for the extraction yield from *Mariposa Christia Vespertilionis* leaves. They reported that extraction yield decreased above 25 g/min CO₂ flow rate and increased with co-solvent flow rate from 5 to 30%.

4.3.10 Process optimization for higher extraction yield, TPC, and lower IC₅₀

Among the 30 experimental sets, maximum and the minimum yield, TPC and IC₅₀ achieved were (4.53% and 1.92%), (83.06 ± 3.8 mg GAE/g and 47.58 ± 8.1 mg GAE/g), and (115.17 ± 0.3 µg/mL and 42.11 ± 1.3 µg/mL), respectively. The desirability function tool chose the optimum extraction conditions that gave the highest yield of extraction with maximum TPC and minimum IC₅₀. The optimum SC-CO₂ extraction conditions were pressure: 25.13 MPa, temperature: 47.53°C, CO₂ flow rate: 14.47 g/min, and amount of co-solvent: 2.43%. At this condition, the predicted yield of extraction, TPC, and IC₅₀ was 4.53%, 83.37 mg GAE/g, and 40.2 µg/mL, respectively.

4.3.11 Validation of SC-CO₂ extraction parameters

Following optimization, a verification experiment was conducted under optimal extraction conditions to confirm the experimental and theoretical values of the yield of extraction, TPC, and IC₅₀. Validation experiments at the optimum condition revealed that extraction yield, TPC, and IC₅₀ of 4.38 % and 84.31 ± 3.98 mg GAE/g, and 41.94 ± 3.13µg/mL, respectively (**Table 4.6**). These results were very close to the projected results. This suggests that the formulated models were supposed to be precise and reliable. The percentage recovery described the contrast between optimized SC-CO₂ extract and Soxhlet extract. The ratio of the targeted component in SC-CO₂ extract to Soxhlet extract is the SC-CO₂ extract recovery. At optimum conditions, SC-CO₂ extraction from FL led to the recovery of 48.83%-yield of extraction and 38.1%-TPC.

4.3.12 Characterization of extract obtained at optimum SC-CO₂ extraction conditions

FL extract obtained at optimum SC-CO₂ extraction conditions was further characterized for its total flavonoid content (TFC), quantitative HPLC analysis of phenolic acids and flavonoids (**Table 4.6**), and

Chapter 4

Table 4.6. Extraction yield, TPC, TFC, IC50, and HPLC analysis of extracts

	FL(Sox)	ML(Sox)	FL	ML	MIX	Recovery (%) from FL
Yield (%)	8.97	8.27	4.38	3.9	3.83	48.83
TPC (mg GAE/g)	221.28±3.8	158.69±6.11	84.31±3.98	70.47±4.41	67.79±2.64	38.1
TFC (mg QE/g)	120.29±2.7	73.2±0.67	77.95±1.53	59.46±0.86	62.27±1.96	64.8
IC50 (µg/mL)	4.78±0.05	6.62±0.28	41.94±1.13	53.17±1.62	46.05±1.39	-
Gallic acid (mg/g)	95.49±0.76	85.4±0.32	61.95±0.24	39.35±0.33	53.95±0.27	64.88
Caffeic acid (mg/g)	17.73±0.14	7.55±0.19	0.02	0.19±0.01	0.04	0.11
Ferulic acid (mg/g)	0.13±0.01	0.06±0.01	0.19±0.01	0.27±0.01	0.17	146.15
P-coumaric acid (mg/g)	0.12±0.02	0.11	0.03±0.01	0.01±0.03	0.02	25
Vanillic acid (mg/g)	ND	ND	ND	ND	ND	-
Myricetin (mg/g)	4.48±1.2	4.07±0.04	5.05±0.97	4.46±0.01	4.07±0.33	112.72
Quercetin (mg/g)	ND	ND	0.13	0.05	0.08±0.01	-
Rutin (mg/g)	0.33±0.01	0.24±0.01	ND	ND	ND	-
Kaempferol (mg/g)	ND	ND	ND	ND	ND	-

FL(Sox) and ML(Sox) - extracts from female and male leaves obtained by Soxhlet extraction, respectively. FL - female leaf, ML - male leaf, MIX-50-50% mixture of FL and ML - Extracts obtained by SC-CO₂ extraction at optimum condition.

antibacterial properties (**Table 4.8**). FL's optimal SC-CO₂ extraction setup was also used to extract ML and a 50-50% blend of male and female leaves (MIX). The TFC of FL SC-CO₂ extracts was 77.95 ± 1.53 mg QE/g, encompassing 64.8% of the conventional extract. The HPLC chromatograms of phenolic acids and flavonoids in the extract obtained by Soxhlet and the optimum SC-CO₂ extraction process from FL, ML, and the mixture of leaves (MIX) are given in **Fig. 4.5** and **Fig. 4.6**. The linearity of the established HPLC method was determined with the standard solutions with the concentration range of 10-100 µg/mL

at five concentration levels. The retention time, regression equation, the limit of detection (LOD), and the limit of quantification (LOQ) values of investigated compounds are listed in **Table 4.7**. The standard curves revealed good linear regression ($R^2 > 0.99$) within test ranges. The flavonoids method was more sensitive than phenolic acids, as indicated by the lower values of the LOD and LOQ values.

Table 4.7. Retention time, regression equation, LOD, and LOQ of analyzed compounds

Compounds	Retention time	Regression equation	R^2	LOD ($\mu\text{g/mL}$)	LOQ ($\mu\text{g/mL}$)
Gallic acid	3.7	$Y=38127X+10^6$	0.998	1.16	3.54
Caffeic acid	4.1	$Y=100213X-716173$	0.997	1.57	4.76
Ferulic acid	5.3	$Y=97291X-386832$	0.9974	0.58	1.76
P-coumaric acid	5.1	$Y=152227X+97936$	0.99	0.05	0.16
Vanillic acid	4.4	$Y=46548X+125323$	0.979	0.43	1.3
Myricetin	18	$Y=9877X-15460$	0.998	0.03	0.1
Quercetin	27	$Y=49994X-142127$	0.996	1.56	4.7
Rutin	10.2	$Y=47766X-299204$	0.995	2.02	6.11
Kaempferol	40.8	$Y=166604X-570934$	0.998	0.23	0.71

Gallic acid (61.95 ± 0.24 mg/g) was found to be the most abundant phenolic acid in SC-CO₂ extracts, followed by ferulic acid (0.19 ± 0.01 mg/g), p-coumaric acid (0.03 ± 0.01 mg/g), and caffeic acid (0.02 mg/g). SC-CO₂ extracted ferulic acid better than Soxhlet, with a 146.2% recovery. This proves the benefit of SC-CO₂ selectivity and the drawback of thermal degradation using Soxhlet. Gallic acid, p-coumaric acid, and rutin were, in fact, better extracted using Soxhlet extraction. SC-CO₂ extraction,

Chapter 4

however, remains a safer option than Soxhlet extraction because of its shorter extraction time, lower extraction temperature, and higher selectivity for extracting specific compounds. Rutin was identified only in Soxhlet extract.

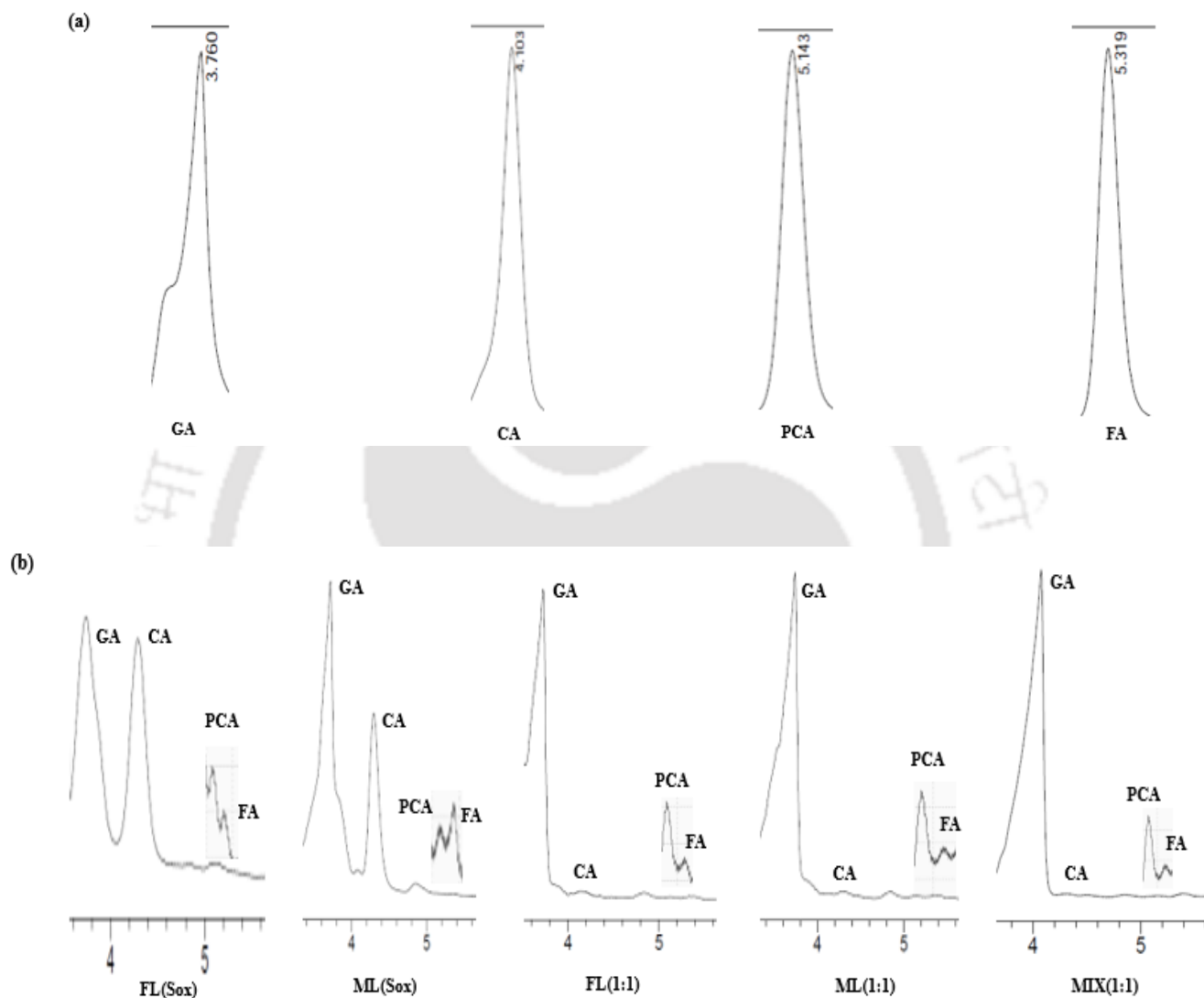


Fig. 4.5. HPLC chromatograms for identification of phenolic acids. (a) HPLC profile of standards: gallic acid (GA), caffeic acid (CA), p-coumaric acid (PCA), and ferulic acid (FA). (b) Identification of phenolic acids in extracts at 310 nm: FL(Sox) and ML(Sox) – extracts from female and male leaf obtained by Soxhlet extraction, respectively. FL(1:1)-female leaf, ML(1:1)-male leaf, MIX(1:1)-mixture of FL and ML extracts obtained from SC-CO₂ extraction at optimum condition

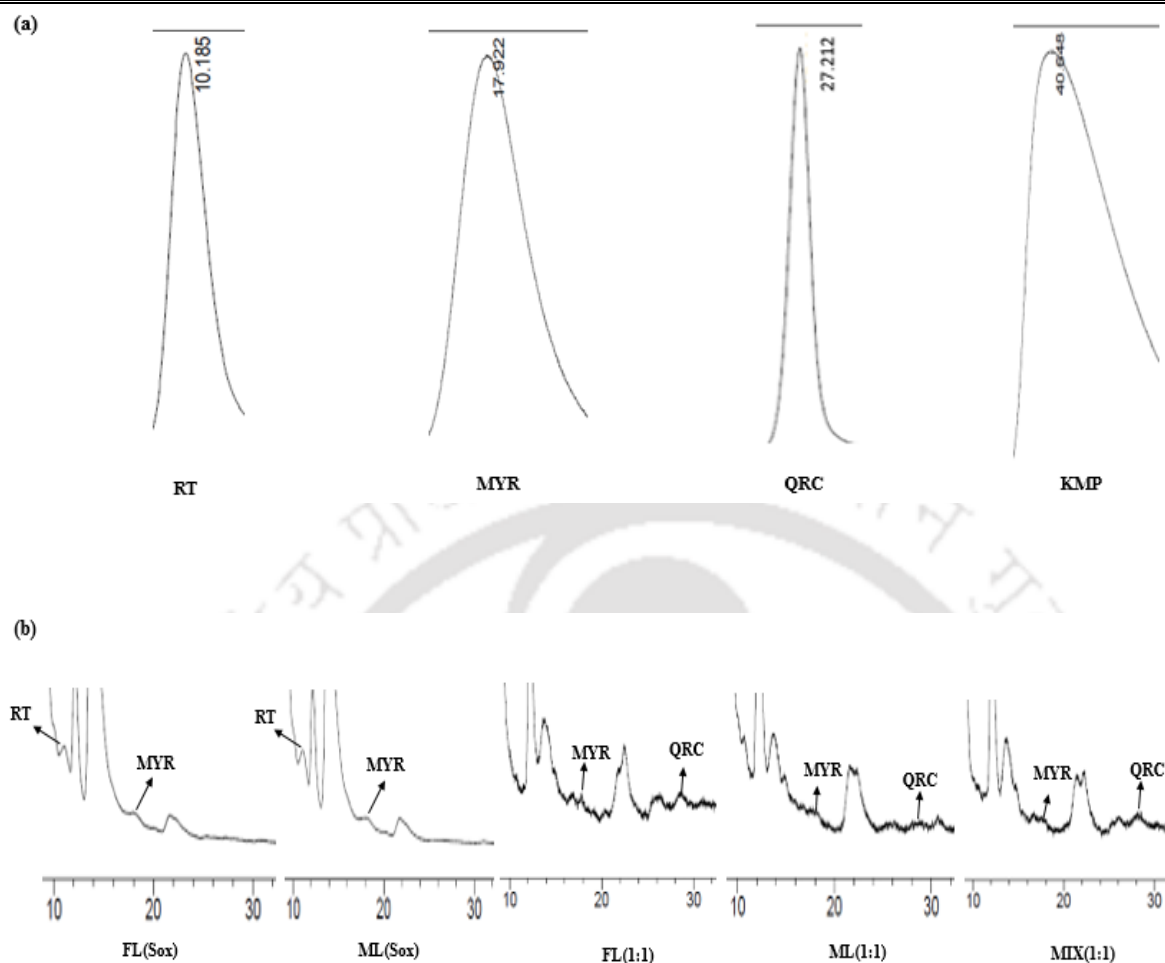


Fig. 4.6. HPLC chromatograms of flavonoid compounds. (a) HPLC profile of standards rutin (RT), myricetin (MRC), quercetin (QRC), and kaempferol (KMP) at 368 nm. (b) Identification of flavonoids in extracts: FL(Sox) and ML(Sox) – extracts from female and male leaves obtained by Soxhlet extraction, respectively. FL(1:1)-female leaf, ML(1:1)-male leaf, MIX(1:1)- mixture of FL and ML extracts obtained from SC-CO₂ extraction at optimum condition

The most abundant flavonoids in FL extract were myricetin (5.05 ± 0.97 mg/g), followed by quercetin (0.13 mg/g). SC-CO₂ extract had significantly greater myricetin contents than Soxhlet extract, with a recovery rate of 112.72%. Only SC-CO₂ extracts contained quercetin. HPLC analysis confirmed that SC-CO₂ extraction was more selective for the extraction of flavonoids (myricetin and quercetin) than phenolic compounds. This demonstrates that SC-CO₂ is a promising alternative over conventional

Chapter 4

solvent extraction for obtaining flavonoid-rich extracts from sea buckthorn leaves. Vanillic acid and kaempferol were not detected in all extracts. Similar investigations were reported by researchers (Pereira et al., 2016; Song et al., 2019).

4.3.13 Antibacterial activity of extract obtained at optimum conditions

The antibacterial activities of Soxhlet extracts from the leaves of *H. salicifolia* are given in **Table 4.8**. The FL extract obtained at optimized SC-CO₂ extraction condition showed significant antibacterial activity against eight bacterial strains as evaluated by MIC (125 to 500 µg/mL) and ZoI (3 to 12.1 ± 0.6 mm) assays. SC-CO₂ extract showed the highest activity against *E. aerogenes* at 125 MIC. There were no substantial differences in the MIC of the extract against other bacterial strains. Soxhlet extract of FL showed the highest antibacterial efficacy with the lowest MIC of 62.5 µg/mL against *S. aureus*, *E. aerogenes*, and *B. subtilis*, 8-fold lower than SC-CO₂ extract of FL. The difference in antibacterial activity of SC-CO₂ and Soxhlet extracts is attributed to the higher content of polyphenol compounds, especially gallic acid and caffeic acid (Ouattara et al., 2011).

The ZoI trend bears consistent with the MIC. SC-CO₂ extract showed the highest activity against *S. epidermidis* with the highest ZoI (12.1 ± 0.6 mm) and the smallest activity against *E. aerogenes* with the lowest ZoI (3 mm). Gram-negative bacteria were most resistant to the extract, and lower values of ZoI were obtained for these bacteria. Gram-positive bacteria lack basic lipopolysaccharide components on their outer membranes and were more vulnerable to antibacterial agents than Gram-negative. Information regarding the polyphenolic content, antioxidant and antibacterial properties of sea buckthorn leaf extract using SC-CO₂ in the literature is rather limited.

Table 4.8. Antibacterial analysis of extracts obtained at optimized conditions

Bacteria	MIC (µg/mL)					ZoI (mm)					Control
	FL(Sox)	ML(Sox)	FL	ML	MIX	FL(Sox)	ML(Sox)	FL	ML	MIX	
<i>S. aureus</i>	62.5	125	500	500	500	9.2±0.3	8.2 ±0.3	5.2±0.1	4.1±0.3	5.1±0.1	0
<i>B. subtilis</i>	62.5	62.5	500	500	500	11±0.5	10.5±1.5	8.3±0.6	7.0	8.5±0.5	0
<i>S. epidermidis</i>	250	250	500	500	500	13.2±0.8	10±0.5	12.1±0.6	8.8±0.3	9.3±0.6	0
<i>M. luteus</i>	125	250	500	500	500	12	11.2±0.3	6.2±0.3	6±0.5	5.0	0
<i>E.coli</i>	125	500	500	500	500	12.3±0.6	10.5±0.5	4.9±0.1	4.0	3.9±0.1	0
<i>E. aerogenes</i>	62.5	125	125	125	125	16.7±1.2	16±1	3.0	4.1±0.1	4.0	0
<i>K. pneumonia</i>	500	500	500	500	500	6.8±0.3	6.7±0.3	6.1±0.1	5.1±0.1	5.0	0
<i>P. aeruginosa</i>	500	500	500	500	500	9.3±0.6	8.2±0.3	6.9±0.3	5.8±0.3	6±0.5	0

MIC- Minimum inhibitory concentration, ZoI - Zone of inhibition, FL(Sox) and ML(Sox) - extracts from female and male leaf obtained by Soxhlet extraction, respectively. FL-female leaf, ML-male leaf, MIX-50-50% mixture of FL and ML - Extracts obtained from SC-CO₂ extraction at optimum condition.

Chapter 4

4.3.14 Comparison between SC-CO₂ extracts of FL, ML, and the mixture of leaves.

The yield and TPC of ML extract were 3.9% and 70.47 ± 4.41 mg GAE/G, respectively, which was lower than the FL extract. Whereas TFC of ML, 59.46 ± 0.86 mg QE/g; and MIX, 62.27 ± 1.96 mg QE/g were slightly higher than FL. The TFC, antioxidant activity, and the gallic acid content of MIX extract lie between the extracts from ML and FL. No difference was observed in the MIC of FL, ML, and MIX extracts. The ZoI of MIX was found to be slightly higher than FL and ML extracts for *B. subtilis*. Cumulatively, the extracts from MIX showed higher antibacterial activity than ML in ZoI assay. This may be due to the benefit of the synergistic effect of bioactive compounds from the leaves of female and male plants.

4.3.4 Summary

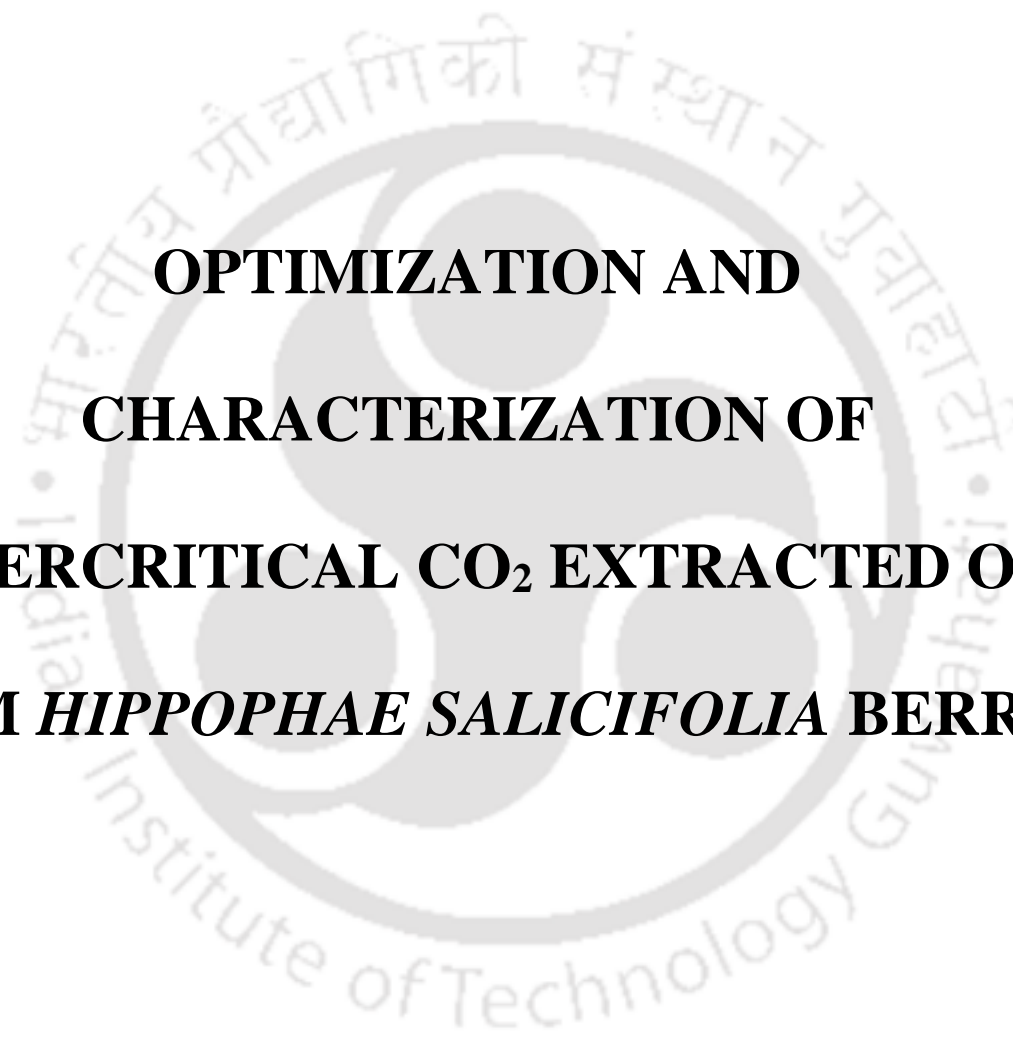
Optimization of SC-CO₂ extraction of polyphenol from *Hippophae salicifolia* D. Don leaves collected from Northeast India is reported for the first time. The major outcomes of the study are given below:

- The use of entrainer showed significant improvement in the extraction yield, TPC, and the antioxidant and antibacterial activity of extracts. The increase in extraction time from 1 h to 3 h increased the yield of extraction, while the TPC and TFC of extracts were reduced when extraction time is extended above 2 h.
- All extraction parameters for polyphenol extraction from sea buckthorn leaf, (pressure (X_1), temperature (X_2), CO₂ flow rate (X_3), cosolvent flow rate (X_4)); all the quadratic terms (X_1^2 , X_2^2 , X_3^2 , X_4^2); and the majority of the cross-terms (X_1X_2 , X_1X_4 , X_2X_3 , X_3X_4) are significantly important parameters with very fewer p-values. On the other hand, the interaction between X_1X_3 , X_2X_4 on the yield of extraction, X_1X_4 on TPC, and X_1X_3 on IC₅₀ are not significant.

Optimization of polyphenol extraction using SC-CO₂

- The optimum condition for maximum yield of extraction with maximum TPC and minimum IC₅₀ occurred at 25.13 MPa, 47.53°C, 14.47 g/min CO₂ flow rate, and 2.43% co-solvent.
- The validation experiment at this condition resulted in 4.38% yield of extraction, 84.31 ± 3.9 mg GAE/g TPC, and 41.94 ± 3.13 µg/mL IC₅₀. Soxhlet extraction performed better to yield of extraction, TPC, IC₅₀, and antibacterial activity than SC-CO₂ extraction.
- SC-CO₂ extraction was more selective for ferulic acid, myricetin, and quercetin extraction. Further research needs to be done on the selectivity of SC-CO₂ extraction for flavonoids.
- The research results indicate the status of utilizing SC-CO₂ extract of *Hippophae salicifolia* leaf as functional foods and ingredients, food supplements, and food preservative





**OPTIMIZATION AND
CHARACTERIZATION OF
SUPERCRITICAL CO₂ EXTRACTED OIL
FROM *HIPPOPHAE SALICIFOLIA* BERRIES**



**OPTIMIZATION AND CHARACTERIZATION OF SUPERCRITICAL CO₂
EXTRACTED OIL FROM *HIPPOPHAE SALICIFOLIA* BERRIES****5.1 Background**

Sea buckthorn (*Hippophae*) fruits are among the most nutritious and vitamin-rich fruits in the plant kingdom. The oil in sea buckthorn berries is the most valuable component. Oil extraction is usually accomplished by cold or screw press, steam-distillation, and solvent (hexane) extraction methods. Despite their higher extraction efficiency, the thermal/oxidative degradation of the extracts and toxic/flammable solvent remnant outweigh the benefits of these conventional methods. Thus, an environmentally friendly approach, like supercritical carbon dioxide (SC-CO₂) extraction, is a potential alternative to overcome these disadvantages. Therefore, this chapter's focus was to optimize oil extraction from *Hippophae salicifolia* berries using SC-CO₂. Optimization was performed to achieve maximum oil yield, with higher β -carotene, and total tocopherol content. The physicochemical, phytochemical, thermal, and mechanical properties of oils including, antioxidant and antibacterial properties are also elaborated on in this chapter.

5.2 Overview

Process parameters (pressure, temperature, and CO₂ flow rate) for SC-CO₂ oil extraction from *Hippophae salicifolia* berries were optimized using the response surface methodology. The flow rate of CO₂ had a maximum effect on oil yield, while pressure showed the highest significant effect on the β -carotene and total tocopherol contents of the oil. 2nd order polynomial model sufficiently represented

the relationship between process variables and responses. The optimum extraction condition for SC-CO₂ extraction of oil was found to be 27.02 MPa, 48.46 °C, 16.45 g/min. The oil extracted at optimum extraction conditions resulted in $12.82 \pm 1.4\%$ oil yield with 126.67 ± 2.9 mg/100 g oil β -carotene and 679.42 ± 1.3 mg/100 g oil total tocopherol contents. UFA content in SC-CO₂ and hexane extracted oils was 92.72% and 91.42%, of which omega-seven fatty acids (palmitoleic acid) comprised 42.98% and 41.14%, respectively. Further, the physicochemical, phytochemical, thermal, and mechanical properties of SC-CO₂ and Soxhlet extracted oils were investigated. The physicochemical properties of both the oils were in the range of the required edible oil standard. The total phenolic content and the antioxidant activity of SC-CO₂ extracted oil were significantly higher than Soxhlet extracted oil. Both the oils showed significant antibacterial activities against eight pathogenic bacterial strains. The thermogravimetric profile showed lower thermal stability up to 185 °C for SC-CO₂ extracted oil. At the same time, the resistance to mechanical stress for SC-CO₂ extracted oil was more substantial than Soxhlet extracted oil. Thus, SC-CO₂ extraction of sea buckthorn berries oil is an effective alternative to conventional solvent extraction for its application in food, cosmetics, and pharmaceutical industries. The schematic diagram for the study in the current chapter is shown in Fig. 5.1.

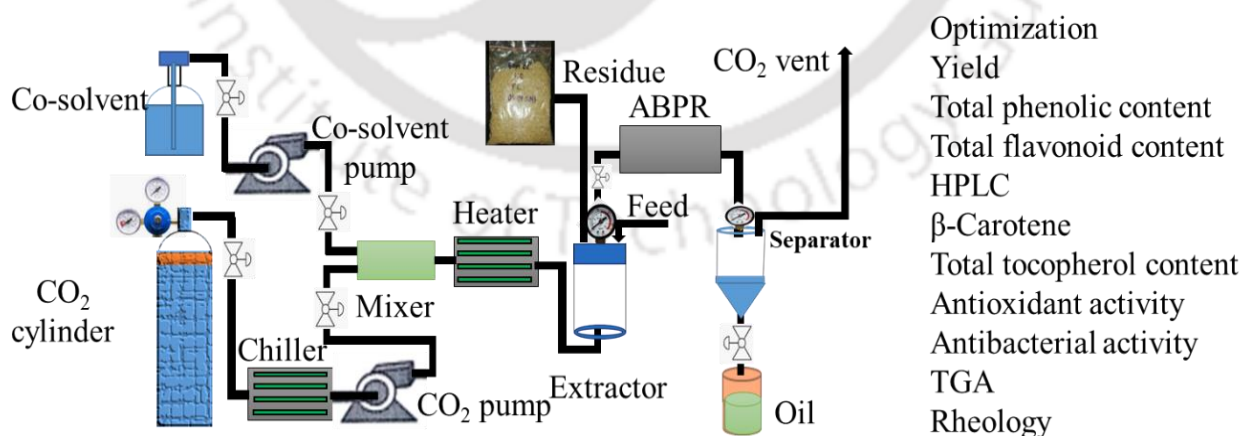


Fig. 5.1: Graphical Abstract

5.3 Results and Discussion

5.3.1 Models fitting and analysis of ANOVA

The interaction between three independent variables X_1 , pressure (MPa); X_2 , temperature ($^{\circ}\text{C}$); and X_3 , CO_2 flow rate (g/min) of SC- CO_2 extraction for sea buckthorn berries oil were examined using a five-level, three-factorial CCD. The coded and uncoded extraction variables and experimental conditions used in this study are given in **Tables 5.1** and **5.2**, respectively. Results were analyzed by multiple regression analysis, and sources of variances determined the optimum extraction conditions (**Table 5.3**).

Table 5.1: Extraction process variables and their levels

Independent variables			Variable levels				
	Symbol	Unit	$-\alpha$	-1	0	+1	$+\alpha$
			(-1.678)				(+1.678)
Pressure	X_1	MPa	8.9	15	24	33	39.1
Temperature	X_2	$^{\circ}\text{C}$	33.2	40	50	60	66.8
CO_2 flow rate	X_3	g/min	6.6	10	15	20	23.4

The models for the oil yield, β -carotene, and total tocopherol contents were adequate to represent the actual relationship between the independent and dependent variables with higher F -values (38.05 - 105.49) and lower p -values (<0.0001). The R^2 values of the developed models were found to represent 97.16, 98.95, and 98.96% of the experimental data for oil yield, β -carotene, and total tocopherol content, respectively. These statistical analyses implied that the experimental data fitted well with the developed 2nd order regression equations given below (Eq 5.1-5.3).

$$\text{Yield (\%)} = 8.65 + 1.1X_1 - 0.36X_2 + 1.2X_3 + 0.88X_1X_2 - 0.3X_1X_3 - 0.46X_2X_3 - 1.89X_1^2 - 0.29X_2^2 - 1.61X_3^2 \quad (5.1)$$

$$\beta\text{-carotenoid (mg / 100g oil)} = 123.07 + 21.13X_1 - 1.22X_2 + 9.35X_3 + 5.2X_1X_2 + 2.45X_1X_3 + 3.54X_2X_3 - 16.28X_1^2 - 11.28X_2^2 - 16.81X_3^2 \quad (5.2)$$

$$\text{Total tocopherol (mg / 100g oil)} = 681.54 + 88.82X_1 - 0.96X_2 + 75.52X_3 + 8.08X_1X_2 - 32.24X_1X_3 - 3.61X_2X_3 - 58.01X_1^2 - 93.11X_2^2 - 173.09X_3^2 \quad (5.3)$$

The plot of model-predicted values against experimental data points envisioned the fitting qualities of the developed model as shown in **Fig. 5.2 (a-c)**. The significance of each parameter and their interaction was analyzed by ANOVA (**Table 5.3**). Individual parameters i.e. pressure (X_1) and CO₂ flow rate (X_3) and interaction terms between pressure and temperature (X_1X_2), showed a significant effect on the oil yield as indicated by their large F -value and small p -value. Temperature (X_2) showed an insignificant contribution to all responses ($p > 0.05$). In addition, the interaction of CO₂ flow rate (X_3) with pressure (X_1X_3) and temperature (X_2X_3) showed an insignificant contribution to the oil yield and total tocopherol content ($p > 0.05$). Pressure (X_1) and CO₂ flow rate (X_3) had similar p -values (< 0.0001) for the oil yield. However, the linear term of CO₂ flow rate (X_3) had a higher F -value of 52.25. From this, it was concluded that the CO₂ flow rate (X_3) had the maximum effect on oil yield. Likewise, pressure (X_1) had a maximum significant effect on the β -carotene content (Eq 5.1) and had the highest significant effect on the total tocopherol content of the oil (Eq 5.3).

5.3.2 Effect of extraction variables on the oil yield

The effect of pressure, temperature, and CO₂ flow rate on the responses (oil yield, β -carotene, and total tocopherol contents of the oil) were analyzed by a three-dimensional response surface plot using the

developed models shown in Eq. 5.1-5.3. The plots were established by changing two process variables simultaneously and fixing the third constant at its central point.

Table 5.2: Central Composite Design for supercritical CO₂ extraction and the corresponding responses

Run	X ₁ :Pressure (MPa)	X ₂ :Temperature (°C)	X ₃ :CO ₂ flow rate (g/min)	Yield (%)	β-carotene (mg/100 g oil)	Total tocopherol (mg/100 g oil)
1	24	50	15	13.05	123.02	698.3
2	33	60	20	9.24	124.28	455.23
3	24	50	15	13.05	123.02	675.3
4	15	60	10	2.1	45.34	191.11
5	8.9	50	15	1.845	42.86	350.23
6	24	33	15	13.17	96.04	438.28
7	24	50	15	12.9	123.02	668.3
8	24	50	15	12.9	123.02	675.3
9	24	50	7	3.27	65.91	108.61
10	33	40	10	5.205	90.11	391.3
11	24	50	15	12.9	123.02	668.3
12	33	40	20	10.215	98.68	467.63
13	39.1	50	15	8.355	112.82	707.29
14	24	50	15	13.05	123.02	698.3
15	33	60	10	10.08	85.39	391.31
16	24	67	15	10.485	86.06	407.09
17	24	50	23	10.5	95.49	391.39
18	15	40	20	9.36	69.61	364.09
19	15	40	10	5.595	54.68	156.78
20	15	60	20	6.15	58.24	381.97

Table 5.3: ANOVA for yield, β -carotenoid, and total tocopherol extraction efficiency for the results obtained from CCD

Source	Yield		β -carotenoid		Total tocopherol	
	F-value	p-value	F-value	p-value	F-value	p-value
Model	38.04	< 0.0001	104.76	< 0.0001	105.49	< 0.0001
X ₁ -Pressure	45.73	< 0.0001	369.64	< 0.0001	150.29	< 0.0001
X ₂ -Temperature	4.87	0.0518	1.24	0.2908	0.0177	0.8969
X ₃ -CO ₂ flow rate	52.25	< 0.0001	69.62	< 0.0001	104.60	< 0.0001
X ₁ X ₂	17.37	0.0019	13.14	0.0047	0.7291	0.4131
X ₁ X ₃	2.05	0.1825	2.93	0.1179	11.62	0.0067
X ₂ X ₃	4.78	0.0536	6.08	0.0334	0.1455	0.7108
X ₁ ²	142.08	< 0.0001	230.95	< 0.0001	67.48	< 0.0001
X ₂ ²	3.40	0.0949	115.75	< 0.0001	181.47	< 0.0001
X ₃ ²	89.34	< 0.0001	211.99	< 0.0001	517.39	< 0.0001

Across all the temperature ranges, the solubility of sea buckthorn oil in SC-CO₂ increased with pressure. The increase in pressure increases the density of CO₂, reinforces the interactions between CO₂ and matrix, enhances the rate of mass transfer and diffusion of CO₂ into the matrix, and thereby improves the oil yield. This effect, however, only lasted so long before a further rise in pressure caused the SC-diffusivity CO₂'s to drop and its contact with the pores to decrease, presumably reducing the solute's ability to dissolve (**Fig 5.3 (a)**). Due to this reason, increasing pressure above 26 MPa decreased the oil yield (Xu et al., 2008).

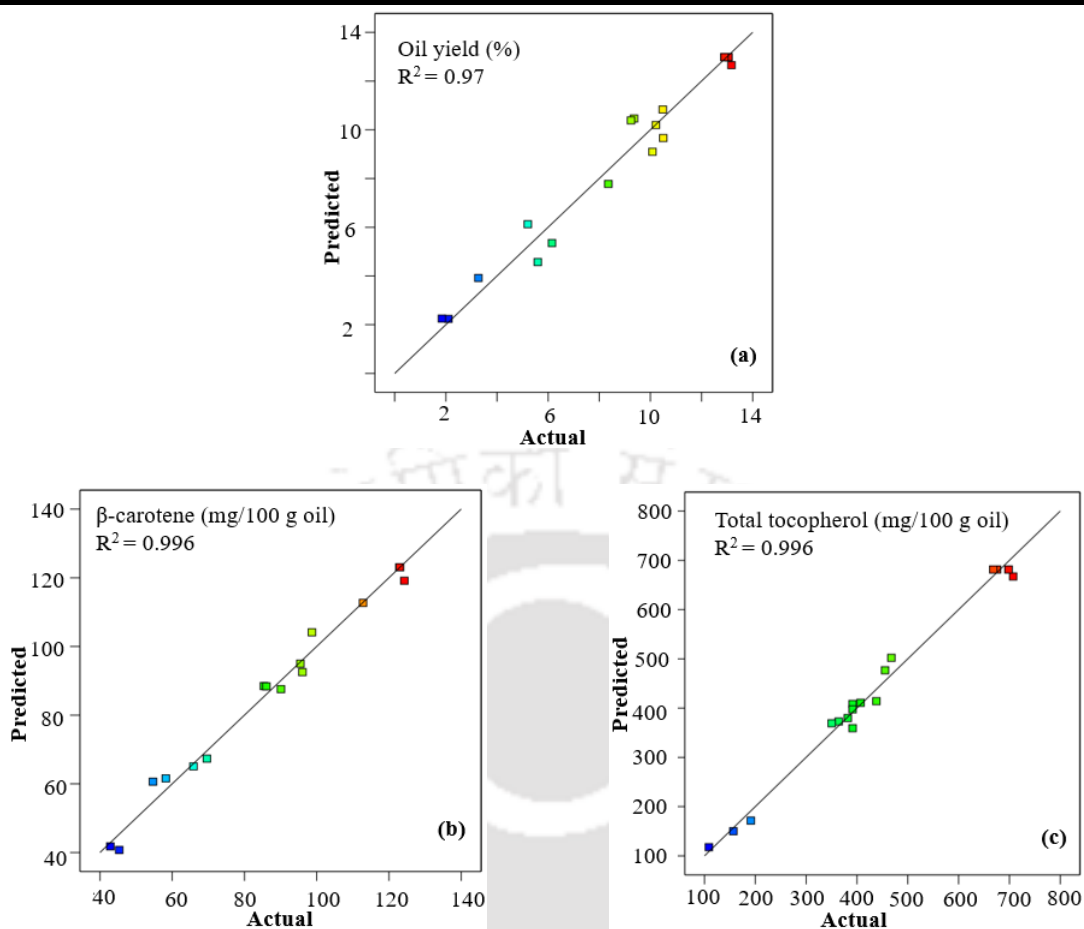


Fig. 5.2: Plots of actual experimental values versus model predicted values for (a) Oil yield, (b) β -carotene, and (c) Total tocopherol content

Furthermore, the solubility of sea buckthorn oil in SC-CO₂ declined with an increase in the temperature at lower pressure (15 MPa), indicating a rise in the temperature at lower pressure resulted in decreased CO₂ solvating power by reducing its density. Conversely, at higher pressure levels (33 MPa), oil yield progressively increased with increasing temperature, promoting the solute's vapor pressure and increasing the solute's dissolution as shown in **Fig 5.3 (a)**. The crossover pressure, above which the temperature effect on the oil extraction began to have the opposite effect, was around 26 MPa. This was comparable with the value specified by Xu et al., (2008) for extracting sea buckthorn oil by SC-CO₂. The CO₂ flow rate was the most critical factor in oil extraction from sea buckthorn berries (**Table 5.3**). The oil yield was

positively correlated with pressure and CO₂ flow rate, but the complicated interplay between the two was inverted as shown in Eq 5.1. These opposing effects can be observed in **Fig. 5.3 (b)**. The highest oil yield was obtained at around 16 g/min CO₂ flow rate and 26 MPa. The effect of increasing CO₂ flow rate on the solubility of oil at lower and higher temperatures showed different behavior. Irrespective of the temperature variation, the increase in CO₂ flow rate from 10 g/min to 16 g/min resulted in an increased oil yield (**Fig. 5.3 (c)**). The decline in oil yield at 60 °C, on the other hand, occurred at a lower CO₂ flow rate (16 g/min) than at 40 °C (18 g/min). This might be related to the fact that the temperature rise decreased CO₂ density, thus adversely affecting the oil yield.

5.3.3 Effect of extraction variables on the β -carotene content in the oil

It was observed that the solubility of β -carotene increased with all extraction variables, as shown in **Fig. 5.3 (d) - (f)**, which was similar to the previous report by Kostrzewa et al., (2019). At pressures between 15 and 33 MPa, the increase in β -carotene solubility was more pronounced at 60 °C than at 40 °C (**Fig. 5.3 (d)**). An increase of pressure at lower temperatures reduces the diffusivity of SC-CO₂ and contact of CO₂ with pores in the plant matrix, hindering solute dissolution and solubility (Khaw et al., 2017). On the contrary, an increase in the pressure at higher temperatures increased the CO₂ density and inspired the specific interactions between the solute molecule and CO₂, increasing the solvating power of CO₂. Additionally, the solubility of β -carotene intensified with temperature rise at higher pressures where the increase in the vapor pressure of the solute was dominant. However, the rise in temperature at lower pressure (15 MPa) resulted in decreased β -carotene extraction due to a decrease in CO₂ density, which was consistent with the trend in literature for the solubility of carotenoid in SC-CO₂ (Kostrzewa et al., 2019). Both pressure and CO₂ flow rate had a significant effect (<0.0001) on the β -carotene content in the oil. In contrast, the impact of the interaction between them showed

no significant effect ($p>0.05$). When the CO₂ flow rate increased, the oil's β -carotene content also increased.

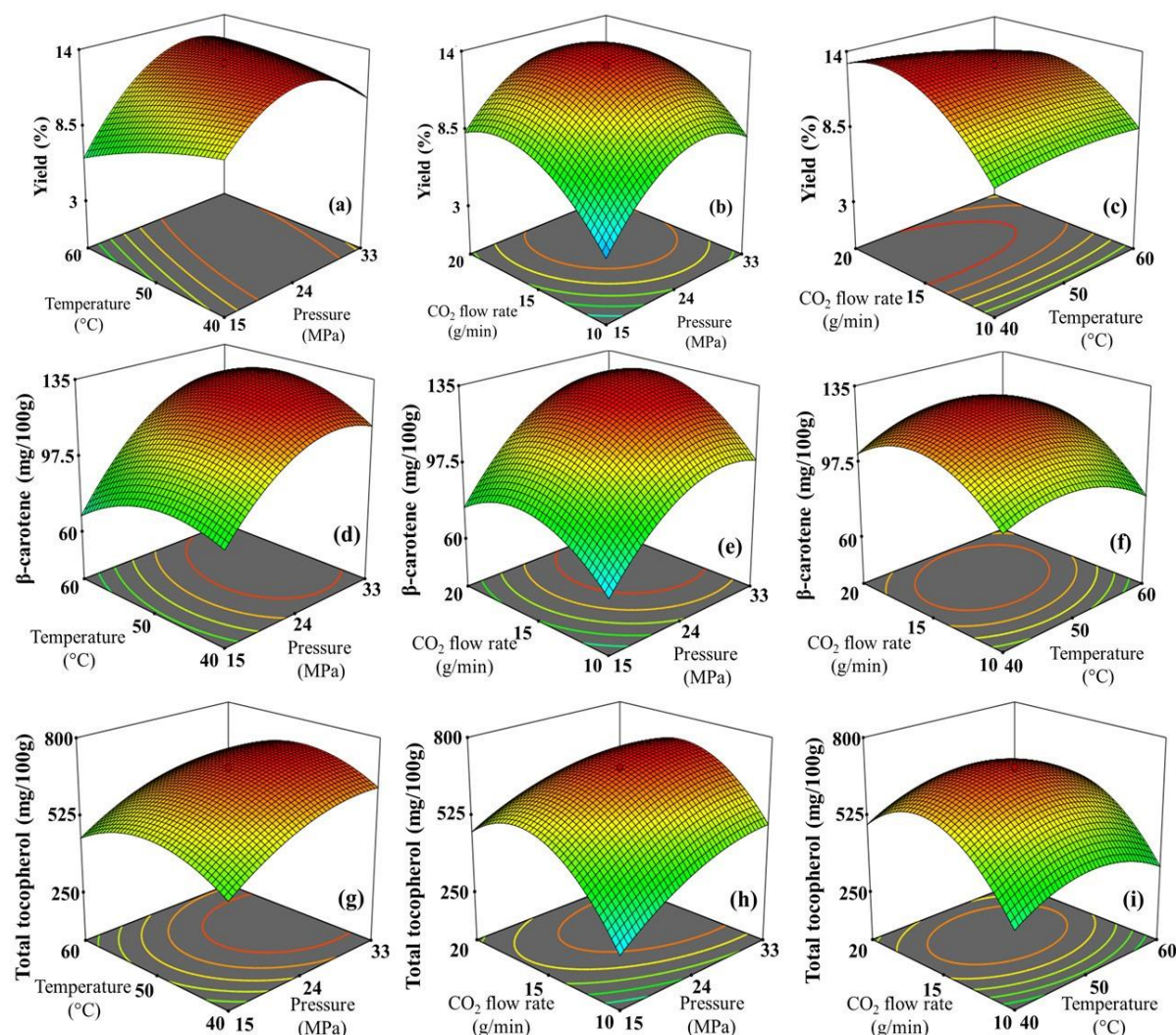


Fig. 5.3: Effect of pressure, temperature, and CO₂ flow rate on oil yield (a–c), on β -carotene (d–f), and Total tocopherol content of the oil (g–i)

The concentration of β -carotene in the extract is influenced by the amount of CO₂ used throughout the entire extraction process (Shi et al., 2007); the higher the flow rate of CO₂, the more the interaction between CO₂ and the sample, which ultimately results in the usage of more CO₂. The highest β -carotene content in the extract was achieved at around 30 MPa and 16 g/min CO₂ flow rate when the temperature is held constant at 40 °C as shown in **Fig. 5.3 (e)**.

Similarly, at 240 MPa, the highest β -carotene content was obtained at 50 °C and 16 g/min CO₂ flow rate (**Fig. 5.3 (f)**).

5.3.4 Effect of extraction variables on the total tocopherol content

In this study, the total tocopherol content in the oil extracts represents the sum of α , γ , and δ -tocopherols. Despite the differences in the extraction conditions, the tocopherol profile of the oil extract from the whole berry of sea buckthorn was majorly dominated by α -tocopherol (~70% of total tocopherols), which coincided with earlier published reports (Cossuta et al., 2007; Xu et al., 2008). The total tocopherol content was found to increase with an increase in the pressure (**Fig. 5.3 (g) and (h)**). At low levels, the CO₂ flow rate had an affirmative linear effect on the tocopherol content. In contrast, at high levels, the CO₂ flow rate had a negative quadratic effect on the tocopherol content of the oil, as presented in **Fig. 5.3 (h)**. The total tocopherol content of the oil decreased with the CO₂ flow rate, in contrast to the oil output, as demonstrated by the negative interaction impact between temperature and CO₂ flow rate. This is because, as the CO₂ flow rate increased, the contact time between the plant matrix and CO₂ required for the equilibrium separation process decreased. The temperature and CO₂ flow rate of 50 °C and 16 g/min, respectively, were the optimal extraction condition to obtain the highest total tocopherol (**Fig. 5.3 (i)**).

5.3.5 Optimization of process parameters

The desirability function in Design-Expert software (7.0.0) was applied to identify an optimum set of process parameters within the stated operating range. The optimum process parameters for maximum oil yield, β -carotene, and total tocopherol content as predicted by the 2nd order model were: P = 27.02 MPa, T = 48.46 °C, and CO₂ flow rate = 16.45 g/min. The maximum oil yield predicted by the model was 13.52 % containing 129.36 mg/100 g β -carotene and total

tocopherol content of 707.54 mg/100 g. The characteristics of the oil obtained at the optimum extraction conditions offered $12.82 \pm 1.4\%$ oil yield with 126.67 ± 2.9 mg/100 g β -carotene and 679.42 ± 1.3 mg/100 g total tocopherol content (**Table 5.4**). These experimental values were within a 3% deviation from the predicted values, indicating that the developed model efficiently optimized the process.

Table 5.4: The oil yield, β -carotene, and tocopherol content of sea buckthorn oils

Responses	SC-CO ₂ extracted oil	Soxhlet extracted oil
Yield (%)	12.82 ± 1.4	14.54 ± 0.47
β -carotenoid (mg/100g oil)	126.67 ± 2.9	274.24 ± 5.6
α -tocopherol (mg/100g oil)	491.76 ± 3.67	541.5 ± 4.7
δ -tocopherol (mg/100g oil)	156.81 ± 3.5	167.47 ± 4.3
γ -tocopherol (mg/100g oil)	30.85 ± 1.27	48.86 ± 2.1
Total tocopherol (mg/100g oil)	679.42 ± 4.3	757.83 ± 6.1

5.3.6 Conventional organic solvent extraction

Table 5.4 shows the oil yield, β -carotene, and total tocopherol content of oil extracted from sea buckthorn berries using Soxhlet and SC-CO₂ extractions. The HPLC chromatograms of tocopherols for standards and oils are shown in **Fig. 5.4**. The Soxhlet extraction resulted in $14.54 \pm 0.47\%$ oil yield, and 144.21 ± 3.1 mg of β -carotene/100 g of oil, and 757.82 ± 6.1 total tocopherols/100 g of oil. Thus, the projected recovery of oil yield, β -carotene, and total tocopherol by SC-CO₂ extraction under optimum conditions were 88.17%, 90.65%, and 94.31%, respectively. The recovery of β -carotene and total tocopherol content in the current study was comparable with earlier published reports by Kagliwal et al. (2012) and Xu et al., (2008).

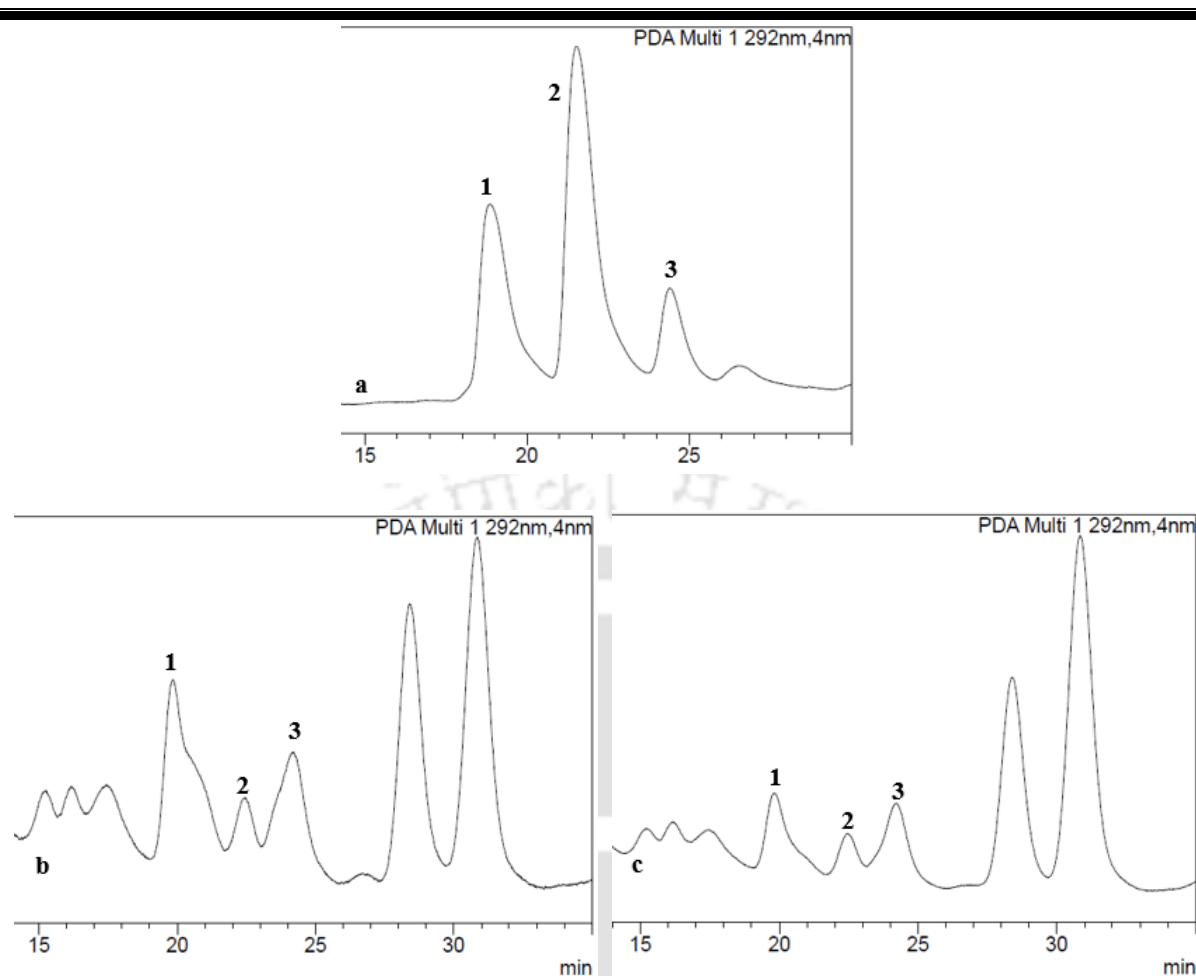


Fig. 5.4: HPLC chromatograms of (a) standards, (b) SC-CO₂ extracted oil, and (c) Soxhlet extracted oil. 1- α -tocopherol, 2 - γ -tocopherol, and 3 - δ -tocopherol

According to Kagliwal et al., (2012), the recovery of β -carotene and tocopherol from *H. rhamnoides* oil extracted at 34.5 MPa, 44 °C, and 80 min was 71.73% and 85.12%, respectively. In another study, for oil extracted from the same species at 27.6 MPa, 34.5 °C, 17 L/h CO₂ flow rate, and 82 min, the recovery of β -carotene and tocopherol was 98.7% and 125.6%, respectively (Xu et al., 2008). The higher recovery of total tocopherol is indicative of the higher solubility pattern of fat-soluble tocopherol in SC-CO₂ than β -carotene. The lower solubility of β -carotene in SC-CO₂ could be due to its relatively larger molecular weight than

tocopherols (Akanda et al., 2012; Shi et al., 2007). It was also noticed that α -tocopherol was the major tocopherol identified in the sea buckthorn berry oil, and it constituted ~ 70% of total tocopherols, followed by δ -tocopherols and γ -tocopherols detected in small amounts as shown in **Table 5.4**. The percentage of α and δ -tocopherols in oil from the berries (62.5-67.9%) and the pulp (74-85%) of sea buckthorn were consistent with the published literature (Zadernowski et al., 2003; Cenkowski et al., 2006). Further, the oil extracted using SC-CO₂ at optimum extraction conditions was analyzed for its fatty acids composition, antioxidant, antibacterial, thermal, and rheological properties and compared with that obtained using Soxhlet.

5.3.7 Fatty acids composition

The Gas Chromatograms of FAMES of SC-CO₂ and Soxhlet extracted oils, and their compositions are given in **Fig. 5.5 and Table 5.5**, respectively. About ten distinct fatty acid peaks were identified in the SC-CO₂ extracted oil: myristic acid (C14:0), palmitic acid (C16:0), palmitoleic acid (C16:1), elaidic acid (C18:1N9T), oleic acid (C18:1N9C), linolelaidic acid (C18:2N6T), linolenic acid (C18:3N1) α -linolenic acid (C18:3N3), eicosanoic acid (C20:0), and 11-eicosenoic acid (C20:1).

The results indicate that the major component of the SC-CO₂ and Soxhlet extracted oils was palmitoleic acid (omega-7 fatty acid) comprised 42.98% and 41.14%, respectively. The composition of UFA, particularly with the presence of omega-7 group, which is rare in the plant kingdom, makes sea buckthorn berry oil unique. The UFA such as; omega 3 (α -linolenic acid), 6 (linolelaidic acid), and 7 (palmitoleic acid) in the sea buckthorn oil that gives skin regeneration, and repair properties were found to be higher in SC-CO₂ extracted oil. Further, α -linolenic acid was identified only in SC-CO₂ extracted oil. α -linolenic acid is an essential omega-3 fatty acid necessary for average human growth and development and is important for

cardiovascular risk reduction (Campos et al., 2008). The oil's fatty acid content is a crucial indicator of its quality; substantial percentages of UFAs could be seen in high-quality oils.

Table 5.5: Fatty acid composition of SC-CO₂ and Soxhlet extracted oils

Fatty acids (%)	SC-CO ₂ extracted oil	Soxhlet extracted oil
Myristic acid (C14:0)	0.38	0.68
Palmitic acid (C16:0)	0.19	0.66
Palmitoleic acid (C16:1)	42.98	41.14
Elaidic acid (C18:1N9T)	2.13	2.1
Oleic acid (C18:1N9C)	22.9	22.82
Linolelaidic acid (C18:2N6T)	9.77	9.6
Linolenic acid (C18:3N1)	14.33	15.53
α-linolenic acid (C18:3N3)	0.18	-
Eicosanoic acid (C20:0)	6.8	7.24
11-Eicosenoic acid (C20:1)	0.34	0.23
MUFA; n:1	68.35	66.29
PUFA; n:n	24.28	25.13
SFA; n:0	7.37	8.58
UFA/SFA	12.57	10.66

SC-CO₂ and Soxhlet extracted oils contained 92.63% and 91.42% of UFA, respectively, implying that sea buckthorn oil has high nutritional and medicinal value. The levels of palmitoleic and oleic acids were similar to previously reported values of 38–39% and 16.5–33.18% for SC-CO₂ extracted sea buckthorn berries oils, respectively (Kagliwal et al., 2012; Xu et al., 2008). They have, however, reported much less UFA (66.9–74.68%) in SC-CO₂ extracted oil. From the above results, it can be concluded that SC-CO₂ extraction is an effective

technique for extracting important lipophilic constituents of sea buckthorn oil with high quality for cosmetics and other high-value applications.

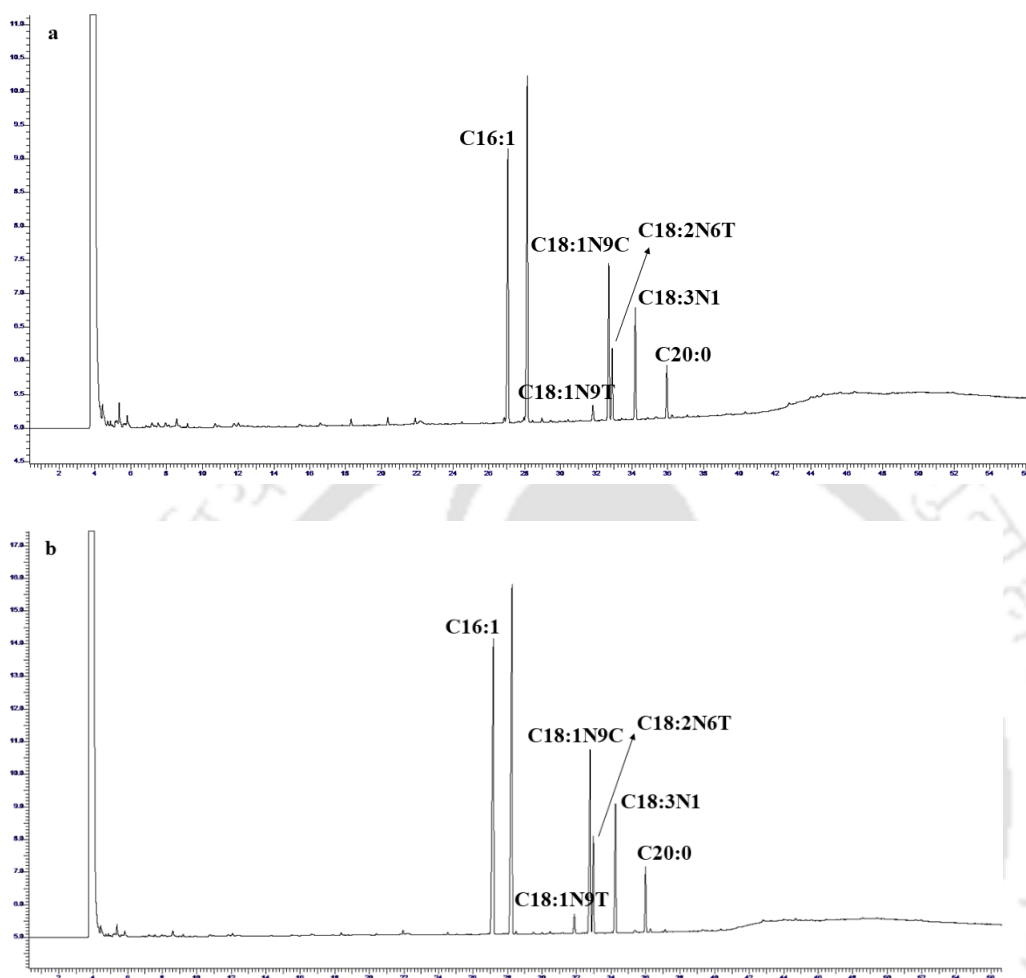


Fig. 5.5: Gas chromatograms of (a) SC-CO₂ extracted oil and (b) Soxhlet extracted oil FAMES

5.3.8 Physicochemical characteristics of oil

Different physicochemical properties such as refractive index, specific gravity, saponification value, unsaponifiable matter, iodine value, peroxide value, and an acid value of SC-CO₂ and conventional Soxhlet extracted oils of sea buckthorn berries were studied. The results of physicochemical studies are presented in **Table 5.6**. The refractive index of Soxhlet extracted oil (1.662) was significantly higher ($p < 0.05$) than SC-CO₂ extracted oil (1.457), and these values were in the range of the standard refractive index (1.448 - 1.477) for vegetable oils (Le

et al., 2018). The decrease in the refractive index of oils indicates the decrease in the state of unsaturation of fatty acids. Consistent with its lower refractive index, the specific gravity of SC-CO₂ extracted oil (0.934) was higher than Soxhlet (0.928) extracted oil. This confirms the higher selectivity of SC-CO₂ to separate short-chain SFA and UFA than Soxhlet. The relative density of both oils was very close to the edible oils. The saponification value is an indicator of the average molecular mass of the fatty acids of glycerides comprising oils. Consistent with the higher specific gravity, the saponification value of SC-CO₂ extracted oil was also significantly higher than Soxhlet extracted oil ($p < 0.05$), indicating that SC-CO₂ better extracts the shorter and low-molecular-weight triacylglycerols acids. The unsaponifiable matter of SC-CO₂ extracted oil was lower than Soxhlet, signifying the more significant percentage of oil-soluble matters other than triglycerides such as carotenoids and tocopherols are better extracted with Soxhlet extraction. In other words, the SC-CO₂ was not lipophilic enough to extract all the non-polar molecules from sea buckthorn berries; however, hexane was capable of extracting these compounds (Gu et al., 2017; Le et al., 2018).

The iodine value measures the percentage of UFA content in the oil. Consistent with the lower refractive index value, SC-CO₂ extracted oil showed a lower iodine value than Soxhlet extracted oil. Similarly, the acid value measures the amount of free fatty acids in the oil. SC-CO₂ extracted oil (8.4 ± 1.5 mg KOH/g) was found to have a lower acid value than Soxhlet extracted oil (10.6 ± 0.7 mg KOH/g). Free fatty acids in the oil can stimulate auto-oxidation reactions and should be within the permissible limit. A low acid value of SC-CO₂ and Soxhlet extracted oils showed good quality. The peroxide value is a crucial parameter for measuring oxygen content in the oil. The peroxide value of SC-CO₂ extracted oil was higher than Soxhlet extracted oil, and the peroxide values of both samples were within the permissible limit. Porto et al., (2016) and Pradhan et al., (2010) reported that SC-CO₂ extracted Moringa and flaxseed oils had lower peroxide values than Soxhlet. The results of physicochemical characterization

of sea buckthorn oils suggest that the oil extracted with SC-CO₂ had better quality than that extracted with Soxhlet (ValleS et al., 2000).

Table 5.6: Physico-chemical characteristics of sea buckthorn oils

Characteristics	SC-CO ₂ extracted oil	Soxhlet extracted oil
Refractive Index at 25 °C	1.457 ± 0.002 ^a	1.662 ± 0.00 ^b
Specific gravity (g/mL)	0.934 ± 0.01 ^a	0.928 ± 0.01 ^a
Saponification Value (mg KOH/g)	239.2 ± 6.7 ^a	210.9 ± 4.2 ^b
Unsaponifiable Matter (%)	2.23 ± 0.1 ^a	2.46 ± 0.02 ^b
Iodine Value (g I ₂ /100g)	69 ± 2.7 ^a	67 ± 2.1 ^a
Acid Value (mg KOH/g)	8.4 ± 0.7 ^a	10.6 ± 1.5 ^b
Peroxide Value (mg eq/kg oil)	3.15 ± 0.12 ^a	3.83 ± 0.25 ^b
Total phenolic and flavonoid content		
TPC (mg GAE/g)	30.13 ± 1.1 ^a	24.59 ± 0.09 ^b
TFC (mg QE/g)	1.58 ± 0.01 ^a	6.43 ± 0.39 ^b
Antioxidant activity (mg/mL)		
DPPH	1.09 ± 0.06 ^a	1.22 ± 0.07 ^a
ABTS	2.59 ± 0.15 ^a	2.83 ± 0.26 ^b

Different superscript letters within a row represent significant differences at $p < 0.05$.

5.3.9 Total phenolic and flavonoid content

Estimation of the total phenolic and flavonoid contents of fruits and vegetables is essential to determine their nutritional and medicinal value. The sea buckthorn berries are a potential source of valued nutrients and bioactive compounds that contribute to their antioxidant and antibacterial activity (Bal et al., 2011). The total phenolic and flavonoid contents of sea buckthorn berries oil obtained from SC-CO₂ extraction and conventional Soxhlet extraction are

tabulated in **Table 5.6**. The SC-CO₂ extracted oil (30.13 ± 1.1 mg GAE/g oil) had significantly higher total phenolic content ($p < 0.05$) than Soxhlet extracted oil (24.59 ± 0.08 mg GAE/g oil). In comparison, total flavonoid content (1.58 ± 0.01 mg QE/g oil) was lower than Soxhlet extracted oil (6.42 ± 0.38 mg QE/g oil). This is mainly due to the differences in the temperature of the two extraction methods. Although both extractions took the same time (2 h), the extraction temperature for Soxhlet extraction (69°C) was considerably higher than the SC-CO₂ extraction temperature (48.46°C). Therefore, the latter had more heat-sensitive polyphenolic compounds than the former. Furthermore, SC-CO₂ has lower lipophilicity than Soxhlet at the ideal extraction pressure and temperature (27.02 MPa, 48.46°C), making it more efficient in extracting polar polyphenolic compounds. The solubility of polyphenolic compounds in SC-CO₂ depends on several thermodynamic properties such as operating pressure, temperature, critical temperature, critical pressure, acentric factor, and molar volume. In favor of the above explanations, Narváez-Cuenca et al., (2020) have reported that phenolic compounds, which are relatively polar, are better extracted in SC-CO₂ than Soxhlet, emphasizing that the total phenolic content in guava seed oil extracted by SC-CO₂ was much higher than hexane extracted oil. In another study, Mohamed et al., (2016) reported that the total phenolic content of *Vitis vinifera* L. seed oils did not significantly differ when extracted by each extraction method.

5.3.10 Antioxidant activity

DPPH and ABTS assays response in terms of their IC₅₀ values for both the extracts is tabulated in **Table 5.6**. Both the SC-CO₂ and Soxhlet extracted oils showed significant antioxidant activity, with SC-CO₂ oil performing better. This could be due to the mild optimal extraction temperature applied for SC-CO₂ extraction, which favors the extraction of heat-sensitive antioxidant compounds. In addition, at optimal extraction pressure and temperature (27.02 MPa, 48.46°C), the hydrophilic affinity of SC-CO₂ towards more active antioxidant

compounds increased. The antioxidant capacity of various seed oils extracted using SC-CO₂ has been investigated, and according to Le et al., (2018) and Mohamed et al., (2016), SC-CO₂ extracted oil had stronger radical scavenging activity than Soxhlet extracted oil. In another study conducted by Kagliwal et al., (2012), the IC₅₀ (DPPH assay) of SC-CO₂ extracted oil of sea buckthorn berry powder was 29.02 mg/mL, which was much higher than 1.09 ± 0.06 mg/mL of the current study. It is known that antioxidant activity depends on various phytochemical components such as total phenolic and flavonoid, tocopherol, and carotenoid content in the oil. Zheng et al., (2017) have studied the phytochemical composition of sea buckthorn pulp oil and reported that the oil's total flavonoid, carotenoid, and polyphenol content have a positive effect on the ABTS assay. They also stated that the tocopherol and phytosterol concentration in the oil contributed more to the DPPH assay. Other studies also reported that the antioxidant activity of the lipophilic extract of sea buckthorn berries and seeds increased significantly with total carotenoid and tocopherol content (Olas et al., 2018; Ting et al., 2011). Thus, it can be concluded that the higher radical scavenging potency of SC-CO₂ extracted oil could be due to the higher level of total phenolic content.

5.3.11 Antibacterial activity

The antibacterial activities of SC-CO₂ and Soxhlet extracted oils were evaluated using a zone of inhibition (ZoI) assay, and the results are presented in **Table 5.7**. Gram-negative and Gram-positive bacteria were used for the antibacterial activity study of oils because they are vital as a food-borne pathogen. Both SC-CO₂ and Soxhlet extracted oils showed the highest bactericidal activity against *S. aureus* with ZoI of 8.5 ± 0.7 mm and 7 mm, respectively. Lowest ZoI was observed for both the oil samples in *E. coli*, followed by *E. aerogenes*. The sea buckthorn oils were more active against Gram-positive bacteria than Gram-negative bacteria. This could be because Gram-negative bacteria have very tough peptidoglycan deposited on

their outer membrane cell wall, which could not easily be penetrated by the oil (Purohit et al., 2021b). Thus, the ZoI study confirmed that SC-CO₂ extracted oil had good antibacterial activity compared to Soxhlet extracted oil.

Table 5.7: Zone of Inhibition (mm) of SC-CO₂ and Soxhlet extracted oils

Extraction medium	Gram-positive bacteria				Gram-negative bacteria			
	<i>S. aureus</i>	<i>B. subtilis</i>	<i>S. epidermidis</i>	<i>M. luteus</i>	<i>E. coli</i>	<i>K. pneumonia</i>	<i>E. aerogenes</i>	<i>P. aeruginosa</i>
SC-CO ₂	8.5±0.7	7±2.8	8±1.4	5±1.4	3±0.7	4.5±2.1	7±1.4	5.5±2.1
n-hexane	7	6.5±2.1	5.5±2.1	6	4±0.7	4.5±0.7	6.5±1.4	7±2.1

5.3.12 Thermal stability

The thermal decomposition behavior of SC-CO₂ and Soxhlet extracted oils were investigated using a thermogravimetric analyzer. The TG and DTG profiles of both oils at a heating rate of 10 °C/min are shown in **Fig. 5.6 (a) and (b)**. The breakdown of larger chemicals into low molecular weight compounds and the volatilization of low molecular weight components are referred to as decomposition. SC-CO₂ and Soxhlet extracted oils showed two stages of decomposition (stage I and stage II), as shown in **Fig. 5.6 (b)**. Hence, in both active thermal degradation stages, decomposition and volatilization processes occur. Stage I decomposition is the most important region to determine the thermal stability of oils because degradation of the UFA begins at the onset temperature of this stage.

The onset temperatures for SC-CO₂ and Soxhlet extracted oils were 185 °C and 203 °C, respectively, implying that the former had less thermal stability. Oils with higher viscosity have higher molecular weight and decompose at a higher temperature than oils with lower viscosity (Gamlin et al., 2002). The value of onset temperatures for Soxhlet extracted oil obtained in the current study (203 °C) are comparable to that of karanja oil (202 °C) (Volli and Purkait, 2014),

linseed oil (202.91°C), sunflower oil (210.66°C) (Li et al., 2018), and lower than that of rapeseed oil (221.45 °C), palm oil (250.22 °C) (Li et al., 2018).

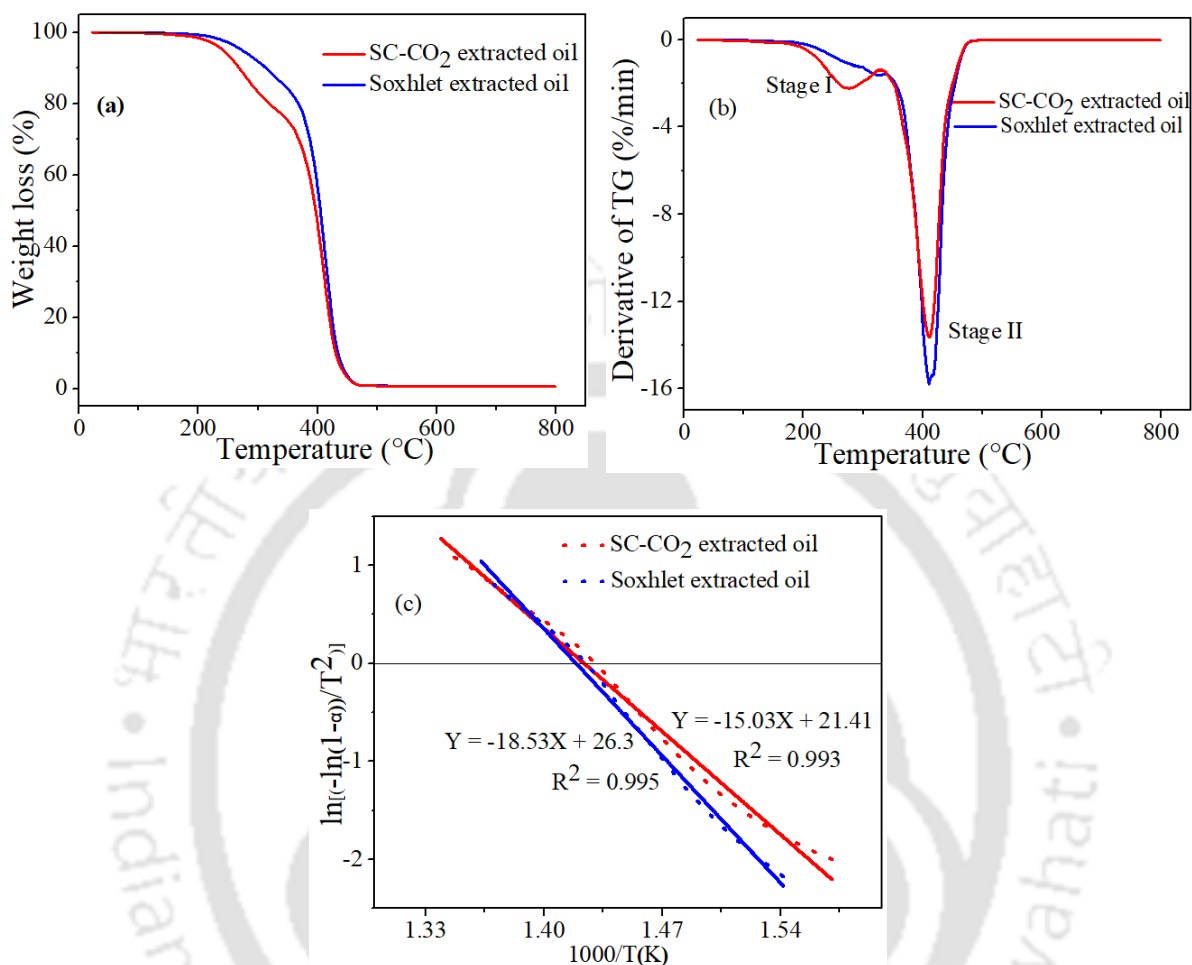


Fig. 5.6: (a) TGA, (b) DTG, and (c) Arrhenius plots for SC-CO₂ and Soxhlet extracted oils

In stage I (**Fig. 5.6 (a) and (b)**), thermal degradation of SC-CO₂ and Soxhlet extracted oils occurred between 185 - 321 °C and 203 - 336 °C, respectively, resulting in 20.47% weight loss (Δ w_t%) for SC-CO₂ extracted oil and 13.35% for Soxhlet extracted oil (**Table 5.8**). The first stage involves the mass loss due to the degradation of triglycerides which produce light volatile compounds, and the decomposition of PUFA. Lighter compounds evolved during the early stage of volatilization. SC-CO₂ extracted oil was more susceptible to thermal degradation than Soxhlet extracted oil. This could be because SC-CO₂ extracted oil has a more concentration of

shorter-chain UFA and low-molecular-weight triacylglycerol acids, which thermally break down faster than SFA and long-chain UFA. This was consistent with the oil compositions and properties that are shown in **Table 5.6**.

Table 5.8: TGA characteristic properties for active pyrolysis stages of SC-CO₂ and conventional Soxhlet extracted oils

Properties	SC-CO ₂ extracted oil		Soxhlet extracted oil	
	Stage I	Stage II	Stage I	Stage II
T _o , °C	159.6	336	166.6	337.9
T _f , °C	326.6	478	336.6	482.6
ΔWt, %	20.47	77.52	13.35	85.57
T _{max} , °C	276.67	410.61	326.6	410
W _{max} , %/min	2.22	13.64	1.48	15.95
E _a (kJ/mol)*	49.28	125	51.17	154.1
Frequency factor (1/min)	10.53	21.41	9.97	26.3

T_o: Initial temperature for the main mass loss (°C). T_f: Final temperature for the main mass loss (°C). T_{max}: Temperature for maximum rate of mass loss (°C). ΔWt: change of mass loss. W_{max}: Maximum mass loss rate (%/min), E_a: activation energy, * R²>0.993.

In the II stage (**Fig. 5.6 (a) and (b)**), thermal degradation of SC-CO₂ extracted oil commenced at a slightly lower temperature at 336 °C and ended at 478 °C, compared to Soxhlet extracted oil (i.e., started at 347 °C and ended at 478 °C) and resulted in weight loss of 77.52% and 85.57%, respectively. This could be attributed to the higher SFA concentration in the Soxhlet extracted oil.

Assuming first-order decomposition, Stage I and II thermal degradation curves of oils fit with the Coats–Redfern model with regression coefficients greater than 0.99. The regression plot

for stage II thermal degradation is presented in **Fig. 5.6 (c)**. The activation energies of SC-CO₂ and Soxhlet extracted oils were nearly identical in Stage I; however, in Stage II, the former (125 kJ/mol) had lower activation energy than the latter (154.1 kJ/mol). The activation energy (E_a) is the minimum energy required to break the chemical bond between the atoms (Reshad et al., 2017). The higher activation energy of Soxhlet extracted oil indicates that the oil was more challenging to decompose thermally owing to the higher molecular weight of UFA and SFA that exhibits a formidable intermolecular force than SC-CO₂ extracted oil. The values of activation energy and frequency factor computed by the Coats-Redfern model are tabulated in **Table 5.8**. The activation energies of sea buckthorn oils were in the range of earlier published reports on soybean (135.4 - 146.6 kJ/mol), mustard (134.2 - 142.1 kJ/mol), olive (119.5 - 142.5 kJ/mol), and karanja (125.7 - 156.5 kJ/mol) (Volli and Purkait, 2014).

5.3.13 Rheological measurement

The rheology study is essential to characterize oils' fundamental flow and deformation properties. Viscosity is a parameter used to describe the quality of oils. The shear stress versus shear rate data of SC-CO₂ and Soxhlet extracted oils measured at 25 °C were fitted to Bingham rheological models as shown in **Fig. 5.7 (a)**. SC-CO₂ and Soxhlet extracted oils fit well with the Bingham plastic model with correlation coefficients of 0.997 and 0.991, respectively. The Bingham yield stress is the shear stress at a zero shear rate. The yield stress for SC-CO₂ and Soxhlet extracted oil was 0.82 Pa and 13.77 Pa. Before the yield stress was attained, the oil was in a solid-like state, or the molecules didn't move until the internal structure was broken. Sunflower oil, cottonseed oil, and palm olein exhibited Bingham plastic behavior (Hassanien and Sharoba, 2014). However, the yield stress of Soxhlet extracted oil was higher than the reported values. Shear stress increased linearly with the shear rate for both oils, implying that oils behaved essentially as Newtonian fluids. The Newtonian flow pattern of the oils is due to

the presence of long-chain molecules (Gu et al., 2019). The Bingham plastic viscosities of SC-CO₂ and Soxhlet extracted oils calculated from slopes of the flow curves were 11.9 mPa.s and 46.31 mPa.s, respectively. The viscosity of soxhlet extracted oil in the current study was higher than that of olive oil (34. mPa.s), rapeseed oil (37.6 mPa.s), soybean oil (40.5 mPa.s), and safflower oil (44.5 mPa.s) (Diamante and Lan, 2014). Hassanien and Sharoba (2014) have established a positive correlation between viscosity and the total SFA composition of the oil. As indicated in **Table 5.6**, Soxhlet extracted oil with a much higher viscosity contains a high percentage of total SFA. Further, the acid value of the SC-CO₂ extracted oil was significantly lower ($p < 0.05$) than Soxhlet-extracted oil (**Table 5.6**). The increase in the free fatty acid content can increase the oil viscosity, which may be because less shear force is enough to initiate the oil to flow (Liu et al., 2012).

Fig. 5.7 (b) depicted the shear-thinning fluid property of Soxhlet extracted oil, in which apparent viscosity decreased with increasing shear rate from 1 to 10 s⁻¹. The shear-thinning fluids are ubiquitous in industrial and biological processes because the fluid will distribute properly in a process where high shearing stresses are employed. On the other hand, the viscosity of SC-CO₂ extracted oil was essentially unaffected by the shear rate.

Fig. 5.7 (C) shows the viscosities of oils at a shear rate of 10 s⁻¹ throughout a temperature range of 10 to 85 °C. The viscosity of both oils decreased with increasing temperature, with higher thermal susceptibility at temperatures below 25 °C and 60 °C for SC-CO₂ and Soxhlet extracted oils, respectively. The SC-CO₂ extracted oil showed lower viscosity at the tested temperature range. The Arrhenius-type equation well describes the variation of oils viscosity with temperature. The linear regression coefficients of ln (Viscosity) versus 1/T(K) for SC-CO₂ and Soxhlet extracted oils were 0.90 and 0.94, respectively. SC-CO₂ extracted oil (71.33 KJ/mol) had a lower flow activation energy than Soxhlet extracted oil (77.82 KJ/mol), supported by steady shear measurements and TGA analysis. This showed that greater energy is needed to

change the viscosity of Soxhlet extracted oil. This is because higher viscous fluid requires higher mean pressure to initiate the flow; thus, the corresponding energy increases according to the viscosity-induced pressure rise. The flow activation energies obtained in the present study were higher than those from other reports, such as in a study by Diamante and Lan, (2014) for olive oil, 24.63 kJ/mole; for grape seed, 21.31 kJ/mole; and for rapeseed, 24.45 kJ/mole.

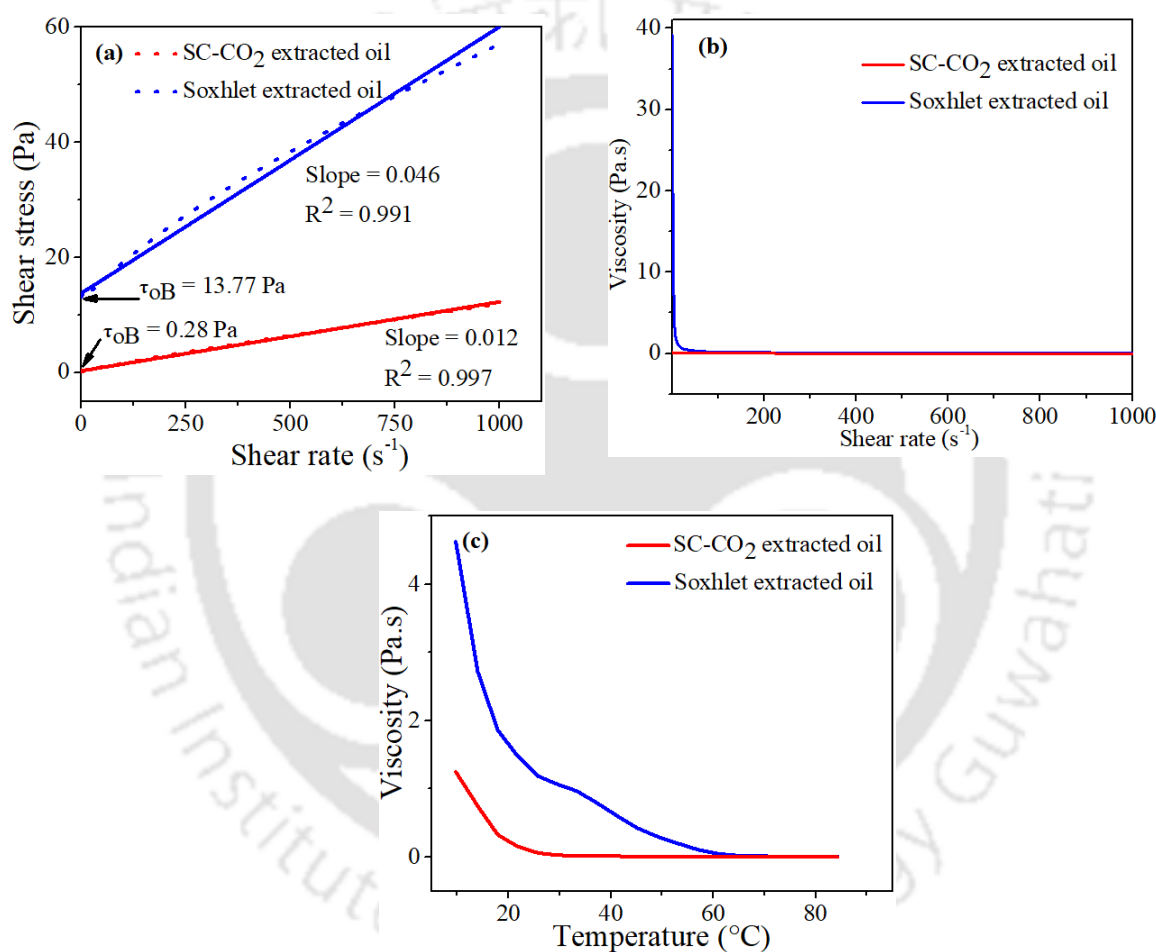


Fig. 5.7: (a) Flow behavior, (b) Effect of the shear rate on the viscosity, (c) Effect of the temperature on the viscosity of SC-CO₂ and Soxhlet extracted oils

5.4 Summary

The current study has provided insights into the optimization and characterization of SC-CO₂ extracted oil from *Hippophae salicifolia* berries. The conclusions are summarized as follows:

- Effect of process variables on oil yield, β -carotene and total tocopherol contents of the oil were sufficiently described and predicted by the 2nd order polynomial model.
- Individual coefficients of pressure and CO₂ flow rate and interaction terms between pressure and temperature significantly affected the oil yield. CO₂ flow rate had a maximum effect on the oil yield. In contrast, the extraction pressure had most significantly affected the oil's β -carotene and total tocopherol contents.
- The optimum values of the process parameters for maximum oil yield, β -carotene, and total tocopherol content as predicted by the model were: 27.02 MPa, 48.46 °C, 16.45 g/min CO₂ flow rate.
- The projected recovery of oil yield, β -carotene, and total tocopherol by SC-CO₂ extraction under optimum conditions were 88.17%, 90.65%, and 94.31%, respectively.
- Omega-7 fatty acid (palmitoleic acid) comprised 42.98% of total oil and was the predominant UFA in SC-CO₂ extracted oil.
- SC-CO₂ extracted oil showed a significant amount of β -carotene, total tocopherol, TPC, and TFC with considerable antioxidant and antibacterial activity.
- SC-CO₂ extracted oil was more susceptible to temperature and showed more resistance to mechanical stress than Soxhlet extracted oil.
- SC-CO₂ extraction of sea buckthorn berries oil is an effective alternative to replace conventional solvent extraction in the food, cosmetics, and pharmaceutical sectors.

**OPTIMIZATION,
CHARACTERIZATION, AND
EVALUATION OF ANTIOXIDANT AND
ANTIBACTERIAL ACTIVITIES OF
SILVER NANOPARTICLES
SYNTHESIZED FROM *HIPPOPHAE
SALICIFOLIA***

Published in

Journal of Inorganic Chemistry Communications. 146, 2022.

[TH-3034_166107031](#)



OPTIMIZATION, CHARACTERIZATION, AND EVALUATION OF ANTIOXIDANT AND ANTIBACTERIAL ACTIVITIES OF SILVER NANOPARTICLES SYNTHESIZED FROM *HIPPOPHAE SALICIFOLIA***6.1 Background**

Nano-biotechnology is a specific research area due to the wide range of prospective applications in food, chemical, and biomedical fields. Silver nanoparticles have received considerable attention for their effective antiviral, antioxidant, and antimicrobial activity. Plant extract-mediated silver nanoparticles (Ag NPs) synthesis is cheap and eco-friendly. This study is concerned with synthesizing Ag NPs using berries and leaves extracts of *Hippophae salicifolia*. Methanol and aqueous extracts were used from successive Soxhlet extraction. Optimizing the process parameters for efficient reduction of Ag⁺ ions is a crucial step in any synthesis process. This study employed a known concentration of extracts for the optimization study. The parameters such as extract concentration, AgNO₃ concentration, pH, temperature, and time were optimized to get the highest possible Ag NPs yield. The increasing concentration of NPs indicated by the rising intensity of the surface plasmon resonance (SPR) peak (Bar et al., 2009). The formation of Ag NPs was confirmed by UV-Vis spectrophotometer. The synthesized Ag NPs were characterized by DLS, FTIR, XRD, EDX, FESEM, and FETEM. Furthermore, the TPC, TFC, and antioxidant and antibacterial activities of the synthesized Ag NPs were evaluated.

6.2 Overview

Ag NPs were successfully synthesized at optimum conditions and characterized. TEM analysis depicted that sea buckthorn leaves and berries extract mediated Ag NPs obtained at optimum conditions are monodispersed spherical with average particles size of 7.87 ± 2.9 nm (nanoparticles synthesized from leaves-aqueous extract) to 13.86 ± 5 nm (nanoparticles synthesized from berries-aqueous extract). Ag NPs synthesized from aqueous extracts are smaller in size than those synthesized from methanol. Antioxidant and antibacterial results suggest that Ag NPs have very high efficacy compared to extracts from which they are synthesized. The Ag NPs obtained from leaves-methanol extract exhibited the highest total phenolic and flavonoid content with the highest antioxidant (IC₅₀: 1.29 ± 0.3 $\mu\text{g/mL}$) and antibacterial activity (MIC: 1.9 $\mu\text{g/mL}$). The minimum inhibitory concentration of Ag NPs ranged from 1.9 to 31.5 $\mu\text{g/mL}$ for eight tested bacterial pathogens. Ag NPs have great antioxidant and antibacterial potential to control and prevent various bacterial infections.

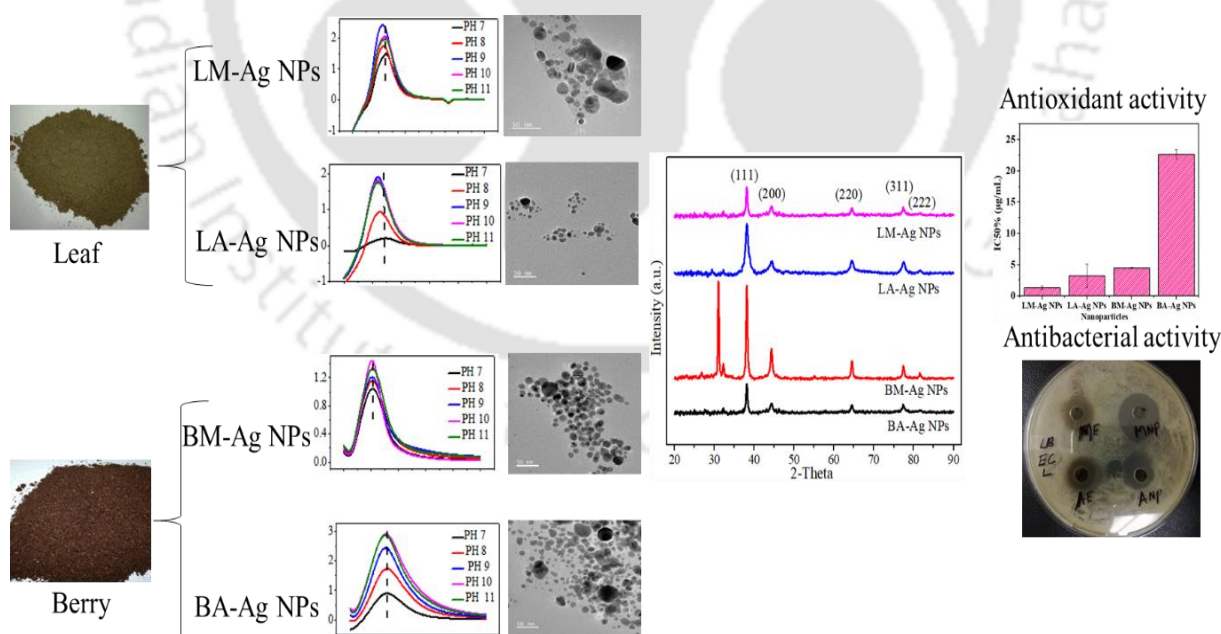


Fig. 6.1: Graphical Abstract

6.3. Results and discussion

6.3.1. Optimization study

Each reaction variable (concentrations of plant extract and AgNO₃, pH, temperature, and time) showed various effects on the reduction rate of Ag⁺ to Ag⁰ as shown in **Fig. 6.3. and 6.4.** Depending on the variation in the reaction settings, the SPR peak between 410 and 445 nm served as confirmation of the generation of monodispersed spherical Ag NPs. SPR is a resonant oscillation that depends on many factors such as; size, shape, surface chemistry, and solvent medium in which particles are dispersed. The SPR absorption indicated that Ag NPs have an excellent particle dispersion without aggregation. **Fig. 6.2.** provides a flowchart for optimization, characterization, and evaluation of antioxidant and antibacterial activities of silver nanoparticles synthesized from *hippophae salicifolia*.

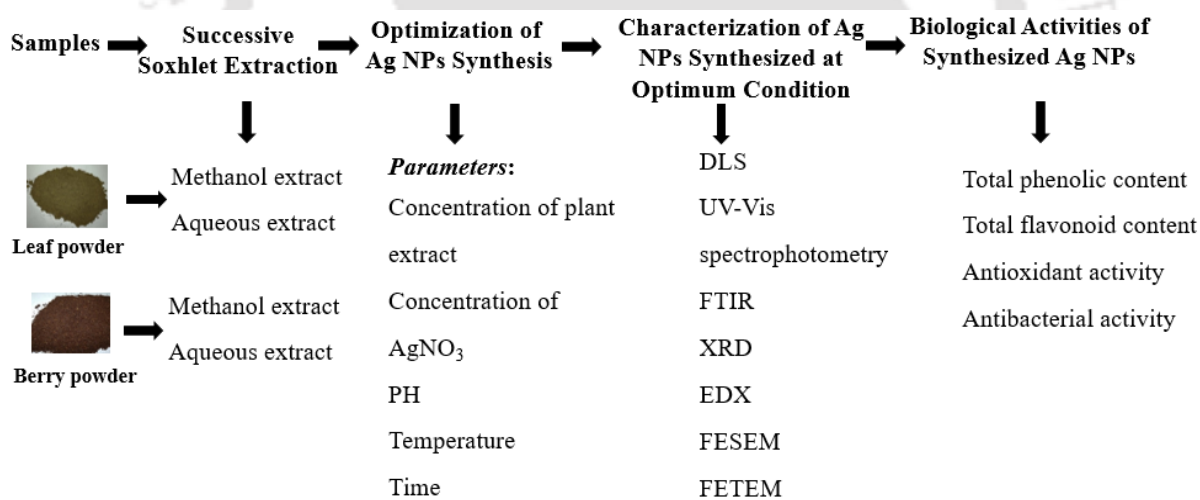


Fig. 6.2: Schematic diagram

6.3.1.1 Effect of extract concentration

The effect of Sea buckthorn leaves and berries extract concentrations on the formation of Ag NPs was studied by mixing AgNO₃ solution (95 mL) and various concentrations of extracts (5 mL). The concentration of leaves and berries extract varied from 500 to 2000 µg/mL and 1000

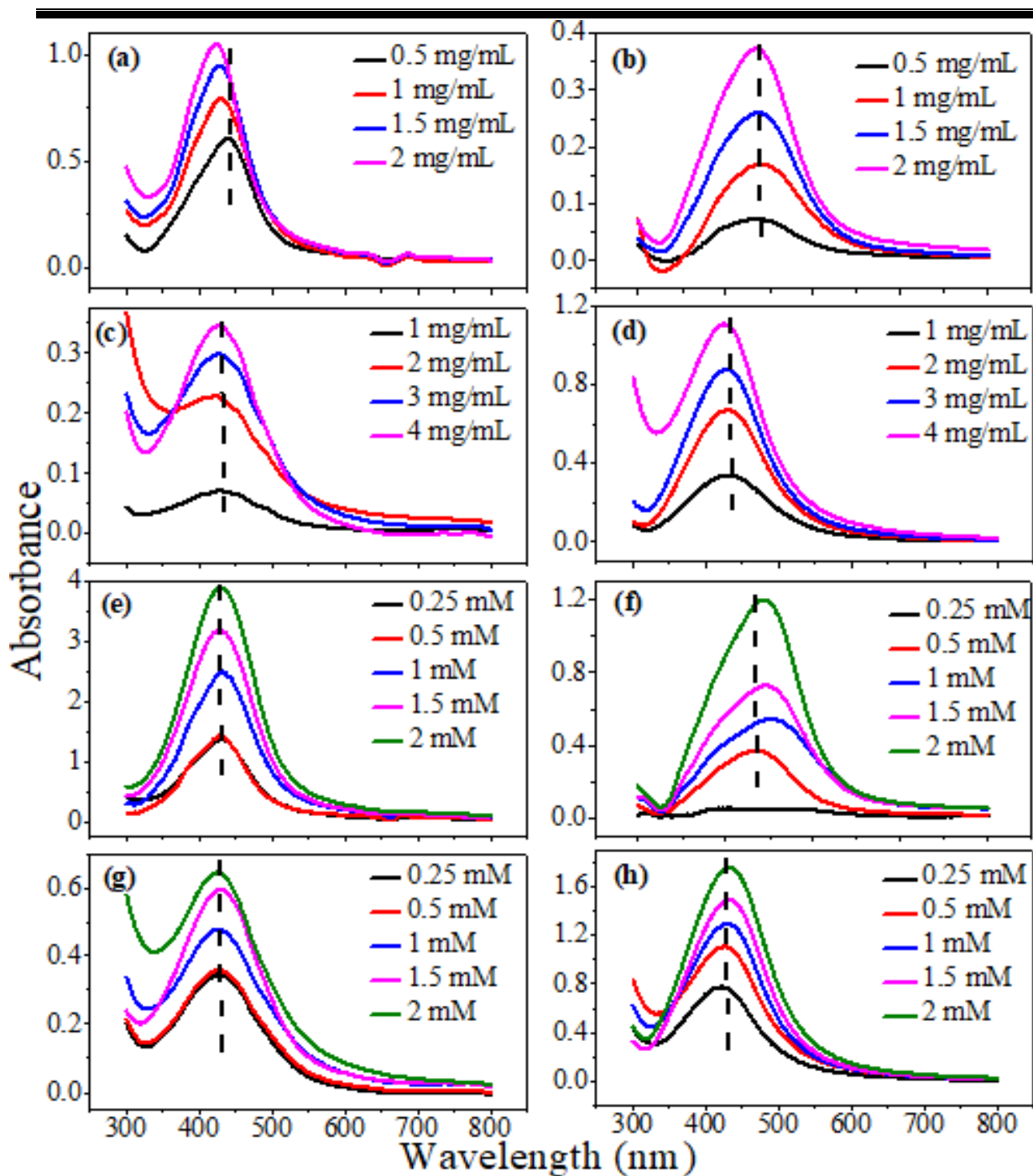


Fig. 6.3: UV-vis spectrum of Ag nanoparticle: (a - d) Effect of extract concentration on (a) LM-Ag NPs, (b) LA-Ag NPs, (c) BM-Ag NPs, (d) BA-Ag NPs. (f - h) Effect of AgNO_3 concentration on (e) LM-Ag NPs, (f) LA-Ag NPs, (g) BM-Ag NPs, (h) BA-Ag NPs. LM-Ag NPs - nanoparticles from leaves-methanol extract, LA-Ag NPs - nanoparticles from leaves-aqueous extract, BM-Ag NPs - nanoparticles from berries-methanol extract, BA-Ag NPs - nanoparticles from berries-aqueous extract

to 4000 $\mu\text{g/mL}$, respectively. With increasing the concentration of extracts, absorption peaks of synthesized Ag NPs increased and underwent a blue shift, as shown in **Fig. 6.3. (a-d)**. The increase in SPR peak indicates the formation of more NPs, while the blue shift confirmed the formation of smaller and spherical NPs (Bar et al., 2009). A shift in the SPR peak position towards lower wavelengths implied that an increase in the extract concentrations leads to the formation of smaller and spherical NPs. As the size of NPs decreases, the energy required to excite the electrons at SPR increases, subsequently causing the absorption peak to shift toward lower wavelengths. Despite the lower concentration, the Ag NPs yield from leaves extract was found to be higher than berries, as evidenced by the higher intensity of SPR peak for leaves colloids. This could be attributed to the higher phenolic and flavonoid content in the leaves than in berries. For a similar reason, Ag NPs from leaves-methanol extract (LM-Ag NPs) and berries-methanol extract (BM-Ag NPs) also showed higher SPR peaks intensity than the corresponding aqueous extracts. Our findings are supported by Khalil et al., (2014), who claim that as the concentration of olive leaf extract increases, the absorption peak sharpens and shifts from 458 to 441 nm. Based on the peak intensity, the optimum extract concentration of leaves and berries extracts were 2000 $\mu\text{g/mL}$ and 4000 $\mu\text{g/mL}$, respectively.

6.3.1.2 Effect of AgNO_3 concentration

The effect of AgNO_3 concentration (0.25 to 2 mM) on the UV-vis spectrum of Ag NPs at optimum extract concentration (for leaves; 2000 $\mu\text{g/mL}$ and for berries; 4000 $\mu\text{g/mL}$) is presented in **Fig. 6.3. (e-h)**. The optical measurements of Ag NPs solutions showed the absorption peaks at 428 nm for LM-Ag NPs, between 436-444 nm for LA-Ag NPs, 424 nm for BM-Ag NPs, and between 421-432 nm for BA-Ag NPs. The UV-vis spectra results revealed that increasing the AgNO_3 concentration increased SPR peaks. For LA-Ag NPs and BA-Ag NPs suspensions, the peak underwent a redshift, implying that the size of Ag NPs increased

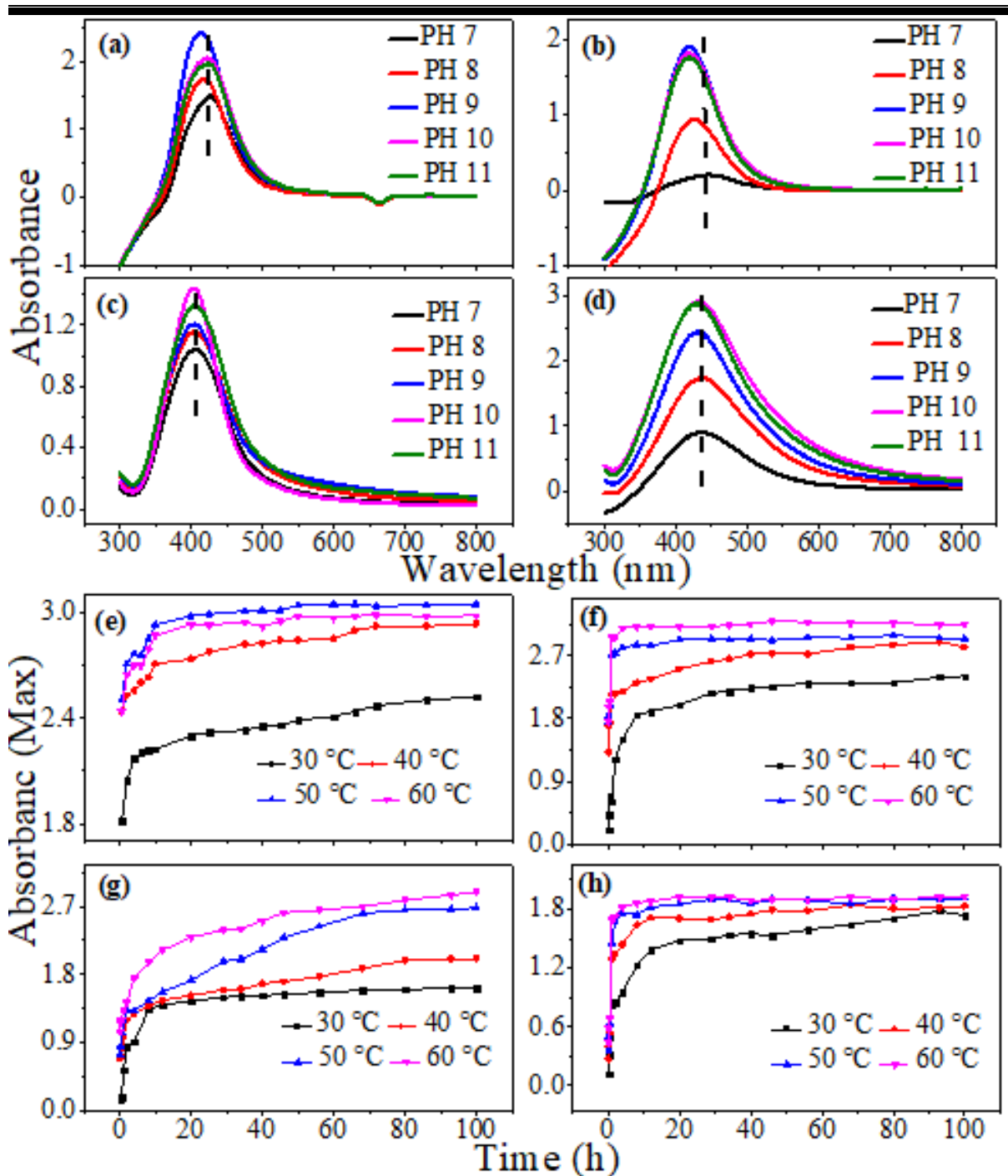


Fig. 6.4: Effect of PH on UV-vis spectrum of Ag nanoparticle: (a - d) Effect of PH on (a) LM-Ag NPs, (b) LA-Ag NPs, (c) BM-Ag NPs, (d) BA-Ag NPs. (e - h) Effect of temperature and time on (e) LM-Ag NPs, (f) LA-Ag NPs, (g) BM-Ag NPs, (h) BA-Ag NPs. LM-Ag NPs - nanoparticles from leaves-methanol extract, LA-Ag NPs - nanoparticles from leaves-aqueous extract, BM-Ag NPs - nanoparticles from berries-methanol extract, BA-Ag NPs - nanoparticles from berries-aqueous extract

6.3.1.3 Effect of pH

pH is considered another critical parameter in the synthesis of Ag NPs. The UV-Vis spectrum of Ag NPs suspension synthesized at variable pH is shown in **Fig. 6.4. (a - d)**. The mixture of methanol-leaves extract, aqueous-leaves extract, methanol-berries extract, and aqueous-berries extract with AgNO_3 had initial pH values of 4.1, 5.6, 3.6, and 4.7, respectively. The pH affects the size, shape, and stability of Ag NPs due to their capability to alter the charge of macromolecules in the suspension (Khalil et al., 2014; Seifipour et al., 2020). A minor increase in pH boosted extract reductant reactivity and resulted in a rapid and dramatic shift in the colloid solution's color. As a result, Ag NP suspensions produced a long-broad range SPR peak that extended above the UV-Vis spectrophotometric maximum limit. Ag NPs suspension of the leaves and berries were diluted 8 and 4 times, respectively, before UV-Vis spectrometer analysis to produce sharp and narrow SPR peaks. In the case of LM-Ag NPs and LA-Ag NPs, SPR peaks became sharper and underwent a blueshift with pH indicating the formation of small-sized Ag NPs particles. The SPR peak for LM-Ag NPs changed from 430 nm (pH 7) to 412 nm (pH 9) and then redshifted toward 424 nm at pH 11. While in the case of LA-Ag NPs, the peak shifted from 445 nm (pH 7) to 419 (pH 11). This implies the availability of more hydroxyl ions in the alkaline condition, which bind to Ag^+ resulting in forming a higher and more stable yield of Ag NPs. The SPR peaks of LM-Ag NPs and LA-Ag NPs suspensions were observed to decline after pH 9. Similarly, the absorption peaks of BM-Ag NPs (428 nm to 427 nm) and BA-Ag NPs (437 nm to 432 nm) showed a very slight blue shift with pH, indicating no significant change in the size of synthesized NPs. The highest SPR absorptions for BM-Ag NPs and BA-Ag NPs were observed at pH 10. Therefore, pH 10 and pH 9 were determined to be the best values for producing Ag NPs from leaves and berries extracts, respectively. Riaz et al., (2021) have reported that the optimal pH for Ag NPs synthesis from green tea leaves at 65 °C was 9. They also discovered that increasing the pH from 7 to 9 reduced the mean diameter

of Ag NPs from 9.9 nm to 5.6 nm and that increasing the pH to 11 caused the SPR peak and mean diameter to decrease.

6.3.1.4 Effect of temperature

After adjusting the extract concentration, AgNO₃, and pH, the reaction temperature and time were simultaneously optimized with the help of a maximum SPR peak versus time plot (**Fig. 6.4 e - h**). The absorption spectra of Ag NP colloids produced at different temperatures (30, 40, 50, and 60 °C) were scanned at intervals of 0.08 h to 100 h. According to several investigations, the synthesis of Ag NPs at room temperature took longer time, lasting between 4 and 7 days (Khalil et al., 2014; Peiris et al., 2017). An increase in temperature can speed up the production of Ag NPs. In our experiment, the SPR peak intensity of LM-Ag NPs increased throughout the entire reaction time. It also increased with reaction temperature from 30 to 50 °C, and decreased as the temperature was further raised to 60 °C. This could be due to the degradation of phytochemicals at elevated temperatures. However, the SPR absorption for LA-Ag NPs, BM-Ag NPs, and BA-Ag NPs increased as the reaction temperature rose from 30 °C to 60 °C. Therefore, the optimal temperature for LM-Ag NPs was determined to be 50 °C. Whereas the optimum temperatures for LA-Ag NPs, BM-Ag NPs, and BA-Ag NPs were measured to be 60 °C. Riaz et al., (2021) have reported that the effect of temperature on the formation of Ag NPs from methanolic extract of green tea leaf is dependent on pH. According to their report, the optimal temperature for synthesizing monodispersed small-sized spherical NPs at 9 pH was 65 °C. Another study by Ahmad et al., (2013) stated that the optimum temperatures and pH for the formation of Ag NPs from aqueous extract of *Hippophae rhamnoides* L. (Sea buckthorn) leaves were 75°C and 7, respectively.

6.3.1.5 Effect of time

The optimum reaction time for the formation of Ag NPs was estimated by analyzing the intensity of the SPR peak at regular time intervals between 0.08 h and 100 h. When the PH of the colloid is adjusted to an optimal value, the creation of Ag NPs appears to commence. However, the time required to complete the transformation from Ag^+ to Ag^0 needs to be optimized. The optimum reaction time was assumed to be the time required to achieve a narrow and stable SPR absorption band and it was determined from the plot of maximum SPR peak versus time. The plot of maximum SPR peak versus time for each Ag NPs suspension is presented in **Fig. 6.4 (e -h)**. At the beginning of the reaction, from 1 to 10 hours, the rate of NP generation for LM-Ag NPs, LA-Ag NPs, and BA-Ag NPs was higher. However, after 10 hours, the strength of absorption peaks was found to be reasonably steady. In previous studies, increasing the reaction time at room temperature resulted in a gradual increase in the absorbance spectrum, followed by a decrease in the absorbance after 4 to 7 days (Khalil et al., 2014; Peiris et al., 2017). The decrease in SPR peak with time indicates the formation of aggregation. In the present study, 10 h of reaction time was sufficient to get a stable LM-Ag NPs, LA-Ag NPs, and BA-Ag NPs colloid solution with a steady SPR peak. Whereas BM-Ag NPs synthesis required a longer time to reduce silver ions as shown in **Fig. 6.4. (g)**. It was noticed that 20 h reaction time was sufficient to complete the reduction of Ag^+ to Ag NPs at 30 ° C, but with the smallest SPR peak. However, as the temperature raised from 40 °C to 60 °C, the reaction time up to 100 h was found to be insufficient to complete the reaction. Sea buckthorn berries are known for higher oil with a higher unsaturated fatty acid content, and methanol dissolves the molecules in a wide range of polarity, including oils. As a result, heating the oil to a higher temperature for a longer time allows the oil to melt and dissociate into the reaction media, improving the interaction between vitamins, fatty acids, and other chemicals

with Ag⁺. Thus, from SPR peak versus time plot, the optimum time for BM-Ag NPs was determined to be 48 h.

Table 6.1: Optimum conditions for the synthesis of Ag NPs

	Extract Conc.	AgNO ₃ Conc.	PH	Temperature	Time
LM-Ag NPs	2 000 µg/mL	2 mM	9	50 °C	10 h
BA-Ag NPs	2 000 µg/mL	2 mM	9	60 °C	10 h
BM-Ag NPs	4 000 µg/mL	2 mM	10	60 °C	48 h
BA-Ag NPs	4 000 µg/mL	2 mM	10	60 °C	10 h

LM-Ag NPs - nanoparticles synthesized from leaves-methanol extract, LA-Ag NPs - nanoparticles synthesized from leaves-aqueous extract, BM-Ag NPs - nanoparticles synthesized from berries-methanol extract, BA-Ag NPs - nanoparticles synthesized from berries-aqueous extract.

6.3.2 Ag NPs yield at optimum condition

Table 6.1 revised the optimal conditions for the production of Ag NPs from methanol and aqueous extracts of sea buckthorn leaves and berries. The yield of Ag NPs generated at optimum conditions from each extract was estimated from SPR peak of the suspension and the weight of Ag-NPs recovered by centrifugation and compared. Based on the SPR peak intensity, the yield of Ag NPs was found in decreasing order of LM-Ag NPs > LA-Ag NPs > BM-Ag NPs > BA-Ag NPs (**Fig. 6.4 e - h**). On the other hand, based on the weight of Ag NPs recovered by centrifugation, the highest yield was 56% for LM-Ag NPs, followed by BM-Ag NPs (44.56%), BA-Ag NPs (37.81%), and LA-Ag NPs (27.73%). Here, we hypothesize that the disparate trends yield of Ag NPs from the SPR peak and weight of those that were recovered after centrifugation may be explained by the challenges associated with centrifuging small-sized NPs.

6.3.3 Characterization of Ag NPs

6.3.3.1 Particle size analysis

DLS analyzed the size of Ag NPs in suspension, and the results are presented in **Table 6.2**. LA-Ag NPs (9.45 ± 0.21 nm) were found to be the smallest in size, followed by LM-Ag NPs (12.75 ± 0.08 nm), BA-Ag NPs (25.65 ± 8.7 nm), and BM-Ag NPs (30.25 ± 2.1 nm). Leaves and berries aqueous extract mediated Ag NPs were smaller in size than those methanol extract mediated NPs. Mani et al., (2021) reported Ag NPs from aqueous extract *B.abla* leaf in size ranged from 20 to 113.6 nm. In another study, the size of Ag NPs made from *Azadirachta indica* aqueous leaf extract was 34 nm. The DLS results were confirmed by XRD and TEM investigation and revealed a similar trend. The average dimension of the Ag NPs evaluated by DLS was generally more significant than the values obtained by TEM examination, as evidence of a low level of NPs aggregation in the suspension. This arises from the fact that DLS assesses a size rather than a physical size, and DLS has a tendency to favor higher size fractions.

Table 6.2: Size of NPs using DLS, XRD, and FETEM analysis

	DLS	XRD	TEM
LM-Ag NPs	12.75 ± 0.08 nm	11.1 nm	9.99 nm
LA-Ag NPs	9.45 ± 0.21 nm	8.56 nm	7.87 nm
BM-Ag NPs	30.25 ± 2.1 nm	22.8 nm	13.86 nm
BA-Ag NPs	25.65 ± 8.7 nm	13.65 nm	10.72 nm

LM-Ag NPs - nanoparticles synthesized from leaves-methanol extract, LA-Ag NPs - nanoparticles synthesized from leaves-aqueous extract, BM-Ag NPs - nanoparticles synthesized from berries-methanol extract, BA-Ag NPs - nanoparticles synthesized from berries-aqueous extract.

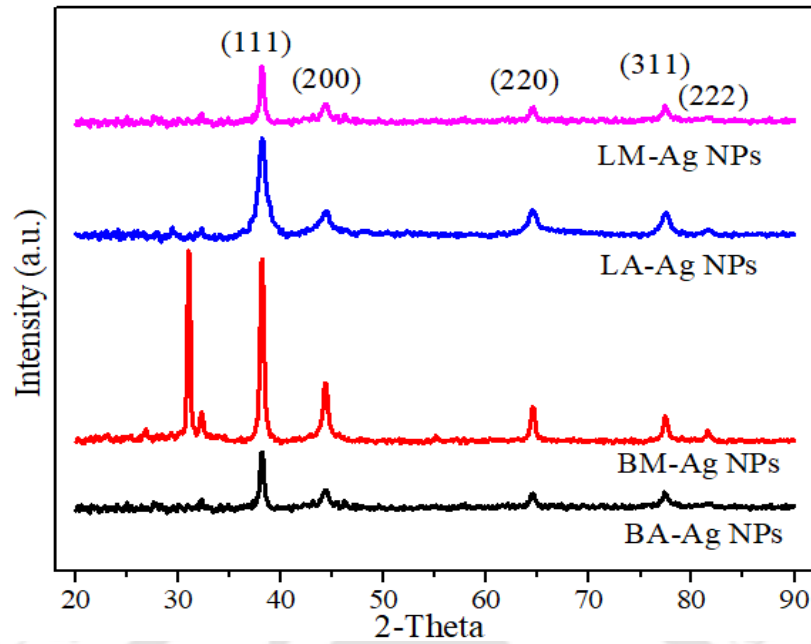


Fig. 6.5: XRD pattern of LM-Ag NPs (nanoparticles synthesized from leaves-methanol extract), LA-Ag NPs (nanoparticles synthesized from leaves-aqueous extract), BM-Ag NPs (nanoparticles synthesized from berries-methanol extract), and BA-Ag NPs (nanoparticles synthesized from berries-aqueous extract)

6.3.3.2 Crystallinity Analysis

The XRD pattern of Ag NPs synthesized using Sea buckthorn leaves, and berries extracts are shown in **Fig. 6.5**. The crystallinity of all synthesized Ag NPs was confirmed by XRD with multiple characteristic Bragg diffraction peaks of silver at 2-tetha value 38.02° , 44.25° , 64.37° , 77.3° , and 81.44° , indexed to (111), (200), (220), (311), and (222) crystal reflection planes of the face-centered cubic structure. The XRD pattern of LM-Ag NPs, LA-Ag NPs, and LA-Ag NPs confirmed the presence of silver in the pure form. Whereas BM-Ag NPs showed crystallographic impurities at 28.3° and 30.98° that could be resulted from the agglomeration of remnant phytochemicals of the plant extract. Bragg's reflections indicated the orientation of the plane in (111) direction was more intense compared to the broad-ended (200), (220), (311),

and (222) reflections. The width of each peak was used to calculate the average particle size and the crystalline size of Ag NPs was calculated from the width of XRD peaks using Debye-Scherrer equation. The average particle size of NPs in increasing order was 8.56 nm, 11.1 nm, 13.65 nm, and 22.8 nm for LA-Ag NPs, LM-Ag NPs, BA-Ag NPs, and BM-Ag NPs, respectively. The average particle size of NPs followed the same pattern as DLS and the SPR peak position in the UV-Vis spectra.

6.3.3.3 Shape and size analysis

FETEM was used to analyze the shape, size, selected area electron diffraction (SAED) pattern, and elemental composition (EDX) of synthesized NPs. The FETEM images of LM-Ag NPs and LA-Ag NPs showed that the particles were nearly spherical with varying sizes, as shown in **Fig. 6.6**. The average particle size distribution is shown using histograms (**Fig. 6.6 a, e, i, m**). In the case of LM-Ag NPs the particle size ranged from 2.23 to 23.43 nm with a mean particle size of 9.99 nm, while for LA-Ag NPs the particles ranged from 2.2 to 16.98 nm with an average particle size of 7.87 nm. The size distribution of spherical BM-Ag NPs varied from 2 to 40.73 nm with an average particle size of 13.86 nm (**Fig. 6.6 e, f, j**). Whereas, BA-Ag NPs image supported that the particles are monodispersed spherical with few hexagons and triangular crystals in size range from 2.49 to 44.09 nm, with an average size of 10.72 nm (**Fig. 6.6 n**). The particle size determined from TEM images was consistent with the XRD and DLS trends. The dimension of LM-Ag NPs (9.99 nm) and LA-Ag NPs (7.87 nm) in the current study was slightly lower than the range of Ag NPs synthesized from the leaves-aqueous extract of *Hippophae rhamnoides* (~10-40 nm) by Kalaiyaran et al., (2017). In another study, Aygün et al., (2020) have reported that the average particle size of *Rheum ribes* extract mediated Ag NPs is 18.2 ± 3.6 nm. So far to the best of our knowledge, no report is available on bio-inspired Ag NPs synthesis from methanol and consecutive aqueous extract of sea buckthorn berries. As

previously validated by DLS and XRD analysis, water extract generated Ag NPs that were smaller in size than methanol extract.

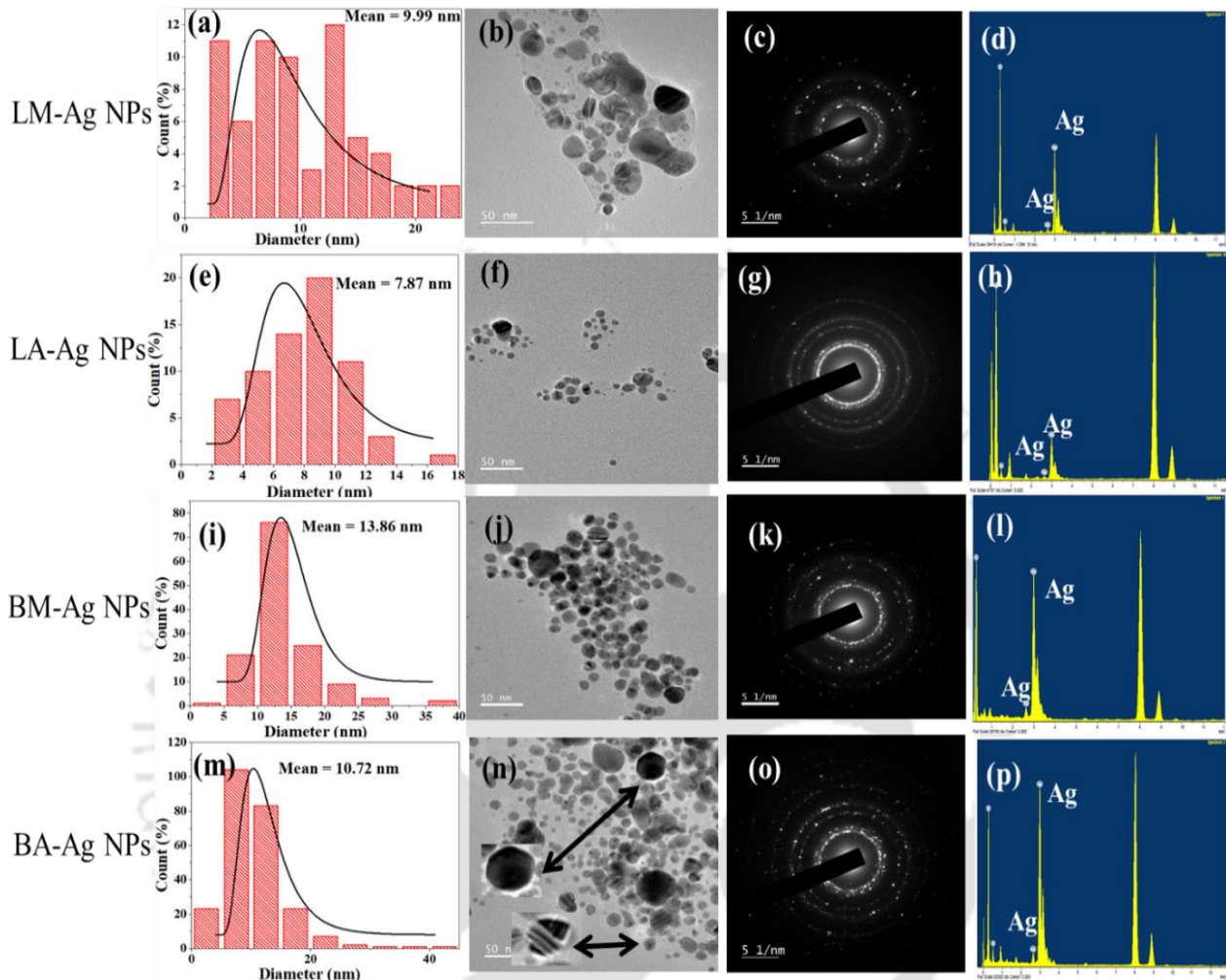


Fig. 6.6: FETEM analysis: Histograms - a, e, i, and m; SEM images - b, f, j, and n; Selected area electron diffraction (SAED) pattern - c, g, k, and o; Elemental (EDX) analysis - d, h, l, and p. LM-Ag NPs - nanoparticles synthesized from leaves-methanol extract, LA-Ag NPs – nanoparticles synthesized from leaves-aqueous extract, BM-Ag NPs - nanoparticles synthesized from berries-methanol extract, BA-Ag NPs - nanoparticles synthesized from berries-aqueous extract

SAED patterns of TEM analysis further verified the crystalline nature of Ag NPs (Fig. 6.6 c, g, k, o). As demonstrated by XRD, the SAED pattern indicates strong crystalline nature with

diffraction rings indexed to a face-centered cubic silver structure. The weak diffused spots for spherical LA-Ag NPs could be attributed to their small particle size and polycrystalline nature. The EDX pattern also depicts a very strong optical absorbance for metallic silver along with background signals for carbon and copper due to X-ray emission from carbon-coated copper grids. **Fig. 6.6 (d, h, l, and p)** showed that Ag content of BA-Ag NPs was the highest, followed by LM-Ag NPs, BM-Ag NPs, and LA-Ag NPs. This notable difference showed the difficulty of collecting smaller size Ag NPs using centrifugation, which justifies the lower yield of LA-Ag NPs.

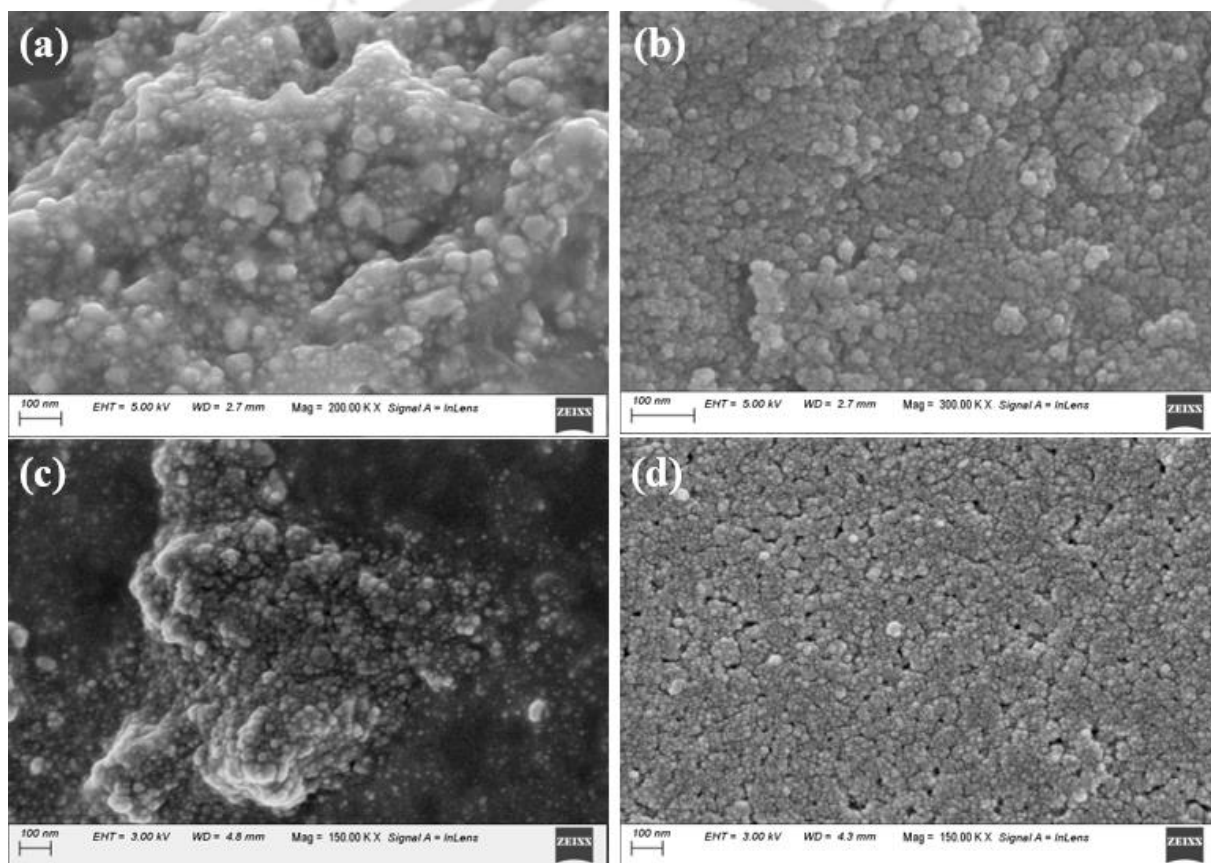


Fig. 6.7: SEM images of synthesized Ag nanoparticles. a - nanoparticles synthesized from leaves-methanol extract, b – nanoparticles synthesized from leaves-aqueous extract, c - nanoparticles synthesized from berries-methanol extract, d - nanoparticles synthesized from berries-aqueous extract

6.3.3.4 Morphological analysis

The FESEM images of all Ag NPs prepared at optimum conditions are shown in **Fig. 6.7 (a – d)**. LM-Ag NPs, LA-Ag NPs, and BM-NPs had the same morphology, spherical and monodispersed. While BA-Ag NPs were found to have a variety of forms, including spherical, hexagonal, and triangular. The images of Ag NPs synthesized from aqueous extracts of leaves and berries have a smooth surface, and the particles are well dispersed with a close compact arrangement. The Ag NPs synthesized from methanol extracts showed some aggregates with spherical morphology and very narrow diameter distributions. The presence of secondary metabolites could cause the aggregation of NPs.

6.3.4 FTIR analysis

FTIR spectral analysis of extracts, supernatants (obtained after collecting Ag NPs), and NPs were carried out to identify compounds accountable for the reduction reaction and stabilization of Ag NPs (**Fig. 6.8 (a - d)**). The broad absorption spectra of extracts, supernatants, and NPs from 3440 to 3116 cm^{-1} were attributed to the strong stretching vibration of phenolic hydroxyl OH. Characteristic absorption bands, at 1058 cm^{-1} (C-O) for a hydroxyl group, at 1074 cm^{-1} for C-N (amines) stretch vibration of the proteins, at 1401 cm^{-1} for C-O stretching phenols, and at 1634 cm^{-1} for N-H bond amine I groups, at 620 cm^{-1} for (-C=C-H:C-H) bending of vibration alkynes bond, at 1068 cm^{-1} for O-H group, and 1634 cm^{-1} for C=C in aromatic compounds and amide I (NH out of plane) were observed for extracts, supernatants, and NPs. Further, the peaks at around 1714 to 1741 cm^{-1} correspond to the stretching vibration of the C=O group of triacylglycerols, which is the characteristic of oils with a high degree of unsaturation. Methanolic extract of sea buckthorn berries showed additional peaks at 2930 and 2856 cm^{-1} , mainly attributed to C-H antisymmetric and C-H symmetric stretching of methyl and methylene of an aliphatic chain of lipids, respectively.

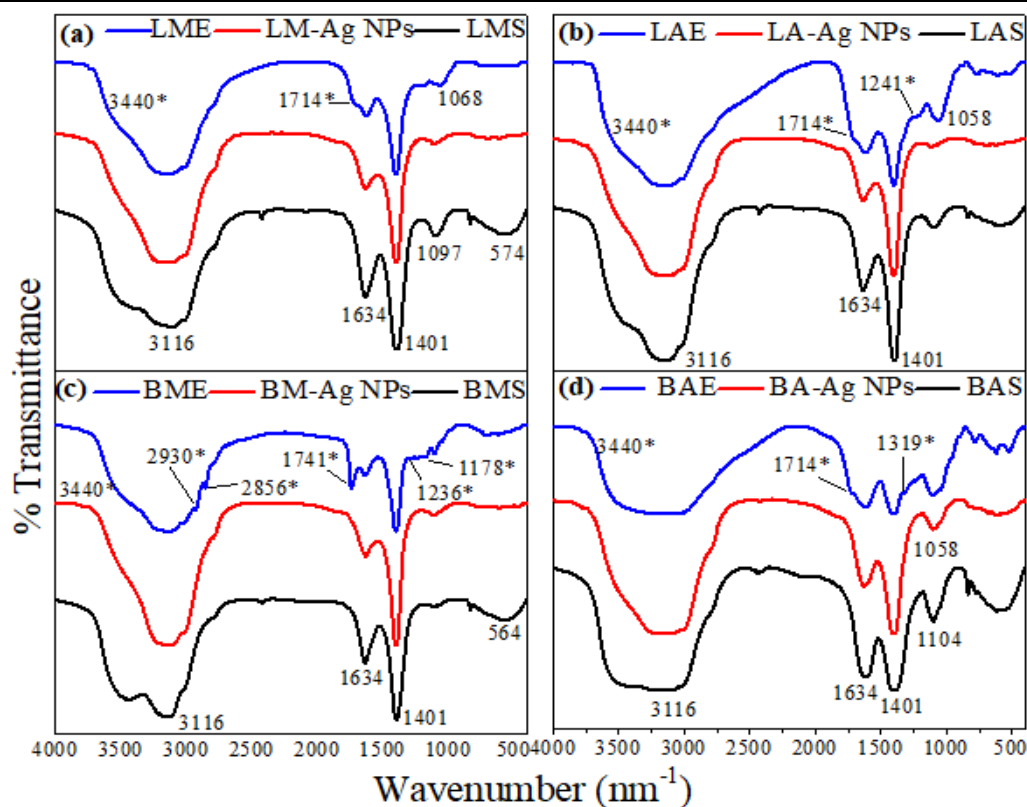


Fig. 6.8: FTIR spectra of (a) LME (leaves-methanol extract), LM-Ag NPs (nanoparticles synthesized from leaves-methanol extract), LMS (supernatant from LM-Ag NPs suspension), (b) LAE (leaves-aqueous extract), LA-Ag NPs (nanoparticles synthesized from leaves-aqueous extract), LAS (supernatant from LA-Ag NPs suspension), (c) BME (berries-methanol extract), BM-Ag NPs (nanoparticles synthesized from berries-methanol extract), BMS (supernatant from BM-Ag NPs suspension), (d) BAE (berries-aqueous extract), BA-Ag NPs (nanoparticles synthesized from berries-aqueous extract), BAS (supernatant from BA-Ag suspension)

Although the majority of the spectra of extracts, supernatants, and NPs indicated a similar pattern of absorption bands, as shown in **Fig. 6.8**, there are minor variances. The FTIR spectrum of Ag NPs showed peaks at 1104, 1401, 1634, and 3116 cm^{-1} along with other small peaks. The inherent peaks of methanol and aqueous-leaves extracts at 3461, 1714, 1241, and 1074 cm^{-1} ; methanol-berries extract at 3437, 2930, 2856, 1741, 1236, and 1178 cm^{-1} ; and berries-

aqueous extract at 3440, 1714, and 1319 cm^{-1} were disappeared in the Ag NPs spectra. It means that the aforementioned peaks, which correspond to phenolics, proteins, benzenes, and sulfuraphane, are critical for reducing Ag^+ to Ag^0 and stabilizing Ag NPs. The capping agents prevent agglomeration and support the stabilization of synthesized Ag NPs.

6.3.5 Total phenolic and flavonoid content

TPC and TFC of the extracts and the synthesized Ag NPs are given in **Table 6.3**. Among the leaves, the TPC of methanol extract (339.7 ± 4 mg GAE/g) was higher than the aqueous extract (294.6 ± 17 mg GAE/g). Whereas, in the case of the berries, the TPC of methanol extract (56.7 ± 2.2 GAE/g) was lower than the aqueous extract (104 ± 0.4 GAE/g). TFC ranged from 135.1 ± 5.3 (aqueous extract) to 294.6 ± 17 mg QE/g (methanol extract) for leaves extracts and from 135.1 ± 5.3 (aqueous extract) to 294.6 ± 17 mg QE/g (methanol extract) for the berries. The TPC of *H. salicifolia* leaf was significantly higher than that of the corresponding berry extracts, as explained by Moges et al., (2021). They have also studied TPC levels in successive extracts from leaves and berries, reporting that TPC was highest in methanol extract of the leaves and aqueous extract of the berries. The TFC of leaves extract was 294.6 ± 17 (methanol extract) and 135.1 ± 5.3 mg QE/g (aqueous extract); and of berries extracts, 15.5 ± 2.2 (methanol extract) and 35.4 ± 1 mg QE/g (aqueous extract). These results were inconsistent with the previous results reported by Moges et al., (2021) on successive extracts from leaves and berries of *H. salicifolia*.

Regarding Ag NPs, the TPC and TFC were found to be highest in LM-Ag NPs (170.8 ± 3 mg GAE/g and 103.5 ± 1.2 mg QE/g) and lowest in BA-Ag NPs (27.3 ± 0.8 mg GAE/g and 10.3 ± 0.5 mg QE/g). BM-Ag NPs had considerably higher TPC and TFC than LA-Ag NPs. The TPC and TFC were higher in the leaves extract mediated Ag NPs than in the berries. Because of

their redox characteristics, which serve as reducing agents, phenolic and flavonoid molecules have high antioxidant potential. Compounds such as phenolics, flavonoids, soluble proteins, and terpenoids are reported to act as capping agents. The TPC levels in Ag NPs were higher than in the aqueous *C. murale* leaves extract from which they are made, according to Abdel-Aziz et al., (2014). In another work by Salari et al., (2018), the TPC and TFC in aqueous *P. farcta* fruit extract mediated Ag NPs were higher than in fruit extract alone.

Table 6.3: TPC, TFC, and antioxidant activities of extracts and Ag NPs obtained at optimized conditions

	TPC (mg GAE/g)	TFC (mg QE/g)	DPPH ($\mu\text{g/mL}$)	ABTS ($\mu\text{g/mL}$)
LME	339.7 \pm 4	294.6 \pm 17	2.76 \pm 0.27	9.62 \pm 0.1
LAE	294.6 \pm 17	135.1 \pm 5.3	3.78 \pm 0.04	9.88 \pm 0.05
BME	56.7 \pm 2.2	15.5 \pm 2.2	25.72 \pm 0.56	39.35 \pm 5.73
BAE	104 \pm 0.4	35.4 \pm 1	42.65 \pm 0.73	40.46 \pm 0.29
LM-Ag NPs	170.8 \pm 3	103.5 \pm 1.2	1.29 \pm 0.3	8.8 \pm 0.6
LA-Ag NPs	55.5 \pm 1.2	24 \pm 0.8	6.21 \pm 1.9	9.36 \pm 1.5
BM-Ag NPs	121.3 \pm 2.6	67.4 \pm 12	4.5 \pm 0.08	21.17 \pm 0.01
BA-Ag NPs	27.3 \pm 0.8	10.3 \pm 0.5	22.65 \pm 0.77	30.46 \pm 1.44

LME-leaves-methanol extract, LAE-leaves-aqueous extract, BME-berries-methanol extract, BAE-berries-aqueous extract, LM-Ag NPs-nanoparticles synthesized from leaves-methanol extract, LA-Ag NPs-nanoparticles synthesized from leaves-aqueous extract, BM-Ag NPs - nanoparticles synthesized from berries-methanol extract, BA-Ag NPs - nanoparticles synthesized from berries-aqueous extract.

6.3.6 Antioxidant activity

The antioxidant activity of methanol and aqueous extract of sea buckthorn leaves and berries as well as NPs synthesized using each extract, was investigated (**Table 6.3**). The DPPH and ABTS assays of methanol extract of leaves and berries exhibited good free radical scavenging activity. The leaves extracts perform better antioxidant action than the corresponding berries extracts. Minimum IC₅₀ was observed for leaves-methanol extract followed by leaves-aqueous extract, berries-methanol extract, and berries-aqueous in both the assays. While in the case of synthesized Ag NPs, LM-Ag NPs exhibited the highest antioxidant activity ($1.29 \pm 0.3 \mu\text{g/mL}$), followed by BM-Ag NPs ($4.5 \pm 0.08 \mu\text{g/mL}$), LA-Ag NPs ($6.21 \pm 1.9 \mu\text{g/mL}$), and BA-Ag NPs ($22.65 \pm 0.77 \mu\text{g/mL}$), in DPPH assay. In the current study ABTS experiment, the IC₅₀ value of leaves extract and leaves extract-mediated Ag NPs was lower than the previously reported value for pure ascorbic acid (10.5 g/mL) (Moges et al., 2021). Further, it was discovered that the antioxidant activity of Ag NPs in the current study was significantly higher than that of gold NPs made from an aqueous extract of *Citrus reticulata* seed. Gold nanoparticles mediated by *citrus reticulata* seed extract demonstrated an IC₅₀ of 87 g/mL against DPPH free radicals (Ahati et al., 2022). The bio-synthesized Ag NPs found to possess a potent reducing ability, higher than plant extracts alone (Kalaiyarasan et al., 2017; Salari et al., 2018). The antioxidant capacity of the synthesized Ag NPs depends largely on the capped phenolic and flavonoid compounds adhered to the surface of Ag NPs. Phenolic and flavonoid compounds help the conversion of silver nitrate to Ag NPs due to their electron-donating ability (Salari et al., 2018). Even though Ag NPs made from methanolic extracts of the leaves and berries are larger, they are more active than those Ag NPs made from aqueous extracts.

6.3.7 Antibacterial activity

6.3.7.1 Minimum inhibitory concentration (MIC)

The antibacterial effect of extracts and Ag NPs was investigated against eight pathogenic organisms. The antibacterial study was conducted using minimum inhibitory concentration (MIC) and diameter of zone of inhibition (ZoI) assays. Plant extracts and synthesized Ag NPs showed significant antibacterial activity against all the tested bacterial strains. The MIC of extracts and Ag NPs are given in **Table 6.4**. In the case of methanolic extract of leaves, the lowest MIC of 31.5 µg/mL was obtained for *B. subtilis*, *S. epidermidis*, and *S. aureus*, and between 62.5 and 125 µg/mL for *P. aeruginosa*, *E. aerogenes*, *K. pneumonia*, and *E. coli*. Whereas, in the case of methanolic berry extract, it varied between 62.5 to 250 µg/mL. Overall, methanolic extracts showed better antibacterial efficacy than aqueous extracts. Regarding Ag NPs, the antibacterial activity was found in decreasing order: LM-Ag NPs > BM-Ag NPs > LA-Ag NP > BA-Ag NPs. LM-Ag NPs exhibited the best antibacterial activity against *B. subtilis* and *M. luteus* at MIC of 1.9 µg/mL and the lowest antibacterial activity against *E. aerogenes* at 15.6 µg/mL MIC. While BA-Ag NPs exhibited the lowest antibacterial activity with MIC ranging from 7.8 µg/mL to 31.5 µg/mL. Reports in the literature indicate that the biosynthesized Ag NPs have strong antibacterial activities (Mani et al., 2021). A similar trend was noticed in the present where synthesized Ag NPs showed significantly higher antibacterial activity against all the eight bacterial strains than plant extracts alone.

Zone of Inhibition (mm)

6.3.7.2 Zone of Inhibition (ZoI)

The ZoI study of extracts and Ag NPs are presented in **Table 6.5**. Leaves extract again showed higher antibacterial activity against all the tested strains with ZoI ranging from 7.5 ± 0.7 to 12.5 ± 0.7 mm. Whereas, berry extracts showed ZoI only for *K. pneumonia*, *S. epidermidis*, *M.*

Table 6.4: Minimum inhibitory concentration ($\mu\text{g/mL}$) of extracts and Ag NPs synthesized at optimal conditions

	Gram-positive bacteria				Gram-negative bacteria			
	<i>S. aureus</i>	<i>B. subtilis</i>	<i>S. epidermidis</i>	<i>M. luteus</i>	<i>E. coli</i>	<i>K. pneumonia</i>	<i>E. aerogenes</i>	<i>P. aeruginosa</i>
LME	31.3	31.3	31.3	62.5	125	125	125	62.5
LAE	62.5	62.5	62.5	125	250	250	250	125
BME	62.5	62.5	62.5	62.5	250	250	250	62.5
BAE	250	125	125	250	250	250	250	125
LM-Ag NPs	7.8	1.9	3.9	1.9	7.8	7.8	15.6	3.9
LA-Ag NPs	7.8	7.8	15.6	31.5	15.6	15.6	31.5	3.9
BM-Ag NPs	7.8	7.8	3.9	7.8	7.8	7.8	15.6	3.9
BA-Ag NPs	7.8	15.6	15.6	15.6	31.5	31.5	31.5	7.8

LME-leaves-methanol extract, LAE-leaves-aqueous extract, BME-berries-methanol extract, BAE-berries-aqueous extract, LM-Ag NPs - nanoparticles synthesized from leaves-methanol extract, LA-Ag NPs - nanoparticles synthesized from leaves-aqueous extract, BM-Ag NPs - nanoparticles synthesized from berries-methanol extract, BA-Ag NPs - nanoparticles synthesized from berries-aqueous extract.

Table 6.5: Zone of Inhibition (mm) of extracts and Ag NPs synthesized at optimal condition

	Gram-positive bacteria				Gram-negative bacteria			
	<i>S. aureus</i>	<i>B. subtilis</i>	<i>S. epidermidis</i>	<i>M. luteus</i>	<i>E. coli</i>	<i>K. pneumonia</i>	<i>E. aerogenes</i>	<i>P. aeruginosa</i>
LME	8.5±0.7	12±1.4	12.5±0.7	10±1.4	11±1.4	9.5±0.7	9.5±0.7	10±1.4
LAE	7	8.5±0.7	8±1.4	8±1.4	9.5±2.1	7.5±0.7	15±1.4	7.5±0.7
BME	10.5±0.7	0	4	1.5±0.7	0	1	0	0
BAE	8.5±0.7	0	5	3	0	1	0	0
LM-Ag NPs	11.5±2.1	18±1.4	16±1.4	12	18.5±0.7	16.5±0.7	6.5±0.7	15±1.4
LA-Ag NPs	7.5±0.7	13.5±2.1	10	8.5±0.7	11	6.5±0.7	9	10
BM-Ag NPs	10.5±0.7	9.5±0.7	10.5±0.7	7.5±2.1	7.5±0.7	9.5±0.7	9	12.5
BA-Ag NPs	9	15.5±0.7	8.5±0.7	11	6	8	7±1.4	10±1.4

LME-leaves-methanol extract, LAE-leaves-aqueous extract, BME-berries-methanol extract, BAE-berries-aqueous extract, LM-Ag NPs - nanoparticles synthesized from leaves-methanol extract, LA-Ag NPs – nanoparticles synthesized from leaves-aqueous extract, BM-Ag NPs - nanoparticles synthesized from berries-methanol extract, BA-Ag NPs - nanoparticles synthesized from berries-aqueous extract.

luteus, and *S. aureus* in the range 1 mm to 10.5 ± 0.7 mm. Among Ag NPs, LM-Ag NPs showed the highest ZoI for *E. coli* (18.5 ± 0.7 mm) and lowest for *E. aerogenes* (6.5 ± 0.7 mm). The lowest ZoI for *EC* (6 mm) was recorded for BA-Ag NPs. Our result suggests that the antibacterial activity of Ag NPs is also more influenced by the capped phenolic and flavonoid compounds than by the size of Ag NPs. The biological effectiveness of Ag NPs increased proportionately with an increase in the specific surface area (decrease in size) which provides better contact with the cell wall of bacteria and increases the surface energy and catalytic reactivity (Haider and Kang, 2014; Padalia et al., 2015). Further, the positive charge on (Ag^+) silver ion interacts with the negative charges on the surface of the cell membrane and disturbs the permeability and respiration functions of the cell. Ag NPs can also penetrate the membrane and kill or denature the bacteria (Jemal et al., 2017; Salari et al., 2018).

6.4 Summary

In the present study, Ag NPs were bio-synthesized using methanol and aqueous extracts of *H. salicifolia* leaves and berries and optimized. The conclusions are summarized as follows:

- This might be the first report to use dried crude plant extracts to optimize the dry bulk of extract concentration for Ag NPs synthesis. *H. salicifolia* leaves and berries extract mediated Ag NPs were successfully synthesized at optimum conditions with an average diameter of 7.87 ± 2.9 nm (LA-Ag NPs) to 13.86 ± 5 nm (BM-Ag NPs) and the shape of a sphere.
- Leaves extract offers higher Ag NPs yield with smaller diameters than berries extract.
- Ag NPs made from aqueous extracts are smaller than methanol extract, yet methanol extract-mediated nanoparticles show better biological activity than aqueous.

- Ag NPs' biological capabilities were shown to be more impacted by the phenolic and flavonoid compounds on their caps than by their size.
- Their significant antioxidant and antibacterial activity validated the bioactivity of Ag NPs, meaningfully higher activities with leaves extract mediated Ag NPs. LM-Ag NPs showed superior inhibition against *E. coli* with the highest ZoI of 18.5 ± 0.7 mm.
- These study results demonstrated that *H. salicifolia* leaves and berries are effective bio-resource/biomaterial for producing biologically active Ag NPs.





The logo of the Indian Institute of Technology Guwahati is a circular emblem. It features a central stylized figure with three circular shapes at its base, resembling a traditional Indian motif. The text "Indian Institute of Technology Guwahati" is written in English around the bottom half of the circle, and its Assamese equivalent "ভাৰতীয় প্ৰযুক্তিগতী সংস্থান গুৱাহাটী" is written along the top half.

OVERALL SUMMARY AND CONCLUSIONS





OVERALL SUMMARY AND CONCLUSIONS**7.1 Overall summary**

This thesis provides a comprehensive report on the dietary and bioactive properties of *Hippophae salicifolia* leaves and whole berries and their application in synthesizing silver nanoparticles. The leaves of *H. salicifolia*, which is cultivated in North-East India, were shown to be primarily more nutrient- and biologically-active than the berries, despite both the berries and the leaves having considerable nutritional and bioactive qualities. Gallic acid, caffeic acid, ferulic acid, p-coumaric acid, quercetin, myricetin, kaempferol, and rutin were among the good polyphenolic compounds found in the extracts of berries and the leaves obtained by successive solvent extraction. The leaves extract also had noticeably higher levels of oxidation and food-borne bacterial inhibition activity. were investigated for their polyphenols, antioxidant and antibacterial properties. The research results indicate the status of SC-CO₂ extracts of *Hippophae salicifolia* leaves and berries. Soxhlet extraction outperformed SC-CO₂ extraction for the leaves in terms of extraction yield, TPC, IC50, and antibacterial activity. For the extraction of ferulic acid, myricetin, and quercetin, SC-CO₂ was more selective. SC-CO₂ extracted oil has physicochemical parameters within the acceptable range for edible oil, and had higher total phenolic content, antioxidant, and antibacterial activity than Soxhlet extracted oil. SC-CO₂ extraction of sea buckthorn berries and leaves is an effective alternative to replace conventional solvent extraction in the food, cosmetics, and pharmaceutical sectors. Further, the findings indicate that Ag NPs synthesized from *H. salicifolia* leaves and berries extract were monodispersed and spherical with significant antioxidant and antibacterial potential for controlling and preventing bacterial infections.

7.2 Conclusions

The findings on the various issues on the nutritional properties, extraction, bioactive properties, and synthesis of silver nanoparticles from *H. salicifolia* D. Don from Northeast India are summarized as follows:

General conclusion:

- The berries and leaves of *H. salicifolia* showed significant dietary and bioactive properties, with the leaves mainly found to be more nutritious and biologically active than the berries.
- Overall the polyphenolic compounds from the leaves were much higher than in berries, while the oil composition in the berries was predominant.
- The effect of process variables on oil yield, β -carotene, and total tocopherol contents of the oil was sufficiently described and predicted by the 2nd order polynomial model. The CO₂ flow rate had a maximum effect on the oil yield, while the extraction pressure had most significantly affected the oil's β -carotene and total tocopherol contents.
- The biological process is cost-effective, ecologically acceptable, and capable of synthesizing Ag NPs at temperatures between 50 and 60 °C and 9–10 pH levels, with methanol and consecutive aqueous extracts of *Hippophae salicifolia* leaves and berries acting as reducing and stabilizing agents.

Specific conclusions:

- Potassium was the predominant element found in the berries and leaves. The second most abundant element in the berries and leaves were sodium and calcium. The leaves sample showed higher sugar, protein, and tannin content than the berries, while vitamin C in the berries was higher than in the leaves.

- Successive Soxhlet extracts (ethyl acetate, acetone, methanol, and aqueous extracts) of whole berries and the mixture of leaves from the male and female plants of Sea buckthorn had higher concentrations of TPC and TFC with higher antioxidant activity than the previous reports for either male or female leaves *H. rhamnoides* variety.
- The berries and leaves extract showed promising polyphenolic compounds such as gallic acid, caffeic acid, ferulic acid, p-coumaric acid, quercetin, myricetin, kaempferol, and rutin, with significant oxidation and food-borne bacterial inhibition activities, meaningfully higher activities with leaves extract.
- SC-CO₂ extraction is a gentle and eco-friendly technique applied to extract polyphenolic compounds from the leaves and oil from the berries. The optimum condition for maximum extraction yield with maximum TPC and minimum IC₅₀ occurred at 25.13 MPa, 47.53°C, 14.47 g/min CO₂ flow rate, and 2.43% cosolvent.
- The validation experiment at this condition resulted in an extraction yield of 4.38%, 84.31±3.9 mg GAE/g TPC, and 41.94±3.13 µg/mL IC₅₀ with good agreement with the predicted values (yield of extraction: 4.53%, TPC: 83.37 mg GAE/g, and IC₅₀: 40.2 µg/mL).
- Extraction of dietary components from seabuckthorn leaves using the Soxhlet extraction technique performed better in terms of extraction yield, TPC, IC₅₀, and antibacterial activity than the SC-CO₂ extraction technique. However, SC-CO₂ extraction was more selective for ferulic acid, myricetin, and quercetin extraction.
- The optimum set of SC-CO₂ oil extraction parameters from *H. salicifolia* that offered maximum oil yield, β-carotene, and total tocopherol content as predicted by the model was: 27.02 MPa, 48.46 °C, 16.45 g/min (CO₂ flow rate). The projected recovery of oil yield, β-

carotene, and total tocopherol under optimum conditions were 88.17%, 90.65%, and 94.31%, respectively.

- Omega-7 fatty acid (palmitoleic acid) comprised 42.98% of total oil and was the predominant UFA in SC-CO₂ extracted oil.
- SC-CO₂ extracted oil had a significant amount of β -carotene, total tocopherol, and total phenolic and flavonoid contents with significant antioxidant and antibacterial activities.
- SC-CO₂ extracted oil was more susceptible to temperature and resistant to mechanical stress than Soxhlet extracted oil.
- SC-CO₂ extraction of sea buckthorn berry oil is an effective alternative to replace the conventional approach in the food, cosmetics, and pharmaceutical sectors.
- The leaves and berries of *Hippophae salicifolia* were extracted successively with methanol and water using the Soxhlet apparatus to be used for synthesizing silver nanoparticles. Variables such as extract concentration, AgNO₃ concentration, pH, temperature, and time were optimized to get the highest possible Ag NPs yield.
- The pH was the most critical parameter in regulating the size and NPs yield.
- Sea buckthorn leaves and berries extract mediated silver nanoparticles were successfully synthesized at optimum conditions with an average diameter of 7.87 ± 2.9 nm (LA-Ag NPs) to 13.86 ± 5 nm (BM-Ag NPs). Leaves extract was found to offer a higher yield of small-sized nanoparticles compared to berry extract.
- The synthesized Ag NPs exhibited a strong antioxidant and antibacterial activity. LM-Ag NPs demonstrated superior activity against *E. coli* with the highest ZoI of 18.5 ± 0.7 mm.

The logo of the Indian Institute of Technology Guwahati is a circular emblem. It features a central stylized figure with three rounded protrusions, resembling a traditional Indian motif. The figure is surrounded by a circular border containing text in both Assamese and English. The Assamese text at the top reads 'গুৱাহাটী প্ৰযুক্তিবিদ্যাৰ গৱেষণা কেন্দ্ৰ' and the English text at the bottom reads 'Indian Institute of Technology Guwahati'.

**RESEARCH CONTRIBUTIONS AND
FUTURE WORK RECOMMENDATIONS**







**RESEARCH CONTRIBUTIONS AND FUTURE WORK
RECOMMENDATIONS****8.1 Research contribution**

- This thesis contributes to the desire for more research into alternative possibilities for natural resource sustainability by identifying phytonutrients in *Hippophae salicifolia* species of sea buckthorn.
- The physicochemical properties of the *Hippophae salicifolia* berries oil obtained from SC-CO₂ extraction are comparable to the highest quality edible oils.
- The NPs have shown exceptionally stronger antioxidant and antibacterial activities than the extracts from which they are synthesized. They have significant antioxidant and antibacterial potential for controlling and preventing bacterial infections.

8.2 Future work recommendations

- Despite its nutritional benefits, sea buckthorn leaves have yet to be widely recognized as a food and food supplement. Efforts must be made to expand the scope and method of the Novel Food Regulation to allow for the use of sea buckthorn leaves as a food and food supplement.
- It is advised that real entrepreneurs consider the sea buckthorn berries and blend of leaves for the manufacture of juice and oil, as well as labor and equipment logistics.

- Berries and leaves of *H. salicifolia* were extracted using traditional Soxhlet and supercritical CO₂. These extracts showed good antioxidant and antibacterial activities. Further study on animal vs. human clinical trials is advised.
- SC-CO₂ extraction was found to be more selective for the isolation of flavonoid compounds in general and ferulic acid, myricetin, and quercetin in particular. Comprehensive research on the optimization and selectivity of SC-CO₂ extraction of flavonoids from sea buckthorn leaf is needed.
- SC-CO₂ extracted sea buckthorn berry oil could be analyzed for its application in the food, cosmetics, and pharmaceutical sectors.
- Ag NPs synthesized from methanol, and aqueous extracts of the berries and sea buckthorn leaves can be studied for their nutraceutical and pharmaceutical application.
- Following clinical testing, Ag NPs are a useful medication for treating pathogenic diseases in humans. Future studies can include more research on the efficient separation and medicinal use of Ag NPs mediated by *H. salicifolia* extract.
- Interaction effect of environmental conditions; soil type, topography, harvesting methods, temperature, RH, types of feedstock, particle-size, moisture content, etc. on the physicochemical properties of sea buckthorn and their effect on the extraction processes can be studied for future.





REFERENCES





References

- A.O.A.C., 2012. Official methods of analysis of AOAC, 19th ed, Association of Official Analytical Chemists International. AOAC International, Arlington, TX.
- Abalkhil, T.A., Alharbi, S.A., Salmen, S.H., Wainwright, M., 2017. Bactericidal activity of biosynthesized silver nanoparticles against human pathogenic bacteria. *Biotechnol. Biotechnol. Equip.* 31, 411–417. <https://doi.org/10.1080/13102818.2016.1267594>
- Ahati, P., Xu, T., Chen, L., Fang, H., 2022. Biosynthesis, characterization and evaluation of anti-bone carcinoma, cytotoxicity, and antioxidant properties of gold nanoparticles mediated by *Citrus reticulata* seed aqueous extract: Introducing a novel chemotherapeutic drug. *Inorg. Chem. Commun.* 143, 109791. <https://doi.org/10.1016/j.inoche.2022.109791>
- Ahmad, B., Ali, J., 2013. Physiochemical, minerals, phytochemical contents, antimicrobial activities evaluation and fourier transform infrared (FTIR) analysis of *Hippophae rhamnoides* L. leaves extracts. *African J. Pharm. Pharmacol.* 7, 375–388. <https://doi.org/10.5897/AJPP12.1246>
- Ahmad, B., Ali, J., Bashir, S., 2013. Optimization and effects of different reaction conditions for the bioinspired synthesis of silver nanoparticles using *hippophae rhamnoides* linn. leaves aqueous extract. *World Appl. Sci. J.* 22, 836–843. <https://doi.org/10.5829/idosi.wasj.2013.22.06.7394>
- Ahmed, S., Ahmad, M., Swami, B.L., Ikram, S., 2016a. A review on plants extract mediated synthesis of silver nanoparticles for antimicrobial applications: A green expertise. *J. Adv. Res.* 7, 17–28. <https://doi.org/10.1016/j.jare.2015.02.007>
- Ahmed, S., Saifullah, Ahmad, M., Swami, B.L., Ikram, S., 2016b. Green synthesis of silver nanoparticles using *Azadirachta indica* aqueous leaf extract. *J. Radiat. Res. Appl. Sci.* 9, 1–
-

References

7. <https://doi.org/10.1016/j.jrras.2015.06.006>

Ahmed, Z., Gupta, S., 2009. Seabuckthorn: A source (donar) in molecular breeding, National conference on Seabuckthorn and Environment, High Altitude Perspectives. DIHAR, Leh-Ladakh-194101 J&K, India.

Akanda, M.J.H., Sarker, M.Z.I., Ferdosh, S., Manap, M.Y.A., Rahman, N.N.N.A., Kadir, M.O.A., 2012. Applications of supercritical fluid extraction (SFE) of palm oil and oil from natural sources. *Molecules* 17, 1764–1794. <https://doi.org/10.3390/molecules17021764>

Akšić, M.F., Tosti, T., Sredojević, M., Milivojević, J., Meland, M., Natić, M., 2019. Comparison of sugar profile between leaves and fruits of blueberry and strawberry cultivars grown in organic and integrated production system. *Plants* 8. <https://doi.org/10.3390/plants8070205>

Alquadeib, B.T., 2019. Development and validation of a new HPLC analytical method for the determination of diclofenac in tablets. *Saudi Pharm. J.* 27, 66–70. <https://doi.org/10.1016/j.jsps.2018.07.020>

Alt, V., Bechert, T., Steinrücke, P., Wagener, M., Seidel, P., Dingeldein, E., Domann, E., Schnettler, R., 2004. An in vitro assessment of the antibacterial properties and cytotoxicity of nanoparticulate silver bone cement. *Biomaterials* 25, 4383–4391. <https://doi.org/10.1016/j.biomaterials.2003.10.078>

Anbarasu, S., Radhakrishnan, M., Suresh, A., Joseph, J., 2015. Phytochemical, ethnomedicinal and pharmacological potentials of seabuckthorn- A mini review. *Int. J. Pharma Bio Sci.* 6, 263–272.

Andersson, S.C., Olsson, M.E., Johansson, E., Rumpunen, K., 2009. Carotenoids in sea buckthorn (*Hippophae rhamnoides* L.) berries during ripening and use of pheophytin a as a maturity marker. *J. Agric. Food Chem.* 57, 250–258. <https://doi.org/10.1021/jf802599f>

-
- Ariff, M.A.M., Yusri, A.M., Razak, N.A.A., Jaapar, J., 2018. Effect of CO₂ flow rate, co-solvent and pressure behavior to yield by supercritical CO₂ extraction of Mariposa Christia Vespertilionis leaves, in: AIP Conference Proceedings 020072. AIP Publishing, pp. 2–7. <https://doi.org/10.1063/1.5080885>
- Arimboor, R., Kumar, K.S., Arumugan, C., 2008. Simultaneous estimation of phenolic acids in sea buckthorn (*Hippophaë rhamnoides*) using RP-HPLC with DAD. *J. Pharm. Biomed. Anal.* 47, 31–38. <https://doi.org/10.1016/j.jpba.2007.11.045>
- Arimboor, R., Venugopalan, V.V., Sarinkumar, K., Arumugan, C., Sawhney, R.C., 2006. Integrated processing of fresh Indian sea buckthorn (*Hippophae rhamnoides*) berries and chemical evaluation of products. *Sci. Food Agric.* 86, 2345–2353.
- Asofiei, I., Calinescu, I., Trifan, A., David, I.G., Gavrilă, A.I., 2016. Microwave-Assisted Batch Extraction of Polyphenols from Sea Buckthorn Leaves. *Chem. Eng. Commun.* 203, 1547–1553. <https://doi.org/10.1080/00986445.2015.1134518>
- Attrey, D.P., Singh, A.K., Katyal, J., Naved, T., 2012. Pharmacognostical Characterization & Preliminary Phytochemical Investigation of Seabuckthorn (*Hippophae rhamnoides* L.) Leaves. *Indo Glob. J. Pharm. Sci.* 2, 108–113.
- Aygün, A., Gülbağça, F., Nas, M.S., Alma, M.H., Çalımlı, M.H., Ustaoglu, B., Altunoglu, Y.C., Baloğlu, M.C., Cellat, K., Şen, F., 2020. Biological synthesis of silver nanoparticles using *Rheum ribes* and evaluation of their anticarcinogenic and antimicrobial potential: A novel approach in phytonanotechnology. *J. Pharm. Biomed. Anal.* 179. <https://doi.org/10.1016/j.jpba.2019.113012>
- Babaeekhou, L., Ghane, M., 2020. Antimicrobial activity of ginger on cariogenic bacteria: molecular networking and molecular docking analyses. *J. Biomol. Struct. Dyn.* 1–12.
-

References

<https://doi.org/10.1080/07391102.2020.1745283>

- Bal, L.M., Meda, V., Naik, S.N., Satya, S., 2011. Sea buckthorn berries: A potential source of valuable nutrients for nutraceuticals and cosmoceuticals. *Food Res. Int.* 44, 1718–1727. <https://doi.org/10.1016/j.foodres.2011.03.002>
- Banerjee, J., Narendhirakannan, R.T., 2011. Biosynthesis of silver nanoparticles from *Syzygium cumini* (L.) seed extract and evaluation of their in vitro antioxidant activities. *Dig. J. Nanomater. Biostructures* 6, 961–968.
- Bar, H., Bhui, D.K., Sahoo, G.P., Sarkar, P., De, S.P., Misra, A., 2009. Green synthesis of silver nanoparticles using latex of *Jatropha curcas*. *Colloids Surfaces A Physicochem. Eng. Asp.* 339, 134–139. <https://doi.org/10.1016/j.colsurfa.2009.02.008>
- Bauer, A., Kirby, W., Sherris, J., 1966. Antibiotic susceptibility testing by a standardized single disk method. *Am. J. Clin. Pathol.* 43, 493–496.
- Bekker, N.P., Glushenkova, A.I., 2001. COMPONENTS OF CERTAIN SPECIES OF THE ELAEAGNACEAE FAMILY. *Chem. Nat. Compd.* 37, 97–116. <https://doi.org/10.1023/A:1012395332284>
- Beveridge, T., Li, T.S.C., Oomah, B.D., Smith, A., 1999. Sea buckthorn products: Manufacture and composition. *J. Agric. Food Chem* 47, 3480–3488. <https://doi.org/10.1021/jf981331m>
- Bhargava, V. V., Saluja, A.K., Dholwani, K.K., 2013. Detection of Heavy Metal Contents and Proximate Analysis of roots of *Anogeissus latifolia*. *J. Pharmacogn. Phytochem.* 1, 61–65.
- Biel, W., Jaroszewska, A., 2017. The nutritional value of leaves of selected berry species. *Sci. Agric.* 74, 405–410. <https://doi.org/10.1590/1678-992x-2016-0314>
- Bittová, M., Krejzová, E., Roblová, V., Kubán, P., Kubáň, V., 2014. Monitoring of HPLC profiles of selected polyphenolic compounds in sea buckthorn (*Hippophaë rhamnoides* L.) plant parts
-

-
- during annual growth cycle and estimation of their antioxidant potential. *Cent. Eur. J. Chem.* 12, 1152–1161. <https://doi.org/10.2478/s11532-014-0562-y>
- Burčová, Z., Kreps, F., Schmidt, Š., Jablonský, M., Ház, A., Sládková, A., Šurina, I., 2017. Composition of fatty acids and tocopherols in peels, seeds and leaves of Sea buckthorn. *Acta Chim. Slovaca* 10, 29–34. <https://doi.org/10.1515/acs-2017-0005>
- Campos, H., Baylin, A., Willett, W.C., 2008. Linolenic Acid and Risk of Nonfatal Acute Myocardial Infarction. *Circulation* 118, 339–345. <https://doi.org/10.1161/CIRCULATIONAHA.107.762419>
- Cho, C.H., Jang, H., Lee, M., Kang, H., Heo, H.J., Kim, D.-O., 2017. Sea buckthorn (*Hippophae rhamnoides* L.) leaf extracts protect neuronal PC-12 cells from oxidative stress. *J. Microbiol. Biotechnol.* 27, 1257–1265. <https://doi.org/10.4014/jmb.1704.04033>
- Ciesarová, Z., Murkovic, M., Cejpek, K., Kreps, F., Tobolková, B., Koplík, R., Belajová, E., Kukurová, K., Daško, E., Panovská, Z., Revenco, D., Burčová, Z., 2020. Why is sea buckthorn (*Hippophae rhamnoides* L.) so exceptional? A review. *Food Res. Int.* 133, 109170. <https://doi.org/10.1016/j.foodres.2020.109170>
- Cossins, E., Lee, R., Packer, L., 1998. ESR studies of vitamin C regeneration, order of reactivity of natural source phytochemical preparations. *Biochem. Mol. Biol. Int.* 45, 583–97.
- Cossuta, D., Bela Simandi, Hohmann, J., Doleschall, F., Keve, T., 2007. Supercritical carbon dioxide extraction of sea buckthorn (*Hippophae rhamnoides* L.) pomace. *J. Sci. Food Agric.* 87, 2472–2481. <https://doi.org/10.1002/jsfa>
- Cowan, M.M., 1999. Plant products as antimicrobial agents, in: *American Society for Microbiology*. pp. 564–582. <https://doi.org/10.1089/1042031990000000000>
- Criste, A., Urcan, A.C., Bunea, A., Furtuna, F.R.P., Olah, N.K., Madden, R.H., Corcionivoschi,
-

References

- N., 2020. Phytochemical Composition and Biological Activity of Berries and Leaves from Four Romanian Sea Buckthorn (*Hippophae Rhamnoides* L.) Varieties. *Molecules* 25, 1–21.
- Diamante, L.M., Lan, T., 2014. Absolute Viscosities of Vegetable Oils at Different Temperatures and Shear Rate Range of 64.5 to 4835 s⁻¹. *J. Food Process.* <https://doi.org/10.1155/2014/234583>
- Ding, J., Ruan, C.J., Bao, Y.H., Guan, Y., Shan, J.Y., Li, H., Ding, G.J., 2015. Analysis of genetic relationships in sea buckthorn (*Hippophae rhamnoides*) germplasm from China and other countries using ISSR markers. *J. Hortic. Sci. Biotechnol.* 90, 599–606. <https://doi.org/10.1080/14620316.2015.11668721>
- Dong, R., Su, J., Nian, H., Shen, H., Zhai, X., Xin, H., Qin, L., Han, T., 2017. Chemical fingerprint and quantitative analysis of flavonoids for quality control of Sea buckthorn leaves by HPLC and UHPLC-ESI-QTOF-MS. *J. Funct. Foods* 37, 513–522. <https://doi.org/10.1016/j.jff.2017.08.019>
- Dubey, S., Ramana, M. V, Mishra, A., 2017. Comparison of Fatty Acid Profiling and RBC Membrane Stabilization Activity of Seabuckthorn (*Hippophae rhamnoides* and *Hippophae salicifolia*) Seed Oil. *Pharmacogn. J.* 9, 329–335.
- El-chaghaby, G.A., Ahmad, A.F., Ramis, E.S., 2014. Evaluation of the antioxidant and antibacterial properties of various solvents extracts of *Annona squamosa* L. leaves. *Arab. J. Chem.* 7, 227–233. <https://doi.org/10.1016/j.arabjc.2011.06.019>
- Elechiguerra, J.L., Burt, J.L., Morones, J.R., Camacho-Bragado, A., Gao, X., Lara, H.H., Yacaman, M.J., 2005. Interaction of silver nanoparticles with HIV-1. *J. Nanobiotechnology* 3, 1–10. <https://doi.org/10.1186/1477-3155-3-6>
- Ercisli, S., Orhan, E., Ozdemir, O., Sengul, M., 2007. The genotypic effects on the chemical
-

-
- composition and antioxidant activity of sea buckthorn (*Hippophae rhamnoides* L.) berries grown in Turkey. *Sci. Hortic. (Amsterdam)*. 115, 27–33. <https://doi.org/10.1016/j.scienta.2007.07.004>
- Fatima, T., Kesari, V., Watt, I., Wishart, D., Todd, J.F., Schroeder, W.R., Paliyath, G., Krishna, P., 2015. Metabolite profiling and expression analysis of flavonoid, Vitamin C and tocopherol biosynthesis genes in the antioxidant-rich sea buckthorn (*Hippophae rhamnoides* L.). *Phytochemistry* 118, 181–191. <https://doi.org/10.1016/j.phytochem.2015.08.008>
- Floch, F. Le, Tena, M.T., Rios, A., Valcarcel, M., 1998. Supercritical fluid extraction of phenol compounds from olive leaves. *Talanta* 46, 1123–1130.
- Gadkari, P.V., Balarman, M., Kadimi, U.S., 2013. Polyphenols from fresh frozen tea leaves (*Camellia assamica* L.) by supercritical carbon dioxide extraction with ethanol entrainer - application of response surface methodology. *J. Food Sci. Technol.* 52, 720–730. <https://doi.org/10.1007/s13197-013-1085-9>
- Galan, A.M., Calinescu, I., Trifan, A., Winkworth-Smith, C., Calvo-Carrascal, M., Dodds, C., Binner, E., 2017. New insights into the role of selective and volumetric heating during microwave extraction: Investigation of the extraction of polyphenolic compounds from sea buckthorn leaves using microwave-assisted extraction and conventional solvent extraction. *Chem. Eng. Process. - Process Intensif.* 116, 29–39. <https://doi.org/10.1016/j.cep.2017.03.006>
- Gallocchio, F., Belluco, S., Ricci, A., 2015. Nanotechnology and Food: Brief Overview of the Current Scenario. *Procedia Food Sci.* 5, 85–88. <https://doi.org/10.1016/j.profoo.2015.09.022>
- Gamlin, C.D., Dutta, N.K., Choudhury, N.R., Kehoe, D., Matisons, J., 2002. Evaluation of kinetic parameters of thermal and oxidative decomposition of base oils by conventional, isothermal
-

References

-
- and modulated TGA, and pressure DSC. *Thermochim. Acta* 392–393, 357–369.
[https://doi.org/10.1016/S0040-6031\(02\)00121-1](https://doi.org/10.1016/S0040-6031(02)00121-1)
- Gęgotek, A., Jastrząb, A., Jarocka-Karpowicz, I., Muszyńska, M., Skrzydlewska, E., 2018. The Effect of Sea Buckthorn (*Hippophae rhamnoides* L.) Seed Oil on UV-Induced Changes in Lipid Metabolism of Human Skin Cells. *Antioxidants* 7, 110.
<https://doi.org/10.3390/antiox7090110>
- GENENA, A.K., HENSE, H., JUNIOR, A.S., SOUZA, S.M. de, 2008. Rosemary (*Rosmarinus officinalis*) - A study of the composition, antioxidant and antimicrobial activities of extracts obtained with supercritical carbon dioxide. *Cienc. e Tecnol. Aliment.* 28, 463–469.
<https://doi.org/10.1590/S0101-20612008000200030>
- Ghatnur, S.M., Sonale, R.S., Balaraman, M., Kadimi, U.S., 2012. Engineering liposomes of leaf extract of seabuckthorn (SBT) by supercritical carbon dioxide (SCCO₂)-mediated process. *J. Liposome Res.* 22, 215–223. <https://doi.org/10.3109/08982104.2012.658576>
- Gu, L.B., Pang, H.L., Lu, K.K., Liu, H.M., Wang, X. De, Qin, G.Y., 2017. Process optimization and characterization of fragrant oil from red pepper (*Capsicum annuum* L.) seed extracted by subcritical butane extraction. *J. Sci. Food Agric.* 97, 1894–1903.
<https://doi.org/10.1002/jsfa.7992>
- Gu, L.B., Zhang, G.J., Du, L., Du, J., Qi, K., Zhu, X.L., Zhang, X.Y., Jiang, Z.H., 2019. Comparative study on the extraction of *Xanthoceras sorbifolia* Bunge (yellow horn) seed oil using subcritical n-butane, supercritical CO₂, and the Soxhlet method. *Lwt* 111, 548–554.
<https://doi.org/10.1016/j.lwt.2019.05.078>
- Guo, R., Guo, X., Li, T., Fu, X., Liu, R.H., 2017. Comparative assessment of phytochemical profiles, antioxidant and antiproliferative activities of Sea buckthorn (*Hippophae rhamnoides*
-

-
- L.) berries. *Food Chem.* 221, 997–1003. <https://doi.org/10.1016/j.foodchem.2016.11.063>
- Gupta, D., Kaul, V., 2017. Antioxidant Activity Vis-a-Vis Phenolic Content in Leaves of Seabuckthorn from Kargil District (J&K, India): A Preliminary Study. *Natl. Acad. Sci. Lett.* 40, 53–56. <https://doi.org/10.1007/s40009-016-0510-9>
- Gurunathan, S., Kalishwaralal, K., Vaidyanathan, R., Deepak, V., Pandian, S.R.K., Muniyandi, J., Hariharan, N., Eom, S.H., 2009. Biosynthesis, purification and characterization of silver nanoparticles using *Escherichia coli*. *Colloids Surfaces B Biointerfaces* 74, 328–335.
- Haider, A., Kang, I.K., 2014. Preparation of silver nanoparticles and their industrial and biomedical applications: A comprehensive review. *Adv. Mater. Sci. Eng.* 2015. <https://doi.org/10.1155/2015/165257>
- Halliwell, B., Zhao, K., Whiteman, M., 2000. The gastrointestinal tract: A major site of antioxidant action? *Free Radic. Res.* 33, 819–830. <https://doi.org/10.1080/10715760000301341>
- Hassanien, M.F.R., Sharoba, A.M., 2014. Rheological characteristics of vegetable oils as affected by deep frying of French fries. *J. Food Meas. Charact.* 8, 171–179. <https://doi.org/10.1007/s11694-014-9178-3>
- Heinäaho, M., Pusenius, J., Julkunen-Tiitto, R., 2006. Effects of different organic farming methods on the concentration of phenolic compounds in sea buckthorn leaves. *J. Agric. Food Chem.* 54, 7678–7685. <https://doi.org/10.1021/jf061018h>
- Herrero, M., Cifuentes, A., Ibañez, E., 2006. Sub- and supercritical fluid extraction of functional ingredients from different natural sources: Plants, food-by-products, algae and microalgae - A review. *Food Chem.* 98, 136–148. <https://doi.org/10.1016/j.foodchem.2005.05.058>
- Htwe, Y.Z.N., Chow, W.S., Suda, Y., Mariatti, M., 2019. Effect of silver nitrate concentration on the production of silver nanoparticles by green method. *Mater. Today Proc.* 17, 568–573.
-

References

<https://doi.org/10.1016/j.matpr.2019.06.336>

- Husain, M., Prasad Rathore, J., Rasool, A., Kumar Vishwakarma, D., Mahendar, K., Mohit Husain, C., Parrey, A.A., 2018. Seabuckthorn: A multipurpose shrubs species in Ladakh cold desert. *J. Entomol. Zool. Stud.* 6.
- Hussain, M.M., Ali, S., Awan, S., Hussain, M.M., Hussain, I., 2014. Analysis of minerals and vitamins in sea buckthorn (*Hippophae rhamnoides*) pulp collected from Ghizer and Skardu districts of Gilgit-Baltistan. *Int. J. Biosci.* 6655, 144–152. <https://doi.org/10.12692/ijb/4.12.144-152>
- Hussain, N., Irshad, F., Jabeen, Z., Shamsi, I.H., Li, Z., Jiang, L., 2013. Biosynthesis, structural, and functional attributes of tocopherols in planta; Past, present, and future perspectives. *J. Agric. Food Chem.* 61, 6137–6149. <https://doi.org/10.1021/jf4010302>
- Ibrahim, M.H., Jaafar, H.Z.E., Rahmat, A., Rahman, Z.A., 2011. The relationship between phenolics and flavonoids production with total non structural carbohydrate and photosynthetic rate in *Labisia pumila* Benth. under high CO₂ and nitrogen fertilization. *Molecules* 16, 162–174. <https://doi.org/10.3390/molecules16010162>
- Ion, V.A., Parvulescu, O.C., Velcea, D., Popa, O., Ahmadi, M., 2019. Physico-chemical Parameters and Antioxidant Activity of Romanian Sea Buckthorn Berries. *Rev. Chim.* 70, 4187–4192. <https://doi.org/10.37358/RC.19.12.7730>
- Jaroszewska, A., Biel, W., Bojanowska-Czajka, A., Wierzchnicki, R., 2017. Influence of habitat conditions on chemical composition and content of isotopes in sea buckthorn (*Hippophae rhamnoides* L.) leaves. *Acta Sci. Pol. Hortorum Cultus* 16, 3–10.
- Jayashankar, B., Mishra, K.P., L.Ganju, Singh, S.B., 2014. Supercritical extract of Seabuckthorn Leaves (SCE200ET) inhibited endotoxemia by reducing inflammatory cytokines and nitric

-
- oxide synthase 2 expression. *Int. Immunopharmacol.* 20, 89–94.
<https://doi.org/10.1016/j.intimp.2014.02.022>
- Jayashankar, B., Singh, D., Mishra, K., Madhusudana, S., YB, A., Singh, S., Ganju, L., 2016. Supercritical Carbon Dioxide Extract of Seabuckthorn Leaves Enhances Rabies Virus Neutralizing Antibody Titers and CTL Response in Swiss Albino Mice. *J. Vaccines Immunol.* 2, 004–009. <https://doi.org/10.17352/jvi.000013>
- Jayashankar, B., Singh, D., Tanwar, H., Mishra, K.P., Murthy, S., Chanda, S., Mishra, J., Tulswani, R., Misra, K., Singh, S.B., Ganju, L., 2017. Augmentation of humoral and cellular immunity in response to Tetanus and Diphtheria toxoids by supercritical carbon dioxide extracts of *Hippophae rhamnoides* L. leaves. *Int. Immunopharmacol.* 44, 123–136.
<https://doi.org/10.1016/j.intimp.2017.01.012>
- Jemal, K., Sandeep, B. V., Pola, S., 2017. Synthesis, Characterization, and Evaluation of the Antibacterial Activity of *Allophylus serratus* Leaf and Leaf Derived Callus Extracts Mediated Silver Nanoparticles. *J. Nanomater.* 2017. <https://doi.org/10.1155/2017/4213275>
- Jeong, J.H., Lee, J.W., Kim, K.S., Kim, J.-S., Han, S.N., Yu, C.Y., Lee, J.K., Kwon, Y.S., Kim, M.J., 2010. Antioxidant and Antimicrobial Activities of Extracts from a Medicinal, Sea Buckthorn. *J. Korean Soc. Appl. Biol. Chem* 53, 33–38.
<https://doi.org/10.3839/jksabc.2010.006>
- Jeremiah, S.S., Miyakawa, K., Morita, T., Yamaoka, Y., Ryo, A., 2020. Potent antiviral effect of silver nanoparticles on SARS-CoV-2. *Biochem. Biophys. Res. Commun.* 533, 195–200.
<https://doi.org/10.1016/j.bbrc.2020.09.018>
- Jianfeng Xing, 2012. Effects of sea buckthorn (*Hippophaë rhamnoides* L.) pulp oils on the gastric secretion, gastric emptying and its analgesic activity. *J. Med. Plants Res.* 6, 3240–3245.
-

References

<https://doi.org/10.5897/JMPR12.109>

Kagliwal, L.D., Patil, S.C., Pol, A.S., Singhal, R.S., Patravale, V.B., 2011. Separation of bioactives from seabuckthorn seeds by supercritical carbon dioxide extraction methodology through solubility parameter approach. *Sep. Purif. Technol.* 80, 533–540.

<https://doi.org/10.1016/j.seppur.2011.06.008>

Kagliwal, L.D., Pol, A.S., Patil, S.C., Singhal, R.S., Patravale, V.B., 2012. Antioxidant-Rich Extract from Dehydrated Seabuckthorn Berries by Supercritical Carbon Dioxide Extraction. *Food Bioprocess Technol.* 5, 2768–2776. <https://doi.org/10.1007/s11947-011-0613-8>

Kalaiyarsan, T., Bharti, V.K., Chaurasia, O.P., 2017. One pot green preparation of: Seabuckthorn silver nanoparticles (SBT@AgNPs) featuring high stability and longevity, antibacterial, antioxidant potential: A nano disinfectant future perspective. *RSC Adv.* 7, 51130–51141.

<https://doi.org/10.1039/c7ra10262c>

Kallio, H., Baoru, Y., Tahvonen, R., Hakala, M., 2000. Composition of sea buckthorn berries of various origins., in: *International Workshop on Sea Buckthorn*. China, Beijing, pp. 13–19.

Kallio, H., Yang, B., Peippo, P., Tahvonen, R., Pan, R., 2002. Triacylglycerols, glycerophospholipids, tocopherols, and tocotrienols in berries and seeds of two subspecies (ssp. *sinensis* and *mongolica*) of sea buckthorn (*Hippophaë rhamnoides*). *J. Agric. Food Chem.* 50, 3004–3009. <https://doi.org/10.1021/jf011556o>

Kaminskas, A., Briedis, V., Budrionienė, R., Hendrixson, V., Petraitis, R., Z.K., 2006. Fatty acid composition of sea buckthorn (*Hippophae rhamnoides* L.) pulp oil of Lithuanian origin stored at different temperatures. *BIOLOGIJA* 38–40.

Kanayama, Y., Sato, K., Ikeda, H., Tamura, T., Nishiyama, M., Kanahama, K., 2013. Seasonal changes in abiotic stress tolerance and concentrations of tocopherol, sugar, and ascorbic acid

-
- in sea buckthorn leaves and stems. *Sci. Hort.* (Amsterdam). 164, 232–237.
<https://doi.org/10.1016/j.scienta.2013.09.039>
- Karhu, S., 2003. New sea buckthorn cultivars Terhi, Tytti and Tarmo, in: In T. Hovi, S. Karhu, M.-M. Linna, & T. Suojala (Eds.), *Harvest – Horticultural Research Results 2000–2002*. MTT Agrifood Research Finland, Horticulture., Piikkiö, Finland:, pp. 83–84.
- Kashif, M., Ullah, S., 2013. Chemical Composition and Minerals Analysis of *Hippophae rhamnoides*, *Azadirachta indica*, *Punica granatu* and *Ocimum sanctum* Leaves. *World J. Dairy Food Sci.* 8, 67–73. <https://doi.org/10.5829/idosi.wjdfs.2013.8.1.1119>
- Kauppinen, S., 2017. Sea Buckthorn Leaves and the Novel Food Evaluation. *Proc. Latv. Acad. Sci. Sect. B Nat. Exact, Appl. Sci.* 71, 111–114. <https://doi.org/10.1515/prolas-2017-0019>
- Khalil, M.M.H., Ismail, E.H., El-Baghdady, K.Z., Mohamed, D., 2014. Green synthesis of silver nanoparticles using olive leaf extract and its antibacterial activity. *Arab. J. Chem.* 7, 1131–1139. <https://doi.org/10.1016/j.arabjc.2013.04.007>
- Khandelwal, K.R., 2008. *Practical pharmacognosy*, 24th ed. Pragati Books Pvt. Ltd., Pune.
- Khaw, K.-Y., Parat, M.-O., Shaw, P.N., Falconer, J.R., 2017. Solvent supercritical fluid technologies to extract bioactive compounds from natural sources: A review. *Molecules* 22. <https://doi.org/10.3390/molecules22071186>
- Kim, S.J., Hwang, E., Yi, S.S., Song, K.D., Lee, H.K., Heo, T.H., Park, S.K., Jung, Y.J., Jun, H.S., 2017. Sea Buckthorn Leaf Extract Inhibits Glioma Cell Growth by Reducing Reactive Oxygen Species and Promoting Apoptosis. *Appl. Biochem. Biotechnol.* 182, 1663–1674. <https://doi.org/10.1007/s12010-017-2425-4>
- Korekar, G., Stobdan, T., Singh, H., Chaurasia, O., Singh, S., 2011. Phenolic content and antioxidant capacity of various solvent extracts from seabuckthorn (*Hippophae rhamnoides*
-

References

-
- L.) fruit pulp, seeds, leaves and stem bark. *Acta Aliment.* 40, 449–458.
<https://doi.org/10.1556/AAlim.40.2011.4.4>
- Kostrzewa, D., Dobrzyńska-Inger, A., Turczyn, A., 2019. Experimental data and modelling of the solubility of high-carotenoid paprika extract in supercritical carbon dioxide. *Molecules* 24.
<https://doi.org/10.3390/molecules24224174>
- Krejcarová, J., Straková, E., Suchý, P., Herzig, I., Karásková, K., 2015. Sea buckthorn (*Hippophae rhamnoides* L.) as a potential source of nutraceuticals and its therapeutic possibilities - A review. *Acta Vet. Brno* 84, 257–268. <https://doi.org/10.2754/avb201584030257>
- Kuhkheil, A., Badi, H.N., Mehrafarin, A., Abdossi, V., 2017. Chemical constituents of sea buckthorn (*Hippophae rhamnoides* L.) fruit in populations of central Alborz Mountains in Iran. *Res. J. Pharmacogn.* 4, 1–12.
- Kumar, M.S.Y., Dutta, R., Prasad, D., Misra, K., 2011. Subcritical water extraction of antioxidant compounds from Seabuckthorn (*Hippophae rhamnoides*) leaves for the comparative evaluation of antioxidant activity. *Food Chem.* 127, 1309–1316.
<https://doi.org/10.1016/j.foodchem.2011.01.088>
- Kumar, M.S.Y., Tirpude, R.J., Maheshwari, D.T., Bansal, A., Misra, K., 2013. Antioxidant and antimicrobial properties of phenolic rich fraction of Seabuckthorn (*Hippophae rhamnoides* L.) leaves in vitro. *Food Chem.* 141, 3443–3450.
<https://doi.org/10.1016/j.foodchem.2013.06.057>
- Kumar, P.P.N.V., Pammi, S.V.N., Kollu, P., Satyanarayana, K.V.V., Shameem, U., 2014. Green synthesis and characterization of silver nanoparticles using *Boerhaavia diffusa* plant extract and their anti bacterial activity. *Ind. Crop. Prod. journa* 52, 562–566.
<https://doi.org/10.1016/j.indcrop.2013.10.050>
-

-
- Kumar, S., Pandey, A.K., 2013. Chemistry and Biological Activities of Flavonoids: An Overview Shashank. Sci. World J. 2013. [https://doi.org/10.1016/S1572-5995\(05\)80065-1](https://doi.org/10.1016/S1572-5995(05)80065-1)
- Le, A. V., Parks, S.E., Nguyen, M.H., Roach, P.D., 2018. Physicochemical Properties of Gac (*Momordica cochinchinensis* (Lour.) Spreng) Seeds and Their Oil Extracted by Supercritical Carbon Dioxide and Soxhlet Methods. *Technologies* 6, 94. <https://doi.org/10.3390/technologies6040094>
- Lee, H.J., Jeong, S.H., 2005. Bacteriostasis and Skin Innoxiousness of Nanosize Silver Colloids on Textile Fabrics. *Text. Res. J.* 75, 551–556. <https://doi.org/10.1177/0040517505053952>
- Leeuw, R. Van, Kevers, C., Pincemail, J., Defraigne, J.O., Dommès, J., 2014. Antioxidant capacity and phenolic composition of red wines from various grape varieties: Specificity of Pinot Noir. *J. Food Compos. Anal.* 36, 40–50. <https://doi.org/10.1016/j.jfca.2014.07.001>
- Li, J., Liu, J., Sun, X., Liu, Y., 2018. The mathematical prediction model for the oxidative stability of vegetable oils by the main fatty acids composition and thermogravimetric analysis. *Lwt* 96, 51–57. <https://doi.org/10.1016/j.lwt.2018.05.003>
- Li, T.S.C., Schroeder, W.R., 1996. Sea buckthorn (*hippophae rhamnoides* l.): A multipurpose plant. *Horttechnology* 6, 370–380. https://doi.org/10.1300/J044v01n01_04
- Lin, D., Xiao, M., Zhao, J., Li, Z., Xing, B., Li, X., Kong, M., Li, L., Zhang, Q., Liu, Y., Chen, H., Qin, W., Wu, H., Chen, S., 2016. An overview of plant phenolic compounds and their importance in human nutrition and management of type 2 diabetes. *Molecules* 21. <https://doi.org/10.3390/molecules21101374>
- Liu, C., Yang, M., Huang, F., 2012. Influence of extraction processing on rheological properties of rapeseed oils. *JAOCS, J. Am. Oil Chem. Soc.* 89, 73–78. <https://doi.org/10.1007/s11746-011-1892-y>
-

References

-
- Lowry, H.O., Rosebrough, J.N., Farr, L.A., Randall, L.R., 1951. Protein measurement with the Folin phenol reagent. *J. Biol. Chem* 193. https://doi.org/10.1007/978-94-007-0753-5_100521
- Lu, R., 1992. Seabuckthorn: A multipurpose plant species of fragile mountains (No. 20). Katmandu, Nepal,.
- Lushchak, V.I., Semchuk, N.M., 2012. Tocopherol biosynthesis: Chemistry, regulation and effects of environmental factors. *Acta Physiol. Plant.* 34, 1607–1628. <https://doi.org/10.1007/s11738-012-0988-9>
- Mani, M., Pavithra, S., Mohanraj, K., Kumaresan, S., Alotaibi, S.S., Eraqi, M.M., Gandhi, A.D., Babujanarthanam, R., Maaza, M., Kaviyarasu, K., 2021. Studies on the spectrometric analysis of metallic silver nanoparticles (Ag NPs) using *Basella alba* leaf for the antibacterial activities. *Environ. Res.* 199, 111274. <https://doi.org/10.1016/j.envres.2021.111274>
- Maran, J.P., Manikandan, S., Priya, B., Gurumoorthi, P., 2015. Box-Behnken design based multi-response analysis and optimization of supercritical carbon dioxide extraction of bioactive flavonoid compounds from tea (*Camellia sinensis* L.) leaves. *J Food Sci Technol* (January 52, 92–104. <https://doi.org/10.1007/s13197-013-0985-z>
- Michel, T., Destandau, E., Floch, G. Le, Lucchesi, M.E., Elfakir, C., 2012. Antimicrobial, antioxidant and phytochemical investigations of sea buckthorn (*Hippophaë rhamnoides* L.) leaf, stem, root and seed. *Food Chem.* 131, 754–760. <https://doi.org/10.1016/j.foodchem.2011.09.029>
- Mihalcea, L., Turturică, M., Ghinea, I.O., Barbu, V., Ioniță, E., Cotârlet, M., Stănciuc, N., 2017. Encapsulation of carotenoids from sea buckthorn extracted by CO₂ supercritical fluids method within whey proteins isolates matrices. *Innov. Food Sci. Emerg. Technol.* 42, 120–129. <https://doi.org/10.1016/j.ifset.2017.06.008>
-

-
- Moges, A., Barik, C.R., Purohit, S., Goud, V. V., 2021. Dietary and bioactive properties of the berries and leaves from the underutilized *Hippophae salicifolia* D . Don grown in Northeast India. *Food Sci. Biotechnol.* 30, 1555–1569. <https://doi.org/10.1007/s10068-021-00988-8>
- Mohamed, H. Ben, Duba, K.S., Fiori, L., Abdelgawed, H., Tlili, I., Tounekti, T., Zrig, A., 2016. Bioactive compounds and antioxidant activities of different grape (*Vitis vinifera* L.) seed oils extracted by supercritical CO₂ and organic solvent. *LWT - Food Sci. Technol.* 74, 557–562. <https://doi.org/10.1016/j.lwt.2016.08.023>
- Narváez-Cuenca, C.E., Inampues-Charfuelan, M.L., Hurtado-Benavides, A.M., Parada-Alfonso, F., Vincken, J.P., 2020. The phenolic compounds, tocopherols, and phytosterols in the edible oil of guava (*Psidium guava*) seeds obtained by supercritical CO₂ extraction. *J. Food Compos. Anal.* 89, 103467. <https://doi.org/10.1016/j.jfca.2020.103467>
- Nasrollahzadeh, M., Sajadi, S.M., Maham, M., 2014. Green synthesis of palladium nanoparticles using *Hippophae rhamnoides* Linn leaf extract and their catalytic activity for the Suzuki-Miyaura coupling in water. *J. Mol. Catal.* 396, 297–303. <https://doi.org/10.1016/j.molcata.2014.10.019>
- Ncube, N.S., Afolayan, A.J., Okoh, A.I., 2017. Assessment techniques of antimicrobial properties of natural compounds of plant origin: current methods and future trends. *African J. Biotechnol.* 7, 1797–1806. <https://doi.org/10.1016/j.pep.2007.12.009>
- Negi, P.S., Chauhan, A.S., Sadia, G.A., Rohinishree, Y.S., Ramteke, R.S., 2005. Antioxidant and antibacterial activities of various seabuckthorn (*Hippophae rhamnoides* L.) seed extracts. *Food Chem.* 92, 119–124. <https://doi.org/10.1016/j.foodchem.2004.07.009>
- Ngouana, V., Zeuko’O Menkem, E., Youmbi, D.Y., Yimgang, L.V., Toghueo, R.M.K., Boyom, F.F., 2021. Serial Exhaustive Extraction Revealed Antimicrobial and Antioxidant Properties
-

References

-
- of *Platyserium stemaria* (Beauv) Desv. *Biomed Res. Int.* 2021.
<https://doi.org/10.1155/2021/1584141>
- Oh, K.H., Soshnikova, V., Markus, J., Kim, Yeon Ju, Lee, S.C., Singh, P., Castro-Aceituno, V., Ahn, S., Kim, D.H., Shim, Y.J., Kim, Yu Jin, Yang, D.C., 2018. Biosynthesized gold and silver nanoparticles by aqueous fruit extract of *Chaenomeles sinensis* and screening of their biomedical activities. *Artif. Cells, Nanomedicine Biotechnol.* 46, 599–606.
<https://doi.org/10.1080/21691401.2017.1332636>
- Ohashi, S., Saku, S., Yamamoto, K., 2004. Antibacterial activity of silver inorganic agent YDA filler. *J. Oral Rehabil.* 31, 364–367. <https://doi.org/10.1111/j.1365-2842.2004.01200.x>
- Olas, B., 2016. Sea buckthorn as a source of important bioactive compounds in cardiovascular diseases. *Food Chem. Toxicol.* 97, 199–204. <https://doi.org/10.1016/j.fct.2016.09.008>
- Olas, B., Skalski, B., Ulanowska, K., 2018. The anticancer activity of sea buckthorn [*Elaeagnus rhamnoides* (L.) A. Nelson]. *Front. Pharmacol.* 9, 1–8.
<https://doi.org/10.3389/fphar.2018.00232>
- Oprica, L., Olteanu, Z., Zamfirache, M.M., Truta, E., Surdu, S., Rati, I.V., Manzu, C., Milian, G., Rosu, C., 2007. The Content of Soluble Proteins in *Hyppophae rhamnoides* ssp. *carpathica* Varieties Harvested from Different Regions of Romania, in: 3rd International Sea Buchthorn Association Conference. pp. 73–79.
- Ouattara, L., Koudou, J., Karou, D.S., Giacò, L., Capelli, G., Simpoire, J., Fraziano, M., Colizzi, V., Traore, A.S., 2011. In vitro anti *Mycobacterium tuberculosis* H37Rv activity of *Lanea acida* A. Rich. from Burkina Faso. *Pak. J. Biol. Sci* 14, 47–52.
- Padalia, H., Moteriya, P., Chanda, S., 2015. Green synthesis of silver nanoparticles from marigold flower and its synergistic antimicrobial potential. *Arab. J. Chem.* 8, 732–741.
-

-
- <https://doi.org/10.1016/j.arabjc.2014.11.015>
- Parikh, D. V., Fink, T., Rajasekharan, K., Sachinvala, N.D., Sawhney, A.P.S., Calamari, T.A., Parikh, A.D., 2005. Antimicrobial Silver/Sodium Carboxymethyl Cotton Dressings for Burn Wounds. *Text. Res. J.* 75, 134–138. <https://doi.org/10.1177/004051750507500208>
- Patel, C.A., Divakar, K., Santani, D., Solanki, H.K., Thakkar, J.H., 2012. Remedial Prospective of *Hippophae rhamnoides* Linn. (Sea Buckthorn). *ISRN Pharmacol.* 2012, 1–6. <https://doi.org/10.5402/2012/436857>
- Peiris, M.K., Gunasekara, C.P., Jayaweera, P.M., Arachchi, N.D.H., Fernando, N., 2017. Biosynthesized silver nanoparticles: Are they effective antimicrobials? *Mem. Inst. Oswaldo Cruz* 112, 537–543. <https://doi.org/10.1590/0074-02760170023>
- Pereira, P., Cebola, M.-J., Oliveira, M.C., Bernardo-Gil, M.G., 2016. Supercritical fluid extraction vs conventional extraction of myrtle leaves and berries: Comparison of antioxidant activity and identification of bioactive compounds. *J. Supercrit. Fluids* 113, 1–9. <https://doi.org/10.1016/j.supflu.2015.09.006>
- Piltz, J., Law, D., 2007. *IFIA-Laboratory Methods Manual*. Aust. Fodd. Ind. Assoc. Inc, Balwyn.
- Polshettiwar, S.A., Ganjiwale, R.O., Wadher, S.J., Yeole, P.G., 2007. Spectrophotometric estimation of Total tannin in some ayurvedic eye drop. *Ind J Pharm Sci* 69, 574–576.
- Pop, Raluca M., Buzoianu, A.D., Rati, I. V., Socaciu, C., 2014. Untargeted metabolomics for sea buckthorn (*Hippophae Rhamnoides* ssp. *carpatica*) berries and leaves: Fourier transform infrared spectroscopy as a rapid approach for evaluation and discrimination. *Not. Bot. Horti Agrobot. Cluj-Napoca* 42, 545–550. <https://doi.org/10.1583/nbha4229654>
- Pop, R.M., Socaciu, C., Pinte, A., Buzoianu, A.D., Sanders, M.G., Gruppen, H., Vincken, J.-P., 2013. UHPLC/PDA-ESI/MS analysis of the main berry and leaf flavonol glycosides from
-

References

- different Carpathian *Hippophaë rhamnoides* L. Varieties. *Phytochem. Anal.* 24, 484–492.
<https://doi.org/10.1002/pca.2460>
- Pop, Raluca Maria, Weesepeel, Y., Socaciu, C., Pintea, A., Vincken, J.P., Gruppen, H., 2014. Carotenoid composition of berries and leaves from six Romanian sea buckthorn (*Hippophaë rhamnoides* L.) varieties. *Food Chem.* 147, 1–9.
<https://doi.org/10.1016/j.foodchem.2013.09.083>
- Porto, C. Da, Decorti, D., Natolino, A., 2016. Microwave pretreatment of *Moringa oleifera* seed: Effect on oil obtained by pilot-scale supercritical carbon dioxide extraction and Soxhlet apparatus. *J. Supercrit. Fluids* 107, 38–43. <https://doi.org/10.1016/j.supflu.2015.08.006>
- Pourmortazavi, S.M., Taghdiri, M., Makari, V., Rahimi-Nasrabadi, M., 2015. Procedure optimization for green synthesis of silver nanoparticles by aqueous extract of *Eucalyptus oleosa*. *Spectrochim. Acta - Part A Mol. Biomol. Spectrosc.* 136, 1249–1254.
<https://doi.org/10.1016/j.saa.2014.10.010>
- Pradhan, R.C., Meda, V., Rout, P.K., Naik, S., Dalai, A.K., 2010. Supercritical CO₂ extraction of fatty oil from flaxseed and comparison with screw press expression and solvent extraction processes. *J. Food Eng.* 98, 393–397. <https://doi.org/10.1016/j.jfoodeng.2009.11.021>
- Purohit, S., Barik, C.R., Kalita, D., Sahoo, L., Goud, V. V., 2021a. Exploration of nutritional, antioxidant and antibacterial properties of unutilized rind and seed of passion fruit from Northeast India. *J. Food Meas. Charact.* 1–15. <https://doi.org/10.1007/s11694-021-00899-6>
- Purohit, S., Kalita, D., Barik, C.R., Sahoo, L., Goud, V. V., 2021b. Evaluation of thermophysical, biochemical and antibacterial properties of unconventional vegetable oil from Northeast India. *Mater. Sci. Energy Technol.* 4, 81–91. <https://doi.org/10.1016/j.mset.2021.01.004>
- Ranjith, A., Kumar, K.S., Venugopalan, V.V., Arumughan, C., Sawhney, R.C., Singh, V., 2006.
-

-
- Fatty acids, tocopherols, and carotenoids in pulp oil of three sea buckthorn species (*Hippophae rhamnoides*, *H. salicifolia*, and *H. tibetana*) grown in the Indian Himalayas. *JAOCS, J. Am. Oil Chem. Soc.* 83, 359–364. <https://doi.org/10.1007/s11746-006-1213-z>
- Rao, K.J., Paria, S., 2015. *Aegle marmelos* Leaf Extract and Plant Surfactants Mediated Green Synthesis of Au and Ag Nanoparticles by Optimizing Process Parameters Using Taguchi Method. *ACS Sustain. Chem. Eng.* 3, 483–491. <https://doi.org/10.1021/acssuschemeng.5b00022>
- Rathor, R., Sharma, P., Suryakumar, G., Ganju, L., 2015. A pharmacological investigation of *Hippophae salicifolia* (HS) and *Hippophae rhamnoides turkestanica* (HRT) against multiple stress (C-H-R): an experimental study using rat model. *Cell Stress Chaperones* 20, 821–831. <https://doi.org/10.1007/s12192-015-0603-2>
- Re, R., Pellegrini, N., Proteggente, A., Pannala, A., Yang, M., Rice-Evans, C., 1999. Antioxidant Activity Applying an Improved ABTS Radical Cation Decolorization Assay. *Free Radic. Biol. Med.* 26, 1231–1237. [https://doi.org/10.1016/s0891-5849\(98\)00315-3](https://doi.org/10.1016/s0891-5849(98)00315-3)
- Reshad, A.S., Tiwari, P., Goud, V. V., 2017. Thermal Degradation Kinetic Study of Rubber Seed Oil and Its Methyl Esters under Inert Atmosphere. *Energy and Fuels* 31, 9642–9651. <https://doi.org/10.1021/acs.energyfuels.7b02249>
- Riaz, M., Mutreja, V., Sareen, S., Ahmad, B., Faheem, M., Zahid, N., Jabbour, G., Park, J., 2021. Exceptional antibacterial and cytotoxic potency of monodisperse greener AgNPs prepared under optimized pH and temperature. *Sci. Rep.* 11, 1–11. <https://doi.org/10.1038/s41598-021-82555-z>
- Rice-Evans, C.A., Miller, N.J., Paganga, G., 1996. Structure- antioxidant activity relationships of flavonoids and phenolic acid. *Free Radic. Biol. Med.* 20, 933–956.
-

References

- Roberto, M., Junior, M., Leite, A.V., Romanelli, N., Dragano, V., 2010. Supercritical Fluid Extraction and Stabilization of Phenolic Compounds From Natural Sources – Review (Supercritical Extraction and Stabilization of Phenolic Compounds). Chem. Eng. J. 4, 51–60.
- Rodrigues, V.H., Melo, M.M.R. de, Portugal, I., Silva, C.M., 2018. Supercritical fluid extraction of Eucalyptus globulus leaves. Experimental and modelling studies of the influence of operating conditions and biomass pretreatment upon yields and kinetics. Sep. Purif. Technol. 191, 173–181. <https://doi.org/10.1016/j.seppur.2017.09.026>
- ROP, O., ERCİŞLİ, S., MLCEK, J., JURIKOVA, T., HOZA, I., 2014. Antioxidant and radical scavenging activities in fruits of 6 sea buckthorn (*Hippophae rhamnoides* L.) cultivars. Turkish J. Agric. For. 38, 224–232. <https://doi.org/10.3906/tar-1304-86>
- Rupp, M.E., Fitzgerald, T., Marion, N., Helget, V., Puumala, S., Anderson, J.R., Fey, P.D., 2004. Effect of silver-coated urinary catheters: Efficacy, cost-effectiveness, and antimicrobial resistance. Am. J. Infect. Control 32, 445–450. <https://doi.org/10.1016/j.ajic.2004.05.002>
- Sadasivam, S., Manickam, A., 2008. Biochemical Methods, New Delhi, New Age International Publishers, 3rd ed. New Age International (P) Limited, Delhi.
- Saikia, M., Handique, P.J., 2013. Antioxidant and antibacterial activity of leaf, bark, pulp and seed extracts of seabuckthorn (*Hippophae salicifolia* D. Don) of Sikkim Himalayas. J. Med. Plants Res. 7, 1330–1338. <https://doi.org/10.5897/JMPR12.1123>
- Sajfrtová, M., Ličková, I., Wimmerová, M., Sovová, H., Wimmer, Z., 2010. β -sitosterol: Supercritical carbon dioxide extraction from sea buckthorn (*Hippophae rhamnoides* L.) seeds. Int. J. Mol. Sci. 11, 1842–1850. <https://doi.org/10.3390/ijms11041842>
- Sajfrtova, M., Sovova, H., 2012. Solute-matrix and solute-solute interactions during supercritical
-

-
- fluid extraction of sea buckthorn leaves, in: *Procedia Engineering*. Prague, Czech Republic, pp. 1682–1691. <https://doi.org/10.1016/j.proeng.2012.07.561>
- Salari, S., Bahabadi, S.E., Samzadeh-Kermani, A., Yosefzaei, F., 2018. In-vitro Evaluation of Antioxidant and Antibacterial Potential of Green Synthesized Silver Nanoparticles Using *Prosopis farcta* Fruit Extract. *Iran. J. Pharm. Res.* 18, 430–445.
- Samant, S.S., Dhar, U., Palni, L.M.S., 1998. Medicinal Plants of Indian Himalaya: Diversity, Distribution and Potential Value. G. B. Pant Inst. of Himalayan Environment and Development, Almora.
- Sarker, S.D., Nahar, L., Kumarasamy, Y., 2007. Microtitre plate-based antibacterial assay incorporating resazurin as an indicator of cell growth, and its application in the in vitro antibacterial screening of phytochemicals. *Methods* 42, 321–324. <https://doi.org/10.1016/j.ymeth.2007.01.006>
- Seifipour, R., Nozari, M., Pishkar, L., 2020. Green Synthesis of Silver Nanoparticles using *Tragopogon Collinus* Leaf Extract and Study of Their Antibacterial Effects. *J. Inorg. Organomet. Polym. Mater.* 30, 2926–2936. <https://doi.org/10.1007/s10904-020-01441-9>
- Sen, S., De, B., Devanna, N., Chakraborty, R., 2013. Total phenolic, total flavonoid content, and antioxidant capacity of the leaves of *Meyna spinosa* Roxb., an Indian medicinal plant. *Chin. J. Nat. Med.* 11, 149–157. [https://doi.org/10.1016/S1875-5364\(13\)60042-4](https://doi.org/10.1016/S1875-5364(13)60042-4)
- Sharma, B., Deswal, R., 2018. Single pot synthesized gold nanoparticles using *Hippophae rhamnoides* leaf and berry extract showed shape-dependent differential nanobiotechnological applications. *Artif. Cells, Nanomedicine Biotechnol.* 46, 408–418. <https://doi.org/10.1080/21691401.2018.1458034>
- Sharma, U.K., Sharma, K., Sharma, N., Sharma, A., Singh, H.P., Sinha, A.K., 2008. Microwave-
-

References

- assisted efficient extraction of different parts of *Hippophae rhamnoides* for the comparative evaluation of antioxidant activity and quantification of its phenolic constituents by reverse-phase high-performance liquid chromatography (RP-HPLC). *J. Agric. Food Chem.* 56, 374–379. <https://doi.org/10.1021/jf072510j>
- Shi, J., Mittal, G., Kim, E., Xue, S.J., 2007. Solubility of carotenoids in supercritical CO₂. *Food Rev. Int.* 23, 341–371. <https://doi.org/10.1080/87559120701593806>
- Siakavella, I.K., Lamari, F., Papoulis, D., Orkoula, M., Gkolfi, P., Lykouras, M., Avgoustakis, K., Hatziantoniou, S., 2020. Effect of plant extracts on the characteristics of silver nanoparticles for topical application. *Pharmaceutics* 12, 1–17. <https://doi.org/10.3390/pharmaceutics12121244>
- Singh, A., Sharma, B., Deswal, R., 2018. Green silver nanoparticles from novel Brassicaceae cultivars with enhanced antimicrobial potential than earlier reported Brassicaceae members. *J. Trace Elem. Med. Biol.* 47, 1–11. <https://doi.org/10.1016/j.jtemb.2018.01.001>
- Singh, A.K., Deep, P., Dubey, S., Attrey, D.P., Naved, T., 2014. Comparative studies on antioxidant activity, total phenol content and high performance thin layer chromatography analysis of seabuckthorn (*hippophae rhamnoides* l) leaves. *Pharmacogn. J.* 6, 5–8. <https://doi.org/10.5530/pj.2014.5.2>
- Singh, I.P., Ahmad, F., Gore, D.D., Tikoo, K., Bansal, A., Jachak, S.M., Jena, G., 2019. Therapeutic potential of seabuckthorn: a patent review (2000-2018). *Expert Opin. Ther. Pat.* 29, 733–744. <https://doi.org/10.1080/13543776.2019.1648434>
- Sivakumar, P., Nethradevi, C., Renganathan, S., 2012. Synthesis of silver nanoparticles using *Lantana camara* fruit extract and its effect on pathogens. *Asian J. Pharm. Clin. Res.* 5, 97–101.
-

-
- Šne, E., Galoburda, R., Segliņa, D., 2013a. Sea buckthorn vegetative parts - A good source of bioactive compounds. *Proc. Latv. Acad. Sci. Sect. B Nat. Exact, Appl. Sci.* 67, 101–108. <https://doi.org/10.2478/prolas-2013-0016>
- Šne, E., Segliņa, D., Galoburda, R., Krasnova, I., 2013b. Content of phenolic compounds in various sea buckthorn parts. *Proc. Latv. Acad. Sci. Sect. B Nat. Exact, Appl. Sci.* 67, 411–415. <https://doi.org/10.2478/prolas-2013-0073>
- Solana, M., Boschiero, I., Dall'Acqua, S., Bertucco, A., 2014. Extraction of bioactive enriched fractions from *Eruca sativa* leaves by supercritical CO₂ technology using different co-solvents. *J. Supercrit. Fluids* 94, 245–251. <https://doi.org/10.1016/j.supflu.2014.08.022>
- Song, J.Y., Kim, B.S., 2009. Rapid biological synthesis of silver nanoparticles using plant leaf extracts. *Bioprocess Biosyst. Eng.* 32, 79–84. <https://doi.org/10.1007/s00449-008-0224-6>
- Song, L., Liu, P., Yan, Y., Huang, Y., Bai, B., Hou, X., Zhang, L., 2019. Supercritical CO₂ fluid extraction of flavonoid compounds from Xinjiang jujube (*Ziziphus jujuba* Mill.) leaves and associated biological activities and flavonoid compositions. *Ind. Crops Prod.* 139. <https://doi.org/10.1016/j.indcrop.2019.111508>
- Stobdan, T., Chaurasia, O.P., Korekar, G., Mundra, S., Ali, Z., Yadav, A., Singh, S.B., 2010. Attributes of Seabuckthorn (*Hippophae rhamnoides* L.) to Meet Nutritional Requirements in High Altitude. *Def. Sci. J.* 60, 226–230.
- Stobdan, T., Ladakh, L., Korekar, G., Biotech, C., Chaurasia, O.P., Organisation, D., Yadav, A., 2011a. Seabuckthorn Production for Greening and Sustainable Income.
- Stobdan, T., Phunchok, T., 2021. Value chain analysis of SEABUCKTHORN (*Hippophae rhamnoides* L.) in Leh Ladakh. *Leh Ladakh, Jammu & Kashmir*.
- Stobdan, T., Yadav, A., Mishra, G.P., Chaurasia, O.P., Srivastava, R.B., 2011b. Seabuckthorn :
-

References

- The Super Plant. Def. Inst. High Alt. Res. Def. Res. Dev. Organ.
- Sytařová, I., Orsavová, J., Snopek, L., Mlček, J., Byczyński, Ł., Mišurcová, L., 2020. Impact of phenolic compounds and vitamins C and E on antioxidant activity of sea buckthorn (*Hippophaë rhamnoides* L.) berries and leaves of diverse ripening times. *Food Chem.* 310. <https://doi.org/10.1016/j.foodchem.2019.125784>
- Tang, X., Tigerstedt, P.M.A., 2001. Variation of physical and chemical characters within an elite sea buckthorn (*Hippophaë rhamnoides* L.) breeding population. *Sci. Hortic.* 88 88, 203–214.
- Tian, Y., Liimatainen, J., Alanne, A.-L., Lindstedt, A., Liu, P., Sinkkonen, J., Kallio, H., Yang, B., 2017. Phenolic compounds extracted by acidic aqueous ethanol from berries and leaves of different berry plants. *Food Chem.* 220, 266–281. <https://doi.org/10.1016/j.foodchem.2016.09.145>
- Tian, Y., Pukanen, A., Alakomi, H.-L., Uusitupa, A., Saarel, M., Yanga, B., 2018. Antioxidative and antibacterial activities of aqueous ethanol extracts of berries, leaves, and branches of berry plants. *Food Res. Int.* 106, 291–303. <https://doi.org/10.1016/j.foodres.2017.12.071>
- Tiller, M.B., Oswald, B.P., Schuijn, M., 2020. Preliminary Flammability Assessment of Sea Buckthorn from The Netherlands Compared to Known Flammable Shrubs of the Southern and Western. *J. For. Res.* 9, 1–6.
- Ting, H.C., Hsu, Y.W., Tsai, C.F., Lu, F.J., Chou, M.C., Chen, W.K., 2011. The in vitro and in vivo antioxidant properties of seabuckthorn (*Hippophaë rhamnoides* L.) seed oil. *Food Chem.* 125, 652–659. <https://doi.org/10.1016/j.foodchem.2010.09.057>
- Upadhyay, N.K., Kumar, M.S.Y., Gupta, A., 2010. Antioxidant, cytoprotective and antibacterial effects of Sea buckthorn (*Hippophaë rhamnoides* L.) leaves. *Food Chem. Toxicol.* 48, 3443–3448. <https://doi.org/10.1016/j.fct.2010.09.019>
-

-
- Upadhyay, N.K., Kumar, R., Mandotra, S.K., Meena, R.N., Siddiqui, M.S., Sawhney, R.C., Gupta, A., 2009. Safety and healing efficacy of Sea buckthorn (*Hippophae rhamnoides* L.) seed oil on burn wounds in rats. *Food Chem. Toxicol.* 47, 1146–1153. <https://doi.org/10.1016/j.fct.2009.02.002>
- Valadez-Carmona, L., Ortiz-Moreno, A., Ceballos-Reyes, G., Mendiola, J.A., Ibáñez, E., 2018. Valorization of cacao pod husk through supercritical fluid extraction of phenolic compounds. *J. Supercrit. Fluids* 131, 99–105. <https://doi.org/10.1016/j.supflu.2017.09.011>
- ValleS, J.M. del, BelloJ, ThielA, AllenL, Chordia, 2000. Comparison of conventional and supercritical CO₂-extracted rosehip oil. *Brazilian J. Chem. Eng.* 17, 335–348. <https://doi.org/10.1590/S0104-66322000000300010>
- Veggi, P.C., Prado, J.M., Bataglion, G.A., Eberlin, M.N., Meireles, M.A.A., 2014. Obtaining phenolic compounds from jatoba (*Hymenaea courbaril* L.) bark by supercritical fluid extraction. *J. Supercrit. Fluids* 89, 68–77. <https://doi.org/10.1016/j.supflu.2014.02.016>
- Vilas-Franquesa, A., Saldo, J., Juan, B., 2020. Potential of sea buckthorn-based ingredients for the food and feed industry – a review. *Food Prod. Process. Nutr.* 2. <https://doi.org/10.1186/s43014-020-00032-y>
- Volli, V., Purkait, M.K., 2014. Physico-chemical properties and thermal degradation studies of commercial oils in nitrogen atmosphere. *Fuel* 117, 1010–1019. <https://doi.org/10.1016/j.fuel.2013.10.021>
- Vuorinen, A.L., Markkinen, N., Kalpio, M., Linderborg, K.M., Yang, B., Kallio, H.P., 2015. Effect of growth environment on the gene expression and lipids related to triacylglycerol biosynthesis in sea buckthorn (*Hippophaë rhamnoides*) berries. *Food Res. Int.* 77, 608–619. <https://doi.org/10.1016/j.foodres.2015.08.023>
-

References

- Xiangqun Gao, Maria Ohlander, Niklas Jeppsson, Lars Bjork, and V.T., 2000. Changes in antioxidant effects and their relationship to phytonutrients in fruits of sea buckthorn (*Hippophae rhamnoides* L.) during maturation. *J. Agric. Food Chem.* 48, 1485–1490. <https://doi.org/10.1021/jf991072g>
- Xu, X., Gao, Y., Liu, G., Wang, Q., Zhao, J., 2008. Optimization of supercritical carbon dioxide extraction of sea buckthorn (*Hippophaë rhamnoides* L.) oil using response surface methodology. *LWT - Food Sci. Technol.* 41, 1223–1231. <https://doi.org/10.1016/j.lwt.2007.08.002>
- Yang, B., Kallio, H., 2002. Composition and physiological effects of sea buckthorn (*Hippophaë*) lipids. *Trends Food Sci. Technol.* 13, 160–167. [https://doi.org/10.1016/S0924-2244\(02\)00136-X](https://doi.org/10.1016/S0924-2244(02)00136-X)
- Yang, B., Kallio, H.P., 2001. Fatty acid composition of lipids in sea buckthorn (*Hippophaë rhamnoides* L.) berries of different origins. *J. Agric. Food Chem.* 49, 1939–1947. <https://doi.org/10.1021/jf001059s>
- Yao, Y., A., P.M., Tigerstedt, Joy, P., 1992. Variation of Vitamin C Concentration and Character Correlation between and within Natural Sea Buckthorn (*Hippophae rhamnoides* L.) Populations. *Acta Agric. Scand.* 42, 12–17.
- Zadernowski, R., Naczka, M., Amarowicz, R., 2003. Tocopherols in Sea Buckthorn (*Hippophaë rhamnoides* L.) Berry Oil. *JAOCs* 80, 5–8.
- Zadernowski, R., Naczka, M., Czaplicki, S., Rubinskiene, M., Szalkiewicz, M., 2005. Composition of phenolic acids in sea buckthorn (*Hippophae rhamnoides* L.) berries. *J. Am. Oil Chem. Soc.* 82, 175–179. <https://doi.org/10.1007/s11746-005-5169-1>
- Zakynthinos, G., Varzakas, T., Petsios, D., 2016. Sea Buckthorn (*Hippophae Rhamnoides*) Lipids
-

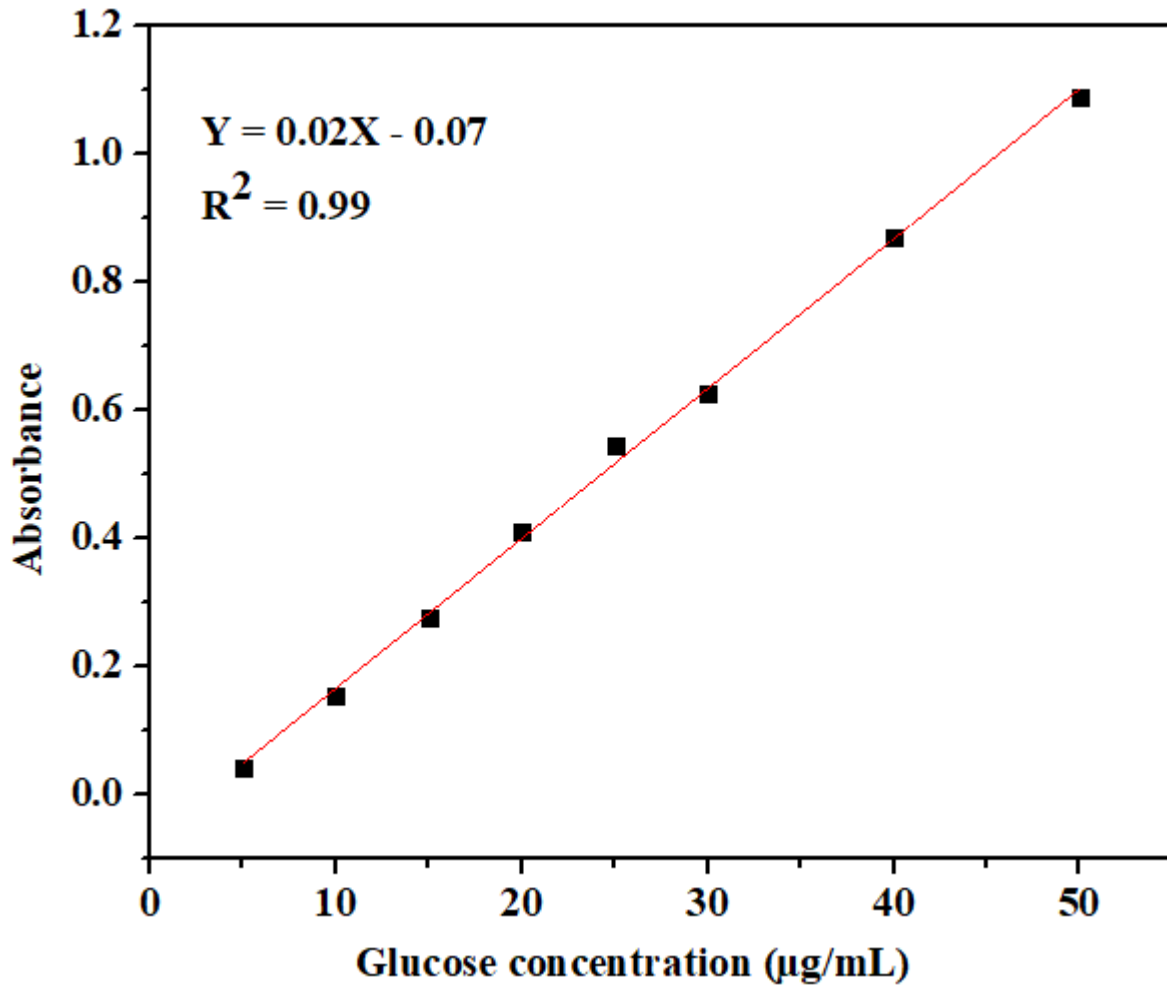
-
- and their Functionality on Health Aspects. *Curr. Res. Nutr. Food Sci. J.* 4, 182–194.
<https://doi.org/10.12944/CRNFSJ.4.3.04>
- Zeb, A., Ullah, S., 2015. Sea buckthorn seed oil protects against the oxidative stress produced by thermally oxidized lipids. *Food Chem.* 186, 6–12.
<https://doi.org/10.1016/j.foodchem.2015.03.053>
- Zheng, L., Shi, L.-K., Zhao, C.-W., Jin, Q.-Z., Wang, X.-G., 2017. Fatty acid, phytochemical, oxidative stability and in vitro antioxidant property of sea buckthorn (*Hippophaë rhamnoides* L.) oils extracted by supercritical and subcritical technologies. *LWT - Food Sci. Technol.* 86, 507–513. <https://doi.org/10.1016/j.lwt.2017.08.042>
- Zielińska, A., Nowak, I., 2017. Abundance of active ingredients in sea-buckthorn oil. *Lipids Health Dis.* 16, 1–11. <https://doi.org/10.1186/s12944-017-0469-7>
- Zulkafli, Z.D., Wang, H., Miyashita, F., Utsumi, N., Tamura, K., 2014. Cosolvent-modified supercritical carbon dioxide extraction of phenolic compounds from bamboo leaves (*Sasa palmata*). *J. Supercrit. Fluids* 94, 123–129. <https://doi.org/10.1016/j.supflu.2014.07.008>
-





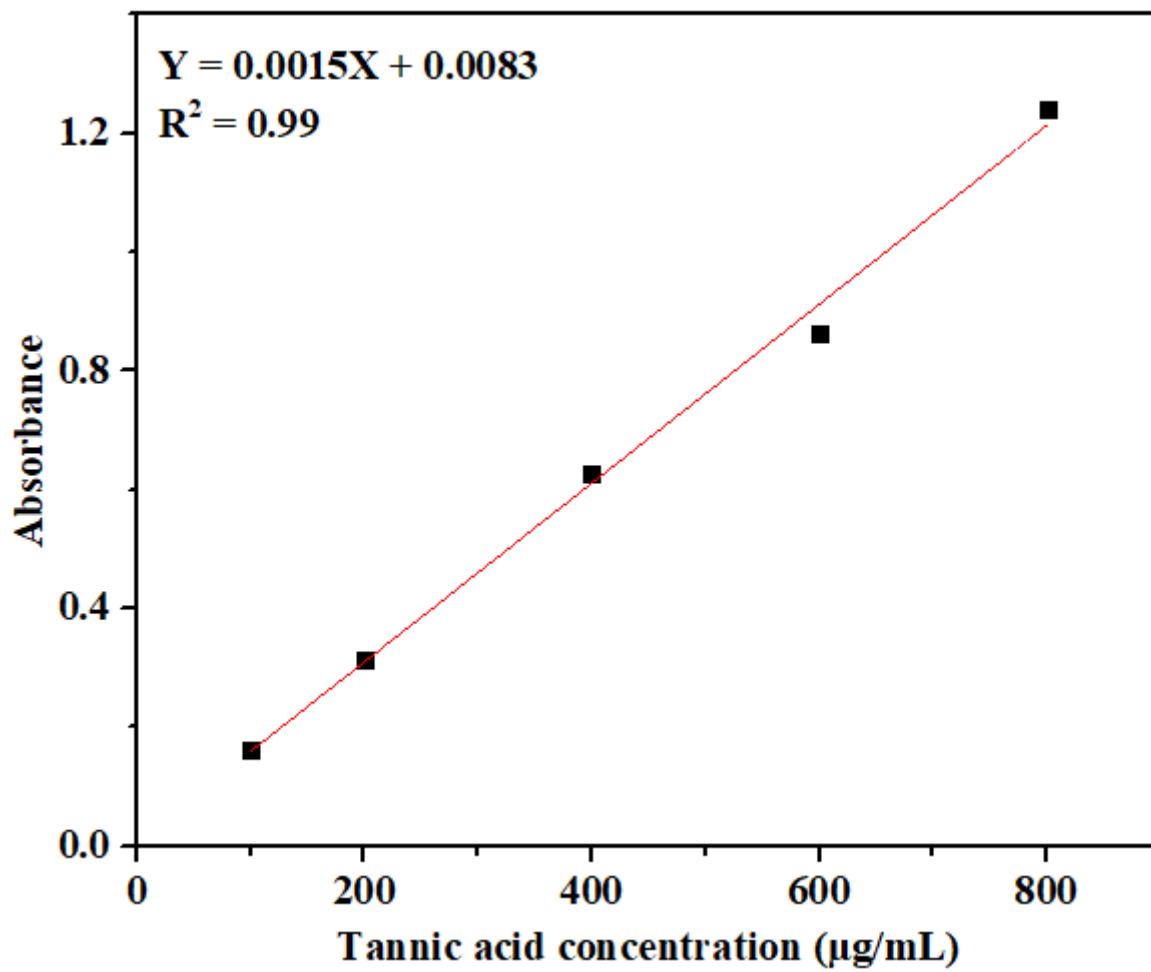
APPENDIX

Appendix 1



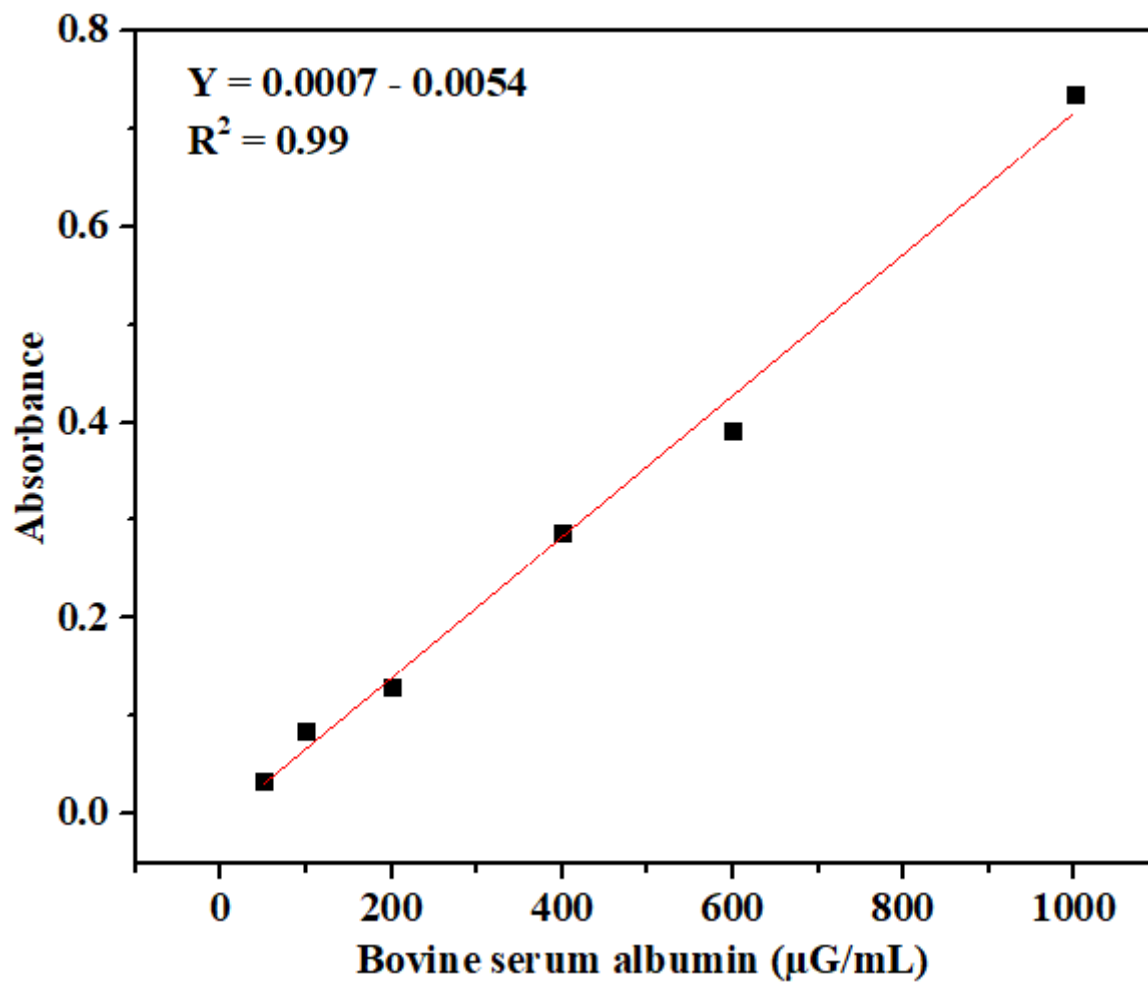
Standard Glucose Calibration Curve

Appendix 2



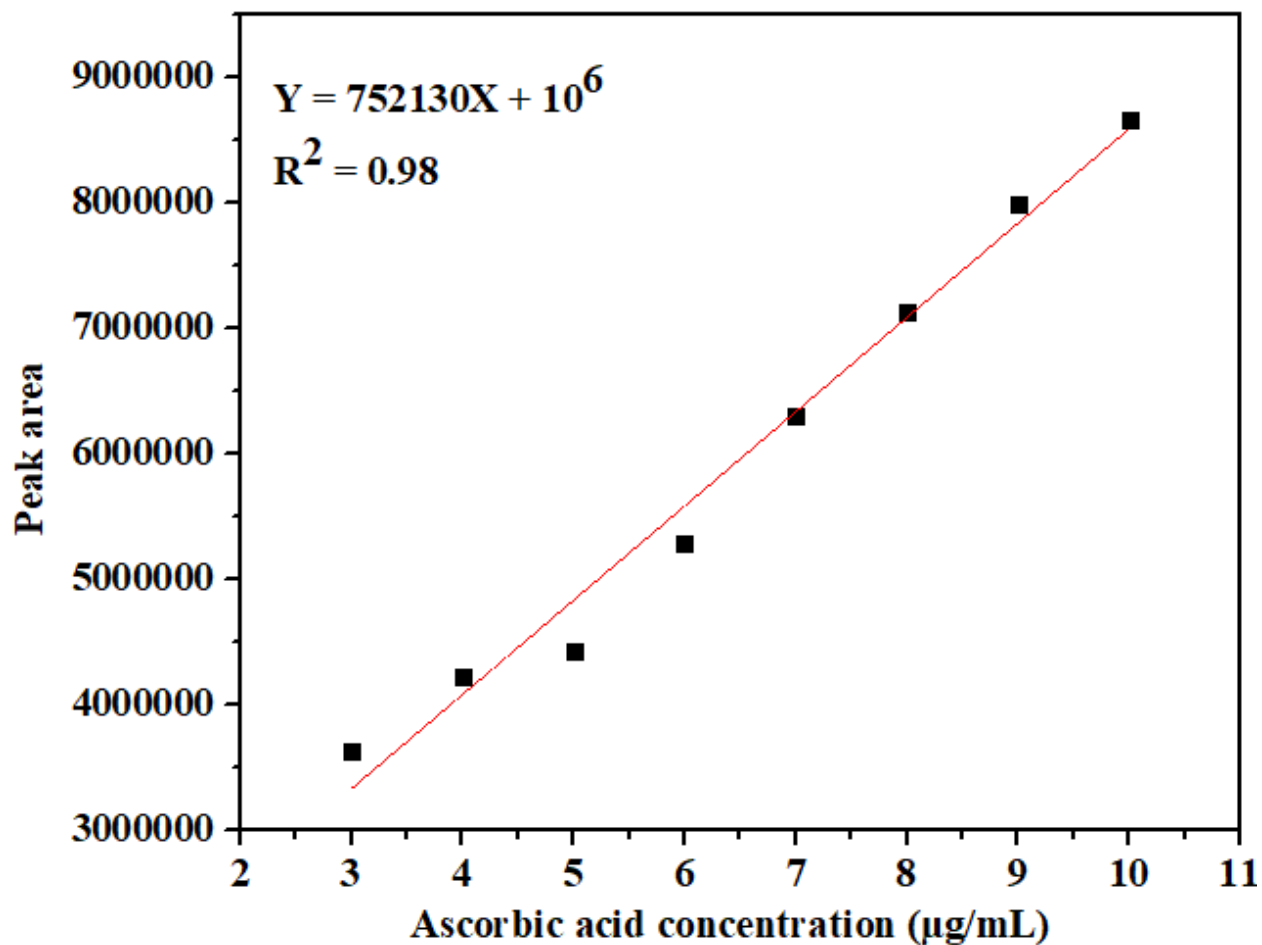
Standard Tannic Acid Calibration Curve

Appendix 3



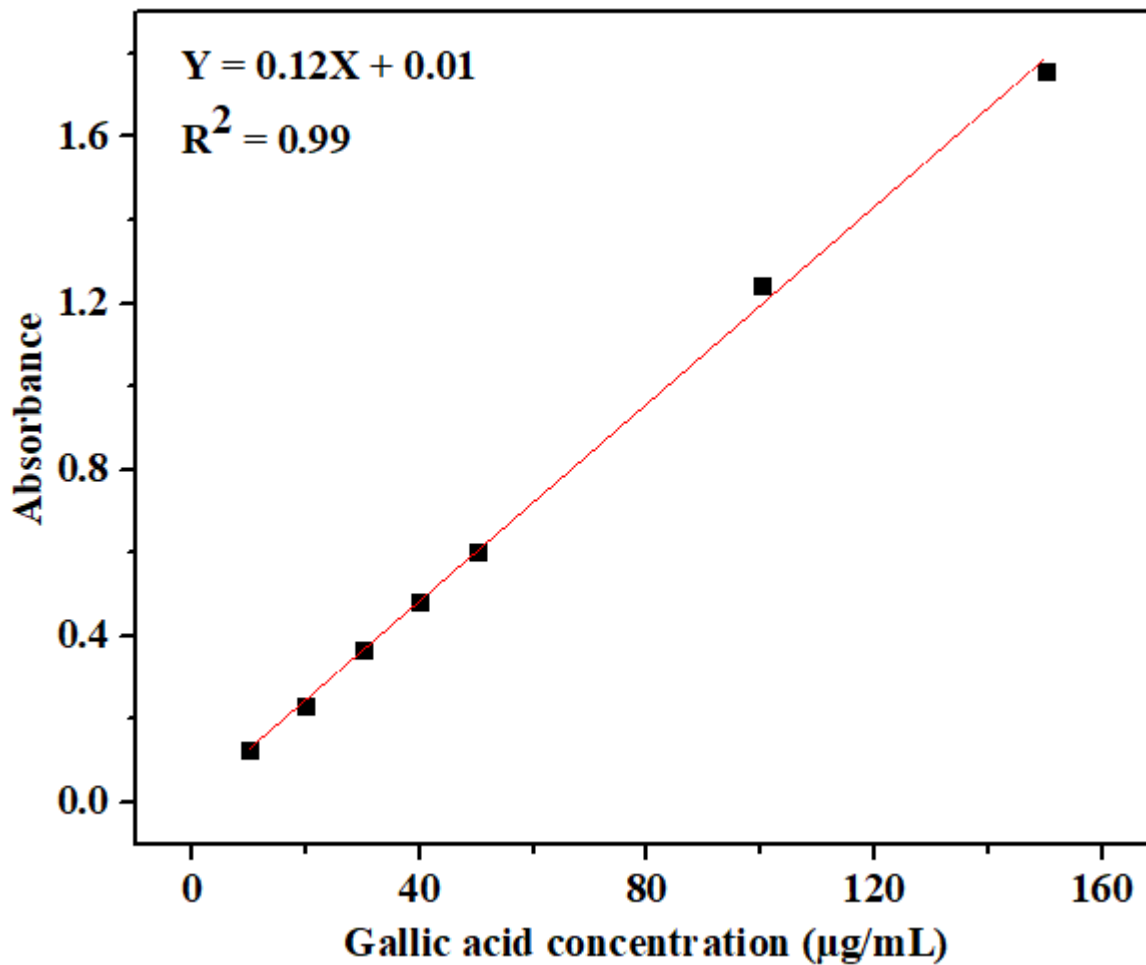
Standard Bovine Serum Albumin Calibration Curve

Appendix 4



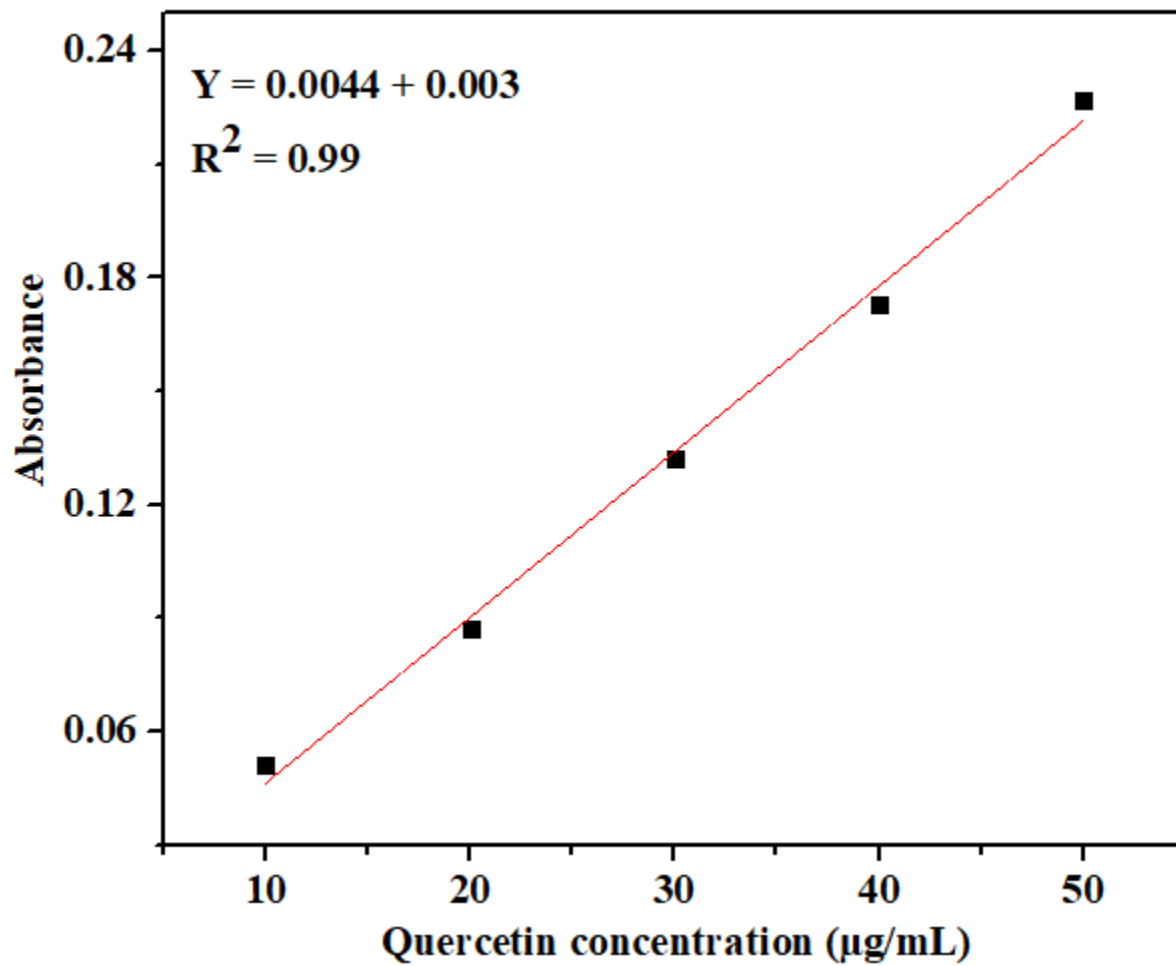
Standard Ascorbic Acid Calibration Curve

Appendix 5



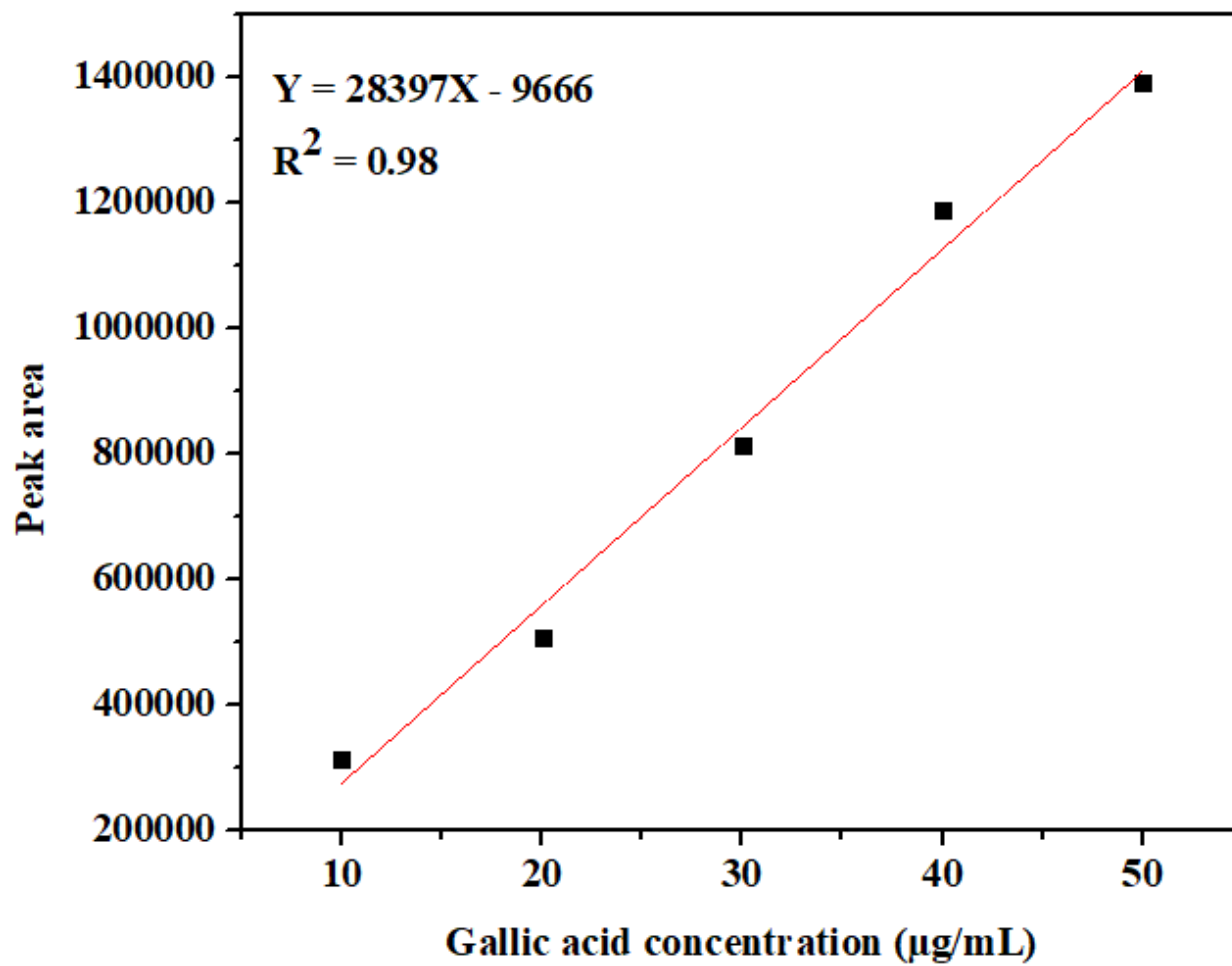
Standard Gallic Acid Calibration Curve

Appendix 6



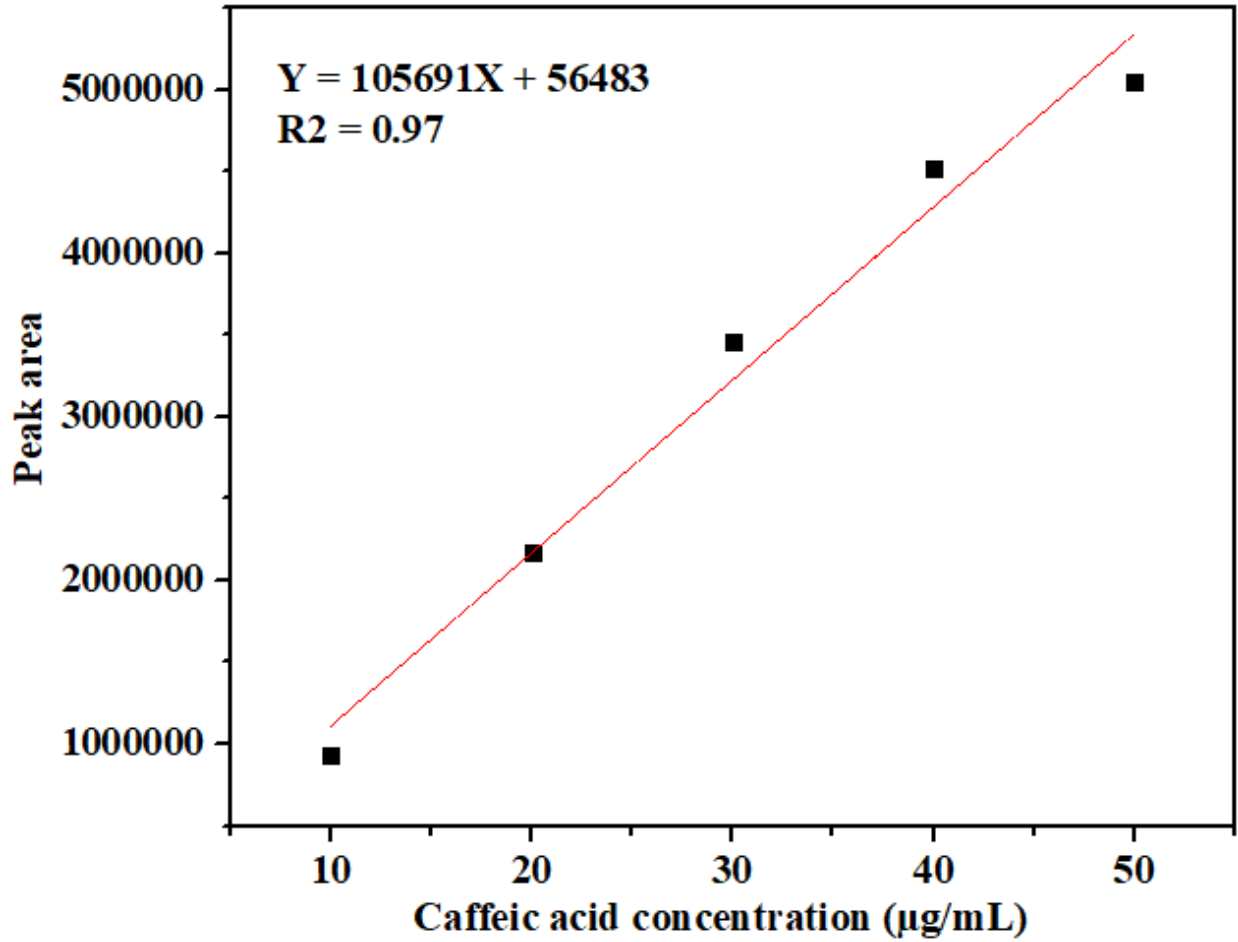
Standard Quercetin Calibration Curve

Appendix 7



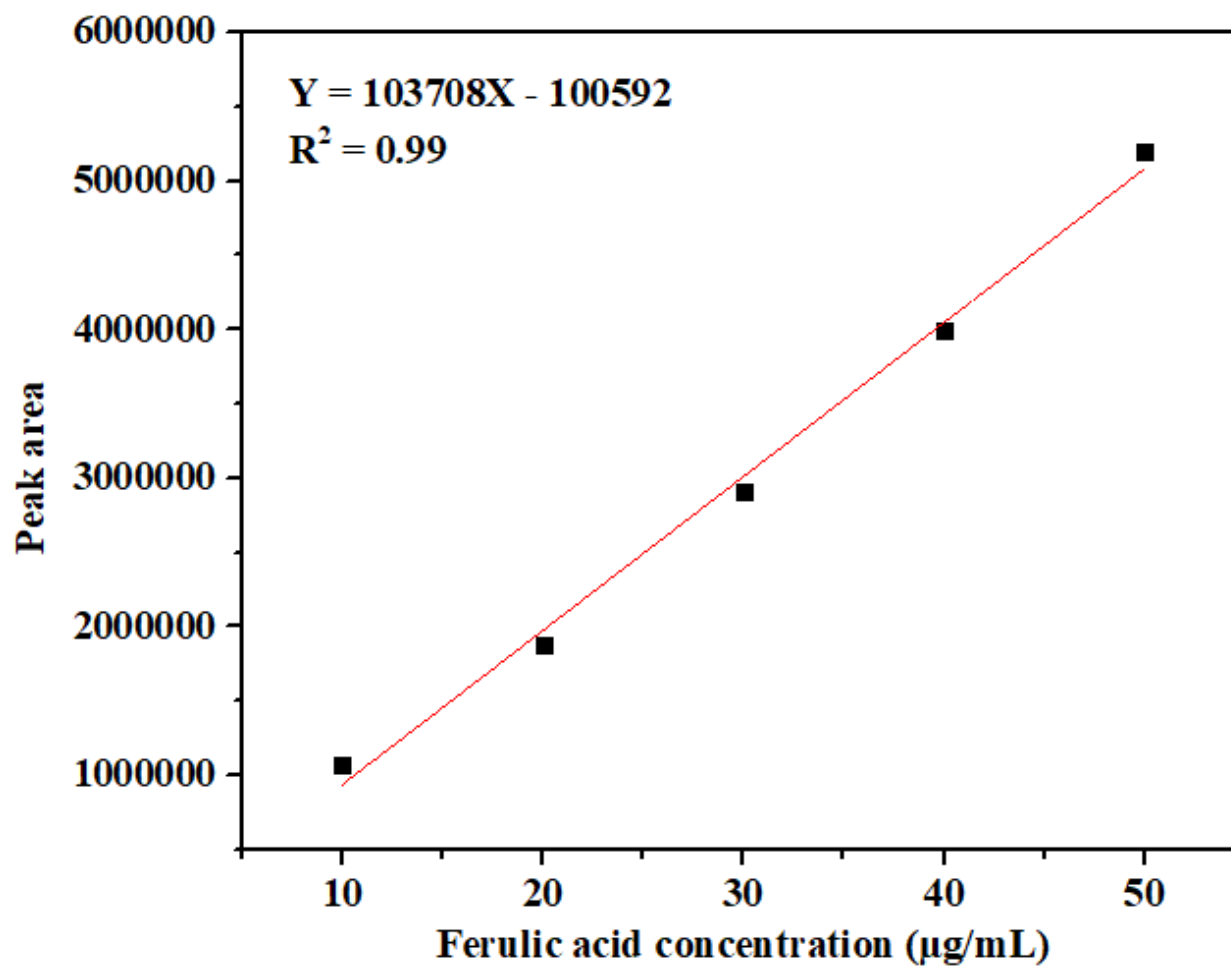
Standard Gallic Acid Calibration Curve

Appendix 8



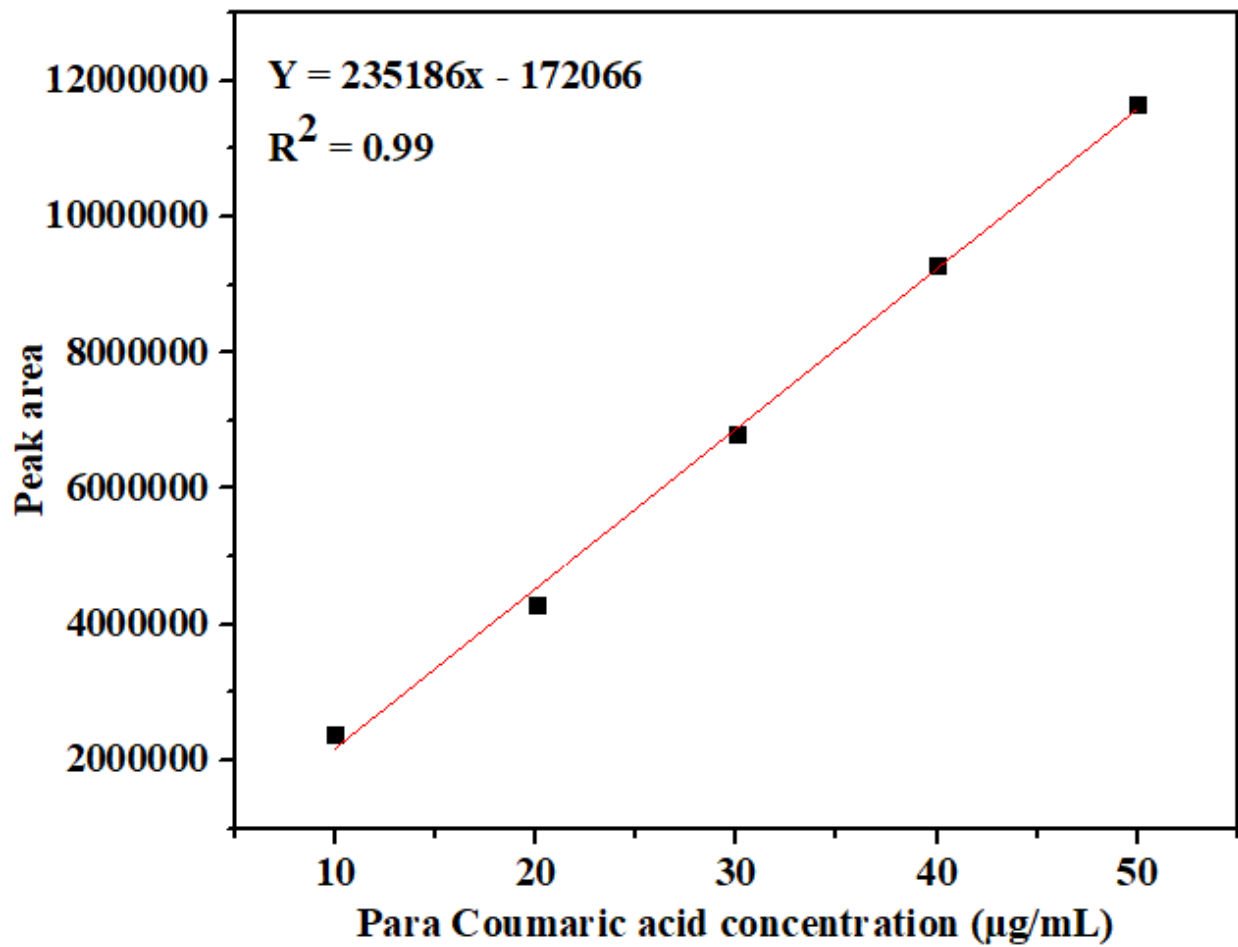
Standard Gallic Acid Calibration Curve

Appendix 9



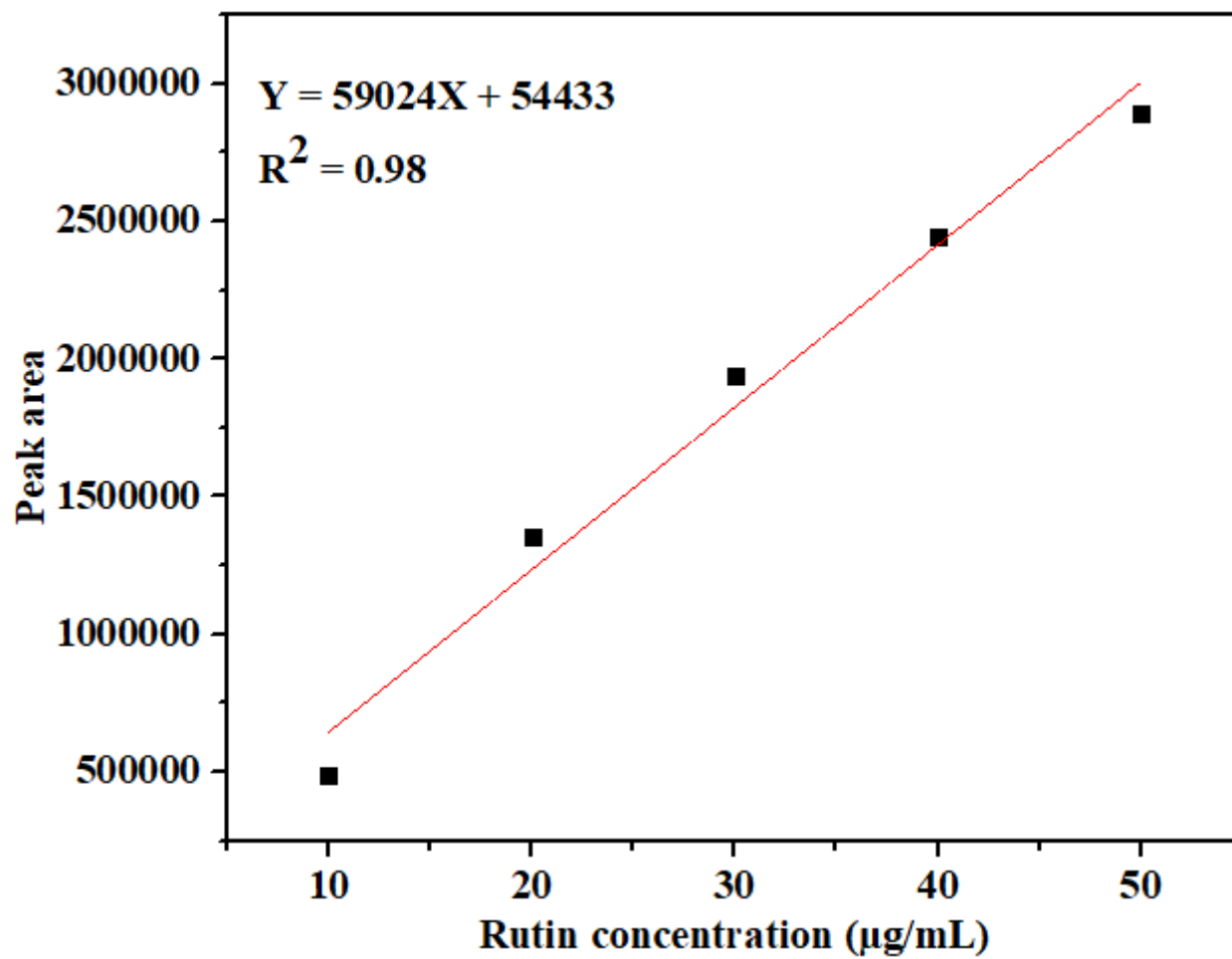
Standard Ferulic Acid Calibration Curve

Appendix 10



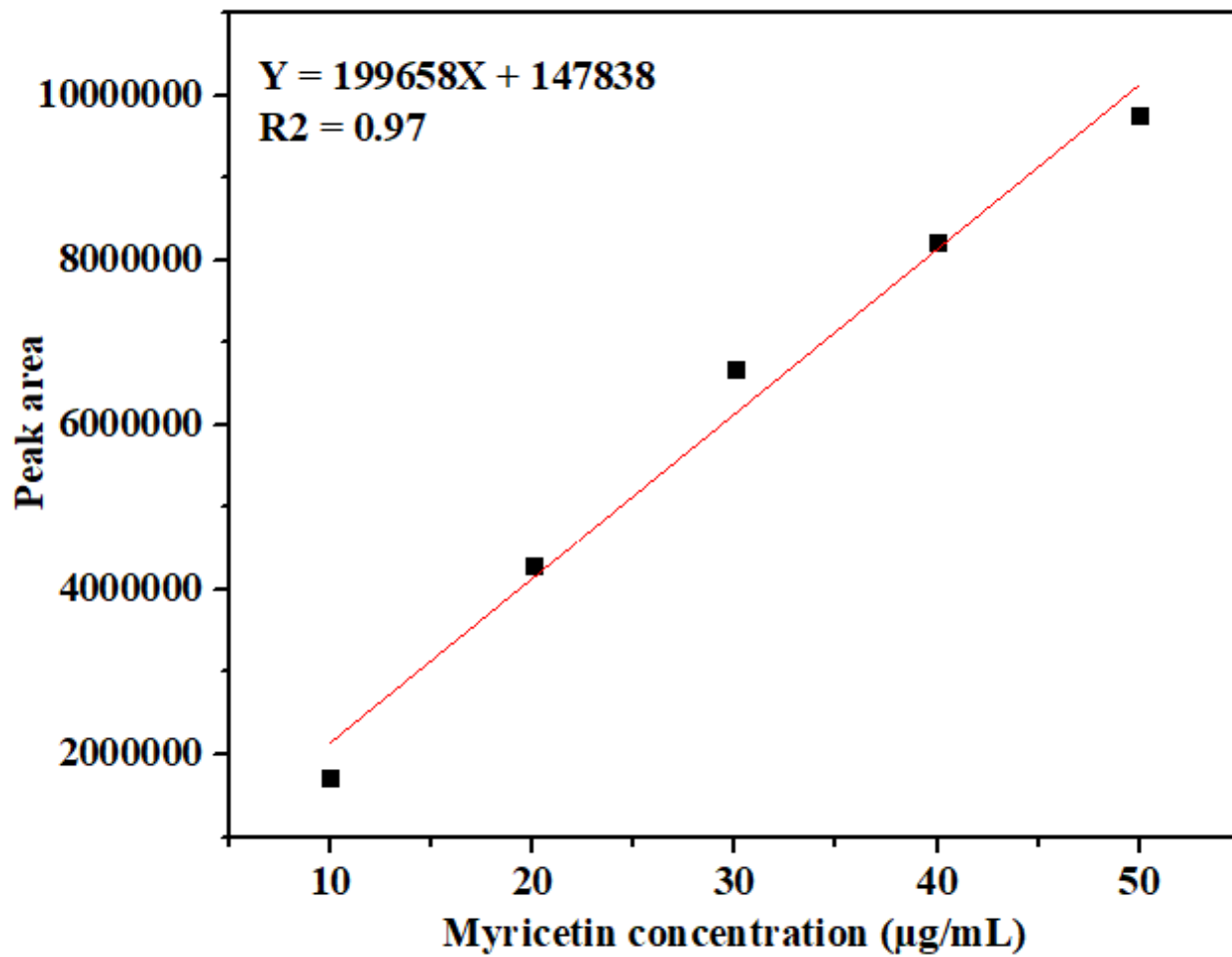
Standard Para Coumaric Acid Calibration Curve

Appendix 11



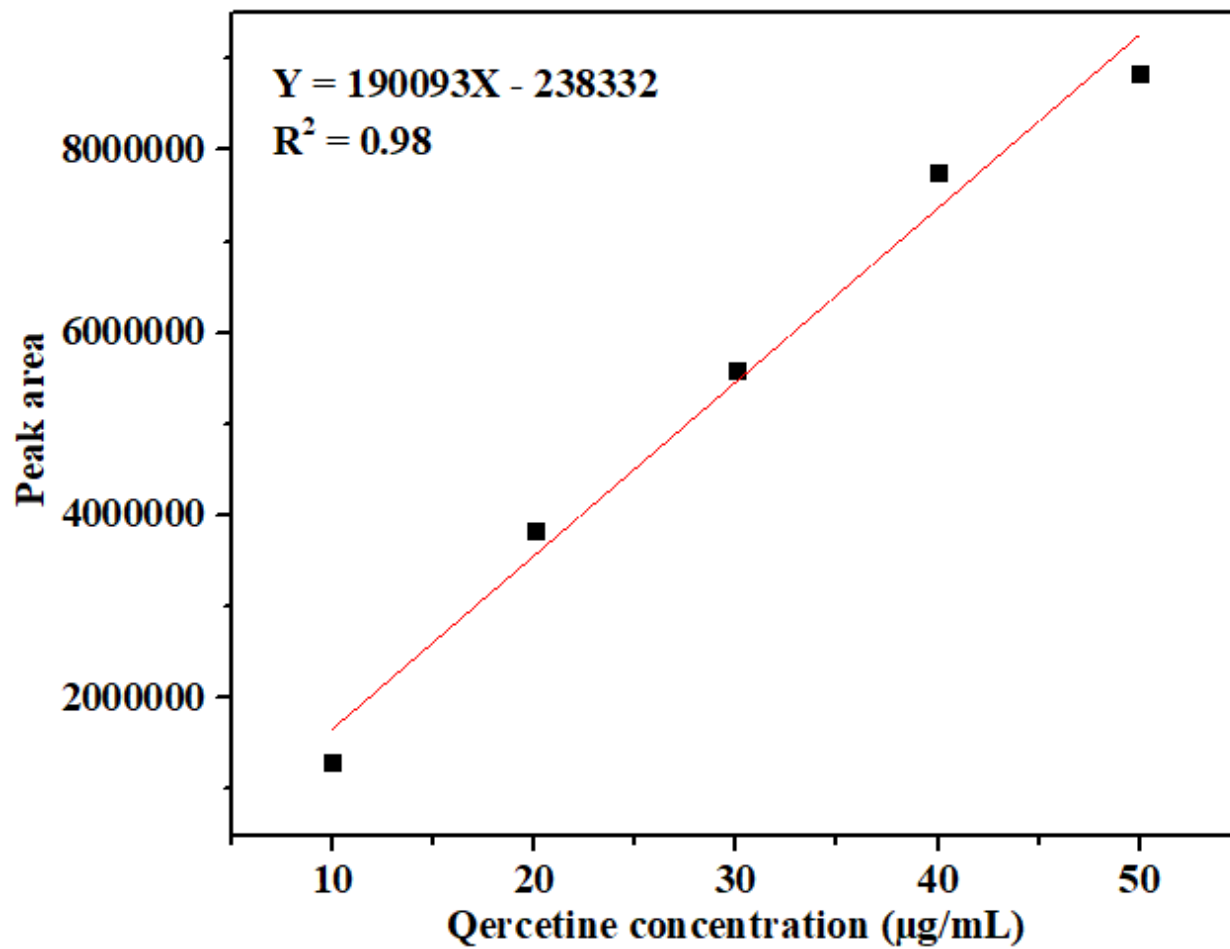
Standard Rutine Calibration Curve

Appendix 12



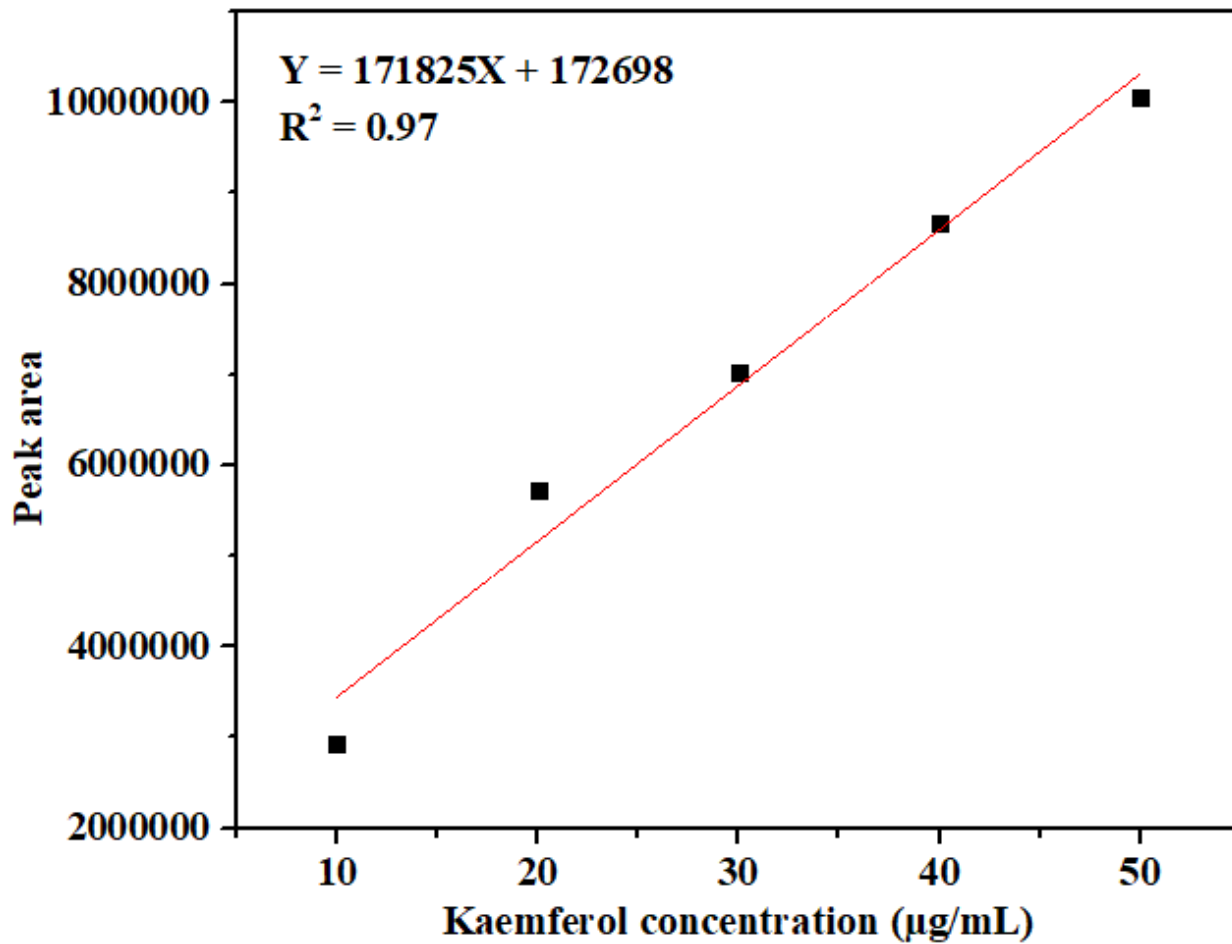
Standard Myricetin Calibration Curve

Appendix 13



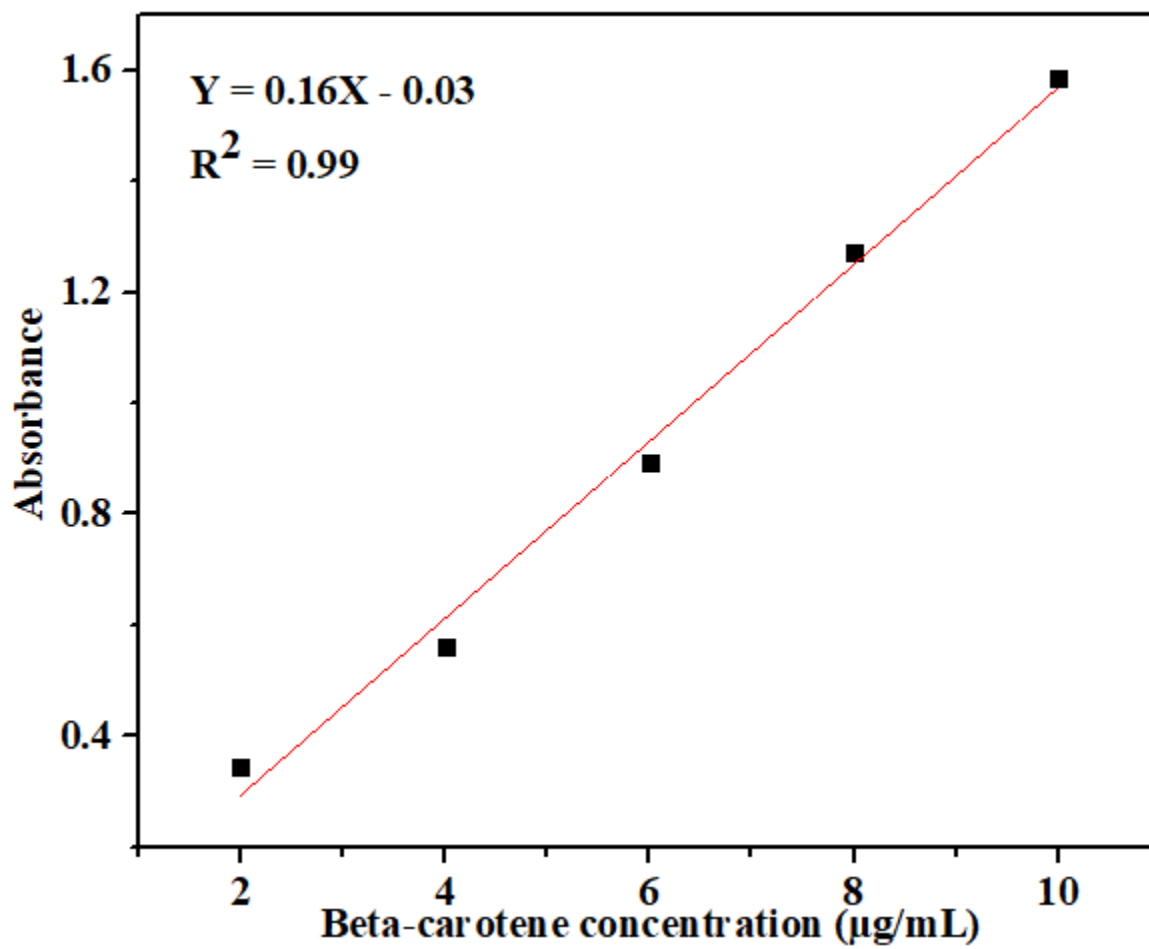
Standard Qercetine Calibration Curve

Appendix 14



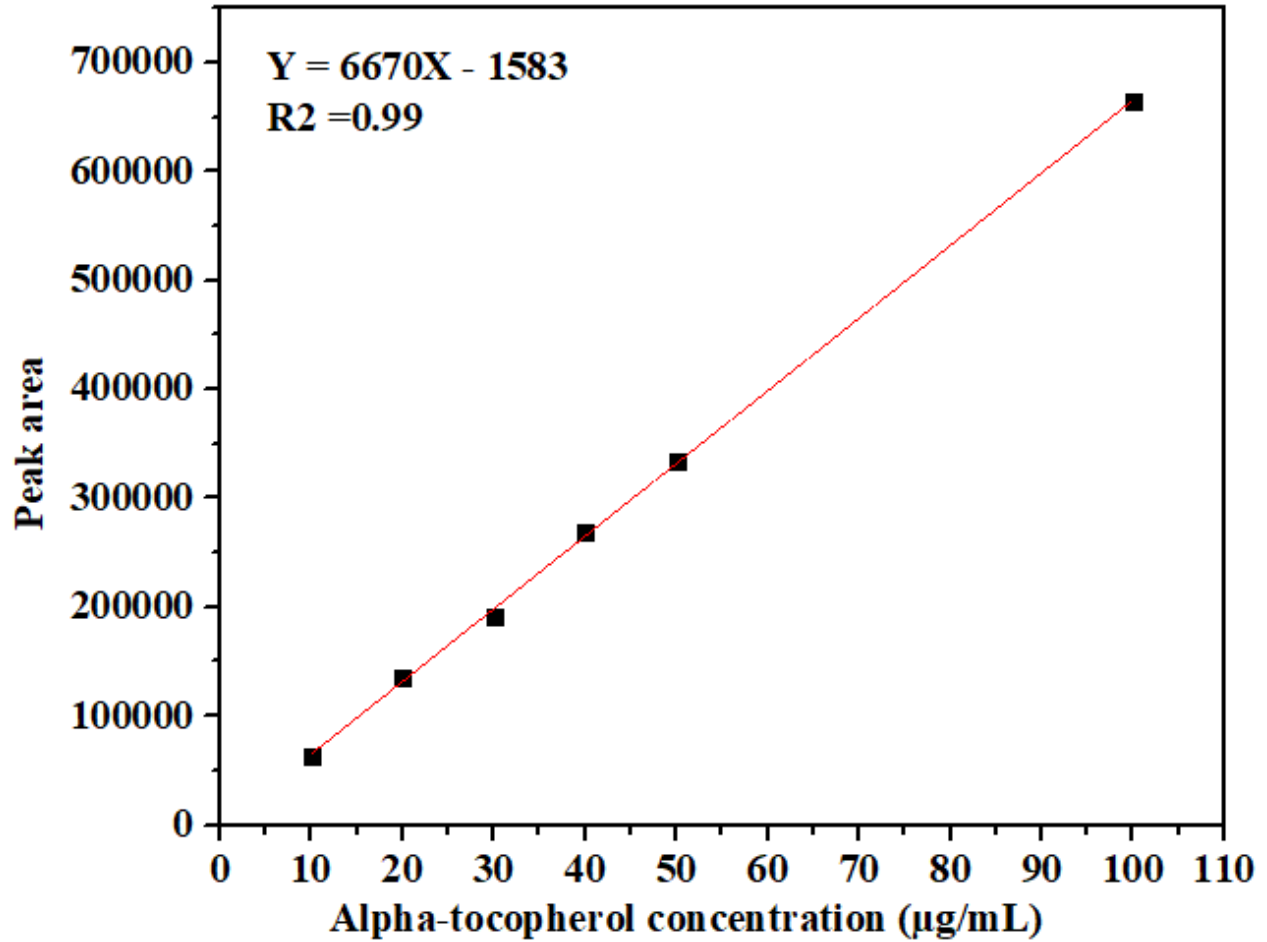
Standard Kaemferol Calibration Curve

Appendix 15



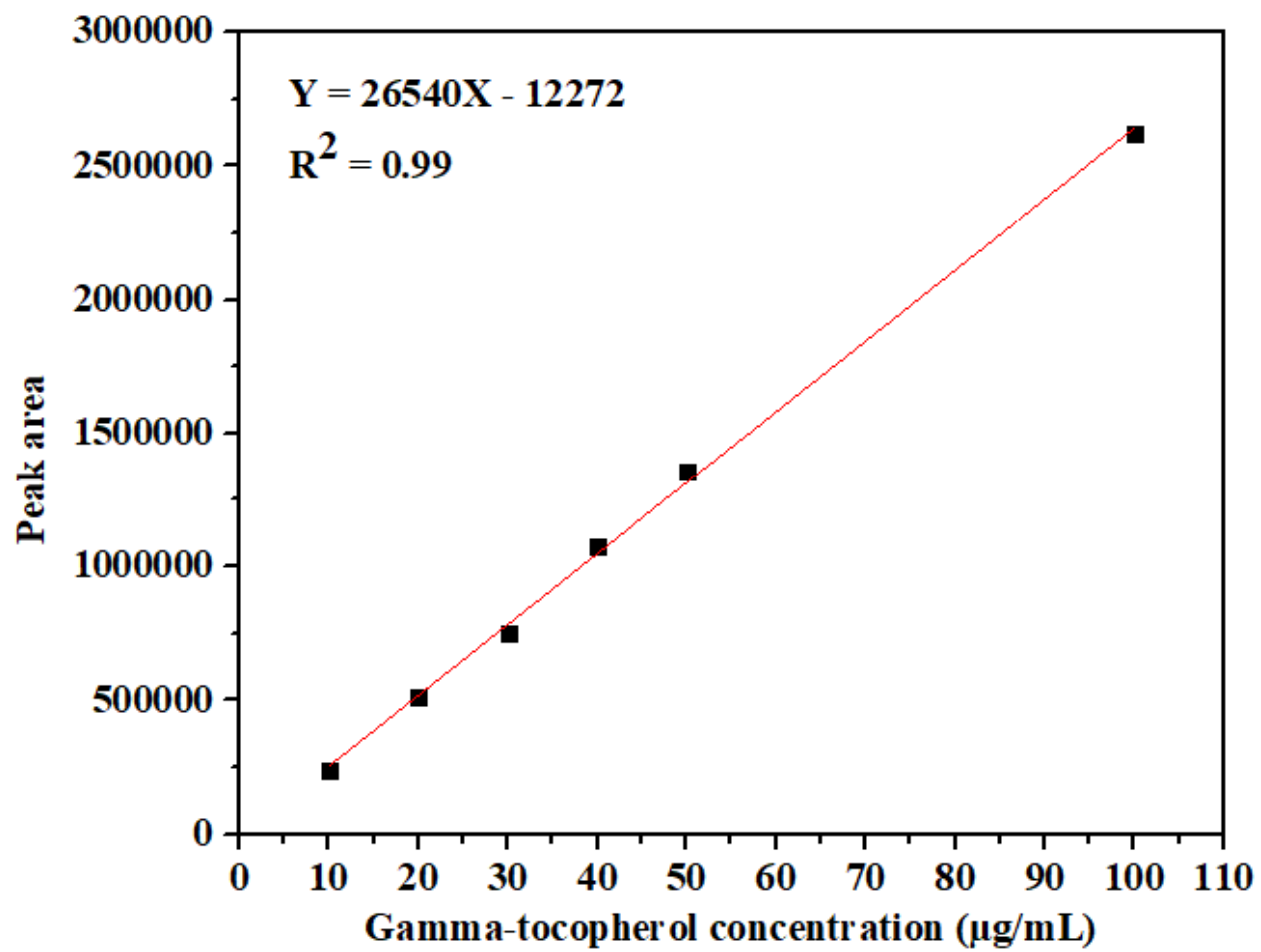
Standard Beta-carotene Calibration Curve

Appendix 16



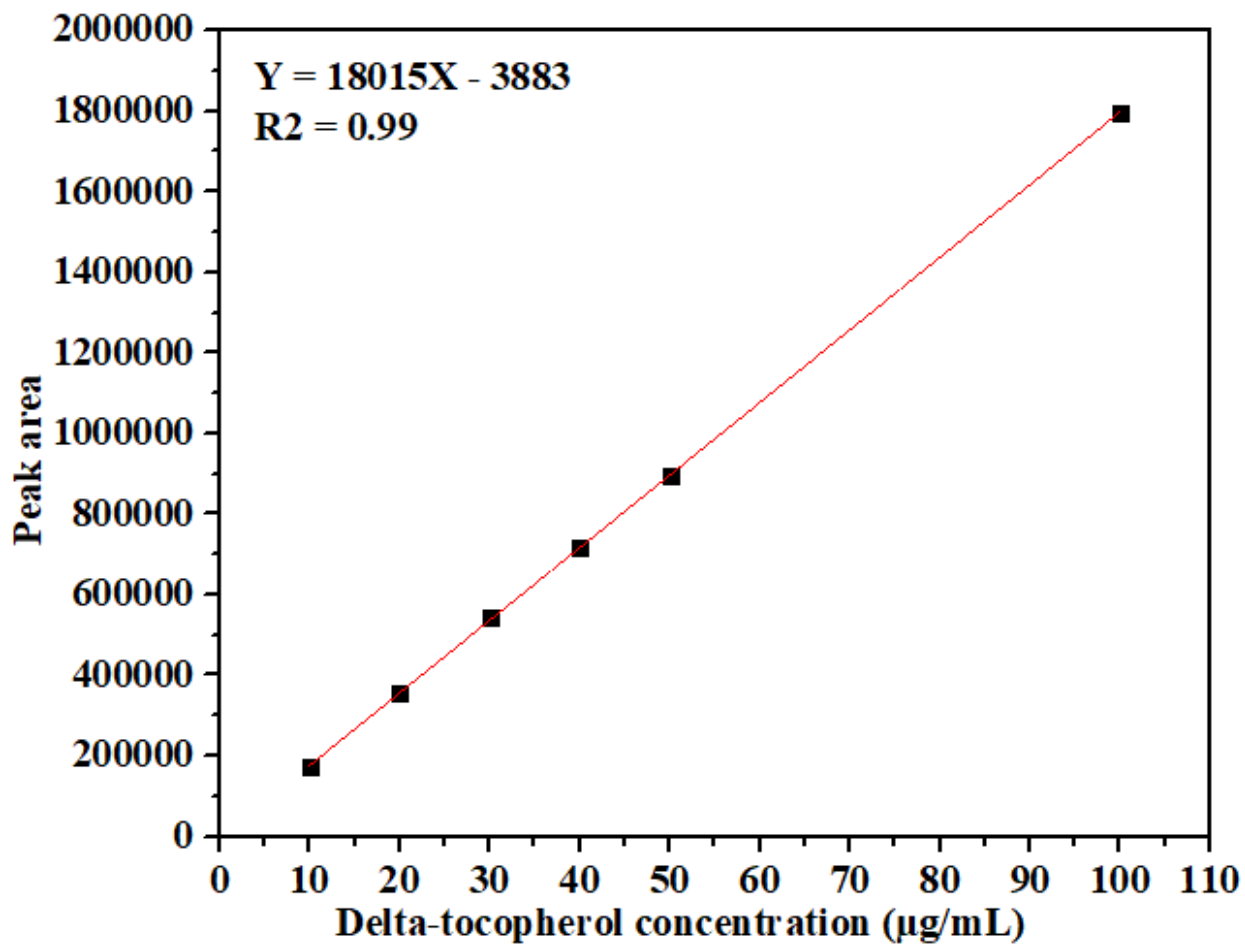
Standard Alpha-tocopherol Calibration Curve

Appendix 17



Standard Gamma-tocopherol Calibration Curve

Appendix 18



Standard Delta-tocopherol Calibration Curve

Research Output

A. Journal publications

- 1) Abebe Moges, Chitta Ranjan Barik, Sukumar Purohit, Vaibhav V. Goud, (2021), Dietary and bioactive properties of the berries and leaves from the underutilized *Hippophae salicifolia* D. Don grown in Northeast India, Journal of food science and biotechnology, 30(12):1555–1569
- 2) Abebe Moges, Chitta Ranjan Barik, Lingaraj Sahoo, Vaibhav V. Goud, (2022) Response surface methodology for optimization of supercritical CO₂ extraction of phenolic compounds from Sea buckthorn leaf, 3 Biotech 12(11):292
- 3) Abebe Moges, Vaibhav V. Goud, Process optimization and characterization of supercritical carbon dioxide extracted oil from *Hippophae salicifolia* D. Don berries, Supercritical fluids, (Manuscript ready to communicate)
- 4) Abebe Moges, Vaibhav V. Goud, (2022), Optimization and characterization of silver nanoparticles synthesized from *Hippophae salicifolia* D. Don and evaluation of in vitro antioxidant and antibacterial activities, Journal of Inorganic Chemistry Communications, 146.

B. Conference

- 1) Abebe Moges Tadesse, Chitta Ranjan Barik, Vaibhav V. Goud, Physicochemical and phytochemical analysis of Sea Buckthorn berries, Technological Innovations for Integration of Food and Health, A focus on North-Eastern India, February 14-16, 2019, Tezpur University, Tezpur, Assam, India.
- 2) Abebe Moges Tadesse, Chitta Ranjan Barik, Sukumar Purohit, Vaibhav V. Goud, Antioxidant and antimicrobial properties of successive extractives of sea buckthorn

(*Hippophae salicifolia* D. Don) berry, 3rd National Conference of Sea Buckthorn Association of India, Dec 19 – 21, 2019, Delhi University Botanical Society (DUBS), Department of Botany, University of Delhi, India.

C. Workshop

- 1) 4th Plant Proteomic Workshop, Dec 23 – 27, 2019, Delhi University Botanical Society (DUBS), Department of Botany, University of Delhi, India.
- 2) National workshop on regulatory compliance for accelerating innovations, June 13, 2019, Department of Biotechnology, Ministry of Science and Technology, India.

